VOLUME 37 SEPTEMBER 1959 NUMBER 9

Canadian Journal of Chemistry

Published by THE NATIONAL RESEARCH COUNCIL
OTTAWA CANADA

Canadian Journal of Chemistry

Under the authority of the Chairman of the Committee of the Privy Council on Scientific and Industrial Research, the National Research Council issues THE CANADIAN JOURNAL OF CHEMISTRY and five other journals devoted to the publication, in English or French, of the results of original scientific research. Matters of general policy concerning these journals are the responsibility of a joint Editorial Board consisting of: members representing the National Research Council of Canada; the Editors of the Journals; and members representing the Royal Society of Canada and four other scientific societies.

The Chemical Institute of Canada has chosen the Canadian Journal of Chemistry as its medium of publication for scientific papers.

Manuscripts for publication should be submitted to Dr. Léo Marion, Editor-in-Chief, Canadian Journal of Chemistry, National Research Council, Ottawa 2, Canada.
(For instructions on preparation of copy, see **Notes to Contributors** (inside back cover).)

Proof, correspondence concerning proof, and orders for reprints should be sent to the Manager, Editorial Office (Research Journals), Division of Administration and Awards, National Research Council, Ottawa 2, Canada.

Subscriptions, renewals, requests for single or back numbers, and all remittances should be sent to Division of Administration and Awards, National Research Council, Ottawa 2, Canada. Remittances should be made payable to the Receiver General of Canada, credit National Research Council.

The journals published, frequency of publication, and prices are:

Canadian Journal of Biochemistry and Physiology	Monthly	$9.00 a year
Canadian Journal of Botany	Bimonthly	$6.00 a year
Canadian Journal of Chemistry	Monthly	$12.00 a year
Canadian Journal of Microbiology	Bimonthly	$6.00 a year
Canadian Journal of Physics	Monthly	$9.00 a year
Canadian Journal of Zoology	Bimonthly	$5.00 a year

The price of regular single numbers of all journals is $2.00.

Canadian Journal of Chemistry

Issued by THE NATIONAL RESEARCH COUNCIL OF CANADA

VOLUME 37 SEPTEMBER 1959 NUMBER 9

THE THERMODYNAMIC PROPERTIES OF THE SYSTEM CELLULOSE – WATER VAPOR[1]

JOHN L. MORRISON[2] AND MATTHEW A. DZIECIUCH[3]

ABSTRACT

The heats of wetting by water of cotton cellulose containing various amounts of adsorbed and desorbed water were measured. These measurements together with those of the water vapor sorption isotherm were used to calculate the integral and differential enthalpies, free energies, and entropies of adsorption. Irreversible effects were avoided by vacuum-drying all samples at room temperature. The differential enthalpy values suggest hydrogen bonding. The differential entropies are explained in terms of changes in both the adsorbate and adsorbent.

The surface area of the cellulose is calculated by applying the Brunauer–Emmett–Teller and Harkins–Jura equations to the adsorption isotherm. The changes in the differential enthalpies and entropies of adsorption follow the same sequence as the changes in film formation given by the surface area calculations.

No hysteresis was observed in the heats of wetting of adsorbed and desorbed samples. It is concluded that the hysteresis of the sorption isotherm is an entropy phenomenon. This supports Barkas' explanation of hysteresis in terms of plastic deformation of a gel.

INTRODUCTION

Measurement of the amounts, the vapor pressures, and the energies involved when water vapor is added to and removed from fibrous natural polymers have made it possible to calculate in detail the thermodynamic properties of the systems silk fibroin – water vapor and wool keratin – water vapor (1, 2, 3). The present report includes the same kind of measurements on the system cellulose – water vapor.

Wahba also made similar measurements on the cellulose – water vapor system (4). However, we believe that Wahba's drying procedures introduce an irreversible effect. A similar but larger effect is shown in the work of Argue and Maass (5), who made the first detailed measurements of the heats of wetting of cellulose by water.

Babbitt (6) made a comprehensive analysis of the adsorption isotherm of the cellulose – water vapor system and was the first to apply the Brunauer, Emmett, and Teller adsorption isotherm equation (7) to this system. In the present work, surface area measurements have assisted us in interpreting the thermodynamic properties.

EXPERIMENTAL

Calorimetric measurement of the heats of wetting by liquid water of cellulose equilibrated with various amounts of adsorbed and desorbed water vapor is the basis of the

[1]*Manuscript received April 13, 1959.*

Contribution from the Department of Chemistry, University of Alberta, Edmonton, Alberta. Based on a thesis submitted to the Faculty of Graduate Studies, University of Alberta, in partial fulfillment of the requirements for the M.Sc. degree, June, 1958. Presented in part to the 133rd Meeting of the American Chemical Society, San Francisco, California, U.S.A., April 13–18, 1958.

[2]*Formerly Professor of Chemistry, University of Alberta, Edmonton, Alberta. Present address: Connaught Medical Research Laboratories, University of Toronto, Toronto, Ontario.*

[3]*Graduate student, University of Alberta, 1956–58.*

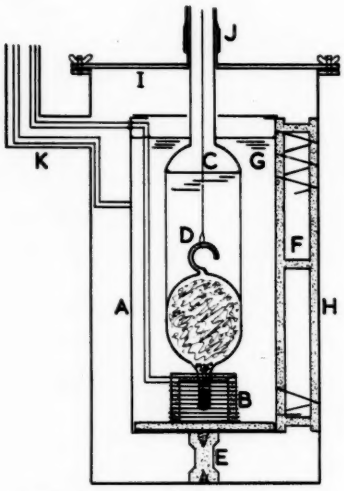

FIG. 1. The adiabatic calorimeter.

enthalpy calculations. Measurement of the adsorption and desorption isotherms is the basis of the corresponding free energy calculations. The entropies of sorption then follow from the well-known equation connecting the three thermodynamic functions.

Calorimeter

The adiabatic calorimeter (Fig. 1) was a simplified version of one by Howard and Culbertson (8). An inner cylindrical copper can, A, 2 inches in diameter by 5.5 inches long, was secured on a small lucite pedestal E inside an outer concentric copper jacket H with an air gap of 0.75 inch. A thermel F of 21 pairs of copper–constantan junctions supported on a light lucite frame was placed between the concentric walls. A 100-ohm manganin wire, non-inductively wound on a lucite frame, served as a calibration heater coil B and was placed in the bottom of the inner can.

The flanged lid I of the outer can had a central brass tube to act as a bearing for the glass reaction cell D. A side tube K from the outer can carried the wiring of the thermels and heater. The complete assembly rested in a well-stirred crock containing water. A rubber tube J was clamped to the lid-bearing to prevent leakage of water from the crock into the calorimeter.

Adiabatic control, sensed by the thermel and a sensitive galvanometer, was obtained manually by hot and cold water streams. Temperature changes were measured by a pair of thermistors (Stantel Type F, Standard Telephone and Cables, Ltd., England, total resistance about 3500 Ω at 25° C) immersed in the outer water bath and connected to a wheatstone bridge reading to 0.1 Ω. (Simultaneously, for some experiments, the resistance was measured by a Sargent Recorder, Model S-72150.) Electrical duplication of the heat changes was obtained with a circuit (9) which included an electronic voltage stabilizer to give a constant voltage (5 to 10 v). Between particular heat of wetting experiments, the outer crock was maintained at constant temperature by a thermoregulator and heater assembly, and at least 20 hours was allowed for the calorimeter and reaction cell to come to thermal equilibrium. All experiments were started at about 24.5° C.

A double compartment glass reaction cell D was used for contacting the cellulose and liquid water (Fig. 1). The cellulose in the lower compartment was sealed under vacuum. This ensured complete wetting when the breaking of the glass septum by pulling on a looped wire C allowed the water in the upper compartment to enter the lower one. The glass tube of the reaction cell passes through the calorimeter lid and is suspended by a coupling to a reciprocating stirring device. The main parts of the reaction cell are suspended in a heat transfer fluid G (light grade vacuum pump oil) in the inner can. After a sample has been prepared, the vacuum seal which is finally made at the lower end of the reaction cell is pinched into a paddle shape to act as a stirrer. This stirrer is suspended just inside the electrical heater B, thus securing dissipation of the heat evolved by the heater and by the wetting process. A new glass cell is required for each experiment.

Adsorption Apparatus

The sorption isotherm of cellulose and water vapor was determined with a vacuum apparatus similar to that used by Wiig and Juhola (10) for charcoal. About 8 g cellulose were placed in a detachable cylindrical glass bulb fitted with a vacuum stopcock and ground glass joint. The bulb had a central glass tube with several perforations to hasten equilibration. The vapor pressure was measured with an oil (Apiezon B) manometer and cathetometer, and the amount of water in the sample was obtained by detaching and weighing the assembly. Special precautions were taken in experiments near saturation vapor pressure because the top surface of the water bath thermostat had a slightly lower temperature than the bulk of the thermostat. A small heating coil was clasped around the tubes of the adsorption cell and the water reservoir to prevent condensation. The manometer was maintained at a temperature slightly above that of the thermostat. The isotherm was measured at 24.6° C.

Preparation of Cellulose

Standard cellulose was prepared from absorbent cotton (Johnson and Johnson Red Chain) by the same method as that of Argue and Maass (5), with the exception that *the cellulose was never allowed to dry above room temperature.*

All of the samples of cellulose, both for the calorimetry and for the sorption isotherm, were evacuated at room temperature for a minimum of 24 hours by means of a system including a mercury diffusion pump, magnesium perchlorate drying tube, a glass trap in dry ice – acetone mixture, and a rotary oil vacuum pump. "Stick" vacuums were consistently obtained as shown by the McLeod gauge. It was found that evacuation for 2 or 3 days neither reduced the moisture content nor produced a higher heat of wetting than for samples evacuated for 24 hours.

Samples for heat of wetting experiments (about 1 g) were placed in the lower compartment of the reaction cell; a small plug of Pyrex glass wool was inserted to prevent singeing of the cellulose. A vacuum stopcock and a male ground glass joint were sealed to the lower compartment, and the assembly was evacuated to constant weight. The dry weight of the cellulose was obtained by weighing the assembly after removing the grease (Apiezon L) from the ground glass joint with ether. All other joints and all stopcocks were greased with Dow Corning High Vacuum Silicone Grease, but Apiezon L is more easily removed because of its yellow color and hydrocarbon nature.

Samples were prepared with various adsorbed and desorbed water contents by contacting water vapor in an otherwise evacuated line. In each case at least 24 hours (11) were allowed for the final equilibration *after* the addition or removal of water. Also, at

least 24 hours were allowed for saturation with water vapor *before* the water was partially removed for the desorption experiments. Thus, at least 48 hours were required to prepare adsorption samples and 72 hours to prepare desorption samples for the calorimeter.

The correction for the heat of bulb-breaking (12) when water entered the evacuated bulb containing cellulose was calculated to be about 0.2 cal for each cell. A blank run on an empty cell gave a value of about 0.15 cal, so that this was subtracted from the heat of wetting of each sample. It happens that this correction does not affect any of the thermodynamic functions except the net enthalpy ΔH at saturation.

RESULTS AND CALCULATIONS

Drying Temperatures and the Heats of Wetting

The heats of wetting of standard cellulose with varying water contents, both adsorbed and desorbed, are given in Table I and Fig. 2. It would appear that within the experimental error, there is no hysteresis between the "adsorbed" and "desorbed" heats of wetting.

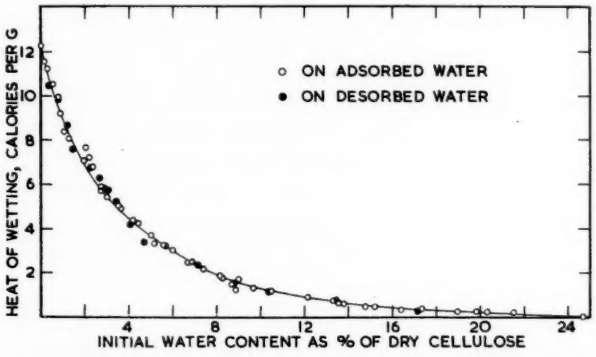

FIG. 2. The heats of wetting by water of cotton cellulose containing various amounts of adsorbed and desorbed water.

TABLE I

Heats of wetting of cotton cellulose by water

Adsorption		Adsorption		Adsorption		Desorption	
Water content, %	Heat of wetting, cal/g	Water content, %	Heat of wetting, cal/g	Water content, %	Heat of wetting, cal/g	Water content, %	Heat of wetting, cal/g
0	12.28	3.46	5.08	12.13	0.92	0.35	10.50
0	12.36	3.60	4.90	13.31	0.74	0.74	9.89
0	12.34	4.12	4.41	13.48	0.66	1.17	8.69
0.17	11.61	4.40	4.25	13.75	0.61	1.38	7.62
0.29	11.30	4.98	3.70	14.78	0.48	1.62	7.13
0.55	10.56	5.13	3.34	15.20	0.45	2.20	6.78
0.77	9.97	5.59	3.24	16.36	0.33	2.61	6.33
0.88	9.21	5.97	3.02	17.28	0.42	2.81	5.90
1.05	8.40	6.66	2.47	18.94	0.25	3.00	5.80
1.28	8.06	6.89	2.49	19.79	0.25	3.38	5.25
1.45	8.05	7.36	2.18	20.28	0.21	4.01	4.18
1.95	7.08	8.14	1.88	21.51	0.23	4.67	3.40
2.06	7.67	8.15	1.80	24.67	0.03	5.67	3.23
2.20	7.22	8.70	1.53	28.43	0	7.11	2.39
2.35	6.80	8.88	1.21	33.31	0	8.76	1.56
2.72	5.93	9.00	1.73	35.59	0	10.37	1.19
2.73	5.74	9.67	1.31			13.40	0.73
2.97	5.46	10.44	1.17			17.20	0.34

There is more scatter in the heats of wetting of samples below 3% water content than above. We believe that this is due to difficulty in removing the last traces of water from the cellulose rather than to errors in the calorimetry.

The heats of wetting obtained here are significantly higher than those obtained by Argue and Maass (5) and Wahba (4). For example, our value for dry cellulose was 12.33 cal/g whereas theirs were 10.16 and 10.72 respectively.

Argue and Maass heated their samples in air at 100° C, while Wahba heated his cellulose *in vacuo* at 65° C. In contrast, our samples were never permitted to go above room temperature. Kouris, Ruck, and Mason (13) also found that drying cellulosic material (a purified sulphite pulp) at elevated temperatures lowers the heat of wetting significantly compared with drying at room temperature.

There is some evidence that the cellulose–water system undergoes a change around 40° to 50° C. For example, Collins (14) found a parallel break in the curves of the cross-sectional area changes *and* the regain when plotted against temperature, with a complete change in direction occurring in the range 40° to 50° C.

Wahba and Nashed (15), on the basis of the experimental determination of adsorption isotherms at different temperatures, found that the isosteric heats of adsorption decreased markedly above an optimum temperature of from 40° to 50° C for "unstabilized" cellulose. They attribute this change to the development of new adsorbing centers above the optimum temperature.

The absence of hysteresis in the heats of wetting probably was found because the samples were dried at room temperature. Wahba and Nashed (16) found some hysteresis when they dried cellulose at 65° C and Argue and Maass (5) found even more when they dried it at 100° C.

The scatter in the heat of wetting values at very low moisture contents may arise from a high energy of activation for the transfer of water out of and into the cellulose fibers. Thus, room temperature drying increases the difficulty of obtaining reproducible drying. If we had used smaller samples, and evacuated them for longer times, the scatter probably would be reduced. Above the moisture content of the monolayer value (later), the scatter is much smaller in spite of the smaller amount of heat to be measured. It follows quite reasonably that the energy of activation for the removal of the upper layers is much less than for the first layer of sorbed water.

Thermodynamic Calculations

The heat of wetting data are used to calculate the integral and differential net enthalpies of sorption ΔH and $\overline{\Delta H}$ in calories per 100 g cellulose (above the heat of condensation of water vapor to liquid).

The adsorption isotherm (Table II and Fig. 3) is used to calculate the integral and differential free energies of adsorption, following the method of Dole and McLaren (17), see also (1, 2), which is similar to that of Wahba (4).

Finally, the integral and differential net entropies of adsorption are calculated from the enthalpies and free energies by the equations

$$\Delta S = (\Delta H - \Delta F)/T \quad \text{and} \quad \overline{\Delta S} = (\overline{\Delta H} - \overline{\Delta F})/T.$$

The various thermodynamic data are given in Table III and the differential properties are plotted in Fig. 4.

Adsorption Areas

Babbitt (6) applied the Brunauer, Emmett, and Teller (B.E.T.) equation (7) to Urquhart and Williams' cellulose – water vapor isotherm (18). Bull applied the same

TABLE II

Sorption isotherms of water vapor on cellulose at 24.6° C

Relative pressure	Adsorption, %	Desorption, %	Relative pressure	Adsorption, %	Desorption, %
0.025	1.00	1.18	0.55	5.97	7.03
0.05	1.49	1.71	0.60	6.52	7.66
0.075	1.86	2.10	0.65	7.13	8.31
0.10	2.13	2.45	0.70	7.81	9.02
0.15	2.65	3.02	0.75	8.58	9.84
0.20	3.09	3.52	0.80	9.53	10.88
0.25	3.48	3.94	0.85	10.72	12.21
0.30	3.87	4.37	0.90	12.55	14.0
0.35	4.22	4.84	0.95	15.25	16.7
0.40	4.61	5.37	0.975	17.0	19.2
0.45	5.02	5.92	0.99	19.1	21.3
0.50	5.47	6.47	1.00	~25	~25

TABLE III

Calculated thermodynamic properties of the cellulose–water system

n	P/P_0	$-\Delta H$	$-\Delta F$	$-\Delta S$	$-\overline{\Delta H}$	$-\overline{\Delta F}$	$-\overline{\Delta S}$
0	0	0	0	0	7600	—	—
.025	.008	165	83	0.28	5730	3100	8.83
.05	.021	297	148	0.50	4640	2300	7.86
.075	.042	405	202	0.68	4050	1900	7.22
.10	.071	498	247	0.84	3350	1570	5.98
.15	.156	640	313	1.10	2230	1095	3.81
.175	.207	695	337	1.20	1935	930	3.37
.20	.265	740	358	1.28	1720	785	3.14
.25	.387	820	391	1.47	1480	565	3.07
.30	.492	888	416	1.58	1360	420	3.15
.35	.582	952	434	1.74	1130	320	2.72
.40	.656	1005	448	1.87	860	250	2.05
.45	.720	1047	459	1.97	690	197	1.65
.50	.773	1080	468	2.05	525	152	1.25
.55	.817	1105	475	2.11	380	118	0.88
.60	.853	1122	481	2.16	330	94	0.79
.65	.881	1140	485	2.20	315	76	0.80
.70	.901	1154	488	2.24	250	62	0.63
.75	.919	1165	491	2.26	210	48	0.54
.80	.932	1176	493	2.29	180	38	0.48
.90	.965	1195	496	2.35	95	23	0.24
1.0	.984	1204	497	2.37	75	13	0.21
1.1	.990	1208	497.5	2.39	50	6	0.15
1.2	.995	1218	497.5	2.42	30	—	—
1.3	.998	1225	—	—	20	—	—
1.4	.9995	1230	—	—	—	—	—

NOTE: n, moles per 100 g cellulose; ΔH and ΔF, calories per 100 g cellulose; $\overline{\Delta H}$ and $\overline{\Delta F}$, calories per mole of water; ΔS, entropy units per 100 g cellulose; $\overline{\Delta S}$, entropy units per mole of water.

equation to a large number of protein – water vapor adsorption isotherms (19). In both cases the B.E.T. equation fitted the lower part of the adsorption isotherm.

Dunford and Morrison (20) have shown that the Harkins–Jura (H.J.) equation (21) applied to the upper part of Bull's isotherms and, by using Liang's correlation (22), they found the *same* monolayer content for both the B.E.T. and H.J. equations.

Applying these equations to the present isotherm, we obtain monolayer contents of 3.19 and 3.29 g water per 100 g cellulose for the B.E.T. and H.J. equations, respectively. The relative pressures over which these equations apply are 0.075 to 0.30 *and* 0.68 to

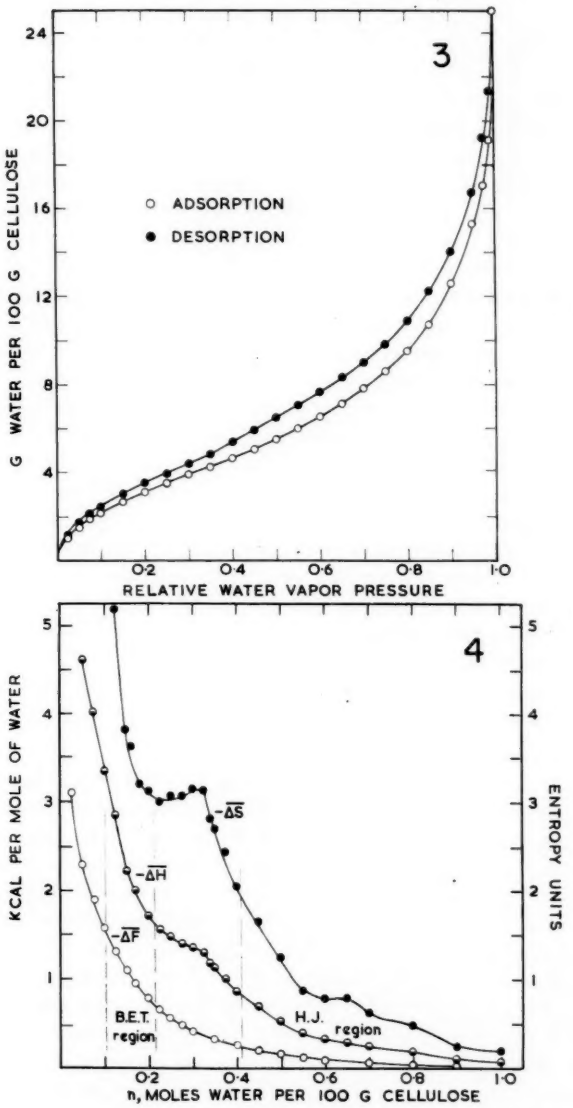

FIG. 3. The adsorption and desorption isotherms of water vapor on cotton cellulose. The points here are from smoothed curves obtained from measurements that extended over 3 months and included a total of 83 points; a minimum of 24 hours was allowed between each point.

FIG. 4. The net differential enthalpy, free energy, and entropy of adsorption of water by cotton cellulose.

1.0, respectively. For comparison, Wahba's data (4) yielded monolayer contents of 3.080 *and* 3.085 g, for the relative pressure range of 0.075 to 0.37 *and* 0.60 to 1.0, respectively. Urquhart and Williams' data (18) gave monolayer values of 3.38 and 3.60 g respectively.

DISCUSSION

Isotherm Equations and Areas

The application of theoretical adsorption equations to water vapor – natural polymer systems such as the present one helps us to interpret the thermodynamic data. The finding that at least two different equations, the B.E.T. and the H.J. equations, are required to account for the major part of the adsorption isotherm suggests either or both of two interpretations, (*a*) that a phase change occurs in the state of the adsorbed film (21) or (*b*) that a new phase appears as the relative pressure increases.

We note here that the B.E.T. equation is based on an immobile film with adsorption on definite sites, while the H.J. equation is based on a mobile condensed film.

Following the suggestion of Dunford and Morrison (20) with respect to the adsorption of water vapor by proteins, we consider that the adsorption of water vapor by cellulose from the dry state to saturation takes place as follows: a monolayer of immobilized water molecules is completed well before a relative pressure of 0.5 is reached, while further adsorption occurs *above* this monolayer; no surface is developed beyond that occupied by the monolayer; some multilayers, also immobile, are built up until the onset of a condensed film occurs at a relative pressure of about 0.6. Since the H.J. equation is based on *monolayer* film formation, it is suggested that the condensed film may appear as a new phase above an underlying "iceberg" phase of immobilized water (23).

The interpretation given here is in part confirmed by the observations of Hermans and co-workers (24). When the density of cotton cellulose is plotted against water content, a very well-defined maximum occurs at about 3.1% water content. This corresponds in their terms to the "formation of the first hydrate", and in our terms to the completion of a monolayer of immobilized water. Subsequently, there is evidence from their data of additional hydration up to 10 to 12% water content, succeeded by a density of sorbed water indistinguishable from that of liquid water.

A Comparison of Cellulose and the Fibrous Proteins

When the differential entropy and enthalpy curves (Fig. 4) of the cellulose – water vapor system are compared with those for silk fibroin and wool keratin (1, 2, 3), it is seen that the curves of the cellulose system are not as *definite* in their features. Whereas the breaks in the $\overline{\Delta H}$ and $\overline{\Delta S}$ curves of the two protein systems are very definite, and these breaks coincide very well with the B.E.T. and H.J. equation ranges, the same features in the corresponding cellulose curves are much less definite. For example, the beginning and end of the B.E.T. ranges of the two proteins coincide with the minimum and maximum respectively of the breaks in the $\overline{\Delta S}$ curves. In contrast, the B.E.T. range for cellulose begins earlier and it ends before the second break in the $\overline{\Delta S}$ curve.

It is possible that in the case of the proteins, the first monolayer is largely completed before the second and higher layers begin to form. In contrast, Babbitt has suggested for cellulose "that condensation begins in the second layer long before the first is completed" (6).

There is much evidence to suggest that cellulose is a much less reproducible material than the fibrous proteins. In our experience with the three fibers, the proteins are much less sensitive to high temperature drying than cellulose. Wool keratin can be dried in vacuum up to 80° C without affecting its heat of wetting (25), and it shows no hysteresis in its heat of wetting curve (2). Probably silk fibroin could also be heated nearly to this temperature without changing its adsorption properties, because on drying at 100° C it shows only a small hysteresis in its heat of wetting curve (1). Moreover, this

hysteresis is in the opposite direction to that observed for cellulose (5). Hutton and Gartside (26) have shown after very careful experiments that silk fibroins of Japanese, Chinese, and Italian origin gave exactly the same sorption isotherms.

In contrast, as already noted, cellulose is very sensitive to its mode of drying (see also Brown and co-workers (27)) and other features of its past history.

Perhaps the most important evidence for the contrast between protein fibers and cellulose is given by Mellon, Korn, and Hoover (28). They found that complete solution and reprecipitation of fibroin and keratin did not essentially alter their sorption isotherms. On the other hand, it is well known that solution and reprecipitation of cellulose always result in very large increases in the amount of water adsorbed.

Differential Enthalpy and Hydrogen Bonding

Although less definite than the fibrous proteins, nevertheless cellulose reveals the same kinds of breaks in its differential enthalpy and entropy curves. The enthalpy $\overline{\Delta H}$ decreases rapidly and levels off somewhat at -1.4 kcal per mole water adsorbed. This is comparable to the first layer heat value, -1.44, which Babbitt obtained for cellulose from one of the constants in the B.E.T. equation (6). It is also similar to the value obtained in this laboratory for mercerized cotton cellulose (29).

The value, -1.4, is significantly lower than the corresponding one, -2.4, which was obtained for both fibroin and keratin (1, 2, 3). As in the latter cases, we consider that the value -1.4 corresponds to a single hydrogen bond between water molecules and cellulose. Since the $\overline{\Delta H}$ values are net ones above the heat of condensation to liquid water, the hydrogen bond values would be $-4.5+(-1.4) = -5.9$ kcal per mole water, which is reasonable (30).

The high initial values of $\overline{\Delta H}$ may be due in part to the formation of two or more hydrogen bonds (15) per adsorbed water molecule; also, there may be a contribution from the release of tensions within the excessively dried cellulose. After the break in the region of monolayer formation, $\overline{\Delta H}$ decreases continuously up to saturation vapor pressure when it is indistinguishable from that of condensation on liquid water.

Entropy Changes

The differential entropy of adsorption for the cellulose – water vapor system is given in Fig. 4. The entropy curve exhibits a minimum similar to that of the fibrous proteins (3). Kelsey and Clarke (31) have a break in their $\overline{\Delta S}$ curve for a wood – water vapor system at about 8% to 9% water content. Since their wood adsorbed about 1.65 times as much water as pure cellulose, their observation is consistent with our maximum at a moisture content of 5.4%.

The explanation of the entropy curve is based on the assumption that both the adsorbate and adsorbent are contributing to $\overline{\Delta S}$ and $\overline{\Delta H}$. It is considered that after the *minimum* in $\overline{\Delta S}$ ($n = 0.25$) the contribution of the adsorbent is negligible on the *adsorption* side.

Pure adsorption, being an ordering process, contributes negative entropy ($-\overline{\Delta S}$ = +value). On the other hand, the disorganization of a highly dried gel (cellulose, fibroin, etc.) by water, contributes positive entropy ($-\overline{\Delta S}$ = −value). The high initial values of $-\overline{\Delta S}$ are probably due to adsorption of water, while the very rapid decrease to a minimum may be due in part to the disordering of the dried gel and in part to the replacement of two or more hydrogen bonds per water molecule by one per molecule. Then $-\overline{\Delta S}$ recovers up to a maximum. Here it is suggested that the disordering of the gel is

largely completed and the ordering due to adsorption asserts itself sufficiently to give a net recovery in $-\overline{\Delta S}$.

Adsorption into the second layer is less ordering than into the first so that $-\overline{\Delta S}$ continues to fall off after the maximum.

There is only a suggestion of a second break in the $-\overline{\Delta S}$ curve at $n = 0.70$, which corresponds to the pronounced break in the fibroin and keratin curves (1, 2, 3). A revision of a former explanation (3) is given here for the second and final break. It has already been suggested that well before the final break is reached, the contribution of the adsorbent to $-\overline{\Delta S}$ is negligible. The final break is considered to be a recovery in $-\overline{\Delta S}$ *after* the onset of a mobile film.

The transition from an immobile to a mobile film, *or* the appearance of a new mobile film above the immobile one, probably is marked by the beginning of the H.J. range, and is a disordering effect ($-\overline{\Delta S} = -$value). Thus, the net $-\overline{\Delta S}$ decreases more rapidly than if such a transition did not occur. But, after it has occurred, further adsorption (an ordering effect) continues and there is some recovery in $-\overline{\Delta S}$. Finally, the entropy changes become indistinguishable from condensation on liquid water.

Hysteresis

The adsorption–desorption isotherm for the cellulose – water vapor system exhibits a well-known hysteresis. Everett and Whitton (32) have discussed the validity of calculating thermodynamic properties of systems which exhibit such a permanent hysteresis. They have shown that these systems are thermodynamically stable, and differ from more familiar thermodynamic systems in having at least one other (an internal) variable.

It has been found that there is no hysteresis in the enthalpies of adsorption and desorption of water vapor on cellulose (also wool keratin and probably silk fibroin). Since the sorption curves determine the free energy functions, it follows that hysteresis in these systems is an entropy phenomenon.

The absence of hysteresis in the enthalpy seems to rule out the suggestion that hysteresis in the sorption isotherm involves the uncovering of new, more active sites on the desorption branch. Thus, Wahba and Nashed (15) suggest that the water molecules are more tightly held on the desorption side so that the vapor pressure is lower than on the adsorption side for the same amount of water sorbed.

If the hysteresis in the sorption isotherm is an entropy phenomenon, we would look for a difference in the arrangements (ordering) of the system on the two sides of the hysteresis loop rather than a difference in the bonding energies (enthalpies). It is difficult to conceive of the water alone having a different arrangement on the two sides of the loop, without the cellulose also being different. In fact, it is more usual that the adsorbent determines the arrangement of the adsorbate than the opposite. The general observation that the hysteresis of the water sorption isotherms of these fibrous systems is an entropy phenomenon supports Barkas' explanation of these hystereses (33).

Barkas explains hysteresis in terms of plastic deformation of a gel on the desorption of water vapor. This sets up internal stresses which affect the vapor pressure in a way analogous to the effect of an external hydrostatic pressure on the vapor pressure of a liquid. Thus, the vapor pressure on the desorption side is decreased by increased stresses on that side of the hysteresis loop.

We are suggesting that on the adsorption side of the hysteresis, the stresses of a completely dried gel have been largely removed in the low vapor pressure region of water uptake and that beyond about a monolayer, the isotherm is essentially stress-free up to saturation. Otherwise, it is difficult to understand the fit of the B.E.T. and H.J. equations

to the lower and upper parts of the adsorption isotherms with the same area being found for both equations. Attempts to fit these equations to the desorption side have been unsatisfactory. In the case of cellulose, the points do not lie on a 'good' straight line; and when the 'best' one is drawn, the H.J. monolayer area is at least 10% higher than the B.E.T. area.

Barkas predicted that there should be a hysteresis in the volume of the gel on the two sides of the loop. He found such to be the case for the wood – water vapor system (34). However, he calculated that in the case of *solid* filaments the volume hysteresis would be too small to observe experimentally. Hermans and his co-workers (24) confirmed this in the case of solid filaments of regenerated cellulose.

However, Collins (14), in some work apparently overlooked by Barkas, observed a definite hysteresis in the diameter of cotton cellulose fibers which have been treated with 15% NaOH to smooth them. Here, the same result as Barkas found for wood was observed in that the volume on the desorption side was greater than on the adsorption side.

Correspondingly, the differential entropy curve of desorption lies below that of adsorption. Since these are negative entropies, the desorption side has a higher positive entropy and is, therefore, more disordered than the adsorption side. This observation is consistent with the volume hysteresis.

A calculation based on Collins' measurements and on Urquhart and Williams' sorption isotherm for cellulose treated with 15% NaOH (35) shows, for example, that at 8% water content, the cross-sectional area changes are 9.7% on the adsorption side and 11% on the desorption. At 13% water content, the cross-section changes are 15.3% and 17.3% respectively.

Recently, Chakravarty (36) observed a similar hysteresis in the cross-sectional areas of single jute fibers at different relative humidities. However, Chakravarty found that there was no measurable hysteresis below a relative humidity of 25%, which corresponds to about one monolayer content for cellulose. This observation when taken together with Hermans and his co-workers' observations on isotropic solid filaments suggests that hysteresis may be largely an interfibrillar phenomenon rather than one within any single microfibril.

In conclusion, our work emphasizes the importance of measuring and reporting both the adsorption and desorption isotherms of systems which exhibit hysteresis. Unfortunately, this has not been done in many cases reported in the literature. For example, Bull in his classical work (19) measured the adsorption isotherms of about 18 protein materials. In the case of five of these (silk, wool, collagen, gelatin, and lyophilized egg albumin) he stated that "equilibrium was approached from both the wet and dry side of the equilibrium point". He found that "there is some hysteresis between a relative pressure of 0.15 and 0.65 while above and below these humidities the agreement is very good. In reporting the adsorption curves for the above five proteins, an average of the adsorption and desorption curves has been given." Here, Bull has assumed that hysteresis is a transient phenomenon; moreover, in calculating the "average of the adsorption and desorption curves", he does not indicate which of the two averages he used, the average at equal relative vapor pressure or at equal water content.

ACKNOWLEDGMENT

The authors are pleased to acknowledge grants in aid of this work made by the National Research Council of Canada.

REFERENCES

1. DUNFORD, H. B. and MORRISON, J. L. Can. J. Chem. **33**, 904 (1955).
2. MORRISON, J. L. and HANLAN, J. F. Proc. Second Intern. Congr. Surface Activity (London), **2**, 322 (1957).
3. MORRISON, J. L. and HANLAN, J. F. Nature, **179**, 528 (1957).
4. WAHBA, M. J. Phys. & Colloid Chem. **54**, 1148 (1950).
5. ARGUE, G. H. and MAASS, O. Can. J. Research, **12**, 564 (1935).
6. BABBITT, J. D. Can. J. Research, A, **20**, 143 (1942).
7. BRUNAUER, S., EMMETT, P. H., and TELLER, E. J. Am. Chem. Soc. **60**, 309 (1938).
8. HOWARD, F. L. and CULBERTSON, J. L. J. Am. Chem. Soc. **72**, 1185 (1950).
9. STURTEVANT, J. M. *In* Physical methods of organic chemistry. Vol. I. *Edited by* A. Weissberger. Interscience Publishers Inc., New York. 1945. p. 331.
10. WIIG, E. O. and JUHOLA, A. J. J. Am. Chem. Soc. **71**, 561 (1949).
11. ASHPOLE, D. K. Proc. Roy. Soc. (London), A, **212**, 112 (1952).
12. GUDERJAHN, C. A., PAYNTER, D. A., BERGHAUSEN, P. E., and GOOD, R. J. J. Chem. Phys. **28**, 520 (1958).
13. KOURIS, M., RUCK, H., and MASON, S. G. Can. J. Chem. **36**, 931 (1958).
14. COLLINS, G. E. J. Textile Inst. **21**, T311 (1930).
15. WAHBA, M. and NASHED, S. J. Textile Inst. **48**, T1 (1957).
16. WAHBA, M. and NASHED, S. Proc. Egyptian Acad. Sci. **8**, 128 (1952).
17. DOLE, M. and MCLAREN, A. D. J. Am. Chem. Soc. **69**, 651 (1947).
18. URQUHART, A. R. and WILLIAMS, A. M. J. Textile Inst. **15**, T559 (1924).
19. BULL, H. B. J. Am. Chem. Soc. **66**, 1499 (1944).
20. DUNFORD, H. B. and MORRISON, J. L. Can. J. Chem. **32**, 558 (1954).
21. JURA, G. and HARKINS, W. D. J. Am. Chem. Soc. **68**, 1941 (1946).
22. LIANG, S. C. J. Phys. & Colloid Chem. **55**, 1410 (1951).
23. KLOTZ, I. M. Science, **128**, 815 (1958).
24. HERMANS, P. H. Physics and chemistry of cellulose fibers. Elsevier Pub. Co., Inc., N.Y. 1949.
25. BRIGHT, N., CARSON, T., and DUFF, G. M. J. Textile Inst. **44**, T587 (1953).
26. HUTTON, E. A. and GARTSIDE, J. J. Textile Inst. **40**, T161 (1949).
27. BRICKMAN, W. J., DUNFORD, H. B., TORY, E. M., MORRISON, J. L., and BROWN, R. K. Can. J. Chem. **31**, 550 (1953).
28. MELLON, E. F., KORN, A. H., and HOOVER, S. R. J. Am. Chem. Soc. **71**, 2761 (1949).
29. CHAPMAN, R. and MORRISON, J. L. Unpublished results.
30. COULSON, C. A. Research, **10**, 149 (1957).
31. KELSEY, K. E. and CLARKE, L. N. Australian J. Appl. Sci. **7**, 160 (1956).
32. EVERETT, D. H. and WHITTON, W. I. Trans. Faraday Soc. **48**, 749 (1952).
33. BARKAS, W. W. Trans. Faraday Soc. **38**, 194 (1942).
34. BARKAS, W. W. Nature, **162**, 32 (1948).
35. URQUHART, A. R. and WILLIAMS, A. M. J. Textile Inst. **16**, T155 (1925).
36. CHAKRAVARTY, A. C. Textile Research J. **28**, 878 (1958).

ADDITION OF PHENYL ISOTHIOCYANATE TO PYRROLES[1]

E. BULLOCK[2] AND R. J. ABRAHAM[2]

ABSTRACT

Pyrrole and alkyl pyrroles react spontaneously with phenyl isothiocyanate to produce C-substituted derivatives. The structures of the products are confirmed by physical methods. The reaction is catalyzed by organic bases.

Alkyl pyrroles react with phenyl isocyanate; the speed of reaction varies widely, depending on the substituents on the pyrrole ring. Where the pyrrole has a free α-position, the product is considered to be the α-anilide, e.g., I*a*. Reaction with α, α'-disubstituted pyrroles is slow and is thought to yield β-anilides, e.g. II*a* (1).

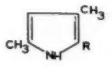

I

(*a*) R = CO.NH.Ph
(*b*) R = CS.NH.Ph

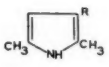

II

(*a*) R = CO.NH.Ph
(*b*) R = CS.NH.Ph

Generally, phenyl isocyanate reacts only sluggishly with "active" carbon atoms (e.g. with acetoacetic ester (2)) though the formation of IV from Fischer's Base (III) is rapid (3).

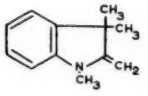

III

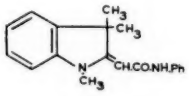

IV

Phenyl isothiocyanate is less reactive than the oxygen analogue towards water (4), amines (5), and acetoacetic ester, though it reacts readily with sodioethyl acetoacetate (11). The reaction with pyrroles is often rapid and the products are easily isolated (no competing side reaction with water). The thioanilides are converted to the corresponding anilides by alkaline peroxide.

In the ultraviolet, I*b* has a single absorption band of high intensity, while II*b* has two weaker bands at shorter wavelengths. This corresponds well with the difference in absorption of the α-(VII*a*) and β-(VII*b*) carboxylic acids (7).

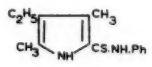

V

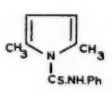

VI

VII

(*a*) R = COOEt, R_1 = H
(*b*) R = H, R_1 = COOEt

[1]*Manuscript received April 16, 1959.*
Contribution from the Division of Pure Chemistry, National Research Council, Ottawa, Canada.
Issued as N.R.C. No. 5272.
[2]*National Research Council Postdoctorate Fellow.*

N.M.R. spectra were recorded on several of these derivatives. The cryptopyrrole adduct shows no signal due to pyrrole C—H protons (8) and is therefore the α-thioanilide V (Fig. 1*a*). This compound is very similar (e.g. in infrared and ultraviolet spectra) to I*b*, which must therefore belong to the α-series, a fact confirmed by the proton resonance (Fig. 1*b*).

The nuclear magnetic resonance spectrum of II*b* confirms the structure since, apart from the single β-proton signal (Fig. 1*c*) the presence of two different sets of $-CH_3$ protons (Fig. 1*d*) rules out the symmetrical N-substituted compound (VI).

There is a qualitative relationship between the degree of alkyl substitution on the pyrrole nucleus and the rate of reaction with isothiocyanate in the α-series (Table I). The work on the anilides (1) shows a similar trend.

TABLE I

Reaction rates of substituted pyrroles

	Reaction (heating time)	Derivative	Yield (%)
Pyrrole	7 hours	α	3
α-Methyl	40 minutes	α	88
2,4-Dimethyl	10 minutes	α	90
2,4-Dimethyl-3-ethyl	2 minutes	α	100 (approx.)
2,3,4-Trimethyl	1 minute	α	100
2,3-Dimethyl	15 minutes	α	95
3,4-Dimethyl	5 minutes	α	73
2,5-Dimethyl	12 hours	β	7
2,3,5-Trimethyl	1½ hours	β	45

The reaction is base-catalyzed and solvent-sensitive. In several cases dissolution of the reactants (10%) in NN-dimethyl formamide (cf. 9) gives almost quantitative yields of thioanilides after 12 hours at room temperature and is the most convenient method of preparation; similar solutions in heptane yield no isolable product after 7 days.

Addition of triethylamine to mixtures of phenyl isothiocyanate with pyrrole, 2,4-, and 2,5-dimethyl pyrrole causes a marked increase in reaction rate and in the yield of the anilide.

The reaction with 2,3,5-trimethylpyrrole is interesting since it is faster than that of pyrrole and is comparable with α-methyl pyrrole. Thus, despite the steric effect of two adjacent methyl groups this β-position approaches the α-position of the simpler compound in reactivity.

Unlike the oxygen analogue, phenyl isothiocyanate failed to react with tetramethyl pyrrole (cf. 13) under vigorous conditions.

The variation of reaction rate with substitution may be due to two effects: (*a*) a general increase in the reactivity of the pyrrole ring with alkyl substitution and (*b*) the similarly increasing basicity of the pyrroles.

The close similarity of the reactions of isothiocyanates and isocyanates suggests that the mechanisms are analogous. The base catalysis observed for the pyrrole reaction indicates that as in the "normal" reaction with amines formation of a reactive complex (10) probably involving the pyrrole nitrogen atom is an intermediate step.

EXPERIMENTAL

Melting points are uncorrected.

Pyrryl carbanilides were prepared for comparison purposes according to Treibs and Ott (1).

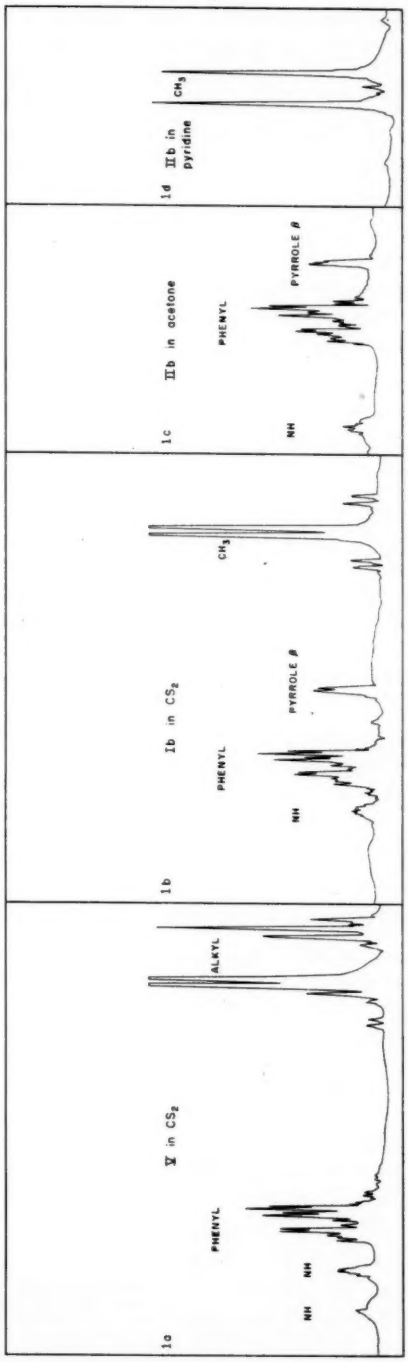

FIG. 1. N.M.R. spectra of pyrryl thiocarbanilides.

General Procedure for Isothiocyanate Reactions

The pyrrole was treated with approximately 10% excess of phenyl isothiocyanate and the mixture heated on the steam bath, the conditions being given for individual compounds in Table I. When the reaction mixture became very viscous, cold heptane was added; the product usually solidified when scratched with a glass rod. The solid was filtered and washed with heptane, then crystallized from a small volume of ether to which heptane was carefully added.

Pyrrole-2-thiocarbanilide

The reaction was far from complete after 7 hours and isolation of the product was made difficult by the presence of the reactants. The product was soluble in many organic solvents but was finally crystallized from heptane to yellow plates, m.p. 96–97° (3%). Calc. for $C_{11}H_{10}N_2S$: C, 65.31; H, 4.98; N, 13.85. Found: C, 64.96; H, 4.86; N, 13.92.

2-Methylpyrrole-5-thiocarbanilide

The thioanilide crystallized to thick yellow needles (88%), m.p. 109.5–111°. Calc. for $C_{12}H_{12}N_2S$: C, 66.62; H, 5.59; N, 12.95. Found: C, 66.46; H, 5.41; N, 12.65.

2,4-Dimethylpyrrole-5-thiocarbanilide

The product (90%) was crystallized to long yellow needles, m.p. 112–115°. Calc. for $C_{13}N_{14}N_2S$: C, 67.79; H, 6.13; N, 12.17. Found: C, 67.73; H, 5.76; N, 11.95. Ultraviolet spectrum: λ_{max} 344, λ_{infl} 218 mμ; log ϵ_{max} 4.38, log ϵ_{infl} 4.12 (95% ethanol). Infrared spectrum (nujol mull): 3380, 3340, 1603, 1500, 1482, 1448, 1427, 1375, 1355, 1315, 1288, 1235, 1207, 1155, 1027, 1008, 986, 945, 892, 820, 802, 744, 695, 680, 642 cm^{-1}.

2,5-Dimethylpyrrole-3-thiocarbanilide

The reactants were heated on the steam bath for 12 hours after which time the reaction mixture was black. The product was isolated by sublimation (0.5 mm, 150°) from the black solid obtained on addition of heptane to the reaction mixture, as small white needles, m.p. 194° (7%). Calc. for $C_{13}H_{14}N_2S$: C, 67.79; H, 6.13; N, 12.17. Found: C, 67.96; H, 5.77; N, 12.13. Ultraviolet spectrum: λ_{max} 319–325, 263, 217 mμ; log ϵ_{max} 4.09, 4.09, 4.32 (95% ethanol). Infrared spectrum (nujol mull): 3170, 1595, 1527, 1493, 1372, 1337, 1315, 1304, 1285, 1219, 1199, 1127, 1067, 1025, 1002, 966, 910, 790, 755, 712, 700, 682, 653 cm^{-1}.

In $CHCl_3$ solution, the NH band resolves to two peaks at 3380, 3440 cm^{-1}.

2,3-Dimethylpyrrole-5-thiocarbanilide.—2,3-Dimethylpyrrole-5-thiocarbanilide was isolated as thick yellow needles (95%), m.p. 144–145°. Calc. for $C_{13}H_{14}N_2S$: C, 67.79; H, 6.13; N, 12.17. Found: C, 68.13; H, 6.00; H, 12.15.

3,4-Dimethylpyrrole-2-thiocarbanilide.—3,4-Dimethylpyrrole-2-thiocarbanilide was obtained as yellow needles (73%), m.p. 118–119.5. Calc. for $C_{13}H_{14}N_2S$: C, 67.79; H, 6.13; N, 12.17. Found: C, 67.75; H, 6.06; N, 12.01.

2,4-Dimethyl-3-ethylpyrrole-5-thiocarbanilide

An almost quantitative yield of the product was isolated as thick yellow needles, m.p. 98–99°. Calc. for $C_{15}H_{18}N_2S$: C, 69.72; H, 7.02; N, 10.84. Found: C, 69.93; H, 6.87; N, 10.91.

2,3,4-Trimethylpyrrole-5-thiocarbanilide.—2,3,4-Trimethylpyrrole-5-thiocarbanilide was obtained in quantitative yield, m.p. 123–124°. Calc. for $C_{14}H_{16}N_2S$: C, 68.34; H, 6.60; N, 11.21. Found: C, 68.74; H, 6.49; N, 11.11.

2,3,5-Trimethylpyrrole-4-thiocarbanilide.—2,3,5-Trimethylpyrrole-4-thiocarbanilide was formed in good yield when the reactants were heated alone (or with triethylamine) for 1½ hours on the steam bath. Shorter reaction times yielded a product which was difficult to purify owing to the presence of starting material. Addition of heptane gave a dark gummy solid which when washed with ether yielded a yellow powder which was crystallized from chloroform–heptane as yellow prisms, m.p. 195–196° (45%). Calc. for $C_{14}H_{16}N_2S$: C, 68.34; H, 6.60; N, 11.21. Found: C, 68.12; H, 6.47; N, 11.37. Ultraviolet spectrum: λ_{max} 313 (broad), λ_{infl} 292 mμ; log ϵ_{max} 4.16, log ϵ_{infl} 4.10 (95% ethanol).

2,3,4,5-Tetramethylpyrrole.—2,3,4,5-Tetramethylpyrrole yielded no derivative under the following conditions: heating for 1 minute, 1 hour, 3 hours, heating for 3 hours then 24 hours at room temperature, standing for 48 hours at room temperature.

Oxidation of Thioanilides to Anilides (6)

Thioanilide (0.2 g) was dissolved in ethanol–water (10:1) in which 1 pellet of sodium hydroxide was dissolved. Hydrogen peroxide solution (100 vol., 1 ml) was added to the cold solution dropwise with shaking, and crystalline material appeared in the mixture soon after the addition of all the peroxide. After 30 minutes the product was isolated by pouring the reaction mixture into water (100 ml) and crystallized from chloroform–heptane.

(*i*) 2-Methylpyrrole-5-thiocarbanilide yielded 0.11 g of the corresponding anilide, m.p. 174–176° alone or mixed with authentic material (lit. 173° (1)).

(*ii*) 2,4-Dimethylpyrrole-5-carbanilide (0.15 g), m.p. 161° (lit. (1) 163°), was isolated.

(*iii*) Cryptopyrrole-5-thiocarbanilide yielded the corresponding anilide (0.06 g), m.p. 128–129° alone or mixed with authentic material (lit. (1) 137° for sublimed material or 131° (12)).

Comparison of Catalyzed and Uncatalyzed Reactions

The pyrrole (1 ml) was mixed with phenyl isothiocyanate (1 ml, 1.13 g) in each of two vessels to one of which triethylamine (3 drops) was added. The reactions were stopped by the addition of heptane (50 ml) and the product filtered off.

In the pyrrole case a black solid was produced in the catalyzed reaction from which two products, one white unidentified, the other the yellow thioanilide, were isolated and separated by fractional crystallization. In the other cases the crude solid was dried and weighed for comparison (a single recrystallization of these materials yielded products of good melting point).

Compound	Heating time	Uncatalyzed	Catalyzed
Pyrrole	6 hours	0.025 g 1.5%	0.17 g 10%
2,4-Dimethylpyrrole	2 minutes	1.40 g 73%	1.66 g 86%
2,5-Dimethylpyrrole	2½ hours	0 0	0.21 g 11%

ACKNOWLEDGMENTS

Analyses are by Mr. H. Seguin and the infrared spectra were recorded by Mr. R. Lauzon.

REFERENCES

1. TREIBS, A. and OTT, W. Ann. **577**, 19 (1952).
2. DIECKMANN, W. Ber. **33**, 2002 (1900).
3. COENEN, M. Chem. Ber. **80**, 546 (1947).

4. CAIN, J. C. and COHEN, J. B. J. Chem. Soc. 328 (1891).
5. BUU HOI, N. P., XUONG, N. G., and SUU, V. T. J. Chem. Soc. 2815 (1958).
6. MCKAY, A. F., SKULSKI, M., and GARMAISE, D. L. Can. J. Chem. **36**, 150 (1958).
7. COOKSON, G. H. J. Chem. Soc. 2789 (1953).
8. ABRAHAM, R. J. and BERNSTEIN, H. J. Can. J. Chem. **37**, 1056 (1959).
9. LIEBER, E. and RAMACHANDRAN, J. Chem. & Ind. 1406 (1958).
10. BAKER, J. W. and BAILEY, D. N. J. Chem. Soc. 4649 (1957).
11. WORRALL, D. E. J. Am. Chem. Soc. **40**, 418 (1918).
12. FISCHER, H., SÖS, O., and WEILGUNY, F. G. Ann. **481**, 159 (1930).
13. TREIBS, A. and DERRA-SCHERER, H. Ann. **589**, 196 (1954).

MOLTEN SALTS

THE DENSITY AND ELECTRICAL CONDUCTIVITY OF THE SYSTEMS: $AgNO_3$–$Ba(NO_3)_2$, –$Ca(NO_3)_2$, AND –$Mg(NO_3)_2$ [1]

J. W. Murphy and F. E. W. Wetmore

ABSTRACT

The density and electrical conductivity of the systems $AgNO_3$–$Ba(NO_3)_2$, –$Ca(NO_3)_2$, and –$Mg(NO_3)_2$ have been determined from 210 to 320° and from 0 to 20 equiv. %. The addition of magnesium nitrate causes the greatest shrinkage of the equivalent volume and reduction of the conductivity, barium nitrate the least.

The low conductivity of the binary melts is explained in terms of a mechanism involving restricted jumps and variation of the energy barrier with temperature and kind of ion added.

To date there have been few systematic studies of the density and electrical conductivity of binary salt melts comprising other than uni-univalent salts. This report concerns melts of silver nitrate with additions of barium, calcium, and magnesium nitrates.

EXPERIMENTAL

Materials

The silver nitrate was of reagent grade with a limit of 0.02% impurity, dried by oven-heating and finally by fusion. Barium nitrate of reagent grade was dried in an oven in which the temperature was slowly raised to a point just short of fusion. Calcium nitrate was prepared from reagent tetrahydrate by holding it at 300° for more than a day and heating it to 450° for an hour before use. Magnesium nitrate was prepared from reagent hexahydrate by vacuum-exsiccation from 50° slowly up to 150° (1); the weight of the charge was determined periodically. The salts were stored under dry air. Dryness of the melts was assured by the fact that their properties (density, conductivity, and freezing point) were not altered by longer periods of drying or by being held at high temperatures for several days during the runs; it is also significant that on heating the melts through more than 100° and returning them to the original temperature, the properties were not changed.

Apparatus

The apparatus used for the determination of density and conductivity differed from that used by Spooner (2) in only a few respects. The furnace was fitted with top and bottom plate heaters, which improved the homogeneity of the temperature of the melt. The silica conductivity cell was similar to that used by Lorenz and Kalmus (3), open at the bottom and having the lower electrode in the main body of the melt; the position of this electrode was found to be not critical.

Calibration with potassium chloride solution (4) showed the cell constant to be 801.93 cm^{-1} at 25°; appropriate correction was made for the expansion of the silica at higher temperatures. The bridge circuit was similar to that recommended by Jones and Josephs (5); both ratio arms were 1000 ohms. The signal leaving the bridge could be sent through a wide-band (400 to 10,000 c.p.s.) filter or through one sharply peaked. The amplitude and phase angle of the signal were observed on a cathode ray tube.

[1]*Manuscript received April 20, 1959.*
Contribution from the Department of Chemistry, University of Toronto, Toronto, Ontario.

Procedure

Preliminary determinations of the apparent resistance of the melts with frequencies from 400 to 10,000 c.p.s. showed that it varied inversely as the square root of the frequency. The small polarization, not exceeding 0.05%, was thereafter conveniently determined by measuring the apparent resistance at two frequencies, 1000 and 4000 c.p.s.

Both conductivity and density measurements were made at intervals of about 12°, first with rising temperature and then with falling. The results fell on one smooth curve. Melts containing 1, 2, 3, 4, 5, 10, and 20 equiv. % of calcium and magnesium nitrate were studied; the dictate of solubility limited the addition of barium nitrate to 5 equiv. %.

RESULTS

From the measured buoyancies and resistances were derived equations of density and specific conductivity as functions of temperature. From these equations the equivalent volume and equivalent conductivity were calculated for intervals of 10°. The deviations of the original data from the equations indicated that the equivalent volumes of Table I are precise within 0.04%, the conductivities of Table II within 0.1%.

The equivalent volume of a melt, whether unary or binary, is the volume of 1 equivalent of nitrate ion with its associated equivalent of cation. Calculation of the shrinkage to be expected from simple replacement of silver ion by an equivalent amount of divalent ion (one-half as many) can be based on the reported (6) radii of the ions. The absolute values must depend on the assumption of the volume to be ascribed to an ion, varying, for example, from an extreme of $4.2\,r^3$ (spherical) to the other extreme of $8\,r^3$ (cubic). The relative shrinkages do not depend on this assumption; they are 1.0:2.0:2.5 for Ba:Ca:Mg. The actual shrinkages shown in Table I are $2.5N_2$, $5.5N_2$, and $7.3N_2$, corresponding to 1.0:2.2:2.9. In the melt, compared with the condition for which the radii were determined, the magnesium ion is most closely bound to the nitrate ions, the barium ion least.

TABLE I

Equivalent volume (cm^3 g-equiv.$^{-1}$) of the systems $AgNO_3$–$M(NO_3)_2$

Temp., °C	Equiv. %, divalent nitrate					
	0	3	5	10	20	M
210	42.82	42.74				Ba
		42.66	42.56	42.27	41.70	Ca
		42.60	42.46	42.07	41.47	Mg
230	43.07	42.99				Ba
		42.90	42.80	42.52	41.94	Ca
		42.85	42.71	42.32	41.72	Mg
260	43.44	43.36	43.32			Ba
		43.28	43.18	42.89	42.30	Ca
		43.22	43.08	42.69	42.10	Mg
290	43.83	43.75	43.70			Ba
		43.66	43.56	43.26	42.67	Ca
		43.60	43.47	43.07	42.48	Mg
320	44.22	44.14	44.10			Ba
		44.05	43.94	43.65	43.05	Ca
		43.99	43.86	43.46	42.87	Mg

Flood, Forland, and Grjotheim (7) suggested that the addition of divalent salt to univalent salt with a common ion could create vacancies in the melt. The shrinkages found here are of a magnitude which indicates the possibility of only small formation of vacancies, if any.

If ideality in conductivity is defined as the absence of effect of the presence of one ion on the mobility of another, then $\Lambda = N_1\Lambda_1^0 + N_2\Lambda_2^0$, in which N_i is the equivalent fraction of component i and Λ_i^0 is the equivalent conductivity of pure component i, is the condition of ideality. Since the melting points of the divalent nitrates lie well above the decomposition temperature of silver nitrate, comparison of real with ideal behavior is restricted to melts containing a high proportion of silver nitrate.

TABLE II

Equivalent conductivity (ohms cm^{-2} g-equiv.$^{-1}$) of the systems $AgNO_3$–$M(NO_3)_2$

Temp., °C	Equiv. %, divalent nitrate					
	0	3	5	10	20	M
210	27.76	26.31				Ba
		26.05	24.86	22.11	16.91	Ca
		25.76	24.59	21.63	16.30	Mg
230	31.99	30.48				Ba
		30.19	28.94	25.99	20.33	Ca
		29.85	28.58	25.34	19.53	Mg
260	38.18	36.56	35.46			Ba
		36.23	34.88	31.70	25.46	Ca
		35.84	34.43	30.84	24.35	Mg
290	44.15	42.44	41.32			Ba
		42.06	40.63	37.27	30.61	Ca
		41.61	40.10	36.25	29.15	Mg
320	49.92	48.10	46.97			Ba
		47.68	46.16	42.71	35.78	Ca
		47.17	45.61	41.56	33.92	Mg

Table II and the solid curves of Fig. 1 show the real behavior; the broken line indicates the ideal contribution of silver nitrate alone, $N_1\Lambda_1^0$. The conductivity of the melt is much less than that of silver nitrate diluted by a non-conducting substance; assumption of lack of conductivity on the part of the divalent nitrate will therefore not alone explain the low conductivity.

Van Artsdalen and Yaffe (8) pointed out that shrinkage of the equivalent volume (quasi-lattice) would increase the electrostatic energy barrier for the conducting species. At 260° a melt containing 20 equiv. % magnesium nitrate, for example, shows a conductivity 20% less than $N_1\Lambda_1^0$. The volume is only 3% less than that of silver nitrate, corresponding to 1% reduction in interionic spacing and 2% increase in coulomb force. This increase in the energy barrier can account for about one-third of the observed decrease.

The suggestion of Van Artsdalen and Yaffe can be extended by supposing that silver ion is the important carrier of charge and that it moves by jumping from one cation site to another, but not to a site occupied by a cation closely bound to its anion neighbors. In comparison with pure silver nitrate there would be in the binary melt only N_1 as many silver ions and only some N_1 as many sites to which jumps are possible. The contribution of silver nitrate, without allowance for an increase in the energy barrier,

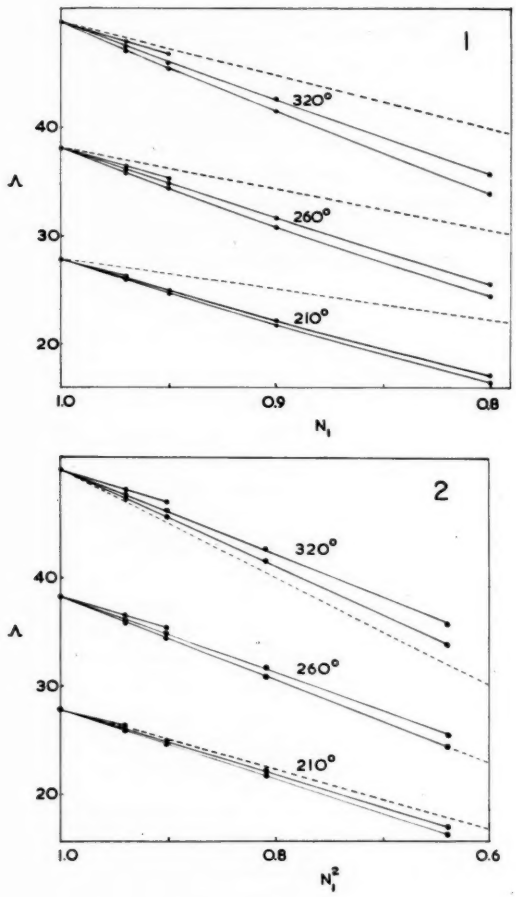

FIG. 1. The equivalent conductivity of silver nitrate with addition of divalent nitrate. The broken line shows the value of $N_1\Lambda_1^0$. In descending order the three solid curves in each group refer to barium, calcium, and magnesium nitrate, respectively.

FIG. 2. The equivalent conductivity of silver nitrate with addition of divalent nitrate. The broken line shows the value of $N_1^2\Lambda_1^0$. In descending order the three solid lines in each group refer to barium, calcium, and magnesium nitrate, respectively.

would be approximately $N_1^2\Lambda_1^0$. The solid lines of Fig. 2 show that Λ is essentially linear in N_1^2, but not exactly equal to $N_1^2\Lambda_1^0$. The deviations with change of temperature and divalent ion are in qualitative agreement with the views expressed above. The energy of activation of the conduction process decreases with rising temperature (2), and it can be seen from the expression $\Lambda = A.\exp(-E/RT)$ that the increase in the energy barrier with shrinkage of the quasi-lattice will be most pronounced at low temperature. The fall of conductivity should be greatest for addition of magnesium ion, least for barium ion. Both of these expectations are borne out.

ACKNOWLEDGMENTS

The authors gratefully acknowledge the financial support received from the National Research Council of Canada and the Advisory Committee on Scientific Research of this University.

REFERENCES

1. SHOMATE, C. and KELLEY, K. K. J. Am. Chem. Soc. **66**, 1490 (1944).
2. SPOONER, R. C. and WETMORE, F. E. W. Can. J. Chem. **29**, 777 (1951).
3. LORENZ, R. and KALMUS, H. T. Z. physik. Chem. **59**, 17 (1907).
4. JONES, G. and PRENDERGAST, M. J. Am. Chem. Soc. **59**, 731 (1937).
5. JONES, G. and JOSEPHS, R. C. J. Am. Chem. Soc. **50**, 1049 (1928).
6. PAULING, L. The nature of the chemical bond. Cornell Univ. Press, Ithaca, N.Y. 1939. p. 326.
7. FLOOD, H., FORLAND, T., and GRJOTHEIM, K. The physical chemistry of melts. Inst. of Mining and Metallurgy. London. 1953. p. 46.
8. VAN ARTSDALEN, E. R. and YAFFE, I. S. J. Phys. Chem. **59**, 118 (1955).

THE NUCLEAR MAGNETIC RESONANCE SPECTRA OF TRIARYL CARBONIUM IONS[1]

R. B. MOODIE,[2] T. M. CONNOR,[3] AND ROSS STEWART

ABSTRACT

The N.M.R. spectra of the triphenylmethyl cation and several of its derivatives substituted with methyl, methoxyl, and *tert*-butyl groups in the meta or para position have been obtained in trifluoroacetic acid – trifluoroacetic anhydride solution. The ring protons and substituent protons are all shifted to lower fields, i.e. are less shielded in the carbonium ions than in the neutral compounds of similar structure. The chemical shifts for the substituent protons are greater for para than for meta substituents and for mono- rather than tri-substituted ions. With each ion only a single peak was observed for the substituent protons but the ring protons were, in some cases, well resolved. The theoretical implications of these results are discussed.

INTRODUCTION

Triaryl carbinols are known to ionize in strongly acid solution to give carbonium ions.

$$Ar_3COH + 2H^+ \rightleftharpoons Ar_3C^+ + H_3O^+$$

The stability of these ions depends mainly on the extent of resonance interaction between the central electron-deficient carbon atom and the aromatic rings. Substituents which can aid this charge dispersal are known to have very large stabilizing effects on the carbonium ion. Thus the equilibrium constant for the ionization of tri-*p*-anisylcarbinol is larger by a factor of 3×10^7 than that of unsubstituted triphenylcarbinol (1). The effect of substituents in the meta position is much smaller since direct resonance interaction is not possible.

There are in addition two steric factors which are known to influence this electronic interaction. They are, first, the effect of bulky ring substituents such as *tert*-butyl in inhibiting solvation of the rings (2), and second, the steric interaction at the ortho positions. This latter effect precludes the formation of the electronically favored planar structure. The actual structure is open to question and it has been suggested that only one or two of the rings are conjugated with the central carbon atom (3). There is evidence, however, that favors, at least for the symmetrically substituted ions, a symmetrical "propeller" structure in which the π orbitals of each ring overlap to the same extent with the central carbon atom's p orbital (4, 5).

This paper reports a study of the nuclear magnetic resonance spectra of some substituted triarylmethyl cations in which the frequency of the aromatic and substituent proton resonances gives information about the distribution of the positive charge. The only previously reported N.M.R. spectra of carbonium ions are those of some protonated aromatic hydrocarbons (6) and the tropylium cation (7).

In order to compare the chemical shifts with those of neutral compounds containing similar groups, we sought a solvent which was sufficiently acidic to cause complete ionization of the triarylcarbinols, which would dissolve such compounds as toluene and anisole, and which was free from proton resonances in the region to be studied. A solution of trifluoroacetic acid in trifluoroacetic anhydride was found to be a suitable solvent system.

[1]*Manuscript received May 11, 1959.*
Contribution from the Chemistry Department, University of British Columbia, Vancouver, B.C., Canada.
[2]*National Research Council Postdoctoral Fellow, 1958–59.*
[3]*Holder of a National Research Council Studentship 1957–59.*

EXPERIMENTAL

The nuclear magnetic resonance spectra were recorded on a Varian 4300 spectrometer at 40 Mc, using an external water marker. In some cases the aromatic proton resonances were also examined at 60 Mc. Shifts were measured using conventional side band and interpolation techniques. Since all the solutions were dilute and the volume susceptibilities of the triarylmethyl cations are expected to be similar, the bulk susceptibility corrections are negligible so that the measured shifts can be compared directly. In each case the sample consisted of a 10% solution of the carbinol in a solvent of 1.5 *M* trifluoroacetic acid in trifluoroacetic anhydride sealed off *in vacuo*. The diamagnetic properties of the solvent were not appreciably changed over the range 1.5 to 3 *M* acid since the position of the proton resonances of toluene did not change.

The visible spectra of 3×10^{-4} *M* triphenylcarbinol (λ_{max} 410 mμ, ϵ 43,500, λ_{max} 425 mμ, ϵ 42,200) and of 1.5×10^{-4} *M* tri-*p*-anisyl carbinol (λ_{max} 478 mμ, ϵ 87,000) in the trifluoroacetic acid – trifluoroacetic anhydride solvent were measured with a Cary Model 14 recording spectrophotometer using cells of 0.1-cm path length. The spectrum appeared to be unchanged in more concentrated solutions (ca. 4×10^{-2} *M*) using cells of 10^{-3}-cm path length, but the volatility of the solvent precluded any precise determination with these cells.

The absorption maxima and extinction coefficients are very similar to those of the carbonium ions in sulphuric acid solution (triphenylmethyl cation: λ_{max} 404 mμ, ϵ 40,000, λ_{max} 431 mμ, ϵ 40,000 (2), tri-*p*-anisylmethyl cation: λ_{max} 483 mμ, ϵ 91,000 (8)). It was assumed that complete ionization also occurred in the slightly more concentrated solutions used for the N.M.R. spectral measurements. The N.M.R. spectra would, however, not necessarily reveal the presence of a small amount of the unionized triarylmethyl trifluoroacetate since in the equilibrium below,

$$CF_3CO_2CAr_3 \rightleftharpoons Ar_3C^+ + CF_3CO_2^-,$$

the rate of interconversion of the ionized and unionized forms may be too fast for separate substituent proton resonances to be observed.

The N.M.R. and visible spectra of *m*-methoxyphenyl diphenylcarbinol and tri-*m*-methoxyphenylcarbinol in this solvent were found to be quite different from the other carbinols studied. There seems to us to be some doubt as to the nature of the colored species formed in this solvent and their spectra are not further discussed here.

Preparation of Carbinols

The carbinols in Table I were prepared from the indicated starting materials by conventional Grignard syntheses.

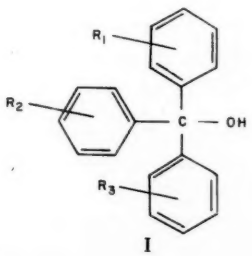

I

TABLE I

Preparation of carbinols

	R_1	R_2	R_3	Starting materials	M.p., °C (found)	M.p., °C (literature)
I	*p*-Me	—	—	*p*-MeC_6H_4Br, $(C_6H_5)_2CO$	76–9	78–9 (9)
II	*p*-Me	*p*-Me	—	C_6H_5Br, $(p\text{-}MeC_6H_4)_2CO$	73	75 (10)
III	*p*-Me	*p*-Me	*p*-Me	*p*-MeC_6H_4Br, $(p\text{-}MeC_6H_4)_2CO$	94–5	94 (11)
IV	*m*-Me	—	—	*m*-MeC_6H_4Br, $(C_6H_5)_2CO$	62–5	67 (12)
V	*m*-Me	*m*-Me	*m*-Me	*m*-MeC_6H_4Br, *m*-MeC_6H_4COOMe	70–2	69–71 (13)
VI	*p*-MeO	—	—	*p*-$MeOC_6H_4Br$, $(C_6H_5)_2CO$	60	60 (14) 82 (15)
VII	*p*-MeO	*p*-MeO	*p*-MeO	*p*-$MeOC_6H_4Br$, *p*-$MeOC_6H_4COOMe$	82–3	81–2 (2)
VIII	*m*-MeO	—	—	*m*-$MeOC_6H_4Br$, $(C_6H_5)_2CO$	87–9	88 (14)
IX	*m*-MeO	*m*-MeO	*m*-MeO	*m*-$MeOC_6H_4Br$, *m*-$MeOC_6H_4COOMe$	117–9	119.4 (14)
X	*p*-^{t}Bu	—	—	*p*-$^t BuC_6H_4Br$, $(C_6H_5)_2CO$, HCl	134–6[a]	133–4[a] (16)

[a]These melting points refer to *p-tert*-butylphenyl diphenylchloromethane which was prepared and used directly for the N.M.R. measurements.

Compounds IV and V gave poor yields and were purified by alumina chromatography. Compounds III and VI were purified by conversion to the triarylchloromethane and after several recrystallizations reconversion to the carbinol, as described by Gomberg (15). We are indebted to Mr. L. J. Muenster for the preparation of compound III.

RESULTS AND DISCUSSION

Table II records the chemical shifts of the aromatic and substituent protons measured from an external water marker at 40 Mc. In the case of the aromatic protons, these measurements were made to the largest peak except in the case of the tri-*p*-anisylmethyl cation where the measurement is to the center of the symmetrical quartet.

TABLE II

Chemical shifts of aromatic and substituent protons in cycles per second

Compound from which cation was derived	Aromatic shift (to main peak)	Substituent shift
Triphenylcarbinol	−101.0	—
p-Tolyl diphenylcarbinol (I)	− 98.0	+102.5
Di-*p*-tolyl phenylcarbinol (II)	− 94.75	+104.5
Tri-*p*-tolylcarbinol (III)	− 93.5	+105.5
m-Tolyl diphenylcarbinol (IV)	− 95.5	+112.5
Tri-*m*-tolylcarbinol (V)	− 89.0	+112.5
p-Anisyl diphenylcarbinol (VI)	− 96.0	+ 42.0
Tri-*p*-anisylcarbinol (VII)	− 87.5	+ 47.0
p-tert-Butylphenyl diphenylchloromethane (X)	−101.0	+151.0
Compound		
tert-Butylbenzene	− 76.0	+161.5
Anisole	− 68.0	+ 59.5
Toluene	− 69.0	+124.0

The Substituent Protons

In no cases were multiple substituent proton peaks observed. This is expected for the symmetrical propeller form but is also consistent with the one-ring-conjugated form if one assumes that the interconversion of isomers is too rapid to be detected by N.M.R. No splitting of the substituent proton resonances of the tri-*p*-anisylmethyl and tri-*p*-tolylmethyl cations was observed when the solutions were cooled to −80°.

Greater shielding of the substituent protons is observed in the carbonium ions sub-

stituted in all three para positions compared with those with only one para substituent. In the latter case greater stability would be expected for a structure in which the substituted ring occupies a position of greater conjugation with the central carbon than the other two rings. This effect should be less marked with metasubstituted compounds, where the direct resonance interaction with the substituent is not possible, and in fact no difference was observed in the shielding of the substituent protons for the *m*-tolyl diphenylmethyl and tri-*m*-tolylmethyl cations.

The greater shift between toluene and the tri-*p*-tolylmethyl cation (18.5 c/s) than between anisole and the tri-*p*-anisylmethyl cation (12.5 c/s), in spite of the greater contribution to stability that a methoxy substituent makes, shows the importance of hyperconjugative structures in the former case.

A considerable loss of shielding is also observed going from *tert*-butylbenzene to the *p-tert*-butylphenyl diphenylmethyl cation (10.5 c/s). However, it is not possible to say whether this is purely an inductive effect or involves carbon–carbon hyperconjugation.

The Ring Protons

The effect of the substituents is to increase the shielding of the ring protons as can be seen by comparison with the triphenylmethyl cation (Table II). In the monosubstituted compounds this effect in the substituted ring is partly offset by the presumed greater conjugation it has with the central carbon atom. The result is that the signals from substituted and unsubstituted rings overlap.

The fine structure of the aromatic peaks is shown in Figs. 1–6. Figures 1 and 2 show the spectra of the triphenylmethyl cation at 40 Mc and at 60 Mc respectively and give us some information regarding the distribution of positive charge within the rings.

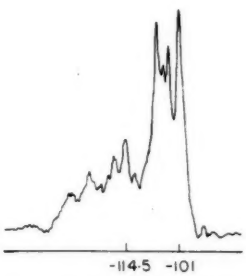

FIG. 1. Spectrum of aromatic protons of the triphenylmethyl cation at 40 Mc.

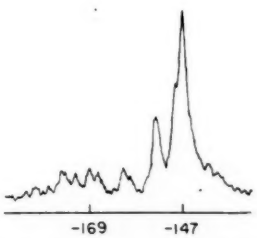

FIG. 2. Spectrum of aromatic protons of the triphenylmethyl cation at 60 Mc.

Resonance theory predicts that the meta protons should be more shielded than either the ortho or para protons in a carbonium ion. (This argument does not apply to molecules like nitrobenzene, for which it has been shown by Corio and Dailey (17) that the ortho hydrogens are least shielded with the meta and para proton peaks superimposed at higher field. The proximity of the latter is reasonable since the Hammett substituent constants (18) for meta and para nitro groups are close, i.e. resonance is of minor importance in nitrobenzene.) The complexity of the triphenylmethyl cation spectrum is due to coupling between aromatic protons and prevents complete identification of the proton signals. The group of peaks at low field however (below 157 c/s), can be assigned to the para protons since they occupy the theoretical value of one fifth of the area of the curve. The meta and ortho proton peaks overlap at higher field. (This agrees with

S.C.M.O. calculations of π electron densities (19).) This is similar to the N.M.R. spectrum of protonated pentamethylbenzene in which the para substituent is the least shielded (6).

A factor which we will call ortho electrostatic interaction may be important in determining the charge distribution in triarylmethyl cations. The propeller form of the ion will be of lowest energy when the three rings are folded close to one another to enable maximum overlap to occur with the central p orbital. The ortho carbons are very close in this form, however, and electrostatic repulsion between these partially positively charged atoms may be expected to render the para positions relatively more positive.

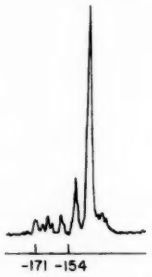

FIG. 3. Spectrum of aromatic protons of p-tolyl diphenylmethyl cation at 60 Mc.

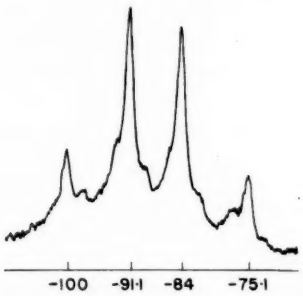

FIG. 4. Spectrum of aromatic protons of tri-p-anisylmethyl cation at 40 Mc.

The spectrum of the mono-para methyl ion (Fig. 3) resembles that of the unsubstituted triphenylmethyl cation with the single peak due to the substituted ring superimposed on the main peak. The peaks at low field are probably due to the para protons in the unsubstituted rings since the area under the peaks below -154 c/s is approximately one seventh of the area under the whole aromatic proton spectrum.

The spectrum of the tri-p-anisylmethyl cation at 40 Mc shows a well-resolved quartet (Fig. 4) due to coupling between ortho and meta positions. Assuming negligible cross ring coupling this quartet may be considered as a superposition of two AB cases in the notation of Bernstein, Pople, and Schneider (20). Using their theory one may calculate the absolute values of the spin-coupling constant, J, and chemical shift, δ, between the ortho and meta protons. J is given directly by the separation of the right- or left-hand pair of lines, which is 8.9 c/s, and the separation of the inner pair of lines (7.1 c/s) is given by $2C-J$ where $C = \frac{1}{2}[\delta^2+J^2]^{\frac{1}{2}}$. This gives a value of $\delta = 13.3$ c/s. Values of J, the ortho coupling constant, found by other authors range from 8.2 c/s to 8.6 c/s (20, 21). This value may also be compared with the value of 8.0 ± 0.5 c/s found for

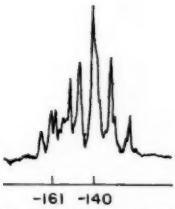

FIG. 5. Spectrum of aromatic protons of *p*-anisyl diphenylmethyl cation at 60 Mc.

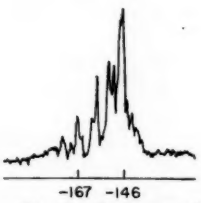

FIG. 6. Spectrum of aromatic protons of *p-tert*-butylphenyl diphenylmethyl cation at 60 Mc.

protonated dianisylethylene in sulphuric acid. In the case of the tri-*p*-tolyl ion, this quartet is not resolved even at 60 Mc, and the aromatic protons give rise to only a single sharp peak.

The spectra of the aromatic protons of the *p*-anisyl diphenylmethyl and *p-tert*-butylphenyl diphenylmethyl cations were recorded at 60 Mc as shown in Figs. 5 and 6. A well-resolved fine structure was observed but no definite assignments could be made.

The meta-methyl-substituted ions illustrate an interesting point. Table II shows that a meta methyl substituent shields the ring protons to a greater extent than does a para methyl substituent. This is because the electron-donating properties of the methyl group function to donate negative charge to the electron-deficient ring but, because of its meta location, it is unable to interact directly by resonance with the central electron-deficient carbon atom.

Di-p-anisylethylene in Sulphuric Acid

The N.M.R. spectrum of 1,1-di-*p*-anisylethylene in sulphuric acid was recorded in connection with other work and its similarity to that of the triarylmethyl cations warrants its being discussed briefly here. The spectrum of the resulting carbonium ion is shown in Fig. 7. Thanks are due to Mr. A. L. Gatzke for the preparation of this compound.

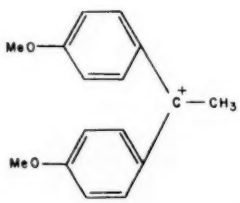

II

Like the tri-*p*-anisylmethyl cation there is a well-resolved quartet due to the coupled ortho and meta protons, the chemical shift between the two halves of the quartet being 32 c/s. The methoxy protons and the methyl protons are at higher field but the high degree of positive charge in the latter, which are in a hyperconjugating position, is reflected in the large shift to low field (−85 c/s) from the cyclohexane marker.

It is of interest to note that the N.M.R. and visible spectra of this compound in trifluoroacetic acid – anhydride solvent is quite different to that in sulphuric acid. Anomalous visible spectra in carboxylic acid solvents for this compound have previously been observed by other workers (8, 22, 23).

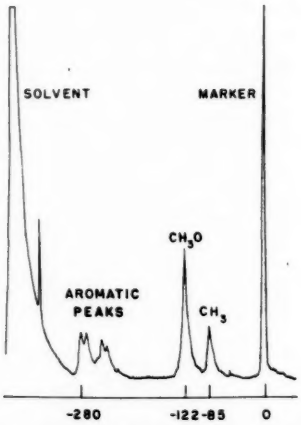

FIG. 7. Spectrum of 1,1-di-*p*-anisylethylene in sulphuric acid at 40 Mc.

ACKNOWLEDGMENTS

The authors wish to thank Dr. K. B. Wiberg and Mr. B. Nist of the University of Washington for allowing us to use their 60-Mc Varian spectrometer. Helpful discussions with Dr. C. Reid are also acknowledged.

Two of us (R.B.M. and T.M.C.) wish to thank the National Research Council for the fellowship and studentship.

REFERENCES

1. DENO, N. C., JARUZELSKI, J. J., and SCHRIESHEIM, A. J. Am. Chem. Soc. **77**, 3044 (1955).
2. SCHUBERT, W. M., ROBINS, J., and HAUN, J. L. J. Am. Chem. Soc. **79**, 910 (1957).
3. DENO, N. C., JARUZELSKI, J. J., and SCHRIESHEIM, A. J. Org. Chem. **19**, 155 (1954).
4. SHARP, D. W. A. and SHEPPARD, N. J. Chem. Soc. 674 (1957).
5. MASON, S. F. *In* Gray, G. W. Steric effects in conjugated systems. Butterworth Scientific Publications, London. 1958. p. 52.
6. MACLEAN, C., VAN DER WAALS, J. H., and MACKOR, E. L. Mol. Phys. **1**, 274 (1958).
7. LETO, J. R., COTTON, F. A., and WAUGH, J. S. Nature, **180**, 978 (1957).
8. GATZKE, A. L. M.Sc. Thesis, University of British Columbia, Vancouver, British Columbia. 1959.
9. WITTIG, G. and CLAUSNIZER, R. Ann. **588**, 145 (1954).
10. MUSTAFA, A., ASKER, W., and HISHMAT, O. H. J. Am. Chem. Soc. **77**, 5127 (1955).
11. BARTLETT, P. D. and JONES, J. E. J. Am. Chem. Soc. **65**, 1837 (1942).
12. BRAND, K., GABEL, W., and ROSENKRANZ, E. Ber. B, **70**, 296 (1937).
13. FABER, A. C. and NAUTA, W. T. Rec. trav. chim. **61**, 469 (1942).
14. MARVEL, C. S., WHITSON, J., and JOHNSTON, H. W. J. Am. Chem. Soc. **66**, 415 (1944).
15. GOMBERG, M. Chem. Revs. **1**, 91 (1924).
16. MARVEL, C. S., MEULLER, M. B., HIMEL, C. M., and KAPLAN, J. F. J. Am. Chem. Soc. **61**, 2771 (1939).
17. CORIO, P. L. and DAILEY, B. P. J. Am. Chem. Soc. **78**, 3043 (1956).
18. HAMMETT, L. P. Physical organic chemistry. McGraw-Hill Book Co., Inc., New York. 1940. p. 184. TAFT, R. W. J. Am. Chem. Soc. **79**, 1045 (1957).
19. POPLE, J. A. J. Phys. Chem. **61**, 6 (1957).
20. BERNSTEIN, H. J., SCHNEIDER, W. G., and POPLE, J. A. Can. J. Chem. **35**, 65 (1957).
21. POPLE, J. A., SCHNEIDER, W. G., and BERNSTEIN, H. J. Can. J. Chem. **35**, 1060 (1957).
22. EVANS, A. G., JONES, N., JONES, P. M. S., and THOMAS, J. H. J. Chem. Soc. 2757 (1956).
23. EVANS, A. G., JONES, P. M. S., and THOMAS, J. H. J. Chem. Soc. 104 (1957).

THE SYSTEM Li^+–Na^+–K^+–SO_4^{--} AND WATER, AT 25.0° C[1]

A. N. CAMPBELL AND E. M. KARTZMARK

ABSTRACT

The above system is a further stage in the study of the five-component system, containing the radicals Li_2, Na_2, K_2, Cl_2, SO_4, and water. The double salts occurring are $Li_2SO_4 \cdot K_2SO_4$ and $3K_2SO_4 \cdot Na_2SO_4$: no ternary salt is formed.

This paper is the fourth instalment of our study of the five-component system containing the radicals Li_2, Na_2, K_2, Cl_2, SO_4, and water, at 25.0° C. So far as we are aware, this is the first complete study which has been made of a five-component system of this type. The work has now been in progress for 4 years: a bibliography is given in references 1 and 2.

According to the Jänecke method of graphic representation the finished study will be represented by a solid model within an equilateral triangular pyramid. All the surfaces of this model have now been studied, the present study being the final one, that of one of the triangular surfaces. It remains only to study the interior of the solid model.

Turning to the present study, the component ternary systems are: (*a*) Li_2SO_4–Na_2SO_4–H_2O; (*b*) Na_2SO_4–K_2SO_4–H_2O; (*c*) Li_2SO_4–K_2SO_4–H_2O. Systems (*a*) and (*c*) have been studied by us and system (*b*) is well known. We have shown (2) that in system (*c*) the double salt $Li_2SO_4 \cdot K_2SO_4$ exists in contact with solution at 25° C, though the solution is not congruently saturating. In system (*a*) no double salt forms (at 25° C) but there is an extensive series of solid solutions of lithium sulphate in sodium sulphate. In system (*b*), the well-known glaserite or Penny's salt ($3K_2SO_4 \cdot Na_2SO_4$) occurs as the end member of a series of solid solutions of potassium sulphate in sodium sulphate.

In the present quaternary system, there is the possibility that ternary salts, containing all three metallic ions, may occur, in addition to the above named double salts, but no such ternary salt has been found.

EXPERIMENTAL

The technique is simple and has been described frequently (1, 2). In previous papers we have referred to the extreme difficulty of determining sulphate radical in the presence of alkalis and we have been forced to such expedients as determining density and viscosity, in order to analyze the systems, procedures which call for extreme experimental accuracy (because of the slight differences in physical property for the different ions), notably in the determination of density. For the present study we turned with relief to the flame photometer as a means of analysis for alkali metals. We used a Beckmann DU instrument with flame photometer attachment. Since this instrument is dependent on constancy of flame intensity, it must be calibrated afresh for each analysis. Standard solutions, containing from 10 to 100 parts per million of lithium sulphate, sodium sulphate, or potassium sulphate, respectively, were made up and preserved in plastic containers. Before each analysis, a curve of instrument reading versus content of given salt was determined experimentally for each salt. The reading for the unknown, in the appropriate region of the spectrum, then gives the salt content in parts per million. Since the unknown always contained the three salts simultaneously present, the possibility existed that

[1]*Manuscript received May 7, 1959.*
Contribution from the Chemistry Department, University of Manitoba, Winnipeg, Manitoba.

TABLE I

Solubilities in the quaternary system at 25° C

Liquid phase in mole %			Nature of solid phase	Moles water/ mole salt
Li_2SO_4	Na_2SO_4	K_2SO_4		
100	—	—	$Li_2SO_4 \cdot H_2O$	17.8
74.6	25.4	—	$Li_2SO_4 \cdot H_2O$ + s.s. of Li_2SO_4 in Na_2SO_4†	13.7
29.0	71.0	—	Na_2SO_4 anhyd. + $Na_2SO_4 \cdot 10H_2O$	18.0
—	100	—	$Na_2SO_4 \cdot 10H_2O$	28.4
95.0	—	5.0	$Li_2SO_4 \cdot H_2O$ + $Li_2SO_4 \cdot K_2SO_4$	15.4
63.0	—	37.0	$Li_2SO_4 \cdot K_2SO_4$ + K_2SO_4	27.5
—*	—	100	K_2SO_4	80.8
—*	77.3	22.7	$Na_2SO_4 \cdot 10H_2O$ + $Na_2SO_4 \cdot 3K_2SO_4$	22.4
—*	37.5	62.5	K_2SO_4 + $Na_2SO_4 \cdot 3K_2SO_4$	44.4
77.0	21.0	2.0	$Li_2SO_4 \cdot H_2O$ + s.s. of Li_2SO_4 in Na_2SO_4	15.8
88.5	4.5	7.0	$Li_2SO_4 \cdot H_2O$ + $Li_2SO_4 \cdot K_2SO_4$	16.1
85.0	10.0	5.0	$Li_2SO_4 \cdot H_2O$ + $Li_2SO_4 \cdot K_2SO_4$ + s.s. of Li_2SO_4 in Na_2SO_4	15.7
83.0	12.0	5.0	$Li_2SO_4 \cdot H_2O$ + s.s. of Li_2SO_4 in Na_2SO_4	16.5
84.9	9.1	6.0	$Li_2SO_4 \cdot H_2O$ + $Li_2SO_4 \cdot K_2SO_4$	16.0
17.2	71.9	10.9	Na_2SO_4 anhyd. + $Na_2SO_4 \cdot 10H_2O$	17.1
13.0	72.5	14.5	Na_2SO_4 anhyd. + $Na_2SO_4 \cdot 10H_2O$ + $Na_2SO_4 \cdot 3K_2SO_4$	18.9
11.7	73.5	14.8	$Na_2SO_4 \cdot 10H_2O$ + $Na_2SO_4 \cdot 3K_2SO_4$	17.7
27.8	58.7	13.5	Na_2SO_4 anhyd. + $Na_2SO_4 \cdot 3K_2SO_4$	15.6
49.5	20.1	30.4	$Li_2SO_4 \cdot K_2SO_4$ + K_2SO_4	23.0
47.3	22.1	30.7	$Na_2SO_4 \cdot 3K_2SO_4$ + $Li_2SO_4 \cdot K_2SO_4$ + K_2SO_4	22.5
27.0	26.0	47.0	$Na_2SO_4 \cdot 3K_2SO_4$ + K_2SO_4	34.2
44.0	21.0	35.0	$Na_2SO_4 \cdot 3K_2SO_4$ + K_2SO_4	25.7
46.0	26.0	28.0	$Na_2SO_4 \cdot 3K_2SO_4$ + $Li_2SO_4 \cdot K_2SO_4$	22.2
29.8	56.8	13.4	Na_2SO_4 anhyd. + $Na_2SO_4 \cdot 3K_2SO_4$	15.1
48.0	46.0	6.0	s.s. of Li_2SO_4 in Na_2SO_4 + $Li_2SO_4 \cdot K_2SO_4$	16.0
53.0	42.0	5.0	s.s. of Li_2SO_4 in Na_2SO_4 + $Li_2SO_4 \cdot K_2SO_4$	16.5
67.0	27.0	6.0	s.s. of Li_2SO_4 in Na_2SO_4 + $Li_2SO_4 \cdot K_2SO_4$	16.7
45.0	32.0	23.0	$Li_2SO_4 \cdot K_2SO_4$ + $Na_2SO_4 \cdot 3K_2SO_4$	19.2
44.0	37.0	19.0	$Li_2SO_4 \cdot K_2SO_4$ + $Na_2SO_4 \cdot 3K_2SO_4$	17.6
42.0	43.0	15.0	$Li_2SO_4 \cdot K_2SO_4$ + $Na_2SO_4 \cdot 3K_2SO_4$	17.2
38.0	53.0	9.0	Na_2SO_4 anhyd. + $Li_2SO_4 \cdot K_2SO_4$ + $Na_2SO_4 \cdot 3K_2SO_4$	16.9

*Reference 3.
†s.s. = solid solution.

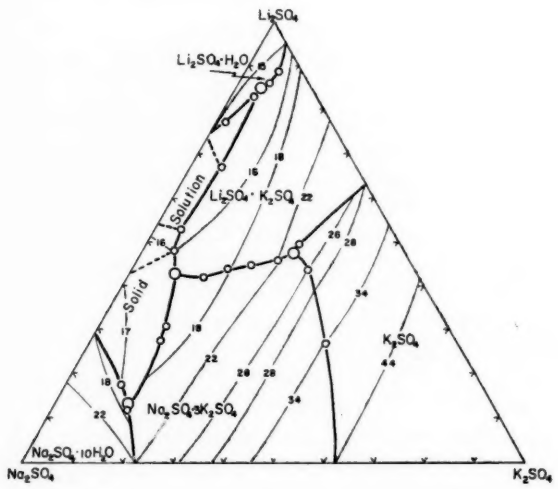

FIG. 1.

one salt might interfere with another, but we convinced ourselves by the analysis of numerous mixtures of known composition that this was not so here. The accuracy is not high, ±1% at best, but, within these limits, the results are completely dependable. In a study which involved the Schreinemakers' method of the "wet rest", this accuracy would scarcely be good enough but it was sufficient for the present study.

RESULTS

The numerical results are given in Table I and represented graphically in Fig. 1. The isohydrores (lines of equal water content) are of necessity, as in all such studies, to some extent hypothetical, at least in their curvature, but such curves are most instructive in evaporation studies.

DISCUSSION

The dotted lines in the area marked "solid solution" (which would normally be the area of anhydrous sodium sulphate) give a rough indication of the composition of the solid phase (solid solution of sodium sulphate in lithium sulphate). Figure 1 also shows the absence of any ternary salt; all the solid phases are to be found already in the component ternary systems. The main areas of the equilibrium diagram are those of K_2SO_4, $K_2SO_4 \cdot Li_2SO_4$, and $3K_2SO_4 \cdot Na_2SO_4$.

REFERENCES

1. CAMPBELL, A. N. and KARTZMARK, E. M. Can. J. Chem. **34**, 672 (1956). CAMPBELL, A. N. KARTZMARK, E. M., and LOVERING, E. G. Can. J. Chem. **36**, 1511 (1958).
2. CAMPBELL, A. N. and KARTZMARK, E. M. Can. J. Chem. **36**, 171 (1958).
3. HAMID M. A. J. Chem. Soc. 199 (1926).

THE REACTION OF SULPHURYL CHLORIDE WITH GLYCOSIDES AND SUGAR ALCOHOLS. PART I[1]

P. D. Bragg, J. K. N. Jones, and J. C. Turner

ABSTRACT

The reaction of sulphuryl chloride with methyl α-D-glucopyranoside, methyl 4,6-*O*-benzylidene-α-D-glucoside, methyl β-D-arabinopyranoside, D-mannitol, 2,5-*O*-methylene-D-mannitol, dulcitol, and sucrose is described.

INTRODUCTION

Helferich and his co-workers in a series of papers (1, 2, 3) described the action of sulphuryl chloride on methyl α- and methyl β-D-glucopyranoside, mannitol, and trehalose. They isolated crystalline products in which the hydroxyl groups had either been replaced by chlorine atoms or bridged by cyclic sulphate groups. The compound derived from methyl α-D-glucopyranoside was shown to contain 2 chlorine atoms and a cyclic sulphate group (1). The cyclic sulphate ring could be opened by treatment with base, and the sulphate group so formed hydrolyzed with hydrochloric or sulphuric acid to yield a dichloro-dideoxy hexose (2).

In the present work, this reaction was applied to glycosides and hexitols, and an attempt was made to determine the structure of the desulphated chloro-sugars.

The dichloro-dideoxy hexose from methyl α-D-glucopyranoside was prepared by Helferich's method (1). On periodate oxidation this compound (I) in 24 hours consumed 2 moles periodate and liberated 2 moles of formic acid.

Although all the periodate was consumed rapidly the second molecule of acid was liberated more slowly suggesting that hydrolysis of the formyl ester (II) was occurring. These results are only consistent with I being 4,6-dichloro-4,6-dideoxy hexose. Periodate oxidation of the methyl glycoside of I (0.87 mole periodate; 26 hours) substantiated this conclusion. Helferich had previously suggested that 1 chlorine atom was at $C_{(6)}$ because of the ease with which it could be removed by alkali (3).

The dichloro-dideoxy hexose was reduced with potassium borohydride. The dichloro-dideoxy hexitol was obtained as an impure syrup which rapidly consumed 1.56 moles periodate liberating 0.73 mole formic acid and formaldehyde (not estimated), which is only consistent with the assignment of chlorine atoms to $C_{(4)}$ and $C_{(6)}$.

The structure of the original compound is therefore probably methyl 4,6-dichloro-4,6-dideoxy-α-D-hexoside 2,3-sulphate. The elimination of the hydroxyl group at $C_{(4)}$ by the chlorine atom might occur with inversion of configuration to give the D-galactose configuration. This problem is now under investigation. The presence of a 2,3-sulphate

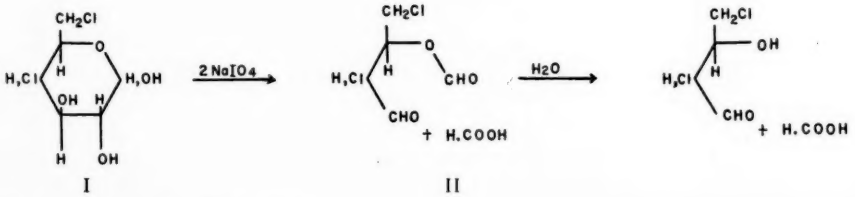

I II

[1]*Manuscript received October 27, 1958.*
Contribution from the Department of Chemistry, Queen's University, Kingston, Ontario.

Can. J. Chem. Vol. 37 (1959)

group was also suggested by the isolation of an analogous methyl 4,6-*O*-benzylidene-α-D-glucoside 2,3-sulphate by the action of sulphuryl chloride on methyl 4,6-*O*-benzylidene-α-D-glucoside.

Hydrolysis of the cyclic sulphate derivative eliminated the methyl glycoside and benzylidene groups and gave glucose only, showing that removal of the sulphate group occurred without inversion of the hydroxyl groups on $C_{(2)}$ and $C_{(3)}$ unless the initial formation of the cyclic ester had also resulted in inversion.

Methyl β-D-arabinopyranoside was converted by sulphuryl chloride to a methyl monochloro-monodeoxy pentoside cyclic sulphate which could be desulphated to yield a monochloro-monodeoxy pentose. The results of periodate oxidation (2 moles periodate consumed with the liberation of 2 moles acid) indicated that the chlorine atom was located on $C_{(4)}$. Periodate oxidation (1.1 moles; 26 hours) of the methyl α-glycoside confirmed this. The monochloro-monodeoxy pentose gave a *p*-nitrophenylosazone without loss of chlorine showing that the chlorine atom was not on $C_{(1)}$ or $C_{(2)}$ of the pentose. The very probable structure of the original compound would therefore be methyl 4-chloro-4-deoxy-β-pentoside 2,3-sulphate.

Both dulcitol and D-mannitol readily give crystalline compounds with sulphuryl chloride and in both cases 4 chlorine atoms and a cyclic sulphate group are introduced. 2,5-*O*-Methylene-D-mannitol gave a trichloro-trideoxy-mono-*O*-methylene hexitol.

The cyclic sulphate ester of the mannitol derivative is very resistant to acid hydrolysis. Very little acetolysis of this compound occurred at 25° C, but appreciable hydrolysis of the sulphate group followed by acetylation occurred at 100° C. Deacetylation of the product then yielded a substance (contaminated with starting material) with a chromatographic mobility consistent with that of a tetrachloro-tetradeoxy hexitol. The impure product consumed 0.77 mole periodate (46 hours) suggesting that the sulphate group in the original compound bridged adjacent hydroxyl groups (presumably on $C_{(3)}$–$C_{(4)}$).

Sucrose yielded a product which appeared to be a mixture of di- and tri-chlorodeoxy sucrose disulphates. The structure of the glucose moiety is similar to that from methyl α-D-glucopyranoside since the same 4,6-dichloro-4,6-dideoxy hexose can be obtained from both. The remaining cyclic sulphate group and chlorine atom are located on the fructose portion of the molecule. The position of these groups was not determined since the vigorous conditions of hydrolysis necessary to cleave the interglycosidic linkage destroyed the fructose moiety, but it is probable by comparison with the anhydrides of sucrose (4), that the sulphate group spans $C_{(3')}$–$C_{(6')}$ or $C_{(1')}$–$C_{(4')}$ with the chlorine atom on $C_{(1')}$ or $C_{(6')}$ respectively.

EXPERIMENTAL

Melting points are uncorrected and were determined on a Kofler microheating stage. Optical rotations were measured at 24° C. All evaporations were carried out under reduced pressure.

General Method

Redistilled sulphuryl chloride (7 ml) was added to a mixture of pyridine (30 ml) and chloroform (100 ml), which had been dried over potassium hydroxide pellets and anhydrous sodium sulphate respectively. The temperature of the solution was maintained at 5° C while the glycoside or hexitol (4 g; dried over phosphoric oxide) was added with vigorous stirring. After 2 hours the reaction mixture was poured into ice water and the chloroform layer separated, well washed with water, and dried (sodium hydrogen carbonate). Concentration afforded a syrup which was decolorized with charcoal if

necessary. Crystallization was spontaneous, but purification by extracting the product into ether was sometimes imperative.

Methyl α-D-Glucopyranoside

With sulphuryl chloride, methyl α-D-glucopyranoside gave long colorless needles (1.8 g) which, recrystallized from ether – light petroleum (40–60° C), had m.p. 104–105° C, $[\alpha]_D$ +140° (*c*, 1.99 in methanol). Analysis: Calc. for $C_7H_{10}O_6Cl_2S$: C, 28.7%, H, 3.4%; Cl, 24.2%; S, 10.9%. Found: C, 28.9%; H, 3.4%; Cl, 24.1%; S, 11.1%.

Methyl Dichloro-dideoxy Hexoside and Dichloro-dideoxy Hexose

The above compound (1.8 g) dissolved in methanol saturated with ammonia at 0° C (50 ml) was kept at room temperature for 24 hours. Concentration gave a partially crystalline syrup which was heated at 100° C for 14 hours with *N* sulphuric acid (50 ml). The acid was neutralized with barium carbonate and the solution deionized by passage through Amberlite IR-120 and Duolite A4 resin columns. The eluate was concentrated to a syrup (0.74 g) which slowly crystallized. An aqueous solution of the syrup was continuously extracted with chloroform. The chloroform extract on evaporation yielded crystals, m.p. 158° C, $[\alpha]_D$ +184° (*c*, 2.1 in water). Analysis: Calc. for $C_7H_{12}O_4Cl_2$: C, 36.3%; H, 5.2%; Cl, 30.7%. Found: C, 36.2%; H, 5.3%; Cl, 31.0%. On concentration of the aqueous solution white needle-shaped crystals were obtained. Recrystallized from ethanol–water, the dichloro-dideoxy hexose had m.p. 183–186° C (decomp.), $[\alpha]_D$ +132° (5 minutes) → 98° (equilibrium; 24 hours) (*c*, 0.69 in methanol). Analysis: Calc. for $C_6H_{10}O_4Cl_2$: C, 33.2%; H, 4.6%. Found: C, 33.6%; H, 4.7%.

The dichloro-dideoxy hexose (115 mg) was reduced for 1 hour with potassium borohydride (365 mg) in water (50 ml). Excess borohydride was destroyed with acetic acid, and after deionization with resin, the major component (R_f 0.56) *n*-butanol:ethanol: water = 3:1:1 was separated as a syrup (47 mg) on paper chromatograms, $[\alpha]_D$ 0° (*c*, 1.0 in water).

Methyl β-D-Arabinoside

Methyl β-D-arabinoside and sulphuryl chloride yielded colorless needles (1.6 g) which, recrystallized from ether – light petroleum (80–100° C), had m.p. 108.5° C, $[\alpha]_D$ −89° (*c*, 0.97 in methanol). Analysis: Calc. for $C_6H_9O_6SCl$: S, 13.1%; Cl, 14.5%. Found: S, 13.3%; Cl, 14.1%.

Methyl Monochloro-monodeoxy Pentoside and Monochloro-monodeoxy Pentose

Both were prepared from the compound derived from methyl β-D-arabinoside by treatment with methanolic ammonia followed by sulphuric acid as described above. The methyl pentoside crystallized as white needles which after recrystallization from ether – light petroleum (b.p. 60–80° C) had m.p. 102–104° C, $[\alpha]_D$ +119° (*c*, 2.25 in water). Analysis: Calc. for $C_6H_{11}O_4Cl$: C, 39.5%; H, 6.0%; Cl, 19.5%. Found: C, 39.6%; H, 6.2%; Cl, 19.8%. Monochloro-monodeoxy pentose had m.p. 128–131° C, $[\alpha]_D$ +57° (10 minutes) → 0° (equilibrium, 6 hours) (*c*, 0.98 in methanol). Analysis: Calc. for $C_5H_9O_4Cl$: C, 35.6%; H, 5.3%. Found: C, 35.8%; H, 5.8%.

The product (95 mg) in 50% acetic acid (2 ml) was added to *p*-nitrophenylhydrazine (0.3 g) in glacial acetic acid (2 ml) and heated at 100° C for 1 hour. Crystals of the *p*-nitrophenylosazone were precipitated. After they were washed with water and ether, they had m.p. 224° C. Analysis: Calc. for $C_{17}H_{17}O_6N_6Cl$: N, 13.7%; Cl, 8.7%. Found: N, 11.7%; Cl, 7.1%.

Methyl 4,6-O-Benzylidene-α-D-glucopyranoside

This reacted with sulphuryl chloride to give long colorless needles (2 g) which slowly darkened over a period of days with liberation of benzaldehyde. When recrystallized

from chloroform – light petroleum it had m.p. 107° C (decomp.). A sodium fusion showed chlorine to be absent from the molecule. Analysis: Calc. for $C_{14}H_{16}O_8S$: S, 9.3%. Found: S, 9.0%. Treatment first with methanolic ammonia and then with sulphuric acid gave chromatographically homogeneous glucose which was characterized as its *p*-nitroanilide derivative, m.p. 186° C, $[\alpha]_D$ +192° (*c*, 0.85 in water).

D-*Mannitol*

With sulphuryl chloride, D-mannitol afforded needle-shaped crystals (1.5 g) which when recrystallized from chloroform – light petroleum had m.p. 105° C, $[\alpha]_D$ +88° (*c*, 2.84 in methanol). Analysis: Calc. for $C_6H_8O_4Cl_4S$: C, 22.6%; H, 2.5%; Cl, 44.7%; S, 10.0%. Found: C, 22.8%; H, 2.8%; Cl, 44.3%; S, 10.4%.

The compound (4.2 g) was heated at 95–100° C for 2½ hours in acetic anhydride (30 ml) and sulphuric acid (1.5 ml). The dark brown solution was poured into ice water, which was then extracted with chloroform. The chloroform extract was washed with an aqueous sodium hydrogen carbonate solution, dried (anhydrous magnesium sulphate), and was concentrated to a syrup. Following decolorization with charcoal, the syrup was deacetylated with sodium methoxide at 5° C. Excess sodium methoxide was removed with carbon dioxide, and after dilution with water, the solution was continuously extracted with ether. Concentration of the ether extract afforded a syrup (0.9 g) which gave a single spot (R_f 0.79) with the periodate–anisidine spray (5) on chromatography in butan-1-ol:ethanol:water (3:1:1) solvent.

Mono-anhydro-trichloro-trideoxy Hexitol

The compound (2.7 g) obtained from mannitol was treated with methanolic ammonia and with sulphuric acid, as previously described, to yield colorless needles (0.6 g) m.p. 102° C, $[\alpha]_D$ 0° (*c*, 0.86 in methanol). Analysis: Calc. for $C_6H_9O_2Cl_3$: C, 32.8%; H, 4.1%; Cl, 48.5%. Found: C, 33.0%; H, 4.1%; Cl, 46.2%.

2,5-O-Methylene-D-*mannitol*

2,5-*O*-Methylene-D-mannitol and sulphuryl chloride yielded a crystalline product (1.1 g); when recrystallized from ethanol–water it had m.p. 116° C and $[\alpha]_D$ −42° (*c*, 1.73 in methanol). Analysis: Calc. for $C_7H_{11}O_3Cl_3$: C, 33.6%; H, 4.4%; Cl, 42.7%. Found: C, 33.7%; H, 4.3%; Cl, 42.9%. In the infrared a hydroxyl peak was obtained. The methylene group was not removed by treatment with *N*-sulphuric acid at 100° C for 5 hours.

Dulcitol

Dulcitol and sulphuryl chloride gave a crystalline product (1.4 g) m.p. 116° C. Analysis: Calc. for $C_6H_8O_4Cl_4S$: C, 22.6%; H, 2.5%; Cl, 44.7%; S, 10.0%. Found: C, 22.6%; H, 2.7%; Cl, 44.3%; S, 10.4%.

Sucrose

Sucrose (4 g) was dissolved in pyridine (80 ml) at the boiling point and the solution then cooled to 5° C. Chloroform (90 ml) was added and the slight precipitate produced was redissolved by the further addition of pyridine (10 ml). Sulphuryl chloride (7 ml) was added dropwise with stirring to the cooled solution (5° C). After 2 hours the liquid was poured into ice water, the chloroform layer washed with water and dried (magnesium sulphate). Concentration gave a syrup (2.9 g), and from a chloroform solution of this the product was precipitated by ether as a pale yellow solid, m.p. 94–99° C. Analysis: Calc. for $C_{12}H_{16}O_{13}S_2Cl_2$: S, 12.7%; Cl, 14.1%. Calc. for $C_{12}H_{15}O_{12}S_2Cl_3$: S, 12.3%; Cl, 20.4%. Found: S, 12.4%; Cl, 16.8%.

Hydrolysis (*N* sulphuric acid, 24 hours) gave a complex mixture of substances but mainly 4,6-dichloro-4,6-dideoxy hexose identical with that derived from methyl α-D-

glucoside. After separation on a cellulose column using *n*-butanol:water (19:1) it had m.p. and mixed m.p. 186° C (decomp.). Calc. for $C_6H_{10}O_4Cl_2$: C, 33.2%; H, 4.6%; Cl, 32.7%. Found: C, 33.4%; H, 4.7%; Cl, 32.6%.

Compounds reacting with the resorcinol spray (ketoses) (6) were largely absent from the hydrolysis mixture.

TABLE I

Substance	Time of oxidation (hours)	Consumption of periodate (mole/molecule)	Acid production (mole/molecule)
Methyl dichloro-dideoxy hexoside	1.08	0.16	
	20	0.79	0.00
	26	0.87	
	43	1.13	0.00
Dichloro-dideoxy hexose	1	1.40	1.14
	4	2.05	1.89
	7	2.05	2.01
	24	2.09	1.96
Dichloro-dideoxy hexitol	1	1.49	
	5	1.56	0.73
	24	1.56	0.73
Methyl monochloro-monodeoxy pentoside	1.08	0.15	
	20	1.01	0.00
	26	1.10	
	43	1.22	0.00
Monochloro-monodeoxy pentose	1	1.62	1.09
	4	1.87	1.42
	7	1.87	1.42
	24	1.93	1.72
Tetrachloro-tetradeoxy hexitol	1	0.46	
	4	0.52	
	23	0.67	0.00
	46	0.77	0.00

Periodate Oxidation of Chloro-sugars

About 25 mg of the substance, accurately weighed, was dissolved in water (50 ml) and 0.3 *M* sodium metaperiodate (2 ml) added. Aliquots were removed at intervals and the consumption of periodate and the production of formic acid measured (7, 8). Dichloro-dideoxy hexitol gave formaldehyde (characterized as the dimedone complex, m.p. 188° C) (9) on periodate oxidation.

Mono-anhydro-trichloro-trideoxy hexitol was not attacked by periodate.

ACKNOWLEDGMENT

Part of this work was supported by the Sugar Research Foundation, Inc., to whom the authors wish to express their thanks.

REFERENCES

1. HELFERICH, B. Ber. **54**, 1082 (1921).
2. HELFERICH, B., LÖWA, A., NIPPE, W., and RIEDEL, H. Ber. **56**, 1083 (1923).
3. HELFERICH, B., SPROEK, G., and BESLER, E. Ber. **58**, 886 (1925).
4. LEMIEUX, R. U. and BARRETTE, J. P. J. Am. Chem. Soc. **80**, 2243 (1958).
5. BRAGG, P. D. and HOUGH, L. J. Chem. Soc. 4050 (1958).
6. HOUGH, L., JONES, J. K. N., and WADMAN, W. H. J. Chem. Soc. 796 (1952).
7. NEUMÜLLER, G. and VASSEUR, E. Arkiv Kemi, **5**, 235 (1953).
8. ANDERSON, D. M. W., GREENWOOD, C. T., and HIRST, E. L. J. Chem. Soc. 225 (1955).
9. BELL, D. J. J. Chem. Soc. 994 (1948).

REACTIONS OF BUTENES AND METHYL BUTENES ON A ZINC OXIDE CATALYST[1]

M. G. HAMPTON[2] AND R. J. CVETANOVIĆ

ABSTRACT

Reactions of butene-1, isobutene, 3-methyl butene-1, and 2-methyl butene-2 on ZnO catalysts have been investigated at 615°. The formation of the observed products is discussed in terms of a sequence of surface processes incorporating dissociation of the bonds in β position to the double bond, with formation of chemisorbed allyl and substituted allyl radicals.

INTRODUCTION

A study of dehydrogenation of butene-1 on semiconducting oxide catalysts between 500 and 650° has been conducted recently in this laboratory (1). The activity and selectivity to butadiene formation of "valency-controlled" ZnO and NiO catalysts were discussed in terms of their electrical properties. Thus, after it was doped with lithia, zinc oxide became inactive, while the catalysts with small additions of gallia, although showing the same activity as pure zinc oxide, were distinctly more selective. An explanation was suggested by assuming an important role in these reactions of "excess" electrons in the *n*-type semiconductors.

The present work has been carried out in an attempt to obtain further information on the mechanism of dehydrogenation on zinc oxide catalysts from a comparative study of the reactions of several structurally related olefins. Zinc oxide containing 1 atom % Ga^{+++} in the lattice was used because of its somewhat greater selectivity (1). The reactions were carried out at 615°.

EXPERIMENTAL

The apparatus used is illustrated in Fig. 1. It consisted of a reactor, circulating pump, boiler, and storage lines. The reactor consisted of a silica tube connected to the rest of the apparatus by pyrex–silica graded seals. The catalyst pellets were placed in a silica spoon as shown. Two leads through tungsten–glass seals were provided for conductivity measurements. Larger flat pellets containing Pt-foil leads were used for conductivity determinations by means of an a-c. bridge. In most of the work small cylindrical pellets of the catalyst ($\frac{1}{8}$ in. × $\frac{1}{8}$ in. × $\frac{1}{8}$ in.) were used. A 14/30 standard joint facilitated catalyst removal and changing. The temperature of the furnace round the reactor was controlled by a chromel–alumel thermocouple placed in a well in the silica tube.

The olefins were introduced to the evacuated 2-liter flask, then mixed with nitrogen to give a total pressure of about 760 mm Hg. The ratio of the olefin to nitrogen was about 1:12 in all experiments. Nitrogen was also let into the reactor system, so that with the water in the boiler boiling vigorously, the total pressure in the reactor section was also about 760 mm. The stopcocks isolating the 2-liter volume from the reaction system could then be opened, and the gases circulated continuously using a reciprocating plunger pump as described by Watson (2). The pumping rate and the volume of the reaction system were such that the gas phase was circulated once in just over 2 minutes. Average run duration was about 30 to 40 minutes, with occasional runs up to 90 minutes. During a run samples of the gas phase were withdrawn at intervals into 50-ml receiving bulbs, and the condensable content frozen out with liquid nitrogen. The permanent

[1]*Manuscript received May 14, 1959.*
Contribution from the Division of Applied Chemistry, National Research Council, Ottawa, Canada.
Issued as N.R.C. No. 5281.
[2]*National Research Council Postdoctorate Fellow 1956–57.*

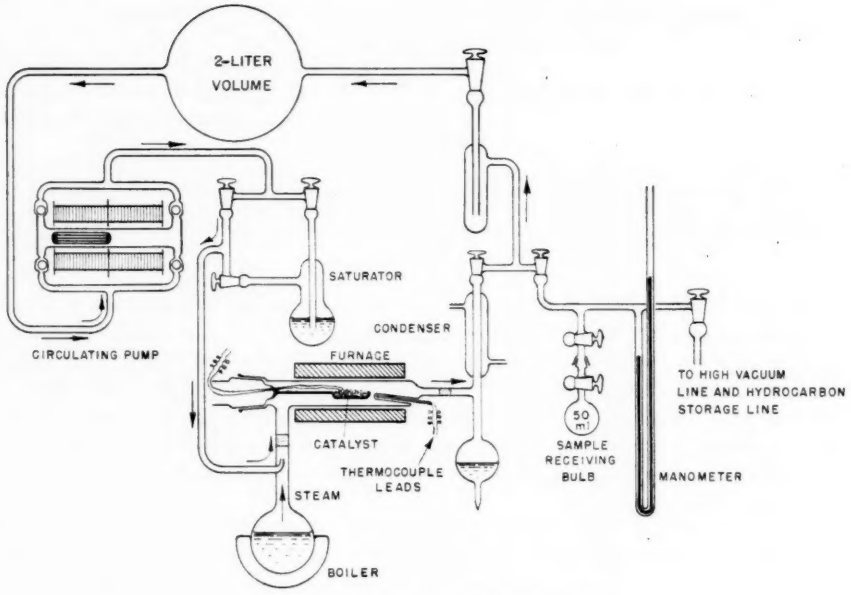

FIG. 1. Diagram of the apparatus.

gases were then pumped away, and the residual samples analyzed by means of a mass spectrometer. Analyses for H_2 and CH_4 in the large excess of non-condensable gas were as a rule not made. To distinguish between certain isomers in the products, gas chromatographic analysis was sometimes used.

Research grade olefins were employed.

RESULTS

Reactions of the following olefins were investigated: butene-1, isobutene, 3-methyl butene-1, and 2-methyl butene-2.

Butene-1

Butene-1 undergoes extensive dehydrogenation, the main products being C_4H_6, C_3H_6, and C_2H_4 in the approximate ratio 2:2:1. The production of butadiene is favored by the presence of moisture, which suppresses side reactions rather than aiding dehydrogenation directly. The results are summarized in Table I. The average dehydrogenation selectivity is about 40% for about 40% decomposition of butene-1.

Isobutene

Isobutene undergoes practically no decomposition and no butadiene is formed. This indicates that no isomerization of the carbon skeleton of the molecule occurs.

3-Methyl Butene-1

3-Methyl butene-1 is very reactive, the main products being C_4H_8 and C_4H_6 in the presence of moisture, that is, the loss of a methyl group is the main reaction. In the presence of oxygen, added to the gas stream, C_5H_8 was the main product, much less C_4H_6 being produced. The presence of oxygen however slowed down the over-all decomposition rate. The results are summarized in Table II.

TABLE I

Dehydrogenation and decomposition of butene-1

Diluting gas	% Reaction* (after 22 min)	Dehydrogenation selectivity, %	Main products†			Catalyst
			Butadiene	Propylene	Ethylene	
Moist N_2	43.4	44.5	14.5	16.0	7.8	ZnO + 1% Ga
Steam + N_2	41.0	41.4	14.8	16.7	7.6	ZnO + 1% Ga
Moist N_2 + 27 mm O_2	40.0	39.0	12.2	12.2	7.9	ZnO + 1% Ga
Dry N_2	62.9	29.6	13.0	21.7	20.0	ZnO + 1% Ga
Steam + N_2	26.0	23.5	5.5	12.3	4.3	Zn metal
Dry N_2	54.1	22.0	11.0	19.6	15.4	Zn metal

*Isomerization is not taken into account in evaluating % reaction.
†Expressed as percentages of the total carbon in the products.

2-Methyl Butene-2

2-Methyl butene-2 produces mainly C_5H_8 and C_4H_8 with only very small amounts of C_4H_6. The results are summarized in Table II. The results show that double-bond isomerization to give 3-methyl butene-1 does not occur, otherwise the products of decomposition of the latter hydrocarbon would also be found. This was confirmed by gas chromatographic analysis.

TABLE II

Dehydrogenation and decomposition of 3-methyl butene-1 and 2-methyl butene-2 on ZnO + 1% Ga

Olefin	Diluting gas	% Reaction* (after 22 min)	Dehydrogenation selectivity, %	Main products†				
				C_5H_8	C_4H_8	C_4H_6	C_3H_6	C_2H_4
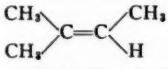 (2-Methyl butene-2)	Steam + N_2	30.0	48.0	13.1	9.4	1.1	3.0	3.0
	Steam + N_2 + 44 mm O_2	42.5	41.2	12.6	8.4	—	9.4	—
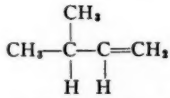 (3-Methyl butene-1)	Steam + N_2	82.8	9.7	5.0	9.0	21.0	11.5	21.5
	Steam + N_2 + 29 mm O_2	56.0	22.1	12.4	10.0	10.2	8.4	8.4

*Isomerization is not taken into account in evaluating % reaction.
†Expressed as percentages of the total carbon in the products.

As the amount of butadiene produced by the decomposition of 2-methyl butene-2 was very small even after about 20 recycles, it appeared that the butene produced in this reaction was mainly the unreactive isobutene. Gas chromatographic analysis of the C_4H_8 fraction showed that the butene consisted of 75% isobutene, 25% *trans*-butene-2, and no *cis*-butene-2 or butene-1.

DISCUSSION

The processes studied in the present work involve dissociation of C—H and C—C bonds at the surface of the catalyst. In general C—C bonds in hydrocarbons are considerably weaker than C—H bonds and this factor alone would favor cracking over dehydrogenation. Selectivity to dehydrogenation is in general determined by the ability of a particular catalyst to dissociate preferentially the C—H bonds. This in general

depends not only on the properties of the catalyst but also on the reaction conditions, such as temperature, contact time, etc. The present experiments were carried out at a single temperature and under conditions which might have favored the cracking processes and somewhat exaggerated their importance. Thus, over a period of time there was some accumulation of metallic zinc on the colder parts of the reaction vessel. For these reasons some of the results were independently checked (3) under similar conditions but with certain additional precautions. The ratio of the dead volume to the catalyst volume in the reaction zone was also reduced. Some differences were observed, particularly a tendency for reduction of cracking relative to dehydrogenation. In the case of 2-methyl butene-2, for example, only isoprene and 2-methyl butene-1 were formed. The main features of the reactions, however, remained very similar. The present results will, therefore, be discussed as obtained under the particular experimental conditions employed. Further study of these processes on the same and some other catalysts at various temperatures is in progress.

The reactions of the individual olefins studied show some characteristic differences. It is known from infrared studies of chemisorbed olefinic hydrocarbons (4) that there are under certain conditions and on some metals at least three and perhaps more than three points of contact (with the necessary corresponding dissociative chemisorption of hydrogen atoms). On hydrogenation–dehydrogenation catalysts the processes of dissociative and associative chemisorption, dehydrogenation and hydrogenation, and of desorption with isomerization or polymerization, are closely related. The predominance of one or the other of these processes depends on the surface concentrations of adsorbed species (in particular that of hydrogen) and on the rates of their formation by adsorption and of their mutual interactions and desorption, both of which are functions of temperature and the nature of the catalyst. The extent of dissociative "stripping" of hydrogen atoms and of the number of contacts with the surface may, therefore, vary widely with the conditions. The kinetic differences observed in the present work should be contrasted with the identical infrared spectra of chemisorbed isomeric *n*-hexenes (4). The adsorbed complexes in the case of 3-methyl butene-1 and 3-methyl butene-2, for example, cannot be identical under conditions of the present work.

In order to explain in a consistent manner the products of dehydrogenation and isomerization observed in the present work a sequence of dissociative processes, following energetically favorable paths, is postulated. This incorporates dissociative chemisorption of the weak C—C and C—H bonds in β position to the double bonds. On the present catalyst at 615° C the weaker β C—C bonds appear to be broken more readily than the stronger β C—H bonds, although this may vary with the type of catalyst used and the temperature. Thus, in the case of butene-1 the breakage of β C—H and β C—C bonds may lead to the formation of butadiene and propylene, respectively. These two compounds are formed in approximately equal amounts in spite of the fact that there are two β C—H bonds and only one β C—C bond indicating that the latter break more readily. In 3-methyl butene-1 there are two β C—C bonds and only one β C—H bond and the reaction involves predominantly cracking to lower hydrocarbons, with butadiene as the main product. The presence of two weak β C—C bonds also explains the high reactivity of this compound. On the other hand, 2-methyl butene-2 possesses no β C—C bonds but only the stronger β C—H bonds, and is consequently much less reactive and direct dehydrogenation is the main reaction. The very low reactivity of isobutene can be partly explained in the same manner, but the main factor appears to be that a conjugated system of double bonds to form C_4H_6 is impossible without rearrangement to a straight chain carbon skeleton. As a result any dissociative chemisorption is eventually

followed by recombination with the initially dissociated H atoms to regenerate isobutene. The dependence of the over-all reactivity under comparable conditions and of the selectivity to dehydrogenation of these olefins on the number of β C—C and β C—H bonds is shown in Table III.

TABLE III

Comparison of the reactivity and selectivity to dehydrogenation with the number of β C—C and β C—H bonds in the olefins

Olefin	% Reaction* (after 22 min)	Dehydrogenation selectivity,* %	Number of β C—C bonds	Number of β C—H bonds
CH_3 CH_3 >C=CH_2	Small	—	None	6
CH_3 CH_3 >C=C< CH_3 H	30.0	48.0	None	9
$CH_3 \cdot CH_2 \cdot CH{=}CH_2$	41.0	41.4	1	2
CH_3 CH_2 >CH·CH=CH_2	82.8	9.7	2	1

*Isomerization is not taken into account in evaluating % reaction.

The dissociation of the bonds in β position to the double bond may constitute the initial step in the catalytic process (a purely dissociative mechanism), or the dissociation may be preceded by an initial interaction of the catalyst with the double bond (a combined associative–dissociative mechanism). The two possibilities are in many respects very similar and are difficult to distinguish experimentally. Both lead to the formation of chemisorbed allyl or substituted allyl radicals. In the purely dissociative mechanism the double-bond shift can be visualized as occurring through a 1,3 switch in the position of attachment of the allylic radical to the surface, and the dissociative process can then be further propagated through the breakage of bonds β to the shifted double bond, with formation of dienes. Some energetic restrictions have to be imposed to accommodate, for example, the lack of isomerization of 3-methyl butene-2 to 3-methyl butene-1.

In the combined associative–dissociative mechanism the energetic restrictions can be introduced by assuming an "orientation" in the initial interaction of the catalyst with the olefin. It can be assumed that (*a*) the initial attachment to the surface takes place at the "less-substituted" of the two carbon atoms of the olefinic double bond, (*b*) a C—H or a C—C bond in β position to the original double bond is broken and a new double bond is formed, (*c*) if there are C—H (or C—C) bonds in β position to the new double bond, these may be broken in turn and dienes formed, (*d*) alternatively and simultaneously recombination may take place with chemisorbed H atoms to regenerate the olefin but with the double bond shifted one position. This is represented for the olefins of interest in connection with the present work in the following scheme.

Isobutene

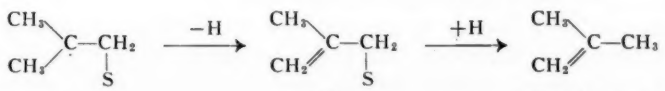

(A) (isobutene)

Butene-1

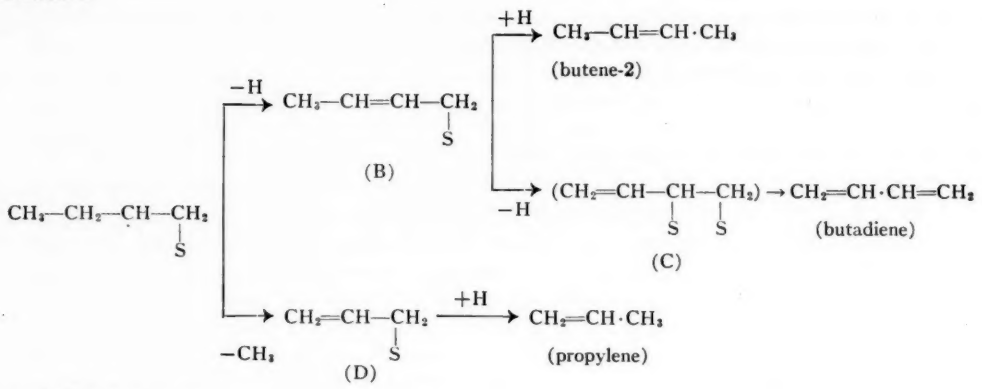

2-Methyl Butene-2

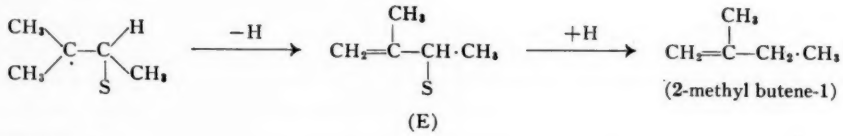

(E)

2-Methyl Butene-1

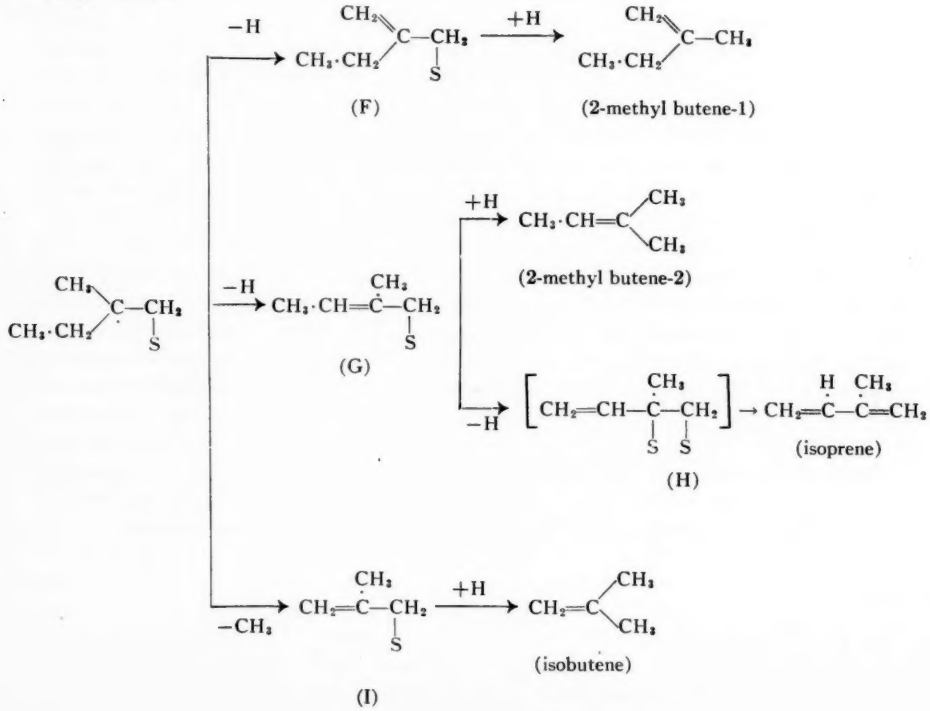

(I)

3-Methyl Butene-1

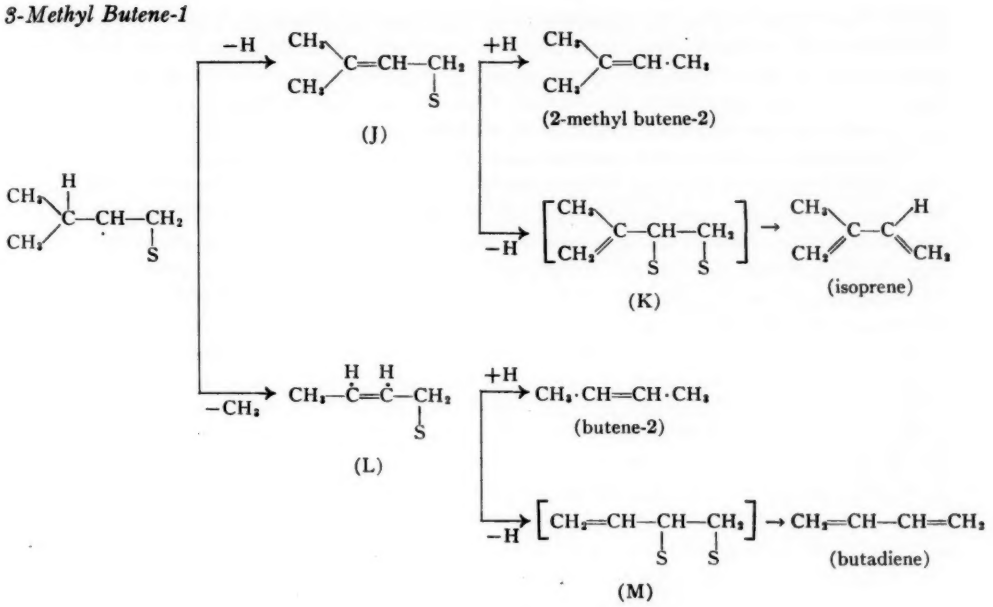

The products predicted in this scheme for various olefins by consistent application of the mechanism summarized in the four points given above agree well with the observed products if, for the moment, the formation of the cracking products ethylene and propylene is disregarded in most cases. Thus, no isomerization of 2-methyl butene-2 to 3-methyl butene-1 is predicted, although the double bond should shift in the opposite direction to form 2-methyl butene-1. This last compound should then produce isoprene and isobutene, which are the main products formed. No butadiene is predicted nor is it formed to any extent. On the other hand, in the case of 3-methyl butene-1, isoprene, butadiene, and butene-2 (but only a trace of butene-1 or isobutene (3)) are all formed in substantial amounts. Furthermore, the primary isomerization product is 2-methyl butene-2, as predicted, rather than 2-methyl butene-1 (3).

In the proposed scheme of reactions no cracking into ethylene and propylene (with one exception) is considered. This type of cracking can be formally explained in a consistent manner by assuming that in the intermediates (B), (G), (J), and (L) the incipient new double bond may break. In the case of the intermediates such as (A), (D), etc. where an analogous split would liberate CH_2, this cracking probably does not occur to any extent. Thus, isobutene is stable, 3-methyl butene-1 forms large amounts of propylene and ethylene, while 2-methyl butene-2 forms very little of these compounds.

The dissociative and associative mechanisms of olefin chemisorption have been the subject of numerous studies and discussions. The difficulty of unambiguous differentiation between the two (and the "hydrogen-switch" mechanism) is well recognized (5) .The number of points of contact indicated for the complexes (A), (B), etc. and their positions in the olefin molecules are necessarily arbitrary. In the case of the complexes (C, H, K, M) preceding dienes the formal application of the associative mechanism leads to 1,2-diadsorbed species with a double bond in 3 position, as shown in the above scheme. The

purely dissociative mechanism discussed earlier, on the other hand, leads to 1,4-diadsorbed molecules with a double bond in 3 position. Formation of transitory double bonds in chemisorbed hydrocarbons, somewhat similar though not identical with those depicted here, was recently postulated by Burwell *et al.* (6) in order to explain racemization of (+)3-methylhexane occurring concurrently with H—D exchange on some metal surfaces.

The condition of the catalytic surface appears to play an important role in determining the relative extents of cracking, dehydrogenation, and isomerization. Thus in the reaction of butene-1 over-all reaction increased but the amount of butadiene formed remained unaltered in the absence of moisture, as shown in Table I. The presence of moisture seems to be essential in suppressing the cracking. The role of moisture may be to prevent the exposure of the Zn atoms by covering the surface with hydroxyl groups. The promotion of cracking by Zn is perhaps due to the relatively strong bond between this metal and CH_3 (7), which is stronger than the corresponding bond with hydrogen.

The sensitivity of the catalytic surface to the ambient atmosphere reflected itself in a strong increase in conductivity, almost to that of metallic zinc as soon as any hydrocarbon was admitted to the system. This held true even when oxygen was present in the gas phase, in spite of the normally observed decrease in conductivity of *n*-type semiconductors as the partial pressure of oxygen is increased.

Under dry conditions appreciable quantities of benzene (up to 14% after 35 to 40 recycles) were formed from butene-1. While the mechanism of formation of benzene is not understood, it is likely that it results from recombination of acetylenic residues. A mixture of butadiene and ethylene failed to yield any benzene under similar reaction conditions.

ACKNOWLEDGMENTS

The authors are thankful to Dr. A. W. Tickner for mass spectrometer analyses and to the Analytical Section of this Division for several gas chromatographic analyses.

REFERENCES

1. Rowlinson, H. C. and Cvetanović, R. J. Advances in Catalysis, **9**, 243 (1957).
2. Watson, J. S. Can. J. Technol. **34**, 373 (1956).
3. Foster, N. F., Barker, G. R., and Cvetanović, R. J. Unpublished results.
4. Eischens, R. P. and Pliskin, W. A. Advances in Catalysis, **10**, 1 (1958).
5. Condon, F. E. Catalysis. *Edited by* P. H. Emmett. Vol. 6. Reinhold Publishing Corp., New York. 1958. Chap. 2.
6. Burwell, R. L., Jr., Shim, B. K. C., and Rowlinson, H. C. J. Am. Chem. Soc. **79**, 5142 (1957).
7. Price, S. J. W. and Trotman-Dickenson, A. F. Trans. Faraday Soc. **53**, 1208 (1957).

OXYMERCURATION OF Δ^5-[2,2,2]-BICYCLOÖCTENE[1]

D. D. K. Chiu and George F Wright

ABSTRACT

It has now been shown that an earlier assignment of configuration in which 1,4-↑↑-ethylene-Δ^5-cyclohexenedicarboxylic acids and their derivatives were presumed to form with mercuric salts 5-↓-hydroxy-6-↓-anionomercuri-1,4-↑↑-ethylenecyclohexanedicarboxylic acid derivatives is incorrect. Instead 5-↓-hydroxy-6-↑-anionomercuri-1,4-↑↑-ethylenecyclohexanedicarboxylic acid derivatives are formed, similarly with the homologous 5-↓-hydroxy-6-↑-anionomercuri-1,4-methylenecyclohexane-2,3-dicarboxylic acid derivatives. This similarity is exemplified by comparable dipole moments. The exception is 5-↓-hydroxy-6-↓-chloromercuri-1,4-↑↑-methylenecyclohexane-2,3-↓↓-dicarboxylic acid, γ-lactone, which has a configuration opposite to all of the others of these series having boat-type cyclohexane ring conformations. The exception is attributed to steric effects.

The oxymercuration of Δ^5-[2,2,2]-bicycloöctene has been reported and the stereochemistry has been specified (1). It has now been proved that this configurational assignment is incorrect. The error may be summarized in terms of two formulae reproduced here, together with their identifying numbers, from page 719 of the previous report (1).

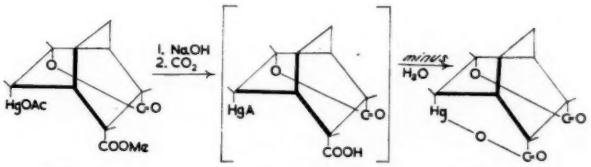

XXI XIII (A=OH) XXIV

According to the statement of McNeely *et al.* (1), the structure of 2-↓-carbomethoxy-5-↓-hydroxy-6-↓-acetoxymercuri-1,4-↑↑-ethylenecyclohexane-3-↓-carboxylic acid, γ-lactone (XXI), was proved by its careful saponification to 5-↓-hydroxy-*anhydro*-[6-↓-hydroxymercuri-2-↓-carboxy]-1,4-↑↑-ethylenecyclohexane-3-↓-carboxylic acid, γ-lactone (XXIV), the molecular weight of which was demonstrated cryoscopically in diphenylmercury. It will be shown that McNeely *et al.* did not have XXIV at all, but, instead, an hydroxymercurial diastereomeric with XIII (A = OH) which was contaminated with its chloromercurial. The content of this mixture has now been shown by a critical study of the X-ray diffraction pattern (1) of what McNeely *et al.* thought to be XXIV.

During the present investigation it has been found that the same dicarboxylic acid, γ-lactone, may be obtained by oxymercuration of 1,4-ethylene-Δ^5-cyclohexene-2,3-↓↓-dicarboxylic anhydride (I) as was formerly obtained from dimethyl 1,4-↑↑-ethylene-Δ^5-cyclohexene-2,3-↓↓-dicarboxylate. The anhydride seems to survive as such in aqueous media. However, a mercuric salt is formed by addition of mercuric chloride to the aqueous solution of the anhydride. Oxymercuration occurs very rapidly in this acidic system, and neutralization is required only to avoid an equilibrium due to the reverse reaction, deoxymercuration. By analogy with the oxymercuration reactions of the 1,4-↑↑-methylene-

[1]*Manuscript received April 8, 1959.*
Contribution from the Department of Chemistry, University of Toronto, Toronto, Ontario, Canada.

Δ^5-cyclohexene system (2) the reaction with the homologue, I, should be acid-catalyzed and should lead to a ↑↓ (*trans*) configuration of the oxy and mercuri addends. Then the product is 5-↓-hydroxy-6-↑-chloromercuri-1,4-↑↑-methylenecyclohexane-2,3-↓↓-dicarboxylic acid, γ-lactone (II), unless lactonization has occurred with inversion.

A re-examination of the oxymercuration of dimethyl 1,4-ethylene-Δ^5-cyclohexene-2,3-↓↓-dicarboxylate (III) shows that inversion during lactonization is very unlikely. The product is clearly dimethyl 5-↓-hydroxy-6-↑-acetoxymercuri-1,4-↑↑-ethylenecyclohexane-2,3-↓↓-dicarboxylate (IV). However, this substance (m.p. 136–137°) is quite unstable. Methanol is eliminated during crystallization and especially at the melting point, whereupon resolidification occurs. The remainder after loss of methanol melts at 188–189°, and is 2-↓-carbomethoxy-5-↓-hydroxy-6-↑-acetoxymercuri-1,4-↑↑-ethylenecyclohexane-3-↓-carboxylic acid, γ-lactone (V). This substance (reported previously (1) as having acetoxymercuri in the ↓ configuration) is thus formed under conditions where inversion is unlikely.

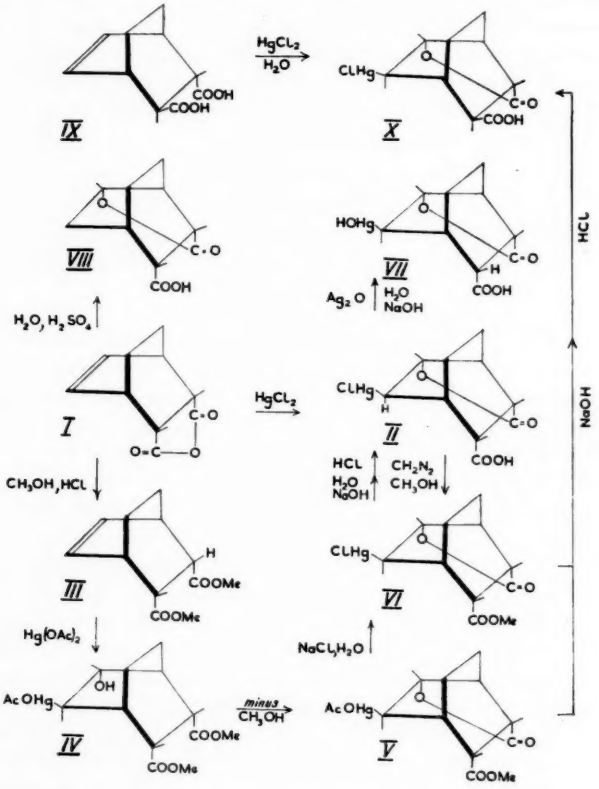

Treatment of V with aqueous sodium chloride converts it to 2-↓-carbomethoxy-5-↓-hydroxy-6-↑-chloromercuri-1,4-↑↑-ethylenecyclohexane-3-↓-carboxylic acid, γ-lactone (VI). This ester may be saponified by use of the stoichiometric quantity of 10% alkali to the acid identical with II. Therefore, it would seem that the anhydride (I) and the ester (III) were oxymercurated to the same product unless some rearrangement occurred during the saponification.

In order to eliminate this possibility we have converted the acid (II) to the ester (VI) by treatment with diazomethane in diethyl ether – methanol. Although this reagent attacks oxymercurials vigorously, forming chloromethylmercuric chloride (3), the esterification may be accomplished in fair yield at a reaction temperature of −80°. The product is identical with the ester (VI), thus precluding rearrangement during the saponification of VI.

When a chloromercurial such as II is treated with alkali the hydroxymercurial, 5-↓-hydroxy-6-↑-hydroxymercuri-1,4-↑↑-ethylenecyclohexane-2,3-dicarboxylic acid, γ-lactone (VII), is expected. In order to ensure absence of chloromercurial, silver oxide should be included, and acidification should be effected with carbonic acid. In these circumstances the product seems to be VII. Although the elemental analyses show percentage errors of 2% for carbon and 13% for hydrogen they are still much closer to theoretical values than was reported by McNeely *et al.* (1) for their substance, which at any rate contained the chloromercurial II according to its X-ray diffraction pattern.

Indeed the poor analysis is more to be expected of the free hydroxymercurial than of the 5-↓-hydroxy-*anhydro*-[6-↑-hydroxymercuri-2-↓-carboxy]-1,4-↑↑-ethylenecyclohexane-3-↓-carboxylic acid, γ-lactone, which McNeely *et al.* thought the product to be. Hydroxymercuri compounds are difficult to purify, partly because they react with carbon dioxide. Of course, the analysis does not differentiate, at best, between the structure VII and that of the diastereomeric 5-↓-hydroxy-*anhydro*-[6-↓-hydroxymercuri-2-↓-carboxy]-1,4-↑↑-ethylenecyclohexane-3-↓-carboxylic acid predicated on the configurational assignment by McNeely *et al.* However, a potentiometric titration in which only 1 equivalent of alkali is consumed vitiates the possibility of this alternative non-lactonic isomer. In any circumstance there is no evidence for the *anhydro* structure and hence no evidence for the ↓↓ addition reported previously.

Proof for structure II is afforded by its high dipole moment (7.30, Table I) which compares with 7.19 Debye for 5-↓-hydroxy-6-↑-chloromercuri-1,4-methylenecyclohexane-2,3-↓↓-dicarboxylic acid, γ-lactone, of proved structure (2). Since the moments of 1,4-↑↑-methylenecyclohexane-2,3-↓↓-dicarboxylic anhydride (4.8 D) (4), 1,4-↑↑-methylenecyclohexane-2-↓-3-↑-dicarboxylic acid (2.19 D), and 5-↓-hydroxy-1,4-↑↑-methylenecyclohexane-2,3-↓↓-dicarboxylic acid, γ-lactone (4.85 D), also are closely comparable with those of the higher homologues (Table I) the structural analogy seems to be reasonable.

A similar comparison can be made between 5-↓-hydroxy-6-↑-chloromercuri-1,4-ethylenecyclohexane-2-↑-3-↓-dicarboxylic acid, γ-lactone (X, 6.91 D), and the methylene homologue (μ = 6.40) (2). The synthesis of X has been effected by prolonged treatment of VI with alkali (1), and also by treatment of 1,4-↑↑-ethylene-Δ^5-cyclohexene-2-↓-3-↑-dicarboxylic acid (IX) (5) with aqueous mercuric chloride. The postulated prototropic configurational shift of 2-carboxyl in II by action of alkali is thus confirmed.

Unfortunately, for a complete demonstration of configurational differences by comparison of dipole moments we have been unable to convert II to the diastereomeric 5-↓-hydroxy-6-↓-anionomercuri-1,4-↑↑-ethylenecyclohexane-2,3-↓↓-dicarboxylic acid, γ-lactone (XIII, A = Cl). When II is treated with hydrazine hydrate a mixture of products is obtained, one of which is the original substance, II. The other seems to be either a hydrolyzate or a polymorph of II since it may be converted to II when it is maintained for a few minutes at a temperature below the melting point. Probably some of XIII is actually formed but we have been unable to isolate it.

In summary the [2,2,2]-bicyclo-2-octenes seem to oxymercurate like the homologous

TABLE I

Dipole moments of 1,4-↑↑-ethylenecyclohexanes in dioxane at 20°

Substance	$d\epsilon/d\omega$	$dV/d\omega$	P_T	R_D calc.	μ, D
1,4-↑↑-Ethylenecyclohexane-2,3-↓↓-dicarboxylic anhydride	15.70	0.180	499	44	4.65
5-↓-Hydroxy-1,4-ethylenecyclohexane-2,3-↓↓-dicarboxylic acid, γ-lactone (VIII)	14.60	0.286	505	45	4.68
5-↓-Hydroxy-6-↑-chloromercuri-1,4-↑↑-ethylenecyclohexane-2,3-↓↓-dicarboxylic acid, γ-lactone (II)	16.15	0.597	1182	61	7.30
5-↓-Hydroxy-6-↑-chloromercuri-1,4-ethylenecyclohexane-2-↑-3-↓-dicarboxylic acid, γ-lactone (X)	14.50	0.581	1065	61	6.91
1,4-↑↑-Ethylenecyclohexane-2-↓-3-↑-dicarboxylic acid (IX)	3.30	0.203	150	47	2.21
Dimethyl 1,4-↑↑-ethylene-Δ^5-cyclohexene-2,3-↓↓-dicarboxylate (III)	3.90	0.120	197	42	2.59
2-↓-Carbomethoxy-5-↓-hydroxy-6-↑-chloromercuri-1,4-↑↑-ethylenecyclohexane-3-↓-carboxylic acid, γ-lactone (VI)	17.03	0.594	1283	66	7.60

[2,2,1]-bicyclo-2-heptenes in a manner which is different from that occurring with cyclohexenes, cyclopentenes, α-terpineol, and the stilbenes. Reaction with the bicyclic compounds seems to be acid-catalyzed. An over-all ↑↓ (*trans*) addition occurs in contradistinction to that observed with the other alkenes. The fixed boat conformation of the bicyclic alkenes may be involved in this abnormality.

One difference in oxymercuration between the bicycloheptene and bicycloöctene series is apparent. Although 1,4-methylene-Δ^5-cyclohexene-2,3-↓↓-dicarboxylic acid seems to oxymercurate by an ionic mechanism, it nevertheless yields a 2,3,5,6-↓↓↓↓-diastereomer. By contrast 1,4-↑↑-ethylene-Δ^5-cyclohexene yields the 2,3,5-↓↓↓-6-↑-diastereomer. It would seem that in one instance (XI) the mercuric ion is endo-co-ordinated, while in XII exo-co-ordination maintains. The difference is thus defined as a steric one.

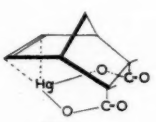

XI

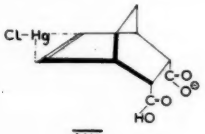

XII

The authors are grateful to the National Research Council for financial aid.

EXPERIMENTAL*

1,4-↑↑-Ethylenecyclohexane-2,3-↓↓-dicarboxylic Anhydride

A solution of 0.20 g (0.00112 mole) of 1,4-↑↑-ethylene-Δ^5-cyclohexene-2,3-↓↓-carboxylic anhydride (6) (I) in 20 ml of absolute ethanol was reduced within 25 minutes by hydrogen in presence of 0.018 g of platinum oxide containing 0.002 g of Darco. The product (0.20 g, 79%, m.p. 176–177°) was crystallized from 1:2 commercial hexane – acetone (30 ml/g), m.p. 186–186.8°. X-Ray diffraction pattern was [10] 5.38; [6] 5.15, 5.02; [5] 3.61; [4] 7.02; [3] 4.60, 3.96, 2.66; [2] 2.96, 3.30, 3.17; [1] 3.04, 3.11, 6.29, 4.15, 3.43, 2.50, 2.19, 2.38, 1.99, 1.93.

Melting points have been corrected against reliable standards (Can. J. Technol. **34, 89 (1956)). The X-ray diffraction patterns are recorded for* Cu K_α *(Ni-filtered) radiation in Å at relative intensities* $[I/I_1]$.

5-↓-Hydroxy-6-↑-chloromercuri-1,4-↑↑-ethylenecyclohexane-2,3-↓↓-dicarboxylic Acid, γ-Lactone (II)

To a solution of 34.0 g (0.191 mole) of I in 2840 ml of water at 80° was added 51.8 g (0.191 mole) of mercuric chloride with vigorous agitation. A precipitate appeared immediately and a test for mercuric ion was almost negative. After 10 hours alkali was added to a pH of 4.5. The system tested negatively (20% alkali) for mercuric or mercurous ion. The precipitate was filtered, thrice washed with distilled water, and vacuum-dried, 73 g (85%), m.p. 197–199° (decomp.). Crystallization from acetone (4 ml/g) raised this melting point to 208–208.5° (decomp.); % C, 27.7; % H, 2.67. The X-ray diffraction pattern was obtained as follows: [10] 8.19; [9] 6.15; [8] 4.16; [6] 3.28; [4] 4.84; [3] 3.81, 5.19, 6.77; [2] 3.94, 5.57, 2.92, 4.10; [1] 3.19, 3.14, 3.01, 2.86, 2.74, 2.64. When the substance was treated for 1 hour with concentrated hydrochloric acid the anhydride (I) was regenerated and identified by mixture melting point (147–148°). When II was dissolved in 4 equivalents of alkali and back-titrated with hydrochloric acid it neutralized 2 equivalents.

Dimethyl 5-↓-Hydroxy-6-↑-chloromercuri-1,4-↓↓-ethylenecyclohexane-2,3-↓↓-dicarboxylate (IV)

A suspension of 12 g (0.0535 mole) of dimethyl 1,4-↑↑-ethylenecyclohexane-2,3-↓↓-dicarboxylate (III) (7, 8) (m.p. 70–70.8°) in a solution of 17 g (0.0535 mole) of mercuric acetate in 120 ml of water was stirred for 8 hours. The filtered precipitate weighed 13.7 g (51%) and melted at 135–137°, with evolution of methanol, demonstrated as the dinitrobenzoate. The melt then resolidified and remelted at 183–185° (decomp.). The diffraction pattern of the filtered precipitate was [10] 6.91; [9] 8.42; [8] 4.09; [7] 5.34, 5.12; [6] 3.53; [5] 3.80; [4] 3.29; [3] 4.84, 2.75. Crystallization of this substance from any medium that we tried, but specifically from methanol (4 ml/g), converted it to 2-↓-carbomethoxy-5-↓-hydroxy-6-↑-acetoxymercuri-1,4-↑↑-ethylenecyclohexane-3-↓-carboxylic acid, γ-lactone (V), m.p. 188.5–189°, X-ray pattern [10] 10.84; [9] 4.56; [8] 6.44, 6.68; [5] 4.27; [4] 3.57; [3] 2.80, 3.75, 8.54. When this product was treated with aqueous sodium chloride it yielded VI.

2-↓-Carbomethoxy-5-↓-hydroxy-6-↑-chloromercuri-1,4-↑↑-ethylenecyclohexane-3-↓-carboxylic Acid, γ-Lactone (VI)

Methanol (800 ml) at 0° was freed from acidic substances by treatment with a solution containing 0.0064 mole of diazomethane in diethyl ether which had previously been dried over potassium hydroxide. Into this colorless methanol–ether mixture was dissolved 0.93 g (0.00216 mole) of 5-↓-hydroxy-6-↑-chloromercuri-2-↓-carboxy-1,4-↑↑-ethylenecyclohexane-3-↓-carboxylic acid, γ-lactone (II), at 0°. This solution at −80° was then mixed with a solution at −80° of ethereal diazomethane (0.0174 mole). The system was allowed to warm to 20° during several hours. Then a gray precipitate was filtered off. The vacuum-evaporated filtrate left 0.65 g, m.p. 182–184° (decomp.). Crystallization from acetone (4 ml/g) gave 0.12 g of unchanged II (mixture melting point). Partial evaporation of the mother liquor gave 0.16 g (17%), m.p. 199–201°. This melting point was raised to 204–205° by crystallization from acetone; a mixture melting point with VI prepared by treatment of V with aqueous sodium chloride was not lowered although admixture with II lowered the melting point 20°.

5-↓-Hydroxy-6-↑-chloromercuri-1,4-↑↑-ethylenecyclohexane-2-↑-3-↓-dicarboxylic Acid, γ-Lactone (X)

To a solution of 0.64 g (0.00327 mole) of 1,4-↑↑-ethylene-Δ^5-cyclohexene-2-↑-3-↓-dicarboxylic acid (IX) (9) in 52 ml of water at 70° was added 0.88 g (0.00327 mole) of mercuric

chloride. After it was cooled to room temperature the system was neutralized to pH 5.6–6.0 (2 ml 10% aqueous sodium hydroxide). A precipitate appeared which redissolved upon addition of 3.5 ml more of the alkali (pH 7.6, no mercuric oxide). After 20 hours the solution was acidified at 0° by addition of 2.2 ml of 10% hydrochloric acid (pH 3.0). The precipitate, 0.81 g (58%), melted at 194–200° (decomp.). Crystallization from acetone (10 ml/g) raised this melting point to 208.5–209°, mixture melting point with II lowered to 194°. No depression was observed upon admixture with the substance obtained by McNeely *et al.* by 1-day saponification (3 equivalents alkali) of 2-↓-carbomethoxy-5-↓-hydroxy-6-↑-acetoxymercuri-1,4-↑↑-ethylenecyclohexane-3-↓-carboxylic acid, γ-lactone, and subsequent acidification with hydrochloric acid. The X-ray diffraction pattern was [10] 4.79; [8] 8.79, 3.24; [7] 1.95; [6] 5.45; [5] 5.98; [4] 6.91; [3] 2.81; [2] 3.00, 2.30; [1] 3.08, 2.70, 2.61. Calc. for $C_{10}H_{11}ClHgO_4$: C, 27.8; H, 2.60. Found: C, 28.0; H, 2.67. Treatment of this product with concentrated hydrochloric acid yielded 1,4-↑↑-ethylene-Δ^5-cyclohexene-2,3-↑↓-dicarboxylic acid, m.p. 210–211°.

5-↓-Hydroxy-6-↑-hydroxymercuri-1,4-ethylenecyclohexane-2,3-↓↓-dicarboxylic Acid, γ-Lactone (VII)

A solution of 3.40 g (0.0073 mole) of 2-↓-carbomethoxy-5-↓-hydroxy-6-↑-acetoxymercuri-1,4-↑↑-ethylenecyclohexane-3-↓-carboxylic acid, γ-lactone (V), in 29 ml of 1% aqueous sodium hydroxide was let stand for 34 hours. The precipitate weighed 1.5 g (53%), m.p. 222–226° (decomp.). This melting point was raised to 239–241° by washing with chloroform, methanol, and diethyl ether. Further purification was effected by solution in 1% aqueous alkali (pH 10) followed by acidification by means of gaseous carbon dioxide. The precipitate, washed with acetone, melted at 244–244.5°. Calc. for $C_{10}H_{12}O_6Hg$: C, 29.1; H, 2.93. Found: C, 28.5; H, 3.17. The X-ray diffraction pattern was found to be [10] 8.72; [9] 6.25; [8] 3.33; [6] 4.27; [5] 2.67; [4] 3.05; [3] 3.65, 4.50, 1.97; [2] 3.92, 3.44, 3.25; [1] 2.03, 7.85, 6.93, 5.55. The same diffraction pattern was obtained for the product obtained when II (0.65 g, 0.0015 mole) in 2.45 ml of 5% aqueous alkali containing 0.46 g (0.002 mole) of silver oxide was filtered and then acidified by means of carbon dioxide gas. A comparison of the diffraction pattern with that reported by McNeely *et al.* shows that their compound must have been a mixture of VII and II.

Treatment of 5-↓-Hydroxy-6-↑-chloromercuri-1,4-↑↑-ethylenecyclohexane-2,3-↓↓-dicarboxylic Acid, γ-Lactone (II), *with Hydrazine Hydrate*

To an alkaline solution of 5.0 g (0.0116 mole) of II in 46.5 ml (0.058 mole) of 5% aqueous sodium hydroxide was added 0.6 ml (0.012 mole) of hydrazine hydrate. After 1 day the filtered system was acidified (pH 3) by use of hydrochloric acid at 0°. Slow precipitation yielded 3.0 g, m.p. 181–183°, which upon crystallization from methanol (10 ml/g) melted at 208–208.5°, mixture melting point with II not lowered (10%). The filtrate upon evaporation left a residue which was crystallized from methanol (1 ml/g), m.p. 207.5–208° (4%). Although this substance seemed to be different from II in respect of its solubility in methanol and also in respect of its X-ray diffraction pattern: [10] 6.41; [8] 8.84; [5] 5.12, 4.19; [4] 3.17; [3] 3.77, 3.46, 4.31; [2] 3.90, 3.26; [1] 4.56, 4.49, 3.39 (and despite the fact that a mixture melting point with II was not depressed), it was evidently configurationally the same as II. Thus when it was heated to 195° for 5 minutes its X-ray diffraction pattern became identical with II. Moreover, it would not form an anhydromercurial when it was converted to the hydroxymercurial by treatment with silver oxide and alkali. It may be a polymorph or, alternatively, the non-lactonic hydroxy acid.

5-↓-Hydroxy-1,4-↑↑-ethylenecyclohexane-2,3-↓↓-dicarboxylic Acid, γ-Lactone (VIII)

The substance was prepared by the recorded method (5) by heating 2.0 g (0.0112 mole) of 1,4-↑↑-ethylenecyclohexane-2,3-↓↓-dicarboxylic anhydride (I) in 22 g of 50% (w/w) sulphuric acid for 5 hours at 90°. After neutralization with sodium bicarbonate (pH 3) the precipitate was dissolved by extraction with chloroform. Evaporation of this solvent left 1.15 g (52%), m.p. 168–178°. Two crystallizations from acetone raised this melting point to 198–198.5°. The X-ray diffraction pattern was [10] 5.82; [9] 5.60; [6] 6.72; [5] 4.29; [4] 3.85, 2.90; [3] 4.94, 4.60; [2] 5.15, 2.98, 4.07; [1] 2.76, 3.18, 3.33. Potentiometric titration showed that 1 equivalent of alkali neutralized this substance. Calc. for $C_{10}H_4O_{12}$: C, 61.2; H, 6.16. Found: C, 61.3; H, 6.11.

1,4-↑↑-Ethylene-Δ⁵-cyclohexene-2,3-↓↑-dicarboxylic Acid (IX)

To a solution of 9.56 g (0.0625 mole) of fumaryl chloride in 55 ml of dry diethyl ether at −10° was gradually added a solution of 10 g (0.125 mole) of 1,3-cyclohexadiene in 55 ml of dry ether at −10°. After 1 hour at this temperature the system was maintained at 25° for 12 hours and then was shaken with 20 ml of 10% aqueous sodium hydroxide for 4 hours. Acidification of the aqueous layer yielded 8.40 g (68%), m.p. 199–204°. Crystallization from commercial hexane – acetone (1:5, 5 ml/g) raised the melting point to 210–211°. Calc. for $C_{10}H_{12}O_4$: C, 61.3; H, 6.16. Found: C, 61.0; H, 6.05.

1,4-Ethylenecyclohexane-2,3-↓↑-dicarboxylic Acid

A solution of 0.20 g (0.002 mole) of 1,4-↑↑-ethylene-Δ⁵-cyclohexene-2,3-↓↑-dicarboxylic acid in 20 ml of absolute ethanol plus 0.02 g of platinum oxide with 0.002 g of Darco was reduced within 35 minutes by 26.7 ml of hydrogen. After filtration of the catalyst the solution was evaporated, leaving 0.20 g (99%), m.p. 234–235°. After crystallization from commercial hexane – acetone (1:5, 60 ml/g) it melted at 235.0–235.5°.

REFERENCES

1. McNeely, K. H., Rodgman, A., and Wright, G. F. J. Org. Chem. **20**, 714 (1955).
2. Abercrombie, M. J., Bharucha, K. R., Rodgman, A., and Wright, G. F. Can. J. Chem. **37**, 1328 (1959).
3. Sawatzky, H. and Wright, G. F. Can. J. Chem. **36**, 1555 (1958).
4. Kwart, H. and Kaplan, L. J. Am. Chem. Soc. **75**, 3356 (1953).
5. Alder, K. and Stein, G. Ann. **514**, 1 (1934).
6. Diels, O. and Alder, K. Ann. **460**, 98 (1928).
7. Bode, H. Ber. **70**, 1167 (1937).
8. West, T. F. J. Chem. Soc. 140 (1941).
9. Alder, K. and Stein, G. Ann. **514**, 197 (1934).

PHOTOCHEMICAL SEPARATION OF MERCURY ISOTOPES

V. FURTHER STUDIES ON THE REACTION OF $Hg^{202}6(^3P_1)$ ATOMS, PHOTOEXCITED IN NATURAL MERCURY VAPOR, WITH HYDROGEN CHLORIDE[1]

J. R. McDowell, C. C. McDonald,[2] and H. E. Gunning

ABSTRACT

A further study has been made of the reaction of $Hg^{202}6(^3P_1)$ atoms, in natural mercury vapor (Hg^N), with hydrogen chloride under flow conditions at room temperature. Emphasis has been placed in this study on the effect of reaction parameters and mercury-recovery techniques on the Hg^{202} content of the solid calomel formed in the reaction.

For pure hydrogen chloride the Hg^{202} content of the calomel was found to be $39.9\pm0.3\%$, compared to the natural abundance of 29.8%. With 20–40 mole % of butadiene-1,3 in the hydrogen chloride, calomels containing 83–84% of Hg^{202} were consistently obtained.

The isotopically specific aspects of the reaction in pure hydrogen chloride can be adequately explained by the sequence:

$$Hg^{202}6(^3P_1) + HCl \rightarrow Hg^{202}Cl + H \quad [1]$$

$$Hg^{202}6(^3P_1) + HCl \rightarrow Hg^{202} + H + Cl \quad [2]$$

$$Cl + Hg^N + M \rightarrow Hg^NCl + M \quad [3]$$

$$H + HCl \rightarrow H_2 + Cl \quad [4]$$

where M in reaction [3] is a third body or the wall. From the Hg^{202}-abundance data and steady-state considerations, it has been shown that the ratio of partitioning of the absorbed radiation to [1] and [2], respectively, $= \Phi_1/\Phi_2 = 0.40\pm0.02$. In short, 29% of the primary reaction proceeds by the isotopically specific step [1].

The Hg^{202} content of the calomel product was found to increase markedly when unsaturated hydrocarbons were added to the hydrogen chloride stream. The addends studied included butadiene-1,3, benzene, isoprene, acetylene, propylene, and ethylene in order of decreasing effectiveness. In the presence of the unsaturated addend (U) two additional reactions were postulated to occur:

$$Cl + U \rightarrow \text{product} \quad [7]$$

$$H + U \rightarrow \text{product}. \quad [8]$$

From steady-state calculations the effectiveness of the addend can be shown to be determined by the rate ratio, k_8/k_4.

For the maximally enriching mixture of hydrogen chloride and butadiene, the effect of variations in lamp temperature and reaction pressure was studied. At lamp temperatures exceeding approximately 35° C, reduced enrichments were obtained owing to emission-line broadening. A progressive reduction in enrichment was also observed with substrate pressures greater than 25 mm, owing presumably to Lorentz-broadening of the hyperfine absorption contours of the Hg^N in the reaction cell.

The Hg^{202} content of the calomel product was determined by resonance radiation absorbiometry. The apparent Hg^{202} abundances of the mercury recovered from the calomel product were found to depend strongly on the method used for isolating the enriched mercury from the calomel. Evidence was obtained for the occurrence of isotopically degradative exchange reactions during the recovery process. A recovery technique was developed which appeared to eliminate this exchange degradation.

INTRODUCTION

In an earlier paper in this series (1), experimental techniques were described for the photoexcitation, in natural mercury vapor (Hg^N), of a specific mercury isotopic species (Hg^1) to the $6(^3P_1)$ state. For mercury-$6(^3P_1)$-photosensitized reactions wherein mercury-containing products are formed, the aforementioned technique of monoisotopic photosensitization may be used to determine the extent to which mercury compounds are formed in the primary process. Primary formation of mercury compounds would be

[1]*Manuscript received April 16, 1959.*
Contribution from the Department of Chemistry, University of Alberta, Edmonton, Alberta.
[2]*Present address: Chemical Department, E. I. du Pont de Nemours Co., Wilmington, Delaware.*

indicated when the mercury product is enriched in the isotope undergoing photoexcitation. For a substrate, XY, the general mechanism may be represented by the sequence:

$$Hg^{i}6(^3P_1) + XY \rightarrow Hg^{i}X + Y \quad [1]$$

$$Hg^{i}6(^3P_1) + XY \rightarrow Hg^{i} + X + Y \quad [2]$$

$$X + Hg^{N} + M \rightarrow Hg^{N}X + M \quad [3]$$

where M represents a third body, including the wall. The two primary processes, [1] and [2], presumably involve the same intermediate. Reaction [3], the isotope-diluting step, may be reduced in importance by the addition of compounds which will react rapidly with the free radicals, X and Y. Under these conditions, products highly enriched in the isotope under photoexcitation can be obtained.

Pertel and Gunning (2, 3) studied the reactions of $Hg^{202}6(^3P_1)$ atoms, in Hg^{N}, with N_2O, O_2, and H_2O under flow conditions. For N_2O and O_2 the HgO product was found to contain the normal abundance (29.8%) of Hg^{202}. However, the HgO product of the water vapor reaction contained 33–35% Hg^{202}. Reaction [1] appears therefore to be significant in the H_2O reaction and unimportant for N_2O and O_2. Evidence in favor of the above-cited general mechanism was obtained by studying the Hg^{202} enrichment when unsaturated addends, such as butadiene-1,3, were added to the water vapor stream. Under these conditions the HgO product was found to contain a maximum of 85% Hg^{202}.

The principles of monoisotopic mercury photosensitization and their application to the study of the mechanisms of reactions involving collisions of the second kind have been reviewed by Gunning (4).

A study has recently been made of the reactions of $Hg^{202}6(^3P_1)$ atoms, in Hg^{N}, with flowing hydrogen chloride (5). Under fast-flow conditions it was found that the pure substrate yielded a calomel product containing 44% Hg^{202}. With butadiene-1,3 and benzene as addends, calomels containing respectively 59% and 55% Hg^{202} were obtained under optimum conditions. In the investigation (5) difficulty was encountered in obtaining good reproducibility in the Hg^{202}-enrichment data. It was suspected that exchange reactions were occurring between Hg^{202} ions and adsorbed Hg^{N} during the recovery for analysis of the isotopic mercury from the calomel product.

The present investigation represents a further study of the reaction of $Hg^{202}6(^3P_1)$ atoms, in Hg^{N}, with flowing hydrogen chloride. The various experimental factors which influence the Hg^{202}-enrichment values have been sought out in order to obtain maximum precision in the kinetic data. Emphasis has been placed on the reaction in the presence of various unsaturated addends, in order to find conditions of maximum isotopic enrichment.

The details of the investigation follow.

EXPERIMENTAL

For detailed descriptions of the experimental techniques employed in this study, reference should be made to earlier papers in this series (5, 3, 1). The particular experimental assembly used was essentially identical with that described in reference 3. The quartz-electrodeless discharge source used in this study contained mercury, 98.3 atom % in Hg^{202}. The lamp-wall temperature was maintained constant to $\pm 0.05°$ C.

In the earlier study (5) of the hydrogen chloride reaction the calomel reaction product was removed from the cell by filling the cell with hot, concentrated, hydrochloric acid. The acid-filled cell was immersed in boiling water until the product had dissolved. After the acid solution had been neutralized with base to a pH of 5–6, the isotopic mercury was recovered by immersing a coil of pure copper wire in the solution.

For this investigation two, totally different, methods were studied for recovering the isotopic mercury for absorbiometric analysis (6). The two recovery procedures will be referred to as the NH_3 method and the HCl method.

In the NH_3 method, 3 ml of concentrated ammonium hydroxide were poured into the reaction cell, and the cell was shaken so that the liquid completely contacted the calomel product, as evidenced by blackening of the product associated with the formation of $HgNH_2Cl + Hg$. After it was drained, the cell was rinsed thoroughly with distilled water, attached via ground joints to a high-vacuum system, and evacuated for 6 hours. While still under evacuation, the cell was heated strongly with a gas–oxygen flame until the product in the cell was completely white in color, indicating that any free mercury had been driven off. The cell was then removed from the evacuation system, and the product was dissolved in a mixture consisting of 2 ml concentrated nitric acid, 3 ml concentrated hydrochloric acid, and 5 ml of water. The aqua regia was allowed to remain in the cell for 10 minutes. After neutralization to pH 4–5 with sodium hydroxide solution, mercury was recovered from the solution with a copper coil.

In the HCl method, 3 ml of concentrated hydrochloric acid, at 100° C, were poured into the cell and allowed to remain there for a specified time. The solution was then drained from the cell, and neutralized as in the NH_3 method. The isotopic mercury was recovered from the solution by plating on copper as before.

The gases used in this investigation were the highest-purity grades available from the Matheson Company, East Rutherford, N.J. The benzene and isoprene used were A.C.S. grade.

RESULTS

In the runs with pure hydrogen chloride the solid product of reaction was observed to form as a white deposit, mainly in the reaction zone. However, some deposit could be observed in the connecting tubing downstream from the reaction cell. The combined product from several runs was examined by X-ray diffraction. The patterns showed that the material was Hg_2Cl_2, with some weak lines indicating, perhaps, a trace of $HgCl_2$. The product was found to be (*a*) insoluble in cold water, (*b*) slightly soluble in cold, concentrated hydrochloric acid, and (*c*) very soluble in hot hydrochloric acid. In the presence of ammonium hydroxide the product turned black. There is therefore little doubt that the white product is finely divided calomel.

When butadiene was added to the hydrogen chloride stream, the white deposit was observed to form as in the runs with pure substrate. However, during the reaction the white deposit became gradually coated with a thin film of transparent polymer. It was further observed that the quantity of white product formed, in a fixed duration of exposure, decreased with increasing mole fraction of butadiene in the stream. The decreasing yield of product with increasing butadiene concentration can obviously be ascribed to competitive quenching of the photoexcited atoms by the butadiene.

In the first series of runs the Hg^{202} abundance in the calomel product was studied as a function of the butadiene concentration in the stream. A fast flow rate was used, which was maintained essentially constant at 304–383 ml/sec at 25° C and reaction pressure. The total pressure was kept at 9.4 ± 2 mm, while the concentration of butadiene was varied from 0–55 mole %. The lamp-wall temperature was held constant at 23.00 ± 0.05° C. For recovery of mercury from the calomel product, the NH_3 method was used. The results are represented graphically in Fig. 1. It will be noted that as the concentration of butadiene is increased, the Hg^{202} abundance rises rapidly to a maximum

value of 75% at 20 mole % of butadiene. At higher butadiene concentrations, the isotopic abundance slowly decreases toward the natural abundance value.

In order to compare directly the effect of recovery methods on the Hg^{202} abundances, a second series of runs was done on the hydrogen chloride–butadiene system. This series differed from the preceding one only in that the isotopic mercury was recovered from the product by the HCl method. The hot acid was left in the cell for 10 minutes before draining.

The results of this series are shown graphically as the upper curve in Fig. 1. The cell pressure was held within the range, 7.4–12.3 mm. The flow rate was maintained at 360 ± 10 ml/sec. For any given run, the lamp-wall temperature was kept constant to $\pm0.05°$ C. The total range of lamp-wall temperature over the series was 23.0–24.0° C.

A comparison of the two curves in Fig. 1 points up clearly the marked effect of recovery methods on the Hg^{202} abundances in the mercury from the solid reaction product. In the second series an average maximum abundance value of 83% was obtained, and this maximum was invariant in butadiene concentration from 20 to at least 40 mole % of butadiene. Even at 70 mole % butadiene the abundance has only decreased to 72%.

It is also pertinent to note that the two recovery methods did not appreciably influence the Hg^{202} abundance for pure hydrogen chloride. The two methods gave an average value of $39.9\pm0.3\%$.

In the HCl method of mercury recovery, it was found that isotopic degradation occurred if the hot acid was left in contact with the product in the reaction cell for more than 10 minutes. The following example is representative of this degradative effect: In one run the acid was left in contact with the product for 5 minutes, after which time the acid was drained and the cell washed thoroughly with distilled water. The mercury recovered from the acid contained 66.2% Hg^{202}. The undissolved deposit in the cell was then treated with another aliquot of hot acid. The acid was left in the cell for 2 hours. The analysis of the recovered mercury gave 52.8% Hg^{202}. Since the normal abundance of Hg^{202} is 29.8%, the fractional enrichment has decreased from 1.22 to 0.77 in the prolonged acid treatment. This represents a degradation of 37%.

In all subsequent runs reported in this paper, the HCl method was used, with the hot acid left in contact with the product for 10 minutes.

In order to assess the importance of lamp-wall temperatures on the hydrogen chloride–butadiene system, the lamp-wall temperature was varied from 4 to 48.5° C. A maximally enriching mixture of hydrogen chloride and butadiene was used, containing 22 mole % of butadiene. Flow rates were kept within the range 350–370 ml/sec at a cell pressure of 10.9 ± 0.6 mm. It should be noted that difficulty was encountered in maintaining constant lamp intensity at 4° C. At this temperature flickering was observed in the blue emission from the lamp. As the lamp-wall temperature was raised, the brilliance of the lamp steadily increased. The rate of production of product was also observed to increase with increasing lamp-wall temperature.

The data on Hg^{202} abundance vs. lamp-wall temperature are shown in Fig. 2. There is some change in the Hg^{202} abundance when the lamp-wall temperature is lowered from 23° C to 4° C. However, in view of the instability of the lamp at 4° C, it is doubtful whether the small decrease is significant. At temperatures beyond 35° C, the Hg^{202} abundance drops sharply. This effect will be discussed later in this paper.

The variation in Hg^{202} content with increasing cell pressure was studied over the range 10–100 mm. The reaction mixture contained 22 mole % of butadiene as in the lamp-wall temperature studies. The flow rate was held constant at 360 ± 10 ml/sec. The lamp temperature was 23.0° C.

The data are graphically represented in Fig. 3. It is quite apparent from the graph that pressure-broadening of the absorption contours is an extremely important factor in studies of this type. Maximum enrichments are only obtained for the hydrogen chloride – butadiene mixture at pressures less than about 25 mm.

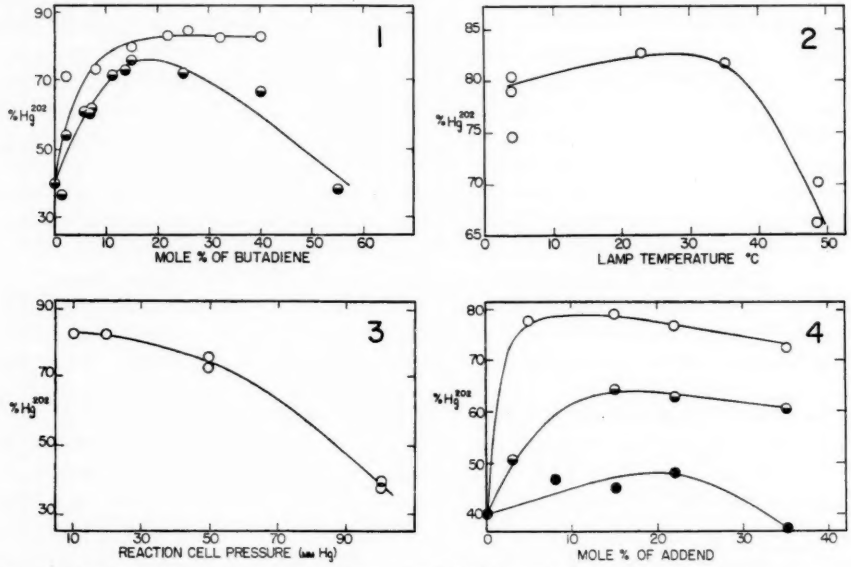

FIG. 1. Hg^{202} abundance vs. mole % of butadiene. ○ HCl method. ◒ NH_3 method.
FIG. 2. Hg^{202} abundance vs. lamp-wall temperature for hydrogen chloride containing 22 mole % of butadiene.
FIG. 3. Hg^{202} abundance vs. reaction cell pressure for hydrogen chloride containing 22 mole % of butadiene.
FIG. 4. Hg^{202} abundance vs. mole % of addend. ○ Benzene. ◒ Isoprene. ● Ethylene.

The efficiency of an unsaturated addend in increasing the Hg^{202} abundance will be related directly to its ability to remove radicals associated with the formation of $Hg^{N}Cl$, if the mechanism proposed in this paper is accepted. A number of addends, in addition to butadiene, were therefore studied in order to obtain a measure of relative efficiencies. In Table I, ethylene, propylene, acetylene, isoprene, benzene, and butadiene are compared with respect to their influence on the Hg^{202} abundance. The concentrations of all addends in the hydrogen chloride stream was 35 mole %. The lamp temperature was 20.0° C. The flow rate was held at 350–375 ml/sec at a total reaction pressure of 10 mm. From Table I, it is apparent that at the chosen concentration of 35 mole %, butadiene is the most efficient addend. In order of decreasing effectiveness follow benzene, isoprene, acetylene, propylene, and ethylene. Surprisingly enough, ethylene is quite ineffective as an addend at the chosen concentration.

Since the effectiveness of an addend could depend upon its concentration, three of the above unsaturated compounds, benzene, isoprene, and ethylene were selected for more detailed study. The results are represented graphically in Fig. 4. While the results at varying concentrations do not change the order of effectiveness of the three addends, they do establish the concentrations at which each addend is maximally effective. The maximum abundances obtained for the three addends were 78.7, 64.0, and 48.1 for benzene, isoprene, and ethylene respectively.

TABLE I

The effect of various unsaturated addends on the Hg^{202} content of the solid product of the reaction of $Hg^{202}6(^3P_1)$ atoms in Hg^N with flowing hydrogen chloride*

Addend	Concentration, mole %	Hg^{202} abundance, atom %
Ethylene	35	37·1
Propylene	35	40·6
Acetylene	35	51·5
Isoprene	35	60·6
Benzene	35	72·3
Butadiene	35	82·0

*Lamp temperature = 20.0° C; flow rate = 350–375 ml/sec; cell pressure = 10 mm.

DISCUSSION

For pure hydrogen chloride the general mechanism proposed in the Introduction becomes:

$$Hg^{202}6(^3P_1) + HCl \rightarrow Hg^{202}Cl + H \quad [1]$$

$$Hg^{202}6(^3P_1) + HCl \rightarrow Hg^{202} + H + Cl \quad [2]$$

$$Cl + Hg^N + M \rightarrow Hg^NCl + M. \quad [3]$$

In the earlier study (5) it was pointed out that Cl atoms are also likely formed by abstraction reactions of the H atoms, generated in [1] and [2], with the substrate

$$H + HCl \rightarrow H_2 + Cl. \quad [4]$$

It would be expected that [4] would be at least as fast as the corresponding abstraction reaction with methyl radicals:

$$CH_3 + HCl \rightarrow CH_4 + Cl. \quad [5]$$

For this reaction Cvetanović and Steacie [7] found a collision yield of 2×10^{-4} at 28° C, corresponding to a maximum activation energy of 5.1 kcal per mole. Reaction [4] could therefore be of considerable importance in the present investigation. On the other hand, the recombination of H and Cl atoms, discussed in the earlier paper (5),

$$H + Cl + M \rightarrow HCl + M, \quad [6]$$

should be unimportant under our conditions owing to the high concentration of Hg^N, which is being constantly replenished in the fast-flow system. Reaction [3], therefore, should account almost exclusively for Cl atom consumption.

For the four-step mechanism, [1]–[4], the relative rate ratio, from steady-state considerations,

$$R_{Hg^NCl}/R_{Hg^{202}Cl} = (1 + \Phi_2)/\Phi_1 = (100-A)/(A-29.8),$$

where Φ_1 and Φ_2 are the relative fractions of the chemically quenched radiation partitioned to [1] and [2] respectively, and A is the percentage Hg^{202} abundance in the recovered calomel. In the present study the A value for pure substrate was found to be 39.9 ± 0.3, whence $(1+\Phi_2)\,(\Phi_1) = 6.0\pm0.2$, and $\Phi_1/\Phi_2 = 0.40\pm0.02$. In the first paper on this reaction (5), an A value of 44% was obtained, corresponding to $\Phi_1/\Phi_2 = 0.68$. In view of the higher analytical reproducibility obtained in this study, together with the fact that the A values were obtained for two totally different methods of mercury recovery, the Φ_1/Φ_2 value of 0.40 ± 0.02 should be more reliable than the earlier one.

It is interesting to compare the value of the ratio, Φ_1/Φ_2, for hydrogen chloride to that obtained in the reaction of $Hg^{202}6(^3P_1)$ atoms, in Hg^N, with water vapor. Pertel and Gunning (2, 3) obtained a value for A of $33.4\pm1.0\%$ for pure substrate. For water vapor the corresponding four-step sequence would be:

$$Hg^{202}6(^3P_1) + HOH \rightarrow Hg^{202}OH + H \quad [1']$$
$$Hg^{202}6(^3P_1) + HOH \rightarrow Hg^{202} + H + OH \quad [2']$$
$$OH + Hg^N + M \rightarrow Hg^NOH + H \quad [3']$$
$$H + HOH \rightarrow H_2 + OH. \quad [4']$$

From the A value $\Phi_1/\Phi_2 = 0.10\pm0.03$. In short, the isotopically specific primary process is some four times more important in hydrogen chloride than in water vapor. It would be expected that the importance of [1] would be related to the stability of the mercury compound formed in the reaction. Since HgCl is considerably more stable than HgOH, compound formation should be favored for hydrogen chloride. The stability consideration would be partially offset, however, by the larger number of vibrational degrees of freedom, available in HgOH, to take up excess energy associated with the quenching process.

It should be emphasized that the Φ_1/Φ_2 values for hydrogen chloride and water vapor are minimum values since any isotopically degradative exchange processes operative either in the reaction, or during recovery of the mercury for analysis, would lower the apparent value of the abundance, and yield a spuriously low value for Φ_1/Φ_2.

As stated earlier in this paper, the major emphasis in the present investigation was placed on the effect of unsaturated addends on the Hg^{202}-abundance values. Here considerable progress was made over the previous investigation (5). Average maximum abundances of 83% were consistently obtained at butadiene concentrations of 20–40 mole %, whereas the highest abundance obtained hitherto was 59% for hydrogen chloride–butadiene mixtures. In this connection the question naturally arises whether degradative reactions have now been completely eliminated in product recovery. In the previous study the calomel was dissolved from the cell in concentrated hydrochloric acid at 100° C. No attempt was made to control the time of contact of the reaction products with the hot acid. From the present study this contact time would appear to be very critical if exchange degradation is to be minimized. Optimum conditions involve a contact time not exceeding 10 minutes, followed by rapid neutralization of the acid extract.

It is instructive to compare the maximum enrichments obtained in the hydrogen chloride and water vapor reactions, for butadiene as the addend. Pertel and Gunning (3) found that the maximally enriched HgO product of the water reaction contained 85% Hg^{202}, at a butadiene concentration of 21 mole %. From Fig. 1, it can be seen that the most highly enriched $Hg^{202}Cl$ contained 84.2% Hg^{202}, and the corresponding butadiene concentration was 26 mole %. Hence the maximum Hg^{202} abundances and the butadiene concentrations are almost identical in the two reactions. Since the HgO product was removed with cold, dilute hydrochloric acid, whereas hot concentrated acid was required to dissolve the HgCl product, and since it has been shown (3) that high acid concentrations favor exchange degradation, it appears probable that exchange reactions are unimportant for the HCl method of calomel recovery. In Fig. 1 the effect of exchange degradation is clearly shown. The consistently lower values obtained by the NH_3 method must be ascribed to this type of isotopic degradation. The fact, apparent from Fig. 1, that exchange degradation becomes more extensive at higher butadiene concentrations, suggests that the controlling factor is the ratio of the quantities of enriched calomel to adsorbed mercury present in the cell. With increasing butadiene concentrations, the

competitive quenching progressively reduces the product yield for a fixed duration of exposure. The quantity of adsorbed mercury on the other hand should be relatively independent of quenching partitioning. The fact that the HCl method, as shown in Fig. 1, leads to maximum Hg^{202} abundances which are invariant in butadiene concentration is further evidence that exchange has been eliminated by using this technique for product recovery.

For the hydrogen chloride reaction the unsaturated addend (U) would serve to remove both Cl and H atoms:

$$Cl + U \rightarrow \text{products} \qquad [7]$$
$$H + U \rightarrow \text{products}. \qquad [8]$$

If, for the mechanism of the reaction with addend, we consider steps [1]–[4], together with [7] and [8], it can be readily shown by steady-state calculations that the effectiveness of the addend at fixed mole fraction is determined by the ratio of k_8/k_4 only. The corresponding steps for the water reaction would be:

$$OH + U \rightarrow \text{products} \qquad [7']$$
$$H + U \rightarrow \text{products}. \qquad [8]$$

The fact that almost identical maximum enrichments are obtained in the hydrogen chloride and water vapor reactions, with butadiene as addend, suggests that reaction [8], which is common to both mechanisms, is the dominant factor in determining the effectiveness of the addend. Maximum enrichment would occur when the H atoms are disappearing almost exclusively by reaction [8]. On this basis other reasons must be sought for the failure to obtain maximum abundances identical with the Hg^{202} content of the lamp isotope (98.3% Hg^{202}).

In order to obtain maximum abundances identical with that of the lamp isotope, the emission line must not overlap hyperfine absorption contours adjacent to that of Hg^{202}. If some overlap is occurring at lamp-wall temperatures of 23° C, it would be expected that a decrease in source temperature would reduce the extent of this overlap. Figure 2 shows clearly that reduced lamp-wall temperature does not improve enrichment. On the other hand, increasing lamp temperature does result in a decreased enrichment, showing thereby that the absorption-line width does indeed increase significantly over the range of lamp temperatures studied. No appreciable overlap occurs until lamp-wall temperatures exceeding 35° C are reached. The problem of lamp-wall temperature is, however, complicated by the fact that the enrichment apparently increases with increasing absorbed intensity (5). This effect may obscure any increase in enrichment associated with a decrease in lamp temperature. The slight maximum in enrichment shown in Fig. 2, at approximately 20° C, may arise from the net effect of the intensity and broadening factors. The problem can only be answered unequivocably by a total isotopic analysis of the maximally enriched products in the hydrogen chloride and water reactions. Mass spectrometric studies are now underway in the laboratories of one of us (H.E.G.) as one result of which considerable light should be shed on the importance of overlap in these reactions.

The results shown in Figs. 2 and 3 on the effects of increasing lamp-wall temperature and substrate pressure on the enrichment point up clearly the importance of broadening factors in emission and absorption of the Hg^{202} enrichment. These data offer further confirmation for the proposed mechanism in that these broadening influences would operate only in the primary act of absorption.

The variation of enrichment with substrate pressure for the maximally enriching hydrogen chloride – butadiene system as shown in Fig. 3 serves to define clearly the pressure beyond which Lorentz-broadening becomes significant. At total pressures below 25 mm the Lorentz effect does not appear detectably to broaden the hyperfine absorption contours.

The broadening influences on the emission line apparently cause appreciable overlap when the lamp-wall temperature is increased from 23° C to 48° C. The Doppler effect is quite inadequate to account for this broadening. An increase of 25° C would result in an increase of emission-line half-width by the Doppler effect of only 0.1 mÅ, whereas the hyperfine contours are separated by approximately 10 mÅ (1). However, with increasing lamp temperature, the vapor pressure of mercury will rise rapidly leading to increased self-reversal (1) of the resonance line. Furthermore, there will be a marked increase in the lamp current. Pressure- and current-broadening will therefore be simultaneously operative at higher lamp temperatures.

In Table I,e % effectiveness of six unsaturated addends are compared, at a concentration of 35 mol the. From the foregoing discussion on the mechanism of the reaction in the presence of addends, it would appear that these relative efficiencies are primarily determined by the rate of addition of H atoms to the double bond, as shown in reaction [8]. In Figs. 1 and 4, the curves for the variation in Hg^{202} abundance with concentration for the four addends show that the order of decreasing effectiveness is butadiene, benzene, isoprene, and ethylene. It should be emphasized that the effectiveness of an addend will be very sensitive to small differences in the activation energy of reaction [8], since absolute rate constant ratios are the determining factor.

From the proposed mechanism, it would be expected that the Hg^{202} abundance should increase with increasing addend concentration, and approach asymptotically the Hg^{202} abundance in the lamp. However, even with butadiene, the most effective addend studied, the abundance maximizes at an average value of 83%, some 15% lower than the Hg^{202} abundance in the mercury present in the lamp. From this investigation, it seems unlikely that the discrepancy can be attributed to broadening either in emission or absorption, since the range of influence of these parameters has been examined in the present investigation. There is apparently some other process operative in these reactions, which leads to degradation of the $Hg^{202}Cl$ formed in [1]. The same situation exists in the water reaction. In the laboratories of one of us (H.E.G.) further investigations are in progress on the detailed kinetics of these reactions. It is hoped that these studies will lead to a more complete understanding of the mechanism involved in reactions of this type.

CONCLUSIONS

By minimizing exchange reactions in product recovery, and determining quantitatively the influence of broadening factors in emission and absorption, the kinetics of the reaction of $Hg^{202}6(^3P_1)$ atoms, in Hg^N, with hydrogen chloride has been placed on a more quantitative basis than proved possible in the earlier study (5). It has now been established that the ratio Φ_1/Φ_2 has the value of 0.40 ± 0.02 at room temperature.

Under the conditions defined in this paper, the hydrogen chloride reaction could be used to advantage in the preparation of Hg^{202} from natural mercury. It has now been shown that enrichments equal to those obtainable in the water reaction can be conveniently produced in the hydrogen chloride system.

In both the hydrogen chloride and water vapor reactions, the effectiveness of an unsaturated addend, in increasing the Hg^{202} abundance in the recovered mercury product, is

apparently determined primarily by the rate of addition of H atoms to the double bond in the addend.

In both the hydrogen chloride and water reactions, the maximum abundances obtained are still some 15 atom % lower than that of the lamp isotope. Mass spectrometric studies now in progress on the total isotopic analysis of the enriched mercury in the solid reaction products and related investigations should be of considerable value in determining the reason for the discrepancy.

ACKNOWLEDGMENTS

This work was supported in part by the National Research Council of Canada through Block Term Grant No. NRC-BT-74. This assistance is most gratefully acknowledged.

One of us (J.R.M.) would like to express his deep appreciation to the International Nickel Company for generous Fellowship support.

REFERENCES

1. OSBORN, K. R., McDONALD, C. C., and GUNNING, H. E. J. Chem. Phys. **26**, 124 (1957).
2. PERTEL, R. and GUNNING, H. E. J. Chem. Phys. **26**, 219 (1957).
3. PERTEL, R. and GUNNING, H. E. Can. J. Chem. **37**, 35 (1959).
4. GUNNING, H. E. Can. J. Chem. **36**, 89 (1958).
5. McDONALD, C. C., McDOWELL, J. R., and GUNNING, H. E. Can. J. Chem. **37**, 930 (1959).
6. OSBORN, K. R. and GUNNING, H. E. J. Opt. Soc. Am. **45**, 552 (1955).
7. CVETANOVIĆ, R. J. and STEACIE, E. W. R. Can. J. Chem. **31**, 158 (1953).

THELEPHORIC ACID[1]

G. READ[2] AND L. C. VINING

ABSTRACT

The electronic and infrared absorption spectra of thelephoric acid and its leucoacetate indicate that the structure at present accepted for the pigment is incorrect. It is suggested from an interpretation of these spectra, together with a re-evaluation of the reported properties of thelephoric acid and its derivatives, that the substance may be a hydroxylated terphenyl containing internal quinhydrone and benzofuran systems (e.g. (V)).

Structure (I), proposed by Kögl, Erxleben, and Jänecke (8), is widely quoted for thelephoric acid, which occurs in several lichens and many of the higher fungi (6, 14). The sparing solubility of a compound of this structure in sodium bicarbonate and sodium carbonate solutions is surprising. Furthermore, (I) does not fall into any of the broad groups of naturally occurring compounds and is difficult to reconcile with accepted theories of biogenesis. Recently Millward and Whiting (10) have shown that synthetic 1,2′-phenanthryl-1,3-butadiene differs in melting point from the hydrocarbon of that structure reported to be formed by zinc dust distillation of acetylthelephoric acid (8). They concede that polymorphism or the unlikely survival of a *cis*-form could account for

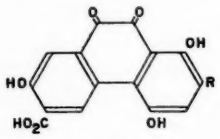

(I)

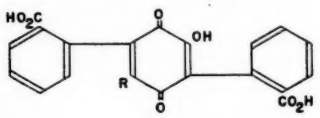

(II)

(I) and (II) R = $\{CH:CH\}_2CO_2H$

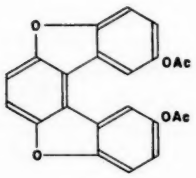

(III)

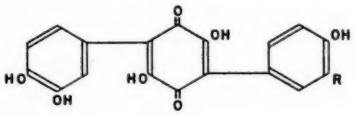

(IV)

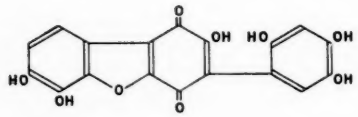

(V)

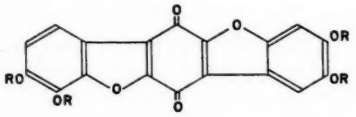

(VI)

[1]*Manuscript received April 24, 1959.*
Contribution from the National Research Council of Canada, Prairie Regional Laboratory, Saskatoon, Saskatchewan.
Issued as N.R.C. No. 5287.
[2]*National Research Council of Canada Postdoctorate Fellow, 1957–59. Present address: The Dyson Perrins Laboratory, Oxford University, Oxford, England.*

the difference, but their doubt concerning the nature of this product seems especially pertinent in view of Kögl and Erxleben's claim that a dienoic acid side chain is lost from muscarufin (II) in a comparable reaction (7). Only limited amounts of material were available for the classical degradations of the pigment (8), and it seemed desirable to confirm the structure by modern physical methods.

Small samples of thelephoric acid and its "leucopentaacetate" were obtained through the generosity of Professor S. Shibata. The infrared spectrum of the pigment was not well defined suggesting heterogeneity. It showed a single peak (1629 cm^{-1}; (s)) in the carbonyl stretching region. The leucoacetate gave peaks in this region at 1760 cm^{-1} (s) (acetate) and 1630 cm^{-1} (w). In view of the absence of any bands attributable to carboxyl groups, the accepted structure for thelephoric acid is clearly untenable. Moreover, the ultraviolet absorption of the leucoacetate (Fig. 1) is inconsistent with that of an acetoxylated phenanthryldienoic acid.

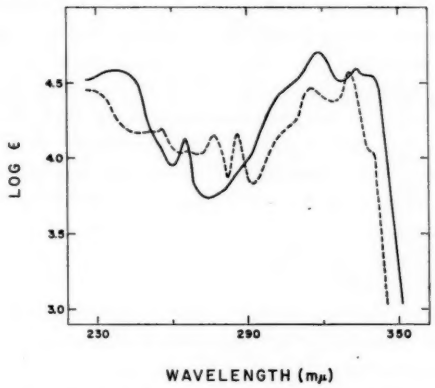

FIG. 1. Absorption spectra of thelephoric acid leucoacetate (——), and 2,11-diacetoxybenzobis-[1,2-*b*,4,3-*b'*]-benzofuran (– – –) (III).

A striking property of thelephoric acid is its intense blue-black color in the solid state, whereas a solution in pyridine is wine-red in color and shows an absorption maximum at only 493 mμ. This suggests a quinhydrone, and the color, insolubility, stability to recrystallization, and color reactions of this material are reminiscent of the internal diphenyl quinhydrone systems examined by Erdtman (3). Thomson has also noted (14) that, like thelephoric acid, 5,6-dihydroxy-1,4-naphthoquinone gives a cornflower-blue solution in aqueous pyridine, and the terphenyl quinone, polyporic acid, behaves similarly (11). A quinhydrone structure would account for the single carbonyl band at 1629 cm^{-1} in the infrared spectrum of thelephoric acid. Other possible assignments for this band are a quinomethine, an extended quinone, or a perihydroxylated quinone, but the last can be excluded by the ultraviolet spectrum of the leucoacetate which, if representing a single chromophore, is incompatible with any fused-ring aromatic system. This spectrum is basically similar to that of dibenzofuran, but bathochromic and hyperchromic displacement of the 280-mμ band suggests a more extended system. It, in fact, closely resembles that of 3-aminodibenzofuran (13), but its absorption in the region of 320 mμ is higher (log ε 4.70 vs. 4.22). The absorption from 290 to 360 mμ shows a marked similarity to that of the terphenyl (III) (Fig. 1), but there are differences between 240 and 290 mμ. The infrared spectra of the leucoacetate and (III) are basically similar and show, in common

with the pigment, weak aromatic absorption bands between 1550 and 1635 cm^{-1}, and strong bands at ca. 1025 (aromatic ether) and 800 cm^{-1} (two adjacent aromatic hydrogens). The pigment and leucoacetate also show a band at ca. 870 cm^{-1} (isolated aromatic hydrogen). The properties of the materials examined are therefore compatible with highly oxygenated terphenyl derivatives, the occurrence of which in higher fungi and lichens has frequently been reported (6, 14).

In attempting to rationalize the published evidence for structure (I) with the current spectral data, the possibility cannot be ruled out that the two samples of thelephoric acid are different. Unfortunately, the material examined by Kögl *et al.* was not obtainable, but in view of the close agreement in properties reported for the two compounds (2), this possibility seems remote. Moreover, a specimen kindly supplied by Dr. J. Gripenberg had an infrared spectrum virtually identical with that of the Japanese sample.

The initial analytical figures obtained by Asahina and Shibata for the pigment (2) agree with $C_{18}H_{10}O_9$, e.g. (V), in addition to the $C_{20}H_{12}O_9.H_2O$ formula adopted. Carbon and hydrogen analyses obtained by both the Japanese and European workers for the acetate fit a $C_{26}H_{16}O_{12}$ molecule, e.g. (VI; R = Ac), while the analyses obtained by Asahina and Shibata for the leucoacetate agree with the required figures for the leucoacetate of (VI; R = Ac). In reported analyses for thelephoric acid, the hydrogen values are all low for $C_{20}H_{12}O_9$, and the carbon values variable (59.89 to 60.99%). Furthermore, Asahina and Shibata could only approach the required analysis for structure (I) by prolonged drying of the sample at elevated temperatures at which (V) might be expected to dehydrate. Analyses obtained would also be given by a 1:1 mixture of (V) and (VI; R = H). Under the conditions used, acetylation and reductive acetylation of such a mixture might be expected to yield a single acetate, e.g. (VI; R = Ac), and leucoacetate. It is therefore suggested that (V) or a closely related isomer represents the structure for thelephoric acid as initially isolated by the Japanese workers. Such a compound might be formally derived from leucomelone (IV; R = H) (1) by hydroxylation to the terphenyl quinone (IV; R = OH), oxidation to a diquinone, rearrangement, and hydroxylation.

The isolation from compounds such as (VI; R = Ac) of the key hydrocarbon from which 2-phenanthroic acid and subsequently phenanthrene were obtained is conceivable if the initial result of zinc dust distillation is a fission of the quinone ring leading to substituted benzofuran and phenyl fragments. A condensation analogous to that in which phenanthrene is formed by pyrolysis of benzofuran and benzene (9) might then yield a phenanthrene derivative such as 2-vinyl phenanthrene (m.p. 116.5–118° C) (12) which is similar in analysis to the reported 1,2-phenanthrylbuta-1,3-diene (m.p. 126° C).

The authors realize that this hypothesis leaves unexplained many aspects of the chemistry of thelephoric acid but hope that it may serve to stimulate further studies by chemists with access to the substance.

EXPERIMENTAL

Infrared spectra of the compounds in pressed potassium bromide disks were measured with a Perkin–Elmer double beam spectrometer, model 21. Because of the poor solubility and the smallness of the samples, solution spectra could not be obtained.

The ultraviolet and visible absorption spectra were measured on a Warren Spectracord double beam recording spectrophotometer, model 3000. Thelephoric acid was examined in pyridine, the remaining samples in freshly purified dioxane. The leucoacetate of thelephoric acid showed λ_{max} 238, 265, 318, and 334 mμ, log ϵ 4.64, 4.18, 4.77, and 4.64 respectively, based on a molecular formula $C_{30}H_{22}O_{14}$.

2,11-Diacetoxybenzobis-[1,2-*b*,4,3-*b'*]-benzofuran (III) was prepared according to the method used by Erdtman (4) and had m.p. 236–238° C. (Erdtman reports m.p. 236–237° C.) Found: C, 70.51%; H, 3.92%. Calculated for $C_{22}H_{14}O_6$: C, 70.58%, H, 3.77%. Ultraviolet absorption maxima at 257, 265.5, 277, 286, 315, 331 mμ, log ε 4.19; 4.04, 4.16, 4.17, 4.46, 4.55 respectively; inflexion at 233 mμ, log ε 4.50. The *p*-terphenyl structure assigned to this compound at the time it was first prepared has since been corrected (5).

ACKNOWLEDGMENTS

The authors wish to express their appreciation to Professor S. Shibata, Tokyo University, Japan, and to Dr. J. Gripenberg, Finland Institute of Technology, Helsingfors, for gifts of samples, and to Miss I. M. Gaffney for measurement of the infrared spectra.

REFERENCES

1. Akagi, M. J. Pharm. Soc. Japan, **62**, 129 (1942).
2. Asahina, Y. and Shibata, S. Chem. Ber. **72**, 1531 (1939).
3. Erdtman, H. Proc. Roy. Soc. A, **143**, 191 (1934).
4. Erdtman, H. Proc. Roy. Soc. A, **143**, 228 (1934).
5. Erdtman, H. and Wachtmeister, C. A. *In* Festschrift Arthur Stoll. Birkhäuser, Basel. 1957. p. 153.
6. Gripenberg, J. Acta Chem. Scand. **12**, 1411 (1958).
7. Kögl, F. and Erxleben, H. Ann. **479**, 11 (1930).
8. Kögl, F., Erxleben, H., and Jänecke, L. Ann. **482**, 105 (1930).
9. Kraemer, G. and Spilker, A. Chem. Ber. **23**, 84 (1890).
10. Millward, B. B. and Whiting, M. C. J. Chem. Soc. 903 (1958).
11. Murray, J. J. Chem. Soc. 1345 (1952).
12. Price, C. C. and Halpern, B. D. J. Am. Chem. Soc. **73**, 818 (1951).
13. Sawicki, E. and Ray, F. E. J. Am. Chem. Soc. **75**, 2519 (1953).
14. Thomson, R. H. Naturally occurring quinones. Butterworth Scientific Publications, London. 1957.

CATALYTIC ACTIVATION OF HYDROGEN IN AQUEOUS SOLUTION BY THE CHLOROPALLADATE(II) ION[1]

J. HALPERN, J. F. HARROD, AND P. E. POTTER[2]

ABSTRACT

The kinetics of the reduction of ferric chloride by molecular hydrogen in aqueous solution, in the presence of chloropalladate(II), were examined. The latter acts as a homogeneous catalyst for the reaction. The rate-law was found to be,

$$-d[H_2]/dt = k[H_2][PdCl_4^{=}]$$

where

$$k = 6.6\times10^{11} \exp[-20{,}000/RT] \text{ liter mole}^{-1} \text{ sec}^{-1}.$$

The mechanism of the reaction is discussed.

INTRODUCTION

Metallic palladium is readily precipitated from aqueous solutions of palladous chloride by reduction with hydrogen. Ipatieff and Tronev (1) found this reaction to be autocatalytic, in line with the well-known heterogeneous catalytic activity of palladium for hydrogenation reactions in general. However, when oxidizing substrates such as ferric chloride were present in the solution, precipitation of the palladium was preceded by an induction period during which the substrate underwent reduction. Since metallic palladium apparently was absent during this stage, this observation suggests that the dissolved palladium salt may be acting as a homogeneous catalyst for the hydrogenation of the substrate. This paper describes a kinetic study of the reaction, the results of which confirm this view.

Previously, the ability to activate hydrogen homogeneously and catalyze its reactions in solution has been demonstrated for ions and complexes of only a few other metals notably copper, silver, mercury, and cobalt (2, 3). Importance has been attached to the study of these systems, not only for their intrinsic interest, but also because of the insight they provide into the mechanism of action of related heterogeneous and enzymic catalysts, which often cannot be elucidated directly because of their greater chemical and kinetic complexity (4).

EXPERIMENTAL

Hydrated palladous oxide, precipitated with NaOH from a solution of reagent grade palladous chloride and washed thoroughly, was dissolved in 3 *M* HCl to give a stock solution of H_2PdCl_4. The concentration of palladium was determined by precipitation with dimethylglyoxime. Hydrogen was obtained from Canadian Liquid Air Co., passed through a "deoxo" catalytic purifier to remove oxygen, and dried over P_2O_5. Other chemicals were of reagent grade.

Several procedures for making the desired kinetic measurements were examined. The most satisfactory of these proved to be the determination of the rate of catalytic reduction

[1]*Manuscript received May 19, 1959.*
Contribution from the Department of Chemistry, University of British Columbia, Vancouver, B.C. Support of this work through grants from the National Research Council of Canada and Imperial Oil Limited is gratefully acknowledged.

[2]*Present address: Inorganic Chemistry Department, Imperial College of Science and Technology, London S.W.7, England.*

of ferric chloride by measuring the volume of hydrogen taken up at constant pressure. The results reported in this paper were obtained by this method, the details of which have been previously described (5). An attempt was also made to examine the kinetics of the catalyzed reduction of dichromate by the procedure used earlier to study the activation of hydrogen by silver salts (6), that is, bubbling hydrogen through the solution and following the decrease in dichromate concentration spectrophotometrically. The overlap of the palladium and dichromate absorption bands and the tendency of metallic palladium (a powerful heterogeneous catalyst) to form prior to complete reduction of the dichromate, limited the accuracy of this procedure but, on the whole, the results obtained by the two methods were in satisfactory accord.

RESULTS AND DISCUSSION

The kinetics of the reduction of ferric chloride, in the presence of palladium chloride, were found to be,

$$[1] \qquad -d[H_2]/dt = k[H_2][PdCl_4^=].$$

Typical rate plots showing the uptake of H_2 are given in Fig. 1. Since the concentrations of $PdCl_4^=$ and of H_2 remain constant while ferric chloride is being reduced the kinetics are of pseudo zero-order. Reduction of palladous chloride itself commenced only when reduction of $FeCl_3$ to $FeCl_2$ was nearly complete and was marked by an increase in the rate of H_2 uptake due to autocatalysis by metallic Pd; prior to this point the reaction is apparently homogeneous.

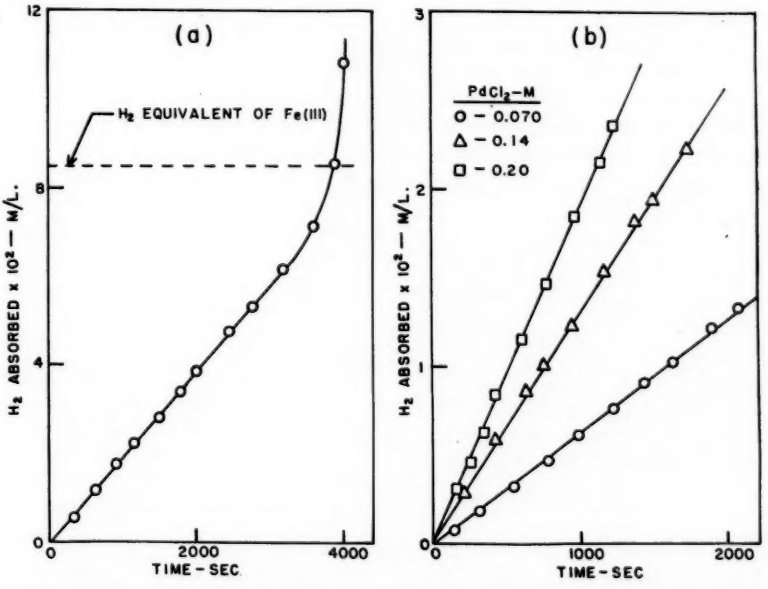

FIG. 1. Typical rate plots at 80°, 450 mm H_2. (*a*) 0.20 *M* $PdCl_2$, 0.17 *M* $FeCl_3$; reduction of $FeCl_3$ carried to completion; (*b*) 0.2 *M* $FeCl_3$, various $PdCl_2$ concentrations.

The kinetic results in Table I are in accord with equation [1]. Values of k, determined from the slopes of the zero-order rate plots using equation [1], are seen to be substantially independent of the initial concentrations of $FeCl_3$, $PdCl_2$, and H_2 over a considerable

range of each. The concentration of H_2 was calculated using the solubility data of Wiebe and Gaddy (7), correcting for the effect of HCl. The latter correction (−18% for 3 *M* HCl) was based on room temperature data (8) but it is unlikely that the error due to this is appreciable.

TABLE I

Summary of kinetic data at 80° C

$[PdCl_4^=]$ (molar)	H_2 (mm)	$[H_2]\times10^4$ (molar)[a]	Initial $[FeCl_3]$ (molar)	Medium	Rate of H_2 uptake $\times10^6$ (mole liter^{-1} sec^{-1})	k (liter mole^{-1} sec^{-1})
0.070	450	3.6	0.20	3 *M* HCl	7.0	0.28
0.113	450	3.6	0.20	3 *M* HCl	11.5	0.28
0.141	450	3.6	0.20	3 *M* HCl	12.5	0.25
0.141	450	3.6	0.10	3 *M* HCl	12.9	0.25
0.188	450	3.6	0.20	3 *M* HCl	17.3	0.26
0.226	450	3.6	0.20	3 *M* HCl	21.5	0.26
0.203	436	3.5	0.15	3 *M* HCl	20.0	0.28
0.203	340	2.7	0.15	3 *M* HCl	14.7	0.27
0.203	275	2.2	0.15	3 *M* HCl	12.8	0.29
0.203	190	1.5	0.15	3 *M* HCl	8.1	0.26
0.203	70	0.5	0.15	3 *M* HCl	3.0	0.27
0.203	450	3.6	0.15	5 *M* HCl	20.7	0.28
0.203	450	3.6	0.15	3 *M* HCl; 2 *M* NaCl	14.9	0.20
0.203	450	3.6	0.15	3 *M* HCl; 2 *M* $NaClO_4$	20.1	0.28
0.203	450	3.6	0.15	3 *M* HCl; 2 *M* $HClO_4$	25.7	0.35

[a]Based on estimated solubility of H_2 in 3 *M* HCl, 6.1×10^{-4} mole atm^{-1}. Data for other media not corrected for variation in solubility.

Varying the HCl concentration from 3 *M* to 5 *M* had no effect on k. Since the predominant palladium species in this region is the chloropalladate(II) ion, $PdCl_4^=$ (9), it appears probable that this is the catalytic species. Addition of 2 *M* $NaClO_4$ was also without effect on the rate while 2 *M* NaCl decreased, and 2 *M* $HClO_4$ increased, the rate slightly. These effects are small and attributable to changes in the solubility of hydrogen since they follow the same pattern as do the activity coefficients of non-electrolytes in general (10, 11).

At HCl concentrations below 3 *M* erratic results were obtained because of the tendency of metallic palladium to form (resulting in complications due to heterogeneous catalysis) prior to complete reduction of the substrate. Similar complications were encountered in experiments using $Pd(ClO_4)_2$ in perchloric acid solution. While these experiments failed to yield quantitative information, it was possible to conclude qualitatively that the catalytic activities of the uncomplexed Pd^{++} ion and the lower chloride complexes are lower than that of $PdCl_4^=$; this was also the case for the ethylenediamine complex.

Kinetic measurements at temperatures ranging from 66 to 87.5° yielded the Arrhenius plot in Fig. 2, fitted by the equation,

$$k = 6.6\times10^{11}\exp[-20{,}000/RT] \text{ liter mole}^{-1}\text{ sec}^{-1}.$$

The frequency factor corresponds to an entropy of activation of −6.8 e.u.; this value is in the normal range for a simple bimolecular reaction in solution, and suggests that there is little charge redistribution during formation of the activated complex.

The kinetics described above resemble those found previously for the activation of hydrogen by Cu^{++}, Ag^+, Hg^{++}, and their complexes (2, 12). In a number of these systems it has been shown that the rate-determining step involves heterolytic splitting of H_2

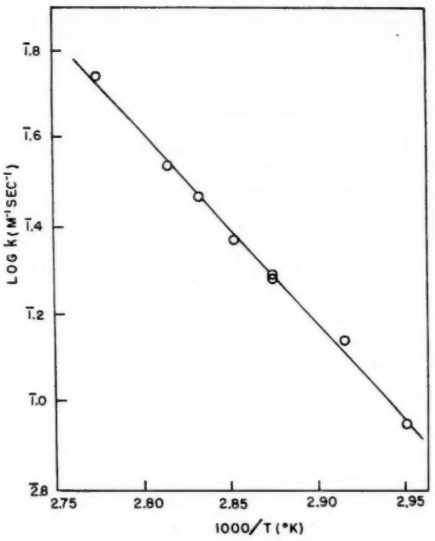

FIG. 2. Arrhenius plot for k.

by the catalytic species* with the formation of a catalyst–hydride complex which is reoxidized in a subsequent rapid reaction with the substrate. It seems likely that the present reaction also proceeds through this type of mechanism, that is,

$$PdCl_4^{=} + H_2 \xrightarrow{k} HPdCl_3^{=} + HCl \qquad [2]$$

$$HPdCl_3^{=} + 2FeCl_3 \xrightarrow{\text{fast}} PdCl_4^{=} + HCl + 2FeCl_2. \qquad [3]$$

Attempts have been made to correlate the catalytic activities of metal ions and complexes with their electron configurations (13, 4). Thus, most of the metal ions which have been found to activate hydrogen in solution have nearly filled or just filled d-shells, and it has been suggested that their catalytic activity is related to their high electron affinities. Attention has also been directed (13, 4) to a link between catalytic activity in homogeneous and heterogeneous systems, suggested by the observation that most of the ions which are catalytically active in solution are "isoelectronic" with metals (Ni, Co, Pd, Pt, etc.) which are good heterogeneous hydrogenation catalysts. The appearance of catalytic activity for a complex of Pd^{++} ($4d^8$; isoelectronic with Ru) is consistent with this pattern. Attention should also be directed to the striking parallel between the postulated hydride intermediate, $HPdCl_3^{=}$, and the electronically analogous complexes of the type $HPtCl(PR_3)_2$, described by Chatt (14).

REFERENCES

1. IPATIEFF, V. V., JR. and TRONEV, V. G. Compt. rend. acad. sci. U.R.S.S. **1**, 624 (1935).
2. HALPERN, J. Quart. Revs. (London), **10**, 463 (1956).
3. WELLER, S. and MILLS, G. A. Advances in Catalysis, **8**, 163 (1956).
4. HALPERN, J. Advances in Catalysis. (In press).

**In the case of* Ag^+, *there is also an alternative path of activation, second-order in* Ag^+, *probably involving homolytic-splitting of* H_2 *in the rate-determining step (12).*

5. CHALK, A. J. and HALPERN, J. J. Am. Chem. Soc. (In press).
6. WEBSTER, A. H. and HALPERN, J. J. Phys. Chem. **60**, 280 (1956).
7. WIEBE, R. and GADDY, V. L. J. Am. Chem. Soc. **56**, 76 (1934).
8. SEIDELL, A. Solubilities of inorganic and metal organic compounds. Vol. 1. 3rd ed. D. Van Nostrand Co., Inc., New York. 1940. p. 557.
9. DROLL, H. A., BLOCK, B. P., and FERNELIUS, W. C. J. Phys. Chem. **61**, 1000 (1957).
10. RANDALL, M. and FAILEY, C. F. Chem. Revs. **4**, 271 (1927).
11. AKERLOF, G. J. Am. Chem. Soc. **57**, 1196 (1935).
12. WEBSTER, A. H. and HALPERN, J. J. Phys. Chem. **61**, 1239, 1245 (1957).
13. HALPERN, J. J. Phys. Chem. **63**, 398 (1959).
14. CHATT, J., DUNCANSON, L. A., and SHAW, B. L. Proc. Chem. Soc. 343 (1957); Chem. & Ind. 859 (1958).

RELATIONS BETWEEN HEATS OF FORMATION FOR INORGANIC SYSTEMS[1]

A. D. WESTLAND

ABSTRACT

Some empirical relationships dealing with the heats of formation of crystalline compounds are interrelated. A more general relation based upon functions derived from heats of formation and applicable to dissolved species as well as crystals is described. The relation may be used as a criterion for thermal data and for estimation of heats of formation. Deviations of literature values from those predicted by the relation are discussed in the light of structural features.

In recent years a number of empirical relations have been found to exist concerning heats of formation or lattice energies of crystalline ionic compounds (1–5). While presenting one of these (4), Hoppe showed it to be a more general case of the relation discovered by Fomin (3). It is the purpose of this paper to show that both of these relations and that of Karapet'yants (5) are special cases of a more general one.

Hoppe derived his method from certain theoretical considerations which were, however, in error. He supposed that the quantity

$$[1] \qquad \nabla^*(\mathrm{F,O})_{\mathrm{Me}} = -\frac{\Delta H^*(\mathrm{MeF}_{2z})}{\text{equivalents}} - \frac{\Delta H^*(\mathrm{MeO}_z)}{\text{equivalents}}$$

in which ΔH^* is the heat of formation of the compound from gaseous atoms in their ground states, would be invariant for the fluorides and oxides of various metals, Me, providing non-coulombic contributions to the lattice bonding are not involved. The conclusion drawn from this was that ∇^*-functions for various series of compounds of a given set of cations would yield a straight line if plotted one against the other. For example, one might plot ∇^*-functions for the nitrates of group I and II metals against the ∇^*-functions for the chlorides of the same metals. The second term in the expression for ∇^* may be taken as the thermal datum for the oxide in each case. Linearity was indeed observed.

The linearity is more correctly rationalized as follows: If we express ΔH^* by means of the Born–Haber cycle using the fundamental electrostatic expressions of Born, we have

$$[2] \qquad -\Delta H^* = \frac{NAe^2}{r^+ + r^-} + \frac{B}{(r^+ + r^-)^n} + \frac{C}{(r^+ + r^-)^6} - I + E - D$$

in which N is Avogadro's number, e is the charge on the ions in electrostatic units, A is the Madelung factor, B is a constant, C is a function of the ionic polarizabilities and zero-point frequencies, I is the sum of the ionization potentials of the metal, E is the electron affinity of the non-metal, D is the dissociation energy of the non-metal, r^+ is the cation radius, r^- is the anion radius, and n is the so-called Born exponent. Upon substitution of this in equation [1], the I terms disappear by subtraction and in plotting one ∇^*-function against another, the $E-D$ terms make up the constant of linearity. Otherwise the ∇^*-functions consist of a linear combination of terms of the form: $(r^+ + a)^{-p}$ where r^+ is a variable taking the values of the radii of the various cations and a is the constant anion radius. The exponent p may have the values 0, n, or 6. The corresponding terms of ΔH^* have decreasing significance in this order.

[1]*Manuscript received March 9, 1959.*
Contribution from the Department of Chemistry, University of Ottawa, Ottawa, Ontario.

Two functions $(r^+ + a_1)^{-p}$ and $(r^+ + a_2)^{-p}$ will be in approximately linear relation one to another, that is the slope at various points of a plot of one function against the other for corresponding values of r^+ will be approximately constant, if

$$[3] \qquad \frac{d(r^+ + a_1)^{-p}}{d(r^+ + a_2)^{-p}} = \left(\frac{r^+ + a_2}{r^+ + a_1}\right)^{p+1}$$

is essentially constant. It follows that the same condition leads to linearity between ∇^*-functions. For $p = 1$ the change in the derivative is never large over the range of values of r^+, a_1, and a_2 encountered in practice. One can easily see upon inserting the ionic radii of alkali halides, oxides, etc., that the maximum change in passing from lithium to caesium amounts to 18%. In terms of the slope of a curve this is not a large change. Thus if a line is being drawn through experimental points governed by this function a departure from linearity is hardly noticed. However, the terms containing higher values of p result in expressions giving plots which are slightly less satisfactory approximations to straight lines.

Since $\nabla^*(F,O)_{Me}$ is not invariant for various metals, Hoppe concluded that there is a certain amount of non-coulombic bonding present. He maintained further that the ∇^*-function is a measure of such non-coulombic bonding. The above development shows that the ∇^*-function indicates not so much departure from purely ionic bonding; rather it simply reflects the change in ionic size.

It is evident that Hoppe's relation is unnecessarily complicated. It is sufficient to plot the quantities ΔH^{**} defined by

$$[4] \qquad -\Delta H^{**} = (-\Delta H_f + S + I)/\text{equivalents}$$

in which ΔH_f is the heat of formation of the compound from the elements in their standard states and S is the sublimation energy of the metal component. This has the advantage that only one thermochemical quantity is required in addition to S and I. The last two quantities are known for most metals to a sufficient degree of accuracy, for good plots are obtained in general. An error of a few per cent in S or I has a negligible effect on the plots in practice.

We are now in a position to compare Hoppe's device with that of Karapet'yants. The latter plotted lattice energies in the same manner that Hoppe plotted ∇^*-functions and obtained straight line plots for compounds of elements in the same valence state. That is, he obtained a straight line for compounds of univalent elements, a different one for bivalent elements, and so on.

By plotting ΔH^{**}-values one combines the two methods to give a more general one. Moreover, since $(r^+ + r^-)^{-p}$ is symmetrical in r^+ and r^-, it follows that series of compounds each containing a common cation instead of a common anion could be employed for setting up a linearity relation. This may be done by defining

$$[5] \qquad -\Delta H^{**} = (-\Delta H_f + D - E)/\text{equivalents}.$$

A better approximation to a straight line plot is possible. If one plots the logarithm of the lattice energies per equivalent, the slope is still more nearly constant in a given case because the exponent p in $(r^+ + a)^{-p}$ is no longer significant, for the expression analogous to [3] is

$$[6] \qquad \frac{d \log (r^+ + a_1)^{-p}}{d \log (r^+ + a_2)^{-p}} = \frac{r^+ + a_2}{r^+ + a_1}.$$

Plots of this sort are shown in Figs. 1 and 2.[2] In the first figure the lines were drawn so as

[2]*These and other heats of formation were taken from the National Bureau of Standards Circular 500.*

to fit the points of the group II metals best. Departure from the line may be expected when there is considerable covalent contribution to the bonding.

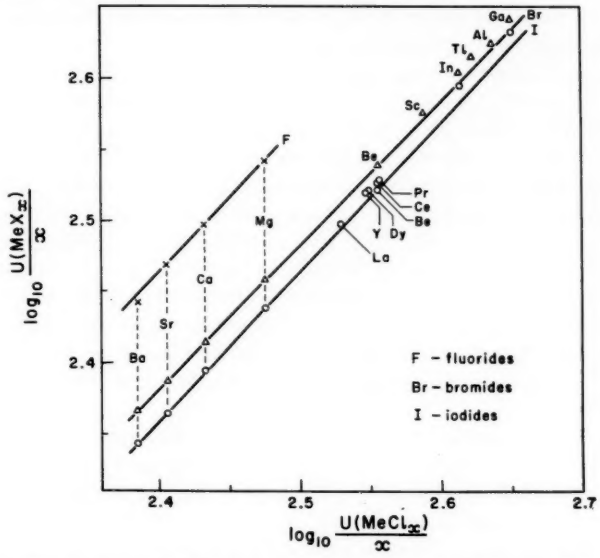

FIG. 1. Logarithmic plots of the lattice energies of fluorides, bromides, and iodides of bi- and ter-valent ions against the lattice energies of the chlorides.

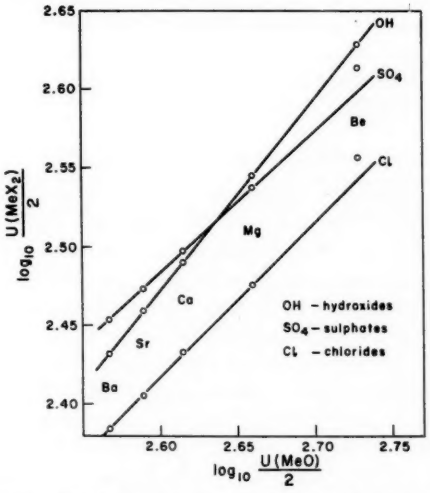

FIG. 2. Logarithmic plots of lattice energies: hydroxides, sulphates, and chlorides of group II*a* elements against the corresponding oxides.

It might be expected that the relation is only as good as the Born equation for lattice energy. It appears to be very much better, however. Thus the form of the Born equation would lead one to expect that the crystal structure, i.e. the value of the Madelung con-

stant, would have to be the same along a series of compounds. Such is not necessarily the case. This is demonstrated in Fig. 2. Thus even though all the group II*a* metal oxides with the exception of BeO have the same crystal structure, this is not true of the sulphates and chlorides for example. Here the magnesium and calcium compounds differ in structure but there is no irregularity in the plots due to this.

It is evident that the difference in the energy due to change in the Madelung factors of the chlorides from magnesium to barium is compensated by some other effect(s). The difference in the Madelung factors of $CaCl_2$ and $MgCl_2$ is not great, so that it would appear that the alteration in ionic radius with change in co-ordination (6) could account for the compensation. The change in co-ordination in this instance is from the asymmetric environment of the chloride ions in $MgCl_2$ to the symmetric environment in $CaCl_2$ and $SrCl_2$. In passing from $SrCl_2$ to $BaCl_2$ there is an increase in co-ordination number; this would be accompanied by an increase in Madelung factor but also an increase of a few per cent in ionic radius. It is remarkable how small is the over-all effect of minor changes in structure. By "minor" is meant such changes as those involving only structures of high co-ordination ($\geqslant 6$). The alkali nitrates provide another example of a series involving several structure changes, but which may yet be related very satisfactorily to the corresponding halides.

If, on the other hand, a structure of 4:4 or 4:2 co-ordination appears in a series otherwise composed of structures of higher co-ordination, a major change in Madelung factor is involved. Such is the case in the series of group II oxides at beryllium. Thus the singularity at this element may be accounted for, provided that the (as yet unknown) chloride structure could be shown to have a Madelung factor close to that of the other group II chlorides. It is significant that there is no discrepancy in a plot of hydroxide and sulphide values against oxide values. In the sulphate–oxide plot there is again a discrepancy at beryllium of exactly the same magnitude as in the chloride–oxide case.

Molecular volume provides an analogous linearity relation. This may, therefore, be used in many cases such as the above-mentioned to decide whether a discrepancy is due to an experimental error or a structural singularity. If the cause is structural, this will in general be reflected in the additivity of atomic increments (7).

APPLICATIONS TO DISSOLVED SPECIES

The coulombic energy of ion–dipole attraction is proportional to $(r^+ + r^-)^{-2}$ in which r is the "thermochemical radius" (8) of the dipole molecule. The polarization energy is proportional to $(r^+ + r^-)^{-4}$. We should therefore expect the linearity relationships to be applicable to heats of solvation (or heats of solution), and this is indeed so.

Figure 3 illustrates the relation between $-\Delta H^{**}$ for solvation of a number of ions and the $-\Delta H^{**}$-values for the corresponding crystalline chlorides. The $-\Delta H^{**}$-values for solvation were obtained by adding $S + I$ to the standard heats of formation of the aqueous ions. It should be noted that the linear relationship demands that either the number of solvent molecules co-ordinated per equivalent of charge on the ion is the same in all cases, or there is a gradual change in effective co-ordination number such that the linearity is preserved. The former condition seems improbable but the latter is quite plausible, representing one more instance of the uniformity of behavior along a series of ions.

A singularity appears in the case of lithium. The point may lie off the curve because of a large covalent contribution to the Li—O bond. This has been suggested previously in explanation of the bond length. It may be seen that the periodic groups are better con-

sidered individually, for a slightly better line could be drawn through the points of the group II*a* metals than that shown and the subgroups of the tervalent metals appear to fall on separate lines.

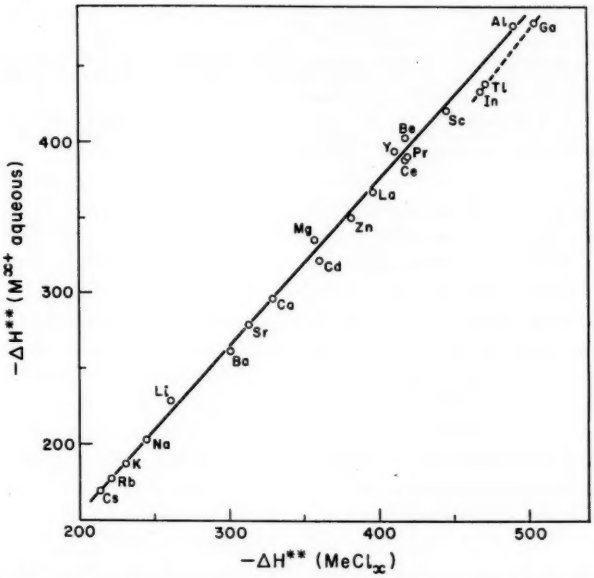

FIG. 3. Plot of $-\Delta H^{**}$-values for uni-, bi-, and ter-valent ions in the aqueous standard state against the corresponding function for anhydrous chlorides.

The heat of formation of a complex compound in aqueous solution may be combined with the solvation energy to obtain the heat of formation of the compound from gaseous ligands and ions (9). The series of group II*a*–EDTA or –citrate complexes serves to demonstrate that the linear relationship extends to these compounds as well. This is hardly a useful fact, however, as the energy of the complex is not much different than the energy of the solvated ion in all cases in which the stability constant is measurable.

REFERENCES

1. LONG, L. H. Quart. Revs. **7**, 134 (1953).
2. KAPUSTINSKII, A. F. Izvest. Akad. Nauk S.S.S.R. Otdel. Khim. Nauk, 568, 581 (1948).
3. FOMIN, V. V. Zhur. Fiz. Khim. **27**, 1689 (1953).
4. HOPPE, R. Z. anorg. u. allgem. Chem. **296**, 104 (1958).
5. KARAPET'YANTS, M. KH. Zhur. Fiz. Khim. **28**, 1136 (1954).
6. GOLDSCHMIDT, V. M. Ber. **60**, 1263 (1927).
7. BLITZ, W. Raumchemie der festen Stoffe. Verlag L. Voss, Leipzig. 1934.
8. KAPUSTINSKII, A. F. Compt. rend. acad. sci. U.R.S.S. **32**, 59 (1941).
9. GEORGE, P. Rec. trav. chim. **75**, 671 (1956).

THE PHOTOOXIDATION OF AZOMETHANE. II[1,2]

R. L. STRONG[3] AND K. O. KUTSCHKE

ABSTRACT

In a further investigation of the photooxidation of azomethane it was found that the yields of all products depend on the fractional conversion in a manner which suggests that some inhibitor is produced. Products from experiments at lower pressures of azomethane are obtained in yields appropriate to the higher conversions. Only very small changes in yields are observed for relatively large variations in light intensity. The implications of these facts to the mechanism of the photooxidation are discussed.

In an earlier investigation of the photooxidation of azomethane (1) it was postulated that formaldehyde should be a major product of the reaction. It proved impossible to detect this product, however, presumably because of the well-known tendency of the material to polymerize at temperatures below 100° C (2).

Preliminary work, indicating that formaldehyde was indeed an important product, was done as follows. The mixture of reaction products, unreacted azomethane, and oxygen was condensed at −196° C in a small side arm attached to a grease-free reaction system. After the side arm was allowed to warm to room temperature, the vapor phase was removed by pumping for several minutes and the side arm sealed off. The invisible residue in the side arm was dissolved in dilute H_2SO_4 and the chromotropic acid test (3) applied to the resulting solution. Positive identification was achieved, which was not due to hydrolysis of residual azomethane as shown by the absence of a test on the unphotolyzed mixture.

A reaction system was constructed based on this technique for the analysis of formaldehyde.

EXPERIMENTAL

The reaction system consisted of a fused quartz reaction cell (4.8 cm i.d., 10 cm long, ~180 cm^3 volume), a glass-enclosed, magnetically driven stirrer, a U-tube through which the cell contents were circulated, and connecting tubing. Reactants were introduced from storage and manometers through a stainless steel diaphragm valve (Hoke, No. 413) and led to the analytical system through a similar valve. The entire system, including the valves but excluding the U-tube, was housed in a thermostatted air oven. Gradients and fluctuations in the region of the cell were less than 1° C. Other parts of the oven had larger gradients so that temperature differences of as much as 5° C existed between the cell and other units in the oven. The U-tube, which extended through the walls of the oven, could be kept at oven temperature with heating tape or cooled to any temperature desired.

Gases were led from the reaction system through heated tubing to a removable U-tube (Dow Corning Silicone greased joints), and thence to a Hg cutoff leading to LeRoy stills (4) and a grease-free gas burette.

[1]*Manuscript received May 8, 1959.*
Contribution from the Division of Pure Chemistry, National Research Council, Ottawa, Canada.
Issued as N.R.C. No. 5290.
[2]*For Part I see ref. 1.*
[3]*National Research Council Postdoctorate Fellow 1954–55. Present address: Department of Chemistry, Rensselaer Polytechnic Institute, Troy, N.Y.*

After an exposure the products were condensed at −196° C in the U-tube of the reaction system and non-condensables (CO, O_2, N_2, and any CH_4) transferred to the gas burette, measured, and analyzed as before (1). Condensables were transferred to the removable U-tube (with the reaction system U-tube above 100° C to ensure depolymerization of formaldehyde) and the outlet valve closed. Three cycles of warming to room temperature and recondensation at −196° C in the removable U-tube followed to polymerize the formaldehyde. The cutoff to the LeRoy still (held at −196° C) was opened and the removable U-tube warmed quickly to room temperature; after 3 minutes the cutoff was closed. Blank experiments showed that this procedure resulted in complete transfer of azomethane in that no formaldehyde could be detected in unoxidized azomethane subjected to the same analysis. Had any azomethane remained, a positive test would have resulted owing to subsequent hydrolysis of the azo compound.

Carbon dioxide and nitrous oxide were removed from the LeRoy still at −155° C and submitted for mass spectrometric analysis. Usually a small amount of formaldehyde escaped polymerization and contaminated the CO_2–N_2O mixture. Formaldehyde contributes to the peak at m/e 30, which was used as the basis for the N_2O–CO_2 analysis. Since a reproducible sensitivity could not be obtained for formaldehyde in the mass spectrometer, so that a correction could not be made using the formaldehyde peak at m/e 29, it is felt that the N_2O results are slightly high. For similar reasons the subsequent formaldehyde determination may be 10–15% low.

In some experiments azomethane was removed from the LeRoy still at −100° C; the residue of liquid products were identified mass spectrometrically and gas chromatographically. The major constituents were water and methanol with the latter in much greater yield; Φ_{CH_3OH} was of the order of unity.

After separation of all other products, air was admitted to the U-tube, the tube removed, and the polymerized formaldehyde dissolved in 1 *N* H_2SO_4 (three washings, 1 cm^3 each). One cm^3 of this solution was pipetted into a 15×150-mm glass-stoppered tube, 10 drops of chromatropic acid (Eastman Kodak P230, 2.5 g dry powder in 25 cm^3 water) added, and the solution acidified with 7 cm^3 of concentrated H_2SO_4. The tube was stoppered, heated for 30 minutes in boiling water, cooled, and diluted to 50 ml in a volumetric flask. Transmission readings were taken at 570 mμ (using a reagent blank in the Beckman DU) and converted to absolute quantities with the aid of the measured extinction coefficient, 1.7×10^4, obtained with standard formaldehyde solutions.

Azomethane was obtained from Dr. L. C. Leitch of these laboratories. Traces of low-boiling impurities were removed at −119° C, while heavier material was retained at −80° C by low temperature distillation *in vacuo*; large head and tail fractions were rejected. The material retained had a vapor pressure of 6.6 mm at −80° C. Oxygen was generated by heating $KMnO_4$ and dried by passage through traps at −196° C.

The optical system—a S-500 Hanovia Hg arc, lenses, stops, and a Corning 5860 filter—produced a nearly parallel beam which filled the cell. More than 95% of the light absorbed was of wavelength 3660 Å (5). The intensity of the light could be varied by the use of neutral density filters of chromel on quartz, whose transmission was calibrated with a Beckman DU spectrophotometer at the wavelength used.

RESULTS

An attempt was made to do experiments under conditions similar to those described in the second experimental section of the earlier work (1). It became apparent, however, that the stirring was not as effective at low pressures in the present system as it had been in the earlier apparatus. This was shown by the lack of reproducibility of nitrogen yields

and the lack of effect when the stirrer was not operated. It was possible to show definitely that formaldehyde was present in large yields, although not as large as had been predicted (1). Moreover, the yield of carbon monoxide was much higher than had been found in Part I. In those experiments in which the liquid product was separated, methanol was found gas chromatographically in approximately the same yield as had been found in the earlier work. It is concluded that formaldehyde is, in fact, a major product under these conditions, but the postulated equality between formaldehyde and methanol was not found. Possibly the necessity of making the experiments at room temperature followed by heating the reaction mixture to ~100° C before analysis contributed to the lack of reproducibility.

A parameter which has received scant attention in photooxidation systems, but which is of major importance in many thermal oxidations, is that of exposure time. Hentz (6) has observed an induction period for the production of carbon monoxide in the photo-oxidation of acetone. An investigation was made of the effect of the time of exposure on the product ratios in the present system. The general form of the product–time curves is shown by the data of Fig. 1. It is difficult to state unequivocally from these data whether

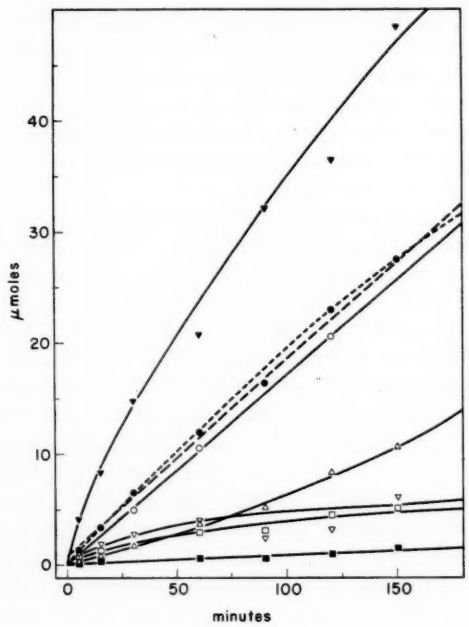

FIG. 1. Variation of products with time at 124° C. Conditions: $p_A \sim 82$ mm, $p_{O_2} \sim 11$ mm, $I_a \sim 1 \times 10^{13}$ quanta/cm³ sec. ○ N_2, $p_{O_2} = 0$; ● N_2, the dotted lines show two possible interpretations; △ CO; ▽ CH_2O; □ N_2O; ■ CO_2; ▼ O_2 consumption.

the nitrogen–time relationship is linear with a small positive intercept or whether it should be extrapolated to the origin as a curve. A careful search was made of possible nitrogen impurities in the reactants and for nitrogen formed in a thermal dark reaction. The total nitrogen expected from such sources was less than about ten per cent of the value of the apparent intercept. This is evidence for curvature in the nitrogen–time plot in the presence of oxygen.

In the absence of oxygen, but with otherwise identical initial conditions, it was observed that the yield of nitrogen was a linear function of time up to rather large fractional decompositions of the order of a few per cent. Thus the ratio of the amount of a product formed in a photooxidation to the amount of nitrogen which would have been formed had oxygen been absent is a measure of the quantum yield of that product since it has been shown that $\Phi_{N_2} = 1$ in the photolysis of azomethane (5). The quantum yields shown in Fig. 2

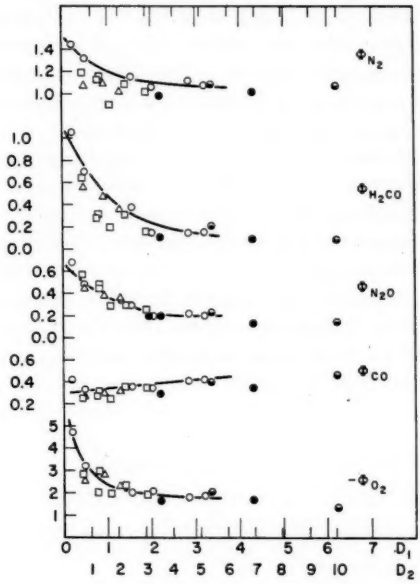

FIG. 2. Variation of product ratios with conversion at 124° C.
○ p_A 82 mm, p_{O_2} 11 mm, I_a 1×10^{13} quanta/cm³ sec.
□ p_A 82 mm, p_{O_2} 11 mm, I_a 3×10^{12} quanta/cm³ sec.
△ p_A 82 mm, p_{O_2} 11 mm, I_a 3×10^{11} quanta/cm³ sec.
● p_A 22 mm, p_{O_2} 11 mm, I_a 0.9×10^{13} quanta/cm³ sec.
◒ p_A 39 mm, p_{O_2} 11 mm, I_a 1.1×10^{13} quanta/cm³ sec.
D_1 and D_2 are approximate measures of the conversion in per cent. The smooth curves were drawn through the open circles and other points plotted later.

were obtained in this manner. The abscissae of Fig. 2 are measures, perhaps arbitrary, of the fractional decomposition of azomethane. D_1 is the ratio of the amount of molecular nitrogen plus that of nitrous oxide found to the amount of azomethane initially introduced in the reaction system (~290 cm³), while D_2 is the similar ratio based on azomethane in the cell alone (~180 cm³). The use of D_1 implies complete and instantaneous efficiency of the stirring mechanism, while D_2 assumes that the stirring is completely ineffective. With the pressures used here it is probable that D_1 is nearer to the true decomposition. Both measures are arbitrary in that it is assumed that each molecule of azomethane which is removed from the system leads either to nitrous oxide or molecular nitrogen. Later work (7) suggests that other nitrogen-containing compounds cannot account for more than 10–15% of the total azomethane disappearance. Thus it would appear that the D_1 abscissae in Fig. 2 are probably accurate to within 10–15%; the relative values are somewhat more precise, of course. Data are shown for N_2, CO, CH_2O, N_2O, and O_2

consumption. The yields of carbon dioxide were always small ($\Phi_{CO_2} \sim 0.1$) and rather badly scattered, owing more to the low value of the yield than to any other factor. For this reason the carbon dioxide data is not included in Fig. 2. No attempt was made to determine methanol in most of the experiments.

DISCUSSION

Two experimental conditions have been investigated in this work, viz., fractional decomposition and light intensity. It is apparent from an examination of Fig. 2 that a variation in light intensity by a factor of about thirty is without large effect, while an increase in the extent of conversion from $\sim 1/2$ to 1% is responsible for a pronounced decrease in the yields of all products except that of carbon monoxide. The first observation is rather surprising, although the second is, perhaps, less so.

In general terms it would seem that as the reaction progresses, some compound is formed which acts as an inhibitor to the main reaction. It is difficult to identify this inhibitor specifically. Because of the low value which has been quoted (8) for the activation energy of the reaction of methyl radicals with formaldehyde, it was thought possible that radicals in the system could react with formaldehyde thus consuming formaldehyde and possibly acting as a source of the carbon monoxide found, as has been suggested before (6, 9). Such a suggestion would, indeed, explain the results, in a qualitative way at least. Assuming that nitrous oxide arises as suggested earlier (1), a competition for radicals will be set up such as reactions [1] and [2]

$$R + CH_2O \rightarrow RH + CHO \qquad [1]$$

$$R + CH_3N_2CH_3 \rightarrow RH + CH_2N_2CH_3 \qquad [2]$$

$$CH_2N_2CH_3 + O_2 \rightarrow CH_2O + N_2O + CH_3. \qquad [3]$$

Step [3] may occur in stages involving $CH_3N_2CH_2O_2$ radicals;* R is some radical in the system. If CHO reacts with oxygen as in [4],

$$CHO + O_2 \rightarrow HO_2 + CO, \qquad [4]$$

it is expected that an induction period should be observed in the production of carbon monoxide, and that the apparent rate of production of formaldehyde should decrease so that the concentration observed approaches a stationary value in time. Moreover, as more radicals are consumed by [1], fewer are available to react in [2] so that the rate of nitrous oxide production and the chain length should decrease with fractional decomposition. If the quantum yield of oxygen consumption is taken as approximately proportional to the probability of chain propagation (reactions [2] and [3]), then both these expectations are realized qualitatively. Further work (7) to be reported later suggests that this concept, while qualitatively correct, cannot withstand quantitative examination in the light of the more extensive data available. Whatever may be the identity of the specific inhibitor produced, it seems obvious that considerable care should be exercised in the interpretation of photooxidation data in which this effect is not studied in detail.

The lack of variation of the quantum yields with intensity also presents considerable difficulties for interpretation. Jolley (10) has observed that the yields of most products from the photooxidation of diethyl ketone vary with intensity according to the equation $\Phi = a + bI_a^{-\frac{1}{2}}$. If the same type of mechanism is applicable here, the numerical value of

*The referee has pointed out that the radical $CH_3N{=}NCH_2{-}OO\cdot$ might also exist in the form $CH_3N{-}\dot{N}CH_2OO$, a formulation which enhances the plausibility of [3] as the over-all reaction.

b must be such that the second term makes a negligible contribution to the yield. The second term involves the formation of a product in a propagation reaction, such as the combination [2] and [3], along with some other reactions which oxidize methyl radicals, presumably to methoxy radicals. The first term, on the other hand, represents the same product formed in an initiation or termination reaction; because of the inverse square root dependence on intensity it would appear that termination was mutual. It is difficult to conceive of a source of nitrous oxide other than [2] and [3]. If this is in fact the sole source of nitrous oxide, then the yields of this product should be the most sensitive to changes in intensity since the first term is missing. The opposite is observed.

A possible explanation is that termination is linear in radicals, e.g., a two-step adduct formation with azomethane, with the first stage rate determining. In this case radical concentration becomes proportional to the first power of light intensity, and the yield of nitrous oxide by the mechanism suggested becomes independent of the light intensity.

A few experiments were done with lower azomethane pressures as indicated in Fig. 1. The yields at lower azomethane pressures are those appropriate to the larger conversions, as determined by extrapolation of the lower conversion data, although a trend to lower yields is just discernible at the lowest pressure for almost all the products. This would be consistent with the decreasing importance of a chain reaction at lower substrate pressures. It has been suggested (11, 12, 13) that the association of a methyl radical and oxygen requires a third body in the usual experimental conditions. The relatively slight effect of azomethane pressure on product yields, if degree of conversion is also considered, is inconsistent with this hypothesis, but the data are insufficient to permit a thorough test.

ACKNOWLEDGMENTS

The authors wish to thank Dr. E. W. R. Steacie for his advice and encouragement during this investigation. They are indebted to Mrs. Frances Kutschke and Mrs. June Garlick for the mass spectrometric analyses.

They are indebted to Dr. Calvert for a manuscript of his paper (ref. 13) prior to publication.

REFERENCES

1. HOEY, G. R. and KUTSCHKE, K. O. Can. J. Chem. **33**, 496 (1955).
2. WALKER, J. F. Formaldehyde. Reinhold Publishing Corp., New York. 1953.
3. BRICKER, C. E. and JOHNSON, H. R. Ind. Eng. Chem. Anal. Ed. **17**, 400 (1945).
4. LEROY, D. J. Can. J. Research, B, **28**, 492 (1950).
5. JONES, M. H. and STEACIE, E. W. R. J. Chem. Phys. **21**, 1018 (1953).
6. HENTZ, R. R. J. Am. Chem. Soc. **75**, 5810 (1953).
7. WENGER, F. and KUTSCHKE, K. O. Unpublished work.
8. KODAMA, S. and TAKEZAKI, Y. J. Chem. Soc. Japan, **73**, 13 (1952).
9. RALEY, J. H., PORTER, L. M., RUST, F. F., and VAUGHAN, W. E. J. Am. Chem. Soc. **73**, 15 (1951).
10. JOLLEY, J. E. J. Am. Chem. Soc. **79**, 1537 (1957).
11. HOARE, D. E. and WALSH, A. D. Trans. Faraday Soc. **53**, 1102 (1957).
12. CHRISTIE, M. I. Proc. Roy. Soc. A, **244**, 411 (1958).
13. SLEPPY, W. C. and CALVERT, J. G. J. Am. Chem. Soc. **81**, 769 (1959).

THE REACTION OF METHYL RADICALS WITH FORMALDEHYDE[1]

A. R. BLAKE[2] AND K. O. KUTSCHKE

ABSTRACT

The pyrolysis of di-*t*-butyl peroxide has been reinvestigated and used as a source of methyl radicals to study the abstraction reaction between methyl radicals and formaldehyde. At low [HCHO]/[peroxide] ratios the system was simple enough for kinetic analysis, and a value of 6.6 kcal/mole was obtained for the activation energy. At higher [HCHO]/[peroxide] ratios the system became very complicated, possibly due to the increased importance of addition reactions.

INTRODUCTION

The reaction between methyl radicals and formaldehyde has been previously studied by Kodama and Takezaki (1) and by Toby and Kutschke (2), who used the photolysis of azomethane as a source of methyl radicals. They obtained values of 5.6 and 6.2 kcal/mole, respectively, for the activation energy of the process. It seemed desirable to re-investigate the reaction using the pyrolysis of di-*t*-butyl peroxide as a source of methyl radicals. This source possesses the advantage that there is little abstraction reaction between methyl radicals and the molecule which produces the radicals.

EXPERIMENTAL

Methyl radicals were produced by the pyrolysis of di-*t*-butyl peroxide in a Pyrex glass reaction vessel (volume = 550 cm^3) the temperature of which was controlled to within 0.1° C. To start the reaction the reactants were expanded into the cell from a preheater maintained at 80° C, at which temperature no measurable decomposition of the peroxide took place in a period of 30 minutes. The reaction was stopped by expansion into a liquid-nitrogen-cooled trap. The products were analyzed by conventional methods. CH_4 and CO were separated from the remaining products at −210° C, and the CO measured as CO_2 after oxidation in a copper oxide furnace at 260° C. Methane was removed directly from the furnace and measured. Ethane was distilled from Ward stills at −180° C. The purity of each fraction was checked mass spectrometrically in some experiments. The remaining mixture of liquid products and unreacted starting materials was removed for further analysis. Liquid product analyses for acetone, *t*-butanol, and acetaldehyde were carried out gas chromatographically on a 10-ft column consisting of 30% nonyl-phthalate on firebrick, with a small proportion of polyethylene glycol added to the phthalate to cut down tailing of the peaks. No substances were detected other than the residual reactants and those products for which analyses are given.

Di-*t*-butyl peroxide, from the Novadel-Agene Corporation, contained traces of acetone and methanol and approximately 1/2% *t*-butanol. The first two were entirely removed by chromatographic purification; the *t*-butanol content was reduced to < 0.1% by this treatment. Isobutane was Phillips Research Grade. Formaldehyde was prepared by heating α-polyoxymethylene followed by distillation *in vacuo*. All these materials were thoroughly outgassed before use.

[1]*Manuscript received May 14, 1959.*
Contribution from the Division of Pure Chemistry, National Research Council, Ottawa, Canada. Issued as N.R.C. No. 5289.
[2]*National Research Council Postdoctorate Fellow 1957–59.*

RESULTS AND DISCUSSION

In preliminary experiments the pyrolysis of di-*t*-butyl peroxide was reinvestigated in the temperature range 101–145° C, alone and in the presence of isobutane. The mechanism for the decomposition is well established (3)

$$\text{peroxide} \rightarrow 2(CH_3)_2CO \qquad [1]$$

$$(CH_3)_2CO \rightarrow CH_3 + (CH_3)_2CO \qquad [2]$$

$$2CH_3 \rightarrow C_2H_6 \qquad [3]$$

$$CH_3 + \text{peroxide} \rightarrow CH_4 + \text{radical} \qquad [4]$$

$$CH_3 + \text{radical} \rightarrow \text{stable products} \qquad [5]$$

$$CH_3 + CH_2 - CH(CH_3) - CH_3 \rightarrow CH_4 + CH_2 - C(CH_3) - CH_3. \qquad [6]$$

Peroxide Alone

The results for the decomposition of peroxide alone are given in Table I. Assuming

TABLE I

Pyrolysis of di-*t*-butyl peroxide

Temp., °C	Peroxide, initial, mm	Time, sec	C_2H_6, μmole	CH_4, μmole	k_1, 10^{-4} sec^{-1}	$k_4/k_3^{\frac{1}{2}}$, (mole cm^{-3})$^{-\frac{1}{2}}$ sec$^{-\frac{1}{2}}$
103.2	18.5	9888	3.30	0.06	0.0056	0.018
111.9	12.0	6467	3.55	0.09	0.0203	0.051
116.4	14.3	3700	4.85	0.12	0.0417	0.070
116.6	13.2	3032	3.55	0.13	0.0410	0.097
120.2	14.3	2704	5.52	0.12	0.0639	0.074
120.5	14.4	2702	4.31	0.12	0.0639	0.090
122.3	13.9	4038	10.2	—	0.084	—
128.9	13.3	1430	6.90	0.33	0.174	0.23
129.5	13.2	1746	9.70	0.17	0.198	0.107
135.2	13.0	700	7.55	0.32	0.392	0.370
138.5	13.8	450	8.00	0.06	0.600	0.080
141.8	16.0	800	20.0	0.30	0.770	0.170
143.2	21.4	488	20.8	0.26	0.970	0.140
145.4	10.1	484	12.3	0.28	1.24	0.189

every molecule of peroxide decomposed gives rise to a molecule of ethane or methane then:

$$k_1 = \frac{1}{t} \ln \frac{a}{a - x}$$

and

$$\frac{R_{CH_4}}{R_{C_2H_6}^{\frac{1}{2}}} = \frac{k_4}{k_3^{\frac{1}{2}}} \cdot \frac{1}{[\text{peroxide}]}$$

where a is the initial peroxide concentration, x the amount of methane and ethane formed, and t the time. A plot of log k_1 against $1/T$ is given in Fig. 1. This leads to a rate constant, $k_1 = 2.5 \times 10^{16} \exp(-38{,}700/RT)$ sec^{-1}, in excellent agreement with those previously determined (3, 4, 5, 6, 7, 8). The amount of methane formed in the reaction was small (usually less than 3% of the ethane) and analysis was difficult. An approximate estimate of $E_4 - \frac{1}{2}E_3$ gave 14.5±2.5 kcal/mole. The correspondence between acetone

formation and total methyl radical recovery was good (Table II).* No *t*-butanol was detected in any experiments

TABLE II

Acetone formation in the pyrolysis of di-*t*-butyl peroxide

Temp., °C	% decomposition of peroxide	Acetone, μmole	$2C_2H_6 + CH_4$, μmole	Divergence, %
119.3	1.52	4.00	4.06	1.5
119.1	1.26	5.64	5.47	3
102.5	0.63	1.35	1.30	3.8
131.5	3.0	3.76	3.76	0

Peroxide in the Presence of Isobutane

These experiments were performed in order to establish that our experimental system produced the same value for E_6 as had been determined by other methods. The results are presented in Table III, and the Arrhenius plot in Fig. 2. The value of $E_6 - \frac{1}{2}E_3 = 7.7$ kcal/mole is in good agreement with the value of 7.6 found by Trotman-Dickenson and

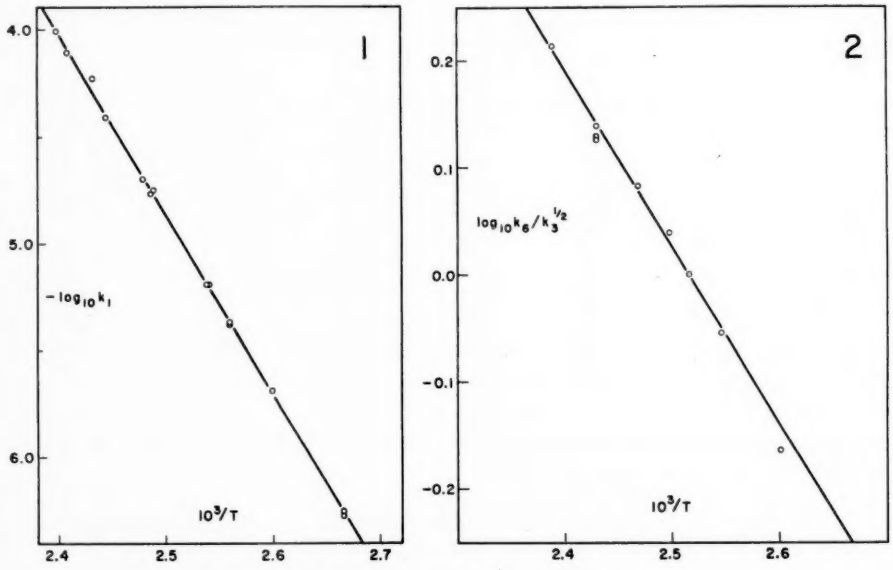

FIG. 1. Arrhenius plot for the pyrolysis of di-*t*-butyl peroxide.
FIG. 2. Arrhenius plot for the reaction of methyl radicals with isobutane.

Steacie (9) from the photolysis of acetone. It is higher than the values of Rebbert and Steacie (10), 7.3 kcal/mole, from the photolysis of $Hg(CH_3)_2$, and Jones and Steacie (11), 6.7 kcal/mole, from the photolysis of azomethane.

*Recently Alexandrova, Yu. A., Yui-Li, K., Pravednikov, A. N., and Medvedev, S. S. (*Doklady Akad. Nauk, S.S.S.R.* **123**, *1029 (1958)) have suggested that acetone can be formed in a bimolecular reaction of t-butoxy radicals, the other product being methyl isobutyl ether. The concentration range (> 0.2 mole/l. in isopropyl benzene solution) in which the effect of this reaction was observed, the lack of methyl isobutyl ether among the products in the present work, and the good balance between acetone and hydrocarbon products found here all suggest that the bimolecular reaction is not of importance in our experimental conditions.*

TABLE III

Pyrolysis of di-*t*-butyl peroxide isobutane mixtures

Temp., °C	Peroxide, 10^{-6} mole/cc	Isobutane, 10^{-6} mole/cc	R_{CH_4}, 10^{-12} mole/cc sec	$R_{C_2H_6}$, 10^{-12} mole/cc sec	$k_6/k_3^{\frac{1}{2}}$, (mole cm^{-3})$^{-\frac{1}{2}}$ sec$^{-\frac{1}{2}}$
145.5	0.280	1.89	13.2	17.4	1.63
137.5	0.391	0.233	1.97	17.2	1.62
137.4	0.330	0.218	1.45	12.5	1.52
137.5	0.265	0.386	2.02	10.0	1.47
137.4	0.273	0.919	13.2	17.4	1.34
137.8	0.326	1.18	3.92	9.15	1.33
137.4	0.306	2.94	5.05	9.45	1.38
131.3	0.330	1.63	3.73	3.35	1.21
126.4	1.22	0.57	2.89	1.48	1.10
124.0	0.292	1.60	1.92	1.42	1.00
119.5	0.310	1.64	1.04	0.526	0.875
111.3	0.330	1.60	0.462	0.173	0.68

It was found that at low isobutane pressures $k_6/k_3^{\frac{1}{2}}$ decreased with increasing isobutane pressure, but above 20 mm Hg there was no change with increasing pressure. Consequently all rate measurements were made above this pressure.

Peroxide in the Presence of Formaldehyde

At low formaldehyde/peroxide ratios (below 0.2, except at high temperatures), the following simple mechanism is obeyed

$$CH_3 + HCHO \rightarrow CH_4 + CHO \quad [7]$$

$$CHO + CH_3 \rightarrow CH_4 + CO \quad [8]$$

$$CHO + CH_3 \rightarrow CH_3CHO \quad [9]$$

along with reactions [1] to [5]. This leads to the expression

$$[I] \qquad R_{CH_4}/R_{C_2H_6}^{\frac{1}{2}} = (k_7/k_3^{\frac{1}{2}})\,[HCHO]\,(1+k_8/(k_8+k_9)).$$

Acetaldehyde is formed in the reaction at low pressures in very small quantities, the value of R_{CH_3CHO}/R_{CO} being < 0.10. Therefore $k_8/(k_8+k_9)$ can be approximated by unity. This approximation will have little effect on the activation energy as the term will certainly have a small temperature coefficient. Throughout this work we have used the approximate expression

$$[II] \qquad R_{CH_4}/R_{C_2H_6}^{\frac{1}{2}} = 2(k_7/k_3^{\frac{1}{2}})\,[HCHO].$$

We consider that reaction [10] probably does not play an important role in the over-all

$$2CHO \rightarrow HCHO + CO \quad [10]$$

reaction scheme, as the methyl radical concentration, as estimated from the absolute rate of ethane formation, is high throughout. It is difficult to check this point in a satisfactory manner experimentally. Table IV shows the experimental results at low formaldehyde/peroxide ratios, and in Fig. 3 the data are plotted according to equation [II]. The Arrhenius plot is given in Fig. 4. This leads to a rate equation

$$k_7/k_3^{\frac{1}{2}} = 3.8\times10^4 \exp(-6600/RT)\ (\text{mole cm}^{-3})^{-\frac{1}{2}}\ \text{sec}^{-\frac{1}{2}}.$$

The activation energy is in good agreement with the value of 6.2 kcal/mole obtained by Toby and Kutschke (2). It is interesting to compare it with the 6.8 kcal/mole obtained

TABLE IV

The pyrolysis of di-*t*-butyl peroxide in the presence of formaldehyde

Temp., °C	f/p*	R_{CH_4}	$R_{C_2H_6}$	R_{CO}	R_{CH_3CHO}	R_{H_2}	$R_{CH_4}/R_{C_2H_6}^{\frac{1}{2}}[P]$
		10^{-11} mole/cm³ sec					(mole cm^{-3})$^{-\frac{1}{2}}$ sec$^{-\frac{1}{2}}$
147.3	0.197	1.03	3.64	0.580			5.65
147.3	0.360	1.66	3.05	—			10.2
147.2	0.396	1.86	3.25	—			10.7
147.2	0.630	2.27	2.57	1.60			17.2
142.5	0.097	1.24	2.28	0.680			3.74
142.5	0.275	2.64	3.20	1.42			7.60
142.2	0.430	1.41	1.43	0.740			12.4
142.2	0.702	1.97	1.16	1.09			18.7
142.2	1.15	3.14	1.27	1.76			26.0
134.5	0.089	0.530	1.68	0.272			2.21
134.5	0.360	0.700	1.48	0.360			3.25
134.7	0.510	1.05	1.39	0.510			4.75
128.2	0.045	0.360	1.31	0.195			0.98
128.9	0.042	0.623	1.91	0.312			1.12
129.0	0.088	0.500	1.09	0.276			1.93
129.0	0.114	0.820	1.21	0.425			2.20
128.9	0.189	0.980	1.07	0.540			3.50
122.1	0.0341	0.656	1.57	0.336			0.670
122.7	0.0415	0.740	1.55	—			0.810
122.2	0.0650	1.10	1.33	0.630			1.16
122.0	0.0625	1.20	1.38	0.670			1.17
122.2	0.100	1.50	1.09	0.820			1.71
142.2	0.430	1.41	1.43	0.609	0.31	0.04	12.4
143.5	0.949	2.59	1.36	1.46	0.34	0.08	21.1
142.2	1.153	3.14	1.25	1.76	0.58	0.18	26.1
142.0	2.825	3.22	0.338	2.34	0.47	0.32	54.5
123.7	0.473	0.247	0.867	0.151	0.05	0.01	8.80
123.7	0.788	0.327	0.658	0.224	0.06	0.01	12.2
123.5	1.809	0.445	0.402	0.327	0.06	0.04	21.8

*f/p = [HCHO]/[peroxide] initial.

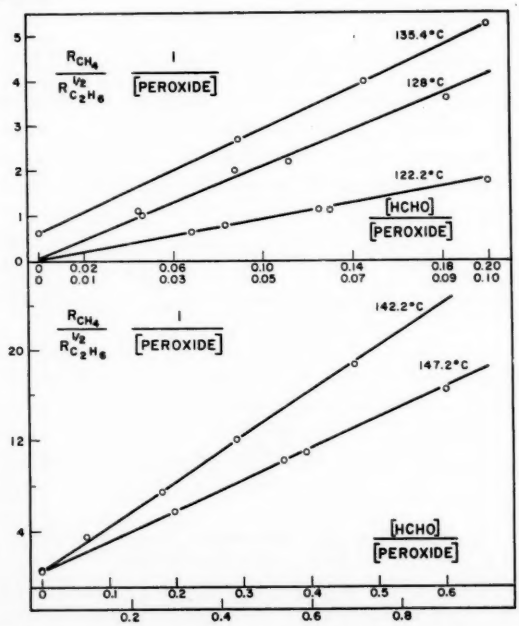

FIG. 3. The pyrolysis of peroxide and formaldehyde at low formaldehyde/peroxide ratios. 147.2° C, lower abscissa scale; 142.2° C, upper abscissa scale; 135.4° C, upper abscissa scale, ordinate origin at 0.5 scale units; 128° C, upper abscissa scale; 122.7° C, lower abscissa scale.

by Ausloos and Steacie (12) for the corresponding reaction with acetaldehyde. Hoare (13) has also determined $k_7/k_3^{\frac{1}{2}}$ at 120° C. He obtained 10.1 (mole cm^{-3})$^{-\frac{1}{2}}$ sec$^{-\frac{1}{2}}$ compared with our value of 7.9 (mole cm^{-3})$^{-\frac{1}{2}}$ sec$^{-\frac{1}{2}}$ at the same temperature.

At higher HCHO/peroxide ratios the system becomes very complicated. Measurable amounts of hydrogen and acetaldehyde are produced and the plots of $R_{CH_4}/R^{\frac{1}{2}}_{C_2H_6}$[peroxide] against [HCHO]/[peroxide] show a very marked deviation from linearity (see, for example, Fig. 5). Some data are shown in the second part of Table IV. This last observation has been made previously in other systems by Brinton and Volman (5) in the reaction between methyl radicals and ethylene imine and by Brinton (14) in the reaction between methyl radicals and ethylene. It seems clear that the deviations are most marked in systems where there is a possibility of methyl radicals undergoing addition reactions. Fuller and Rust (15) have demonstrated recently that alkyl radicals add quite readily to formaldehyde. It is possible that reaction of a second methyl radical

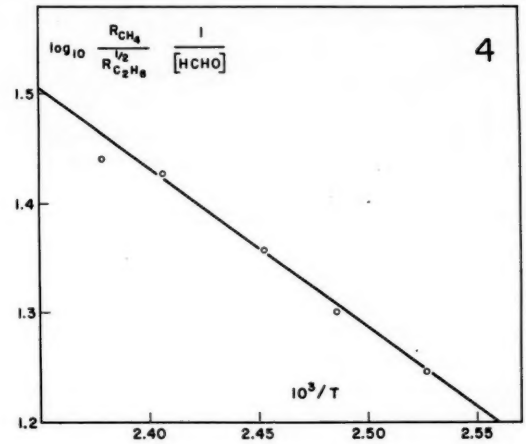

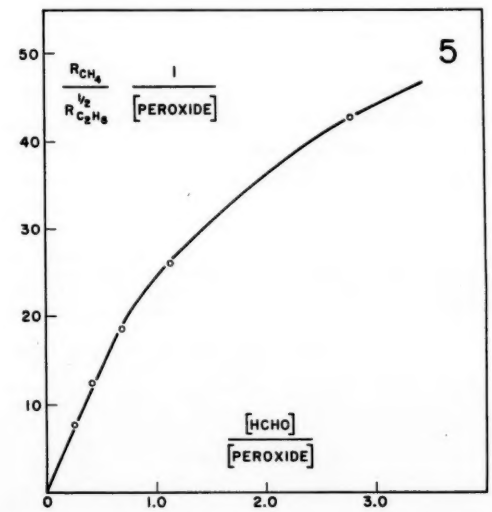

FIG. 4. Arrhenius plot for the reaction of methyl radicals with formaldehyde.
FIG. 5. The pyrolysis of peroxide and formaldehyde at 142.2° C.

with the methyl radical – formaldehyde complex to produce a molecule of ethane could account for the deviations observed.

The ratio of acetaldehyde/CO in these experiments was approximately 0.25. This is not, however, a reliable measure of the relative rates of reactions [8] and [9], as acetaldehyde might also be produced in the decomposition of methyl radical – formaldehyde addition compounds.

ACKNOWLEDGMENTS

We wish to thank Dr. E. W. R. Steacie for his interest in this work, and Miss Bernice Thornton for mass spectrometric analyses.

REFERENCES

1. KODAMA, S. and TAKEZAKI, Y. J. Chem. Soc. Japan, **73**, 13 (1952).
2. TOBY, S. and KUTSCHKE, K. O. Can. J. Chem. **37**, 672 (1959).
3. RALEY, J. H., RUST, F. F., and VAUGHAN, W. E. J. Am. Chem. Soc. **70**, 88 (1948).
4. JAQUISS, M. T., ROBERTS, J. S., and SZWARC, M. J. Am. Chem. Soc. **74**, 6005 (1952).
5. BRINTON, R. K. and VOLMAN, D. H. J. Chem. Phys. **20**, 25 (1952).
6. LOSSING, F. P. and TICKNER, A. W. J. Chem. Phys. **21**, 907 (1953).
7. PRITCHARD, G. O., PRITCHARD, H. O., and TROTMAN-DICKENSON, A. F. J. Chem. Soc. 1425 (1954).
8. BIRSS, F. W., DANBY, C. J., and HINSHELWOOD, C. Proc. Roy. Soc. (London), A, **239**, 154 (1957).
9. TROTMAN-DICKENSON, A. F. and STEACIE, E. W. R. J. Chem. Phys. **19**, 329 (1951).
10. REBBERT, R. E. and STEACIE, E. W. R. J. Chem. Phys. **21**, 1723 (1953).
11. JONES, M. H. J. and STEACIE, E. W. R. Can. J. Chem. **31**, 505 (1953).
12. AUSLOOS, P. and STEACIE, E. W. R. Can. J. Chem. **32**, 593 (1954).
13. HOARE, D. E. Trans. Faraday Soc. **49**, 1292 (1953).
14. BRINTON, R. K. J. Chem. Phys. **29**, 781 (1958).
15. FULLER, G. and RUST, F. F. J. Am. Chem. Soc. **80**, 6148 (1958).

THE INFRARED SPECTRA OF SOME DNP-α-AMINO ACIDS[1, 2]

FELIX FRIEDBERG[3] AND MYLOUS S. O'DELL

ABSTRACT

The infrared spectra of some DNP-α-amino acids were examined using the KBr technique in the region 5000 to 625 cm^{-1}. There is sufficient variation in spectra of closely related DNP-amino acids to allow positive identification even though the spectra on the whole are more strikingly similar than they are different. Differences in varying degrees were also noted between L- and DL-forms.

INTRODUCTION

The DNP[4]-derivatives of amino acids recently have assumed importance in amino acid sequence studies on peptides and proteins (1). While the KBr pellet spectra of a large number of the amino acids (2, 3), and also of their 3-phenyl-2-thiohydantoins (4), are reported in the literature, there is little information with regard to the infrared spectra of DNP-derivatives.[5] This study was undertaken to compare the spectra (*a*) of the DNP-derivatives of amino acids with the spectra of the corresponding free amino acids as given in the literature, (*b*) of the DNP-derivatives of comparable L- and DL-amino acids, and (*c*) of the DNP-derivatives of structurally related acids, to see whether such compounds can be identified by their spectra.

EXPERIMENTAL

The spectra were taken on a Model No. 21 Perkin–Elmer spectrophotometer (equipped with sodium chloride optics). Pellets were made by first mixing the DNP-amino acids with KBr in an agate mortar, and then pressing the material in the Perkin–Elmer die, under evacuation. The DNP-amino acids had been prepared in this laboratory by the method of Levy and Chung (5), and each was crystallized several times and found pure by paper chromatography. Melting points for all derivatives were determined and are essentially in agreement with the values given in literature (6).

DISCUSSION

Table I lists and characterizes the spectral absorption bands in the 5000 to 625 cm^{-1} region. As a result of dipolar ion structure many amino acids possess a characteristic absorption frequency at about 1587 cm^{-1} which is related to the COO^- group, as well as a relatively weak absorption at about 2128 cm^{-1} which may be attributed to NH frequencies in the $-NH_3$ ion. The absence of this absorption peak at 2128 cm^{-1} in the case of DNP-derivatives of amino acids, where the amino group is attached to the dinitrophenyl ring, was therefore expected.

[1]*Manuscript received April 16, 1959.*

Contribution from the Department of Biochemistry, Howard University Medical School, Washington, D.C. This work was supported in part by a grant from the American Cancer Society.

[2]*Spectra deposited with Documentation of Molecular Spectroscopy, Butterworth Scientific Publications, London, England.*

[3]*Work done during tenure of Lederle Medical Faculty Award.*

[4]*DNP is used as an abbreviation for 2,4d-initrophenyl.*

[5]*The first systematic study of the vibrational spectra of α-amino acids was made by Edsall and his co-workers (J. Phys. Chem.* **41**, *133 (1937); J. Chem. Phys.* **4**, *1 (1936);* **5**, *225, 508 (1937); J. Am. Chem. Soc.* **65**, *1767 (1943);* **71**, *474 (1950); and more recently J. Am. Chem. Soc.* **80**, *3807, 3813, 3818, 3823, 3827 (1958). This work is concerned primarily with Raman spectra in aqueous solutions. The first infrared studies were published by Freyman and his co-workers (J. phys. radium,* **7**, *30 (1936)).*

TABLE I

Absorption spectra in the infrared in the 5000–625 cm^{-1} region[a]

DNP-L-arginine 245–250 (*d*)[b]	3311sh 3236SB		2882MB			1658SB 1618SB	1580SB 1570sh	1520SB	1484SS 1464sh 1451sh	1408SB	1387SS	1335SB
DNP-L-alanine 182	3311MS	3058MB			1718SS	1675MB 1623SS	1590SS	1522SS 1502MS	1464WB	1414SB	1359SB	1333sh
DNP-DL-alanine 180.5	3279MS	3058MB			1709SS	1618SS	1587SS	1522SS 1499MS	1464WB	1414SB	1364sh	1333SB
DNP-L-aspartic 186–187	3279MS	3058MB	2857MB		1712SB	1618SS	1590SS	1546MS 1522SS 1499SS		1425SB 1395SS	1361SB	1333SB
Bis-DNP-L-cysteine 155–158	3279MS	3058MB	2907WB		1748SS	1613SB	1590SB	1515SB 1511sh		1427MB	1385MB	1333SB
Di-DNP-L-cystine 118–121	3311sh 3289MS				1745MB	1616SS	1590SS	1520SB		1422MB		1333SB
DNP-glycine 209	3311MS				1712SS	1608SS	1595sh	1517SB 1497SS	1447MS 1441sh	1422sh 1412SB	1362SS	1335SB
Di-DNP-L-histidine 219	3268MS	3058MB			1715MB	1618sh 1613SB	1582SS	1511SB		1416SB 1412sh	1362MS 1359sh	1333sh 1326SB 1321sh
DNP-hydroxy-L-proline 174–178	3425SB 3319sh	3095WB	2950WB		1744SB	1610SB	1588SB	1533SB 1512SB	1464vw 1439MB 1450sh		1384sh	1345SB
DNP-L-isoleucine 109–110	3289MS	3058MB	2924MB	2538vwB	1712SS	1618SS	1587SS	1515SB	1456MB	1412SS	1364MS	1333SB
DNP-DL-isoleucine 174.5	3289WS	3030MB	2915MB 2833sh		1712SS	1621SS	1582SS	1517MS 1502MS	1453WB	1412SS	1377WS 1361MS	1332SB
DNP-L-leucine 102	3289SS	3030SB	2899SB		1712SB	1618SB	1587SB	1513SB 1495SB	1464SB	1422SB	1385SS 1364SS	1325SB

TABLE I (*Continued*)

Absorption spectra in the infrared in the 5000–625 cm^{-1} region[a]

DNP-L-arginine 245–250 (*d*)[b]	1277SB	1250SB		1176sh	1139SB	1094MB		1054MB				948vw	919MB	
DNP-L-alanine 182	1302MS	1261SB	1217MB	1157SS	1140MB	1124MB	1072WB	1057MS				940WB	919WB	
		1230SB												
DNP-DL-alanine 180.5	1292SB	1242SB		1172MB		1119SS		1053MB					916MB	
	1284sh	1232sh		1156MS										
DNP-L-aspartic 186–187	1282SB	1229SB	1220sh	1151SS	1136SS	1109SB		1056SS	1040MB			928SB	915MB	905SB
									1037sh					
Bis-DNP-L-cysteine 155–158	1290SB	1244SB		1171MB	1143SB	1107SB		1050MB					918MB	902WB
		1239sh			1135sh	1100sh							916sh	
Di-DNP-L-cystine 118–121	1299sh				1140sh	1105MB		1058MB					926MB	
	1292SB				1135MB									
DNP-glycine 209	1307SB	1250sh		1155SS	1131SS	1105SS		1056MB		996MS	978WB	945MB	922SS	
	1290SB	1232SB												
Di-DNP-L-histidine 219	1285sh	1230SB	1222sh		1144SB	1103SB		1054MB	1026MB	996SB	971MB	952MB	918MB	
					1133SB							936MB		
DNP-hydroxy-L-proline 174–178	1285sh	1245WB	1210vw	1183MB	1152MS	1125MS	1074MS			997MS	980MS		927WS	903vWB
DNP-L-isoleucine 109–110	1285SB	1244SB	1222SB	1163sh	1147SS	1121MB		1056MB			966WB		921MB	
					1134SB	1101MB							919sh	
DNP-DL-isoleucine 174.5	1290SS	1261sh			1149SS	1124MS		1054WS		1008vw	965WB		918MB	
		1247SB				1098MB								
		1232sh												
		1229sh												
DNP-L-leucine 102	1302MB	1261SB	1206SB	1151SS	1139WB	1094SB	1076SB	1054SB			958MB	939SB	917SB	
	1276SB	1232SB			1125SB									

DNP-L-arginine 245–250 (*d*)[b]			831MS	811MB		763MB	743SB	722MB					645MB
DNP-L-alanine 182			833WB			765WB	743MB	720WB			667WB		
			828WS										
DNP-DL-alanine 180.5			832WB	817WS		763WB	743MB	724WB					
								720sh					
DNP-L-aspartic 186–187		858WB	832MS	807MS	785WB	762WB	744SS	716SB	687WB	680WB	678WB	658WB	644WB
Bis-DNP-L-cysteine 155–158	877WB		833MS	819MB		762WB	745MB	718MB				660WB	
							732MS						
Di-DNP-L-cystine 118–121			832MB				743MB						
DNP-glycine 209	889WB		835MS	818SS		762WS	745SS	714WB	695WB	684WB		657MB	
	886sh												
Di-DNP-L-histidine 219	885WB	870WB	832MB	822MB		759WB	743MS	719MB					
	879vw			818sh									
DNP-hydroxy-L-proline 174–178	882vwB		832vwS	810SS		758WS	743SS	724vwB		689MB		653MB	
DNP-L-isoleucine 109–110			831MS	821MB		765WB	743MS	719WB					
			826MB				733MB						
DNP-DL-isoleucine 174.5			830WS	818MS	791vw	760vw	743MB	717WB	690vw		667vw		644WB
DNP-L-leucine 102			831SB	817SB	774MB	767MS	741SS	711SB	699WB	685MB	665MB		

TABLE I (*Continued*)

Absorption spectra in the infrared in the 5000–625 cm^{-1} region[a]

DNP-DL-leucine 132–133	3322WS		3058WB		2899MB					1712SS	1618SS	1592SS
Di-DNP-L-lysine 178–180	3300WS		3058WB		2890WB					1715MS	1618SS	1587SS
E-DNP-L-lysine 197–200	3333MS				2841SB					1724MS	1618SS	1587SS
DNP-DL-methionine 122	3279MS		3058MB		2874MB					1718SB	1618sh	1590SS
											1608SS	
DNP-L-phenylalanine 191	3279SS	3195sh	3077sh		2882sh		1965WB	1821WB	1742SS	1715sh	1618sh	1580SS
	3247sh	3175sh								1701sh	1608SS	
DNP-DL-phenylalanine 219	3279MS	3205sh	3058sh	3003sh			1980WB	1818WB	1742SS	1701sh	1613SS	1580SS
	3247sh	3185sh								1686sh		
		3145sh										
DNP-L-proline 138	3356WB		3049MB		2833MB					1712SS	1603SS	1577SS
DNP-DL-serine 197–201	3344SS		3077sh	3021sh	2899SB				1757SS		1616SS	1592sh
	3300SS			2959sh								1587SS
				2941sh								
DNP-DL-threonine 178–179	3390SB		3086MS		2899SB				1757SS		1618SS	1587SS
	3333SS											
DNP-L-tryptophan 217–221 (*d*)	3401SS		3096MB		2915MB					1715SS	1613SS	1582SS
	3322MS											
Di-DNP-L-tyrosine 184 (*d*)	3390sh		3058WB								1613SS	1582SS
	3279WB											
Di-DNP-DL-tyrosine 207 (*d*)	3378MS		3058WB							1715SS	1616SS	1582SS
	3279MS											
DNP-L-valine 132–133	3311SS	3215SS		2950SS	2915SS				1748SS		1618SS	1587SS
		3145sh									1616sh	
DNP-DL-valine 187–189	3279MS			3003MvB	2924MB	2571WB				1712SS	1623SS	1587SS
					2890sh							

TABLE I (*Continued*)

Absorption spectra in the infrared in the 5000–625 cm^{-1} region[a]

DNP-DL-leucine 132–133		1517SS	1499MS	1464WS		1422SS	1387vw	1355MS	1332SB	1302MB	1277MB	1261SB	1222MS	
Di-DNP-L-lysine 178–180		1517SS				1416SS			1337SB	1307MB	1269MB		1229MB	
E-DNP-L-lysine 197–200		1522SB				1420SS		1361MS	1330SB	1312SB			1238SB	1195SB
DNP-DL-methionine 122	1541WB	1513SS	1499SB			1420SB		1357MS	1330SS	1307SB	1274SB	1266sh	1244SB	1198MB
						1416sh							1229sh	
DNP-L-phenylalanine 191	1534WB	1515SS	1488SS	1451MS	1437sh	1420sh	1401SB	1362MS	1325SB	1307sh			1236SB	1203sh
							1395sh							
DNP-DL-phenylalanine 219	1538WB	1517SS	1486SS	1451WB	1439sh	1420MB	1393SB	1366MS	1330sh	1314sh	1287sh		1245SS	1205MB
									1321sh	1300sh	1282sh		1235SB	
									1318SS	1294SS				
DNP-L-proline 138		1520SB	1495SS		1447MS	1420MB	1377SS		1326SB	1297sh	1274sh		1221MB	
										1290SB				
DNP-DL-serine 197–201		1513SS	1495SS	1456MS	1431sh	1412SS		1362SS	1335SB	1316SB	1279sh	1266SS	1232SB	1198SB
DNP-DL-threonine 178–179		1520SS	1495SB			1420SB	1395sh	1364SB	1335SS	1316SB	1277SB		1235SB	1206SB
							1389sh	1357sh						
							1381MB							
DNP-L-tryptophan 217–221 (*d*)	1531MS	1515SS	1493MB	1449MS		1418SB		1361sh	1332SB	1290SB	1276SB		1250SB	1198SB
													1227SB	
Di-DNP-L-tryosine 184 (*d*)	1527SB		1502MS			1412MB			1340SB			1266SB		
			1479MS											
Di-DNP-DL-tryosine 207 (*d*)	1531sh	1517SS	1490SS		1439sh	1416SS		1362MB	1330SS	1312sh	1274SB		1248sh	1205SS
													1239SB	
DNP-L-valine 132–133	1541SS	1520SS	1490SS	1466MS	1447sh	1427MS	1406SS	1372SS	1333SB	1299SB			1245SS	
						1425sh	1391sh						1238sh	
													1235sh	
DNP-DL-valine 187–189	1529sh	1520sh	1508SB	1462MS		1412SS		1362MS	1332SB	1309SS	1284SB	1261SB	1242SB	
				1451MS										

TABLE I (*Continued*)

Absorption spectra in the infrared in the 5000–625 cm^{-1} region[a]

DNP-DL-leucine 132–133	1164MS	1148WB	1122MB 1112MB	1095WB		1058WB				958WB			916WS	
Di-DNP-L-lysine 178–180	1181WS	1140MB	1130MB 1107WB			1054WB							917WB	
E-DNP-L-lysine 197–200			1131SB 1122sh 1117SB	1088sh	1076MB	1053MB						922MB		
DNP-DL-methionine 122	1183MS 1170MS	1144SS	1127MS	1100sh 1093MB		1057MB			987WB	966WB 959sh	939WB	921MS	917sh 907WB	
DNP-L-phenylalanine 191	1188SB 1174sh	1156sh 1147SB 1138sh	1130sh	1094sh 1091SB	1071MB	1054SS	1028WB 1026WB	997WB	987WB 976WB	963WB	926MS		913MS	881WB
DNP-DL-phenylalanine 219	1175sh	1159SB 1144SB	1136sh 1131sh	1094SS	1075MS	1054MS	1027WB		983WB	965WB	928WB	923WB 919sh	916sh 909WS	883WB
DNP-L-proline 138	1178MB	1159MS 1145MB	1119MB	1094MB		1063MB	1040WB		976MB				909MB	878WB
DNP-DL-serine 197–201		1153SB	1131sh 1112SB		1067SB	1062sh					934MB		915SB	887MB
DNP-DL-threonine 178–179		1155SB	1126sh 1124sh 1105SB		1083SB	1057SB	1024MB		986WB	966WB	934MB		911MB	
DNP-L-tryptophan 217–221 (*d*)		1143SS	1120MB 1104MB	1093MB		1058MB						923vw	913WB	882WB
Di-DNP-L-tryosine 184 (*d*)	1190MB	1161WS 1144MB	1133sh 1105WB			1064WB 1057sh	1015WB					923MB		889vw
Di-DNP-DL-tryosine 207 (*d*)		1147MB	1121MS 1107MS	1089MB		1062MB		1006WB			939MB 929WB	921vw	914MB	
DNP-L-valine 132–133	1176SS 1174sh 1170sh	1149SS	1125SS 1100SS			1055MS	1029sh			968WS	945WB 926MS			885vwS
DNP-DL-valine 187–189	1174WB	1151SB	1124MB 1100MB			1055WB				953WB		918MB		

TABLE I (*Concluded*)

Absorption spectra in the infrared in the 5000–625 cm^{-1} region[a]

DNP-DL-leucine 132–133		831WS 825WS				763vw	743MS	715WB	709vw	685MB		654WB
Di-DNP-L-lysine 178–180		831WB	817WB			761vw	741MS		709vw 703vw			
E-DNP-L-lysine 197–200		831MS	818MB			763WB	741MS		699MB			
DNP-DL-methionine 122		830MB	817MB	797WB	784WB	762WB	743MS	720WB	714WB	676WB		
DNP-L-phenylalanine 191	849WB	831WB	817SS			768sh 762SS	743MS	717MB	711sh 703SS		661SB	648MB
DNP-DL-phenylalanine 219	855WB	833WB		811MS		765MB	744WB	719MS 717sh	707MS		663sh 662MS	648MB
DNP-L-proline 138		829MS		805MS	773WB	755WS	741SS	724MB		690WB		647WB
DNP-DL-serine 197–201		827SS				768sh 763MB	744SS	715MB		690MB	658MB	
DNP-DL-threonine 178–179	867MB	834sh 828MB				764WB	750MB 744MS	715MB			660WB	
DNP-L-tryptophan 217–221 (*d*)		830MS	821MB			768WB 755MB	741MB		707WB		658WB	
Di-DNP-L-tryosine 184 (*d*)	866vw 855vw	833MB	814vw		784vw	765vw	744MB				667WB	
Di-DNP-DL-tryosine 207 (*d*)		831WB	820MB		778MB	760vw	750MB 742SB		711MB			
DNP-L-valine 132–133		834MS	820SS			762MB	749MB	722SB 718SB				
DNP-DL-valine 187–189		830WB	819MS			761WS	749sh 745MS	720WB		692vw	669WB	

[a] W weak intensity, M medium intensity, S strong intensity, B broad band, S sharp band, sh shoulder, vw very weak band.
[b] These numbers represent uncorrected melting points.

Amino acids have been reported to show marked similarity in their infrared spectra in the region of 1587 to 1333 cm^{-1}. Bands at 1587 and 1408 cm^{-1} have been related, respectively, to the antisymmetrical and symmetrical stretching vibrations of the ionized carboxyl group of the dipolar ions. None of the free amino acids studied lacked the 1408 cm^{-1} band. Among those in which the 1587 cm^{-1} band was not observed were L-threonine and L-proline (3). All of the DNP-derivatives examined by us, however, exhibit the bands at 1587 and 1408 cm^{-1}, and hence the implication is possible that these compounds are dipolar ions. For the free amino acids, a band at 1515 cm^{-1} due to an N–H deformation motion of the α-amino group has been reported, L-leucine, L-serine, and hydroxy-L-proline being among the exceptions (3). Again, there are no such exceptions among the DNP-derivatives studied by us; but we believe that the band here represents antisymmetrical aromatic NO_2 stretch rather than NH-deformation. In the case of free amino acids, bands at 1449 and 1370 cm^{-1} are due to antisymmetrical and symmetrical CH_3 and possibly CH_2 deformation motions, respectively. Among the free amino acids in which the 1449 cm^{-1} band was not apparent were L-valine, L-phenylalanine, hydroxy-L-proline, L-aspartic acid, and L-lysine (3). While the DNP-derivatives of L-aspartic acid and L-lysine (both mono- and di-) and in addition of L-cysteine, L-cystine, L-histidine (di-), L-tyrosine (di-), and DL-threonine do not show the band, those of L- and DL-valine, L- and DL-phenylalanine, and hydroxy-L-proline exhibit it weakly or as a shoulder. In the spectrum of free glycine only, the 1370 cm^{-1} band was lacking (3), and in that of its DNP-derivative it is present. Furthermore, the DNP-derivatives of L-cystine (di-), L-lysine (di-) (unlike the monosubstituted forms), and DNP-L-tyrosine (di-) do not show this band. A 1333 cm^{-1} band has been considered to be related to a CH_2 wagging motion and the only exception among the free amino acids was due to L-alanine (3). None of the DNP-amino acids studied lacks this band. It should be emphasized, however, that bands in the region 1330–1370 will be difficult to interpret, as symmetrical aromatic NO_2 stretch is in this region and is usually intense.

While many free amino acids possessed a band at 2564 cm^{-1}, provisionally assigned to the C–H stretching motion (3), but more likely due to overtone or combinations of the strongly anharmonic $N–H_n$ deformations, it is missing in almost all DNP-derivatives. On the other hand, the spectra of DNP-derivatives with the exception of DNP-L-tyrosine (di-) and DNP-L-arginine possess a band at 1724 cm^{-1}, a band which is not exhibited by the free amino acids.

The spectrum of the racemic form of DNP-alanine differs very little from that of its optically active form. The spectrum of the former does not show the band at 1727 cm^{-1} or that at 1261 cm^{-1}. In the case of DNP-isoleucine, the differences are also not very marked. There is an additional band at 733 cm^{-1} in the spectrum of the active form. The spectrum of the active form of leucine shows additional bands at 1206, 1076, 939, and 775 cm^{-1}. The shoulders at 1420 and at 1203 cm^{-1} of DNP-L-phenylalanine turn into medium broad bands for the DL-form. This L-form has an additional band at 1188, while the DL-form also has an additional band at 1294 cm^{-1}. For tyrosine the shoulder at 3390 cm^{-1} of the L-isomer is a definite dip in the spectrum of the racemic mixture. A striking difference is the absence of the intense and sharp band at 1715 cm^{-1}, the medium band at 1479 cm^{-1}, and the weak one at 1161 cm^{-1} in the DL-form of this amino acid. The DL-form has additional bands at 1362, 1239, 1121, 1089, 939, 750, and 711 cm^{-1}. The shoulder at 1529 cm^{-1} for DNP-DL-valine turns into a definite band for the L-form. The major differences, however, between the spectra for the L- and DL-forms of this amino acid lie between 1429 to 1250 cm^{-1} where the L-form has clearly resolved bands at 1427, 1309, and 1261 cm^{-1}.

The question arises as to whether structurally related DNP-amino acids can be readily differentiated. In the case of DNP-L-proline versus DNP-hydroxy-L-proline, for instance, the former has pronounced additional peaks at 1377, 1290, 1221, 1159, 1094, 1040, and 773 cm^{-1}, the latter at 1245, 997, and 927 cm^{-1}. The 3226-cm^{-1} band, however, reported to be present in the free hydroxy-prolines but not in the spectrum of free proline and assumed to reflect the presence of the —OH group in the former (3), is absent in the spectra of the DNP-derivatives of either L-hydroxyproline or L-proline.

The spectra of DNP-L-valine and DNP-L-isoleucine would be expected to resemble each other. DNP-L-isoleucine has additional bands at 3058, 1222, 1121, and 733 cm^{-1}, DNP-L-valine at 1490, 1427, 1176, and 945 cm^{-1}. In the case of the spectrum of the corresponding free amino acids, L-isoleucine, unlike L-valine, shows a sharp and discrete band at 1462 cm^{-1} (3). Such a distinguishing difference is ruled out for the DNP-derivative of these amino acids.

It would be surprising if the infrared spectra of closely related compounds did not reveal some differences by which pure, individual samples of such compounds could be differentiated from each other. A review of the table suggests that among the DNP-L-amino acids studied the spectra on the whole are more strikingly similar than they are different, and that the use of the spectral tool for purposes of identification is much weaker and less reliable than such procedures as chromatography. There are, however, some DNP-amino acids (e.g., leucine and isoleucine) which are difficult to identify by chromatography and hence spectral analysis after purification would still be of value. Even the spectra of structurally very similar DNP-amino acids show sufficient variation to allow positive identification.[6]

REFERENCES

1. SANGER, F. Biochem. J. **39**, 507 (1945); **45**, 563 (1949).
2. LEIFER, A. and LIPPINCOTT, E. R. J. Am. Chem. Soc. **79**, 5098 (1957).
3. KOEGEL, R. J., GREENSTEIN, J. P., WINITZ, M., BIRNBAUM, S. M., and MCCALLUM, R. A. J. Am. Chem. Soc. **77**, 5708 (1955).
4. RAMACHANDRAN, L. K., EPP, A., and MCCONNELL, W. B. Anal. Chem. **27**, 1734 (1955).
5. LEVY, A. L. and CHUNG, D. J. Am. Chem. Soc. **77**, 2899 (1955).
6. RAO, K. R. and SOBER, H. A. J. Am. Chem. Soc. **76**, 1328 (1954).

[6]*While it is recognized that polymorphism can result in spectral changes due to the alterations in the immediate environments of the vibrating groups, no attempt has been made here to evaluate this factor.*

FREE RADICALS BY MASS SPECTROMETRY

XVI. Hg-PHOTOSENSITIZED DECOMPOSITIONS OF BIACETYL, ACETYLACETONE, AND ACETONYLACETONE[1]

A. G. HARRISON[2] AND F. P. LOSSING

ABSTRACT

The Hg($^3P_1$)-photosensitized decomposition of biacetyl proceeds by a central bond fission. Of the resulting acetyl radicals, at least 27% survive the primary act long enough to react with other radicals, or with a second excited Hg atom. Under conditions of high illumination, there is evidence that Hg($^3S_1$) atoms produced by stepwise excitation also play a part in the reaction by forming excited biacetyl molecules with a lifetime of the order of 1 millisecond. The photosensitized decompositions of acetylacetone and acetonylacetone were examined qualitatively. The former dissociates mainly into an acetyl and an acetonyl radical, and the latter mainly if not exclusively to form CH_3CO and $C_2H_4COCH_3$ radicals. Further reactions of these radicals, and a possible structure for the $C_2H_4COCH_3$ radical, are also discussed.

INTRODUCTION

The photochemical behavior of biacetyl has been the subject of many investigations, mainly as a result of its well-known fluorescence and the complicating factors which this introduces into the mechanism of the acetone photolysis. However, no study of the reaction of biacetyl with excited mercury atoms appears to have been published. Earlier work supplies ample evidence that both CH_3 and CH_3CO radicals are produced in the direct photolysis. The addition of NO was found (1) to suppress the formation of methane and ethane. Blacet and Bell (2, 3) found that the addition of iodine was also effective in this respect, and they concluded that the primary decomposition step at 2654 Å could most probably be written as:

$$CH_3COCOCH_3 + h\nu_{2654} \rightarrow 2CH_3CO. \qquad [1]$$

As a result of energy carry-over, one or both acetyl radicals could dissociate immediately into CH_3 and CO. This work, in agreement with that of Anderson and Rollefson (1), indicated that the decomposition reaction is wholly free radical in nature, and that no molecular rearrangement to form C_2H_6 occurs. Some evidence (4) that ethane could be formed directly by dissociation of a long-lived excited biacetyl molecule has not been substantiated by later work.

The flash photolysis of biacetyl was examined by Porter (5) and by Porter and Norrish (6). Their observations were in agreement with reaction [1] as a primary step, but they concluded that the more complete dissociation

$$CH_3COCOCH_3 + h\nu \rightarrow 2CH_3 + 2CO \qquad [2]$$

predominated, even at 4200 Å. Since the energy available at 4200 Å is insufficient for reaction [2], there is reason to believe that thermal energy from the flash must have been involved. Their conclusions as to the relative occurrence of reactions [1] and [2] are consequently open to question (7).

The photolysis of biacetyl at 2700, 3650, and 4358 Å and its relationship to fluorescence has been discussed in some detail by Noyes and his co-workers (8, 9). They concluded

[1]*Manuscript received April 29, 1959.*
Contribution from the Division of Pure Chemistry, National Research Council, Ottawa, Canada.
Issued as N.R.C. No. 5291.
[2]*National Research Council of Canada Postdoctorate Fellow 1957–59.*

that at 2700 and 3650 Å the primary step [1] given by the earlier work was essentially the correct one, but that the reaction might more correctly be written:

$$CH_3COCOCH_3 + h\nu \rightarrow 2\alpha CH_3CO^* + (2-2\alpha)CH_3CO. \quad [3]$$

The evidence suggested that at 2700 Å one of the acetyl radicals dissociated immediately (i.e. $\alpha = 0.5$) and the primary dissociation was therefore kinetically indistinguishable from a primary dissociation step:

$$CH_3COCOCH_3 + h\nu \rightarrow CH_3 + CH_3COCO \quad [4]$$

followed by an immediate dissociation of the radical:

$$CH_3COCO \rightarrow CH_3CO + CO. \quad [5]$$

At 3650 Å the situation is complicated by the existence of two excited species giving rise to the short-lived and long-lived fluorescences. They found the primary quantum yield at 4358 Å to increase with light intensity. From this observation, and on the basis that the 66 kcal/mole available at 4358 Å is probably insufficient to dissociate biacetyl, they came to the tentative conclusion that the observed dissociation at 4358 Å proceeded by a collision of two excited biacetyl molecules having a lifetime of about 1.8×10^{-3} second. This conclusion, together with the fact that the fluorescence of biacetyl is not excited at wavelengths shorter than 3130 Å (9), is of importance in explaining an unusual feature of the mercury-photosensitized decomposition of biacetyl observed in the present work.

The photochemical behavior of acetylacetone (2,4-pentanedione) and of acetonylacetone (2,5-hexanedione) does not appear to have been investigated before.

EXPERIMENTAL

The mercury-photosensitized reactions were carried out at 55° C in a fast-flow reactor using helium as a carrier. At a point just past the end of the illuminated zone, a small fraction of the reaction stream flowed through an orifice directly into the ionization chamber of a mass spectrometer, enabling observation of free radical products, as well as of stable products, to be made. This apparatus and its operating characteristics have been described (10, 11). A new design of ion source having some modifications to permit a higher pumping speed in the ionization chamber was employed (12).

The effect of light intensity on the biacetyl decomposition was studied by the use of metal screens. Screens with different degrees of transmission were prepared from brass screen having an original transmission of about 39%, by reducing the wire diameter in dilute nitric acid. A rough index of the transmission of the etched screens could be had by measuring the hole-to-wire ratios with a low-power microscope fitted with a micrometer traversing screw. Pieces of suitable width cut from these etched screens were then rolled into cylindrical form so that they could be placed in the annular space between the lamp and the reactor tube. The transmission coefficient for each screen was then measured in place by observing the reduction it caused in the amount of ethylene decomposed in the reactor on illumination by the lamp. The transmission coefficients measured in this way agreed quite closely with those obtained by observation of the hole-to-wire ratios.

MATERIALS

The biacetyl, acetylacetone, and acetonylacetone were Eastman Kodak Co. white label grade, further purified by vacuum distillation. The sample of $Hg(CD_3)_2$ was obtained from Merck and Co. (Montreal).

RESULTS AND DISCUSSION

Biacetyl

A qualitative examination of the products of the mercury-photosensitized reaction of biacetyl, using low-energy electrons for the detection of the parent peaks of free radicals and stable products, showed the presence of CH_3 radicals in considerable abundance. Other parent peaks showing significant increases were those of acetone, ketene, ethane, carbon monoxide, and methane. However, a definite increase for the acetyl radical (mass 43) could not be obtained, even using higher partial pressures of biacetyl. No increase in the mass 85 ($CH_3COCOCH_2$) or mass 71 (CH_3COCO) peaks was found. The failure to detect these radicals using low-energy electrons was not conclusive evidence for their absence, however, since acetyl radicals were also not detected by this means. A further search was made for radicals by means of the addition of mercury dimethyl to the reaction stream. In earlier work (12, 13) it was found that CH_3 radicals produced by the mercury-photosensitized decomposition of $Hg(CH_3)_2$ provided a means for detecting the presence of a free radical R by observation of the formation of the combination product:

$$CH_3 + R \rightarrow CH_3R. \qquad [6]$$

This technique was found to be a valuable aid in detecting radicals for which the sensitivity of detection using low-energy electrons appeared to be rather low. The addition of a small partial pressure of $Hg(CH_3)_2$ to the reaction stream containing biacetyl resulted in a greatly increased yield of acetone, showing that acetyl radicals were present. The combination product of the $CH_3COCOCH_2$ radical with CH_3, on the other hand, was not found, indicating that this radical, which on thermochemical grounds would be stable at 55° C, was not present in significant amounts. To provide a means of detecting the CH_3COCO radical, $Hg(CD_3)_2$ was added to the reaction stream. The combination product $CH_3COCOCD_3$ was not found, although CH_3COCD_3 was produced in abundance. It may be concluded that the CH_3COCO radical, if formed at all, must have dissociated immediately. The addition of CD_3 radicals was found to reduce greatly the yield of CH_3COCH_3, showing that most, if not all, of the acetone was formed by radical combination and not by a molecular rearrangement of biacetyl.

The composition of the reaction products from the biacetyl decomposition was examined quantitatively as a function of the length of the illuminated zone by means of the movable shutter described previously (10, 11). Using 50-volt electrons, mass spectra were obtained at different shutter positions, and analyses were carried out in the usual way. The amounts of biacetyl decomposed, and of the products CO, acetone, ketene, ethane, methane, and methyl produced at the different shutter positions are given in Table I. The amounts of CH_3 were calculated with the assumption that the CH_3^+ contribution

TABLE I

Length of illuminated zone, mm	Biacetyl decomposed, μ	Products from biacetyl, μ						Balance (%) of:	
		CO	$CO(CH_3)_2$	CH_2CO	C_2H_6	CH_3	CH_4	O	C
5	0.096	0.12_1	0.014	0.021	0.020	0.03_5	0.010	81.3	75.5
10	0.221	0.26_9	0.049	0.053	0.049	0.09_6	0.008	83.9	81.9
15	0.401	0.41_8	0.115	0.064	0.085	0.11_4	0.011	73.9	74.4
20	0.566	0.73_6	0.216	0.086	0.146	0.15_1	0.018	91.7	89.1
25	0.790	1.02_8	0.333	0.107	0.212	0.14_7	0.028	92.9	89.6
30	0.996	1.34_6	0.400	0.131	0.276	0.16_7	0.038	94.2	89.5

from the CH_3CO radical was negligible. The actual yields of CH_3 are therefore rather smaller than those given in Table I. The increasing defect in the C and O balances at the shorter lengths of illuminated zone probably results from the inability to include a quantitative measurement for the CH_3CO radical. Although no increase in the mass 43 peak could be detected using low-energy electrons, a small remainder was left in the 50-volt spectra in all cases after correction for contributions from biacetyl and acetone.

The distribution of products is consistent with a primary dissociation into two acetyl radicals:

$$CH_3COCOCH_3 + Hg(^3P_1) \rightarrow CH_3CO + CH_3CO^* + Hg(^1S_0). \quad [7]$$

The present work provides no clear indication as to what fraction of the acetyl radicals formed in this reaction dissociate immediately by the reaction

$$CH_3CO^* \rightarrow CH_3 + CO. \quad [8]$$

However, a significant fraction does survive for an appreciable time, either as a result of receiving insufficient activation in the primary step, or as a result of deactivation:

$$CH_3CO^* + M \rightarrow CH_3CO + M. \quad [9]$$

The following radical combination reactions also occur:

$$CH_3CO + CH_3 \rightarrow CH_3COCH_3 \quad [10]$$

$$2CH_3 \rightarrow C_2H_6. \quad [11]$$

In agreement with the findings of earlier work on acetone (11), the low yield of methane shows that the disproportionation reaction

$$CH_3 + CH_3CO \rightarrow CH_2{=}CO + CH_4 \quad [12]$$

is quite slow compared with reaction [10]. If all the methane were produced by reaction [12] and all the acetone by reaction [10], the ratio k_{12}/k_{10} would be given by the ratio of methane to acetone. At the longest contact time this ratio was 0.095. This probably represents an upper limit to k_{12}/k_{10}. The large excess of ketene over methane supports the conclusion reached in earlier work (11) that acetyl radicals are decomposed by excited mercury atoms as follows:

$$CH_3CO + Hg^* \rightarrow CH_2{=}CO + H + Hg. \quad [13]$$

The fate of the H atom is not known; possibly it reacts with an acetyl radical to give a second molecule of ketene. Since no acetaldehyde is formed, it is evident that ketene is not produced in a primary molecular rearrangement reaction. The rapid decrease in the yield of acetone at shorter contact times supports the evidence given above that acetone was formed by reaction [10] and not by the possible molecular rearrangement:

$$CH_3COCOCH_3 + Hg^* \rightarrow CH_3COCH_3 + CO + Hg. \quad [14]$$

A similar conclusion can be reached for ethane. Assuming, then, that acetone and ketene are formed only by reactions [10] and [13], it may be concluded that at least 0.27 of the acetyl radicals survive the primary dissociation step for a time sufficiently long to permit them to react with methyl radicals or a second excited mercury atom. Whether they survive as a result of deactivation (reaction [9]), or as a result of not being sufficiently excited in reaction [7], cannot be decided from the present results.

A graphical representation of the data on biacetyl, given in Fig. 1, shows an unexpected feature. The amount of biacetyl decomposed did not increase linearly with the length of the illuminated zone as had been found for all other compounds examined, but curved

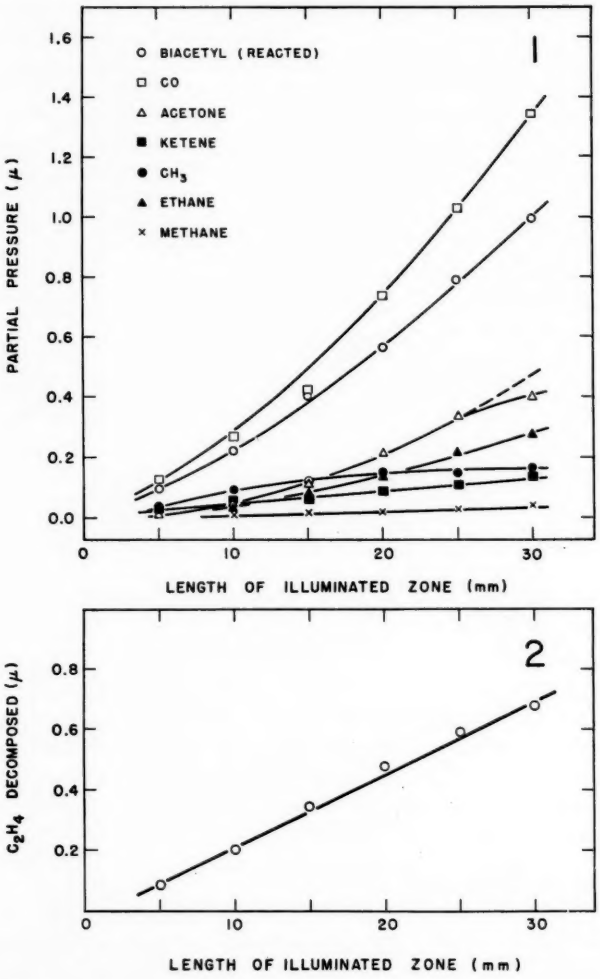

FIG. 1. Decomposition of biacetyl.
FIG. 2. Ethylene decomposed as a function of the length of the illuminated zone.

progressively upward. In order to ensure that this non-linear behavior did not result from inequalities in the amount of 2537-Å radiation entering the reactor at different points along its length (as a result of polymeric deposits, for example), a calibration was carried out using ethylene. As shown in Fig. 2, the relation for ethylene was linear. The curvature evident in Fig. 1 was consequently considered to be a real, and not an instrumental, effect. Such an effect would be produced if an appreciable fraction of the biacetyl decomposed by a process involving an intermediate whose lifetime was not negligible compared to the transit time through the illuminated zone, which was about 1×10^{-3} second. A reasonable assumption would be that this species was the metastable state of biacetyl B**, having a lifetime of 1.8×10^{-3} second. As discussed above, this

species was considered by Noyes and co-workers (8, 9) to account for the dissociation of biacetyl at 4358 Å by a second-order process:

$$2B^{**} \rightarrow B + \text{products.} \qquad [15]$$

If, in the present work, some fraction of the biacetyl were dissociating by this mechanism, the question arises as to how B** could be formed. Since biacetyl shows no fluorescence in the 2380–3130 Å (9) it appears unlikely that B** could be formed by collisions with $^3P_1$ mercury atoms. The radiation from a mercury lamp of the type used in this work does contain an appreciable amount of radiation at longer wavelengths, particularly at 3130, 3650, and 4358 Å. The possibility that B** could be formed by direct absorption of 3650- and 4358-Å radiation was checked by placing a filter, in the form of a split cylinder of Corning 7040 glass, between the lamp and the reactor tube to remove 2537 Å while allowing 3650 Å to pass. With this filter in place, it was found that no measurable decomposition of biacetyl occurred, showing that direct absorption of 3650- or 4358-Å radiation was not responsible for the effect, and that the explanation must be sought in terms of 2537-Å radiation and excited mercury atoms.

The dependence of biacetyl decomposition on the total light intensity was investigated using the metal screens described above, with the result shown in Fig. 3. For purposes of comparison, the dependence for acetone decomposition was also examined. Within the

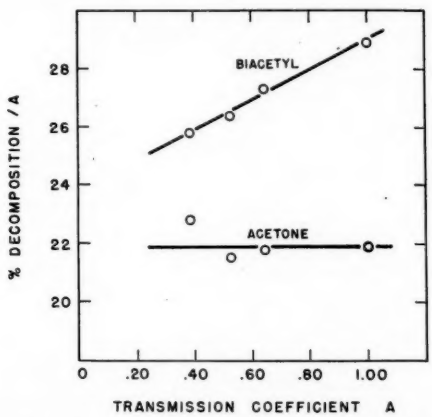

FIG. 3. Dependence of extent of decomposition on the light intensity.

experimental error the amount of acetone decomposed per millisecond was found to be proportional to the amount of light passing through the screen. The amount of biacetyl decomposed, on the other hand, depended on some order of light intensity greater than one. This lends further support to the view that a second-order decomposition process such as reaction [15] must be involved.

A positive identification of this process is not possible from the present work, but it is of interest to speculate as to how the B** state of biacetyl could be activated. Since the incident flux of 2537-Å radiation in the reaction cell is very high (greater than 10^{18} quanta/sec cc (10)) the fraction of the total number of mercury atoms which are at any instant in the $^3P_1$ state is quite appreciable. The probability of absorption of a quantum of 4358 Å by a $^3P_1$ atom to give a mercury atom in the 7^3S_1 state is therefore not negligible. This process of stepwise excitation is well known (14). Since the B**

state of biacetyl is known to be formed by direct absorption of 4358 Å it is not unreasonable to assume that this state could also be formed by a collision in which a $^3S_1$ mercury atom is quenched to a $^3P_1$ atom. On the assumption that the incident radiation I contains a fraction x of 4358-Å radiation, the remainder being 2537 Å, the following interactions may be considered:

[16] $$Hg + h\nu_{2537} \rightarrow Hg^3P_1 \qquad +\frac{d}{dt}[Hg^3P_1] = k_{16}(1-x)I[Hg]$$

[17] $$Hg^3P_1 + h\nu_{4358} \rightarrow Hg^3S_1 \qquad +\frac{d}{dt}[Hg^3S_1] = k_{17}I[Hg^3P_1]$$

[18] $$Hg^3P_1 \rightarrow Hg + h\nu_{2537} \qquad -\frac{d}{dt}[Hg^3P_1] = [Hg^3P_1]/\tau_1$$

[19] $$Hg^3S_1 \rightarrow Hg^3P_1 + h\nu_{4358} \qquad -\frac{d}{dt}[Hg^3S_1] = [Hg^3S_1]/\tau_2$$

[20] $$Hg^3P_1 + B \rightarrow Hg + B^* \qquad -\frac{d}{dt}[Hg^3P_1] = k_{20}[Hg^3P_1][B]$$

[21] $$Hg^3S_1 + B \rightarrow Hg^3P_1 + B^{**} \qquad -\frac{d}{dt}[Hg^3S_1] = k_{21}[Hg^3S_1][B]$$

Application of the steady-state treatment to these equations gives the relation:

[22] $$\frac{[Hg^3S_1]}{[Hg^3P_1]} = \frac{k_{17}x}{k_{16}(1-x)}\frac{[Hg^3P_1]}{[Hg]}\left(\frac{1/\tau_1 + k_{20}[B]}{1/\tau_2 + k_{21}[B]}\right).$$

The lifetime of Hg^3S_1, $\tau_2 = 5.75\times10^{-8}$ second (15), is not greatly different from that of Hg^3P_1, for which $\tau_1 = 1.0\times10^{-7}$ second (14). Since the absorption coefficients are proportional to the reciprocal of the lifetimes, k_{16} and k_{17} are, to a first approximation, nearly equal. Nothing is known about the quenching efficiency of biacetyl for Hg^3S_1 atoms, but if it is assumed that it is not greatly different from that for Hg^3P_1 atoms, then $k_{20} \simeq k_{21}$ and expression [22] reduces to:

[23] $$\frac{[Hg^3S_1]}{[Hg^3P_1]} = \frac{x}{1-x}\frac{[Hg^3P_1]}{[Hg]}f$$

in which the factor f is of the order of unity. On the basis (from Fig. 3) that some 10% of the amount of biacetyl decomposed does so by a second-order process, the right-hand side of equation [23] would have to have a value of about 0.2. Under the existing experimental conditions this may not be beyond the bounds of possibility.

In order to demonstrate conclusively that Hg^3S_1 atoms were the activating agent, it would have been necessary to filter out 4358-Å radiation while allowing 2537 Å to pass. While this might be possible given sufficient space between the lamp and the reactor tube, it could not be accomplished in the 2–3 mm annular space available in the present reaction system.

Acetylacetone and Acetonylacetone

The products of the mercury-photosensitized reactions of acetylacetone and acetonylacetone were very briefly examined, but no quantitative analyses of the products were made. In the decomposition of acetylacetone, the use of low-energy electrons indicated that three free radicals were formed, at mass 15 (methyl), mass 43 (acetyl), and mass 57 (CH_3COCH_2). The stable products were CO, some ethane, ketene, and acetone. Addition

of CH_3 radicals to the reaction stream resulted in an increased yield of acetone and ethane, and the appearance of a peak at mass 72. The latter was attributed to the formation of methyl ethyl ketone by combination of methyl with acetonyl radicals. There was no indication of the formation of $CH_3COCH_2COCH_2CH_3$, suggesting that the $CH_3COCH_2COCH_2$ radical was not present in significant amounts. These qualitative results suggest that acetylacetone decomposes mainly by a split into two radicals:

$$CH_3COCH_2COCH_3 + Hg^* \rightarrow CH_3COCH_2 + CH_3CO. \quad [24]$$

Since the CH_3CO radical could be detected at low-electron energies, it is possible that a considerably larger fraction of the CH_3CO radicals survives the primary step than in the case of biacetyl.

The mode of reaction with acetylacetone with excited mercury atoms is undoubtedly quite complicated in detail. Acetylacetone vapor is 76.5% in the enol form under equilibrium conditions (16) and at first sight it might be thought that the keto and enol forms could be excited at different higher states and dissociate by different modes. However, it appears from the present experiments that CH_3CHO, a reasonable product from the dissociation of an enol-type excited molecule, is not formed to any extent. It is interesting to note that in the mass spectrum (No. 806 in the API Mass Spectral Catalog) there are no ions such as $CH_3{}^+COH$ which might arise from dissociation of an enol-type parent ion. There is no reason to believe, therefore, that the keto–enol tautomerism also exists among the excited and ionic states of acetylacetone.

A qualitative examination of the products formed by the mercury-photosensitized decomposition of acetonylacetone was also carried out in the same way. Using low-energy electrons, products were found having the following parent peaks: mass 15 (CH_3), mass 42 (ketene), and mass 43 (CH_3CO). No increase in the mass 57 peak, corresponding to the acetonyl radical, was found. Other products formed were ethane, acetone, products having parent masses of 70 and 86, and possibly a little ethylene. The addition of CH_3 radicals (from $Hg(CH_3)_2$) to the reaction stream gave a greatly enhanced yield of the products of mass 58 and 86, indicating the presence of radicals of mass 43 and 71. This shows that the predominating mode of dissociation is into two radicals according to the reaction:

$$CH_3COCH_2CH_2COCH_3 + Hg^* \rightarrow CH_3CO + C_2H_4COCH_3 + Hg. \quad [25]$$

Since no methyl ethyl ketone was formed on the addition of CH_3 radicals it may be concluded that the concentration of acetonyl radicals was negligibly small, and that the alternative mode of dissociation

$$CH_3COCH_2CH_2COCH_3 + Hg^* \rightarrow 2CH_3COCH_2 + Hg \quad [26]$$

occurred to a much smaller extent, if at all.

A third mode of dissociation is possible:

$$CH_3COCH_2CH_2COCH_3 + Hg^* \rightarrow CH_3 + COCH_2CH_2COCH_3 + Hg. \quad [27]$$

However, the addition of CD_3 radicals (from $Hg(CD_3)_2$) to the reaction stream did not result in any formation of the combination product $CD_3COCH_2CH_2COCH_3$ at mass 117. Although this experiment strongly suggests that no $COCH_2CH_2COOH_3$ radicals were present, it is possible that some of the radicals at mass 71 arose from reaction [27] followed immediately by a loss of CO from the large radical. On the other hand, the large yield of CH_3CO radicals shows that a large fraction of the radicals of mass 71 was formed by reaction [25]. In view of earlier observations that free radicals may react

rapidly with excited Hg atoms (10, 11) the small amount of product of mass 70 may have been formed by the reaction:

$$C_2H_4COCH_3 + Hg^* \rightarrow CH_2 = CHCOCH_3 + H + Hg. \qquad [28]$$

In view of the unexpected stability of the $C_2H_4COCH_3$ radical, further experiments were carried out in an attempt to obtain a more exact identification. A simple bond rupture as in equation [25] would be expected to give a radical having the structure $\dot{C}H_2CH_2COCH_3$. The addition product of this radical with the added CH_3 radicals would therefore be expected to be methyl *n*-propyl ketone. The mass spectrum of this ketone shows major peaks at masses 86, 71, and 57.[3] Although the observed addition product had major peaks at masses 86 and 71, the peak at mass 57 was much too small for this product to be methyl *n*-propyl ketone. The lack of a mass 57 peak would be explained if the addition product were instead methyl isopropyl ketone, which has major peaks at masses 86 and 71, but not at mass 57. This observation suggests that the large radical formed in reaction [25] had the structure $CH_3\dot{C}HCOCH_3$ rather than the structure $\dot{C}H_2CH_2COCH_3$, presumably as a consequence of a hydrogen atom shift in the excited molecule prior to dissociation. If such were the case the stability of the $C_2H_4COCH_3$ radical would be explained, since for the former one can write two resonating structures:

$$CH_3\dot{C}H{-}\underset{\underset{O}{\|}}{C}CH_3 \leftrightarrow CH_3CH{=}\underset{\underset{O\cdot}{|}}{C}CH_3.$$

The $\dot{C}H_2CH_2COCH_3$ radical, on the other hand, would be expected to dissociate easily into C_2H_4 and $COCH_3$. Without a more definite identification of the ketone addition product, this conclusion as to the identity of the $C_2H_4COCH_3$ radical must be regarded as tentative.

REFERENCES

1. Anderson, H. W. and Rollefson, G. K. J. Am. Chem. Soc. **63**, 816 (1941).
2. Blacet, F. E. and Bell, W. E. Discussions Faraday Soc. **14**, 70 (1953).
3. Blacet, F. E. and Bell, W. E. J. Am. Chem. Soc. **77**, 5332 (1954).
4. Ascah, R. G., Burton, M., Ricci, J. E., and Davis, T. W. J. Chem. Phys. **14**, 487 (1946).
5. Porter, G. Proc. Roy. Soc. (London), A, **200**, 284 (1950).
6. Khan, M. A., Norrish, R. G. W., and Porter, G. Proc. Roy. Soc. (London), A, **219**, 450 (1953).
7. Steacie, E. W. R. Atomic and free radical reactions. 2nd ed. Reinhold Publishing Corp., New York. 1954.
8. Sheats, G. F. and Noyes, W. A., Jr. J. Am. Chem. Soc. **77**, 1421 (1955).
9. Noyes, W. A., Jr., Porter, G. B., and Jolley, J. E. Chem. Revs. **56**, 49 (1956).
10. Lossing, F. P., Marsden, D. G. H., and Farmer, J. B. Can. J. Chem. **34**, 701 (1956).
11. Lossing, F. P. Can. J. Chem. **35**, 305 (1957).
12. Kebarle, P. and Lossing, F. P. Can. J. Chem. **37**, 389 (1959).
13. Collin, J. and Lossing, F. P. Can. J. Chem. **35**, 778 (1957).
14. Mitchell, A. C. G. and Zemansky, M. W. Resonance radiation and excited atoms. Cambridge University Press, London. 1934.
15. Randall, R. H. Phys. Rev. **35**, 1161 (1930).
16. Conant, J. B. and Thompson, A. F., Jr. J. Am. Chem. Soc. **54**, 4039 (1932).

[3]*The data in the Mass Spectral Catalog, API Project 44, are in disagreement as to the spectrum of methyl n-propyl ketone. Spectra Nos. 299 and 378 show a large 57 peak, but No. 651 shows instead a mass 57 peak of only 0.35. A spectrum of methyl n-propyl ketone obtained in the present work agreed with spectra Nos. 299 and 378 in this respect. It is possible that a misprint in No. 651 has given 0.35 instead of 10.35 for the mass 57 peak.*

STERIC INHIBITION OF RESONANCE

V. NITROMESITYLENE[1]

JAMES TROTTER[2]

ABSTRACT

A detailed X-ray investigation of the crystal structure of nitromesitylene has shown that the nitro group is twisted 66° out of the plane of the aromatic ring about the C—N bond. The resulting decrease in resonance interaction compared with a completely planar model has been correlated with the characteristic NO_2 vibration frequencies.

INTRODUCTION

The physical properties of the nitro and acetyl derivatives of mesitylene and durene indicate that resonance interaction between the nitro and acetyl groups and the aromatic rings is markedly reduced in comparison with nitrobenzene and acetophenone, suggesting that the steric effect of the methyl groups prevents the attainment of completely coplanar configurations (1).

The dipole moments, for example, of conjugated aromatic nitro compounds, such as nitrobenzene (I), are larger than those of the corresponding aliphatic molecules, the moment of nitrobenzene in benzene solution being 3.95 Debye units compared with about 3.3 D for an aliphatic nitro compound. The increased dipole moments are due to contributions from ionic structures (II and III) which are at a maximum when the nitro

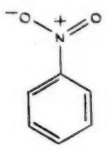

I

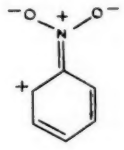

II

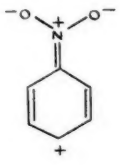

III

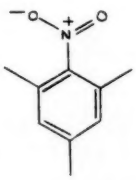

IV

group is coplanar with the aromatic ring. The introduction of methyl groups ortho to the nitro group, as in nitromesitylene (IV), reduces the dipole moment to 3.65 D, suggesting that the nitro group is twisted out of the plane of the benzene nucleus, and the contributions of structures II and III are reduced.

[1]*Manuscript received February 27, 1959.*
Contribution from the Division of Pure Physics, National Research Council, Ottawa, Canada.
Issued as N.R.C. No. 5292.
[2]*National Research Council Postdoctorate Fellow.*

Raman spectra evidence leads to similar conclusions. The Raman shift corresponding to the NO_2 symmetrical stretching vibration is at 1367 cm^{-1} in phenylnitromethane, $Ph.CH_2.NO_2$, where the nitro group is not conjugated with the ring, and at 1341 cm^{-1} in nitrobenzene; the frequency in nitromesitylene is 1363 cm^{-1}, much closer to the value in the non-conjugated molecule, again indicating a significant inhibition of the resonance between the nitro group and the aromatic π-electrons. The ultraviolet absorption spectrum of nitromesitylene also suggests a marked reduction in the resonance interaction.

Similar deviations from coplanarity and consequent resonance inhibition are to be expected in 9-nitroanthracene and 9,10-dinitroanthracene where the nitro group environments are similar to those in nitromesitylene. Detailed investigations of the crystal structures of these anthracene derivatives by X-ray diffraction methods have shown that the nitro groups are twisted markedly out of the planes of the aromatic rings, by 64° in crystals of 9,10-dinitroanthracene, and by 85° in crystals of the 9-nitro derivative. The reductions in resonance interaction resulting from these deviations from coplanarity have been correlated with the infrared spectra and with the bond length variations in the molecules, the energy of resonance interaction between a nitro group and the aromatic π-electrons in 9,10-dinitroanthracene in the solid state being about one-fifth of that in a completely planar model, while for 9-nitroanthracene this resonance energy is negligible. Configurations with 64° twist are the most stable for isolated molecules of both substances, but in crystals of 9-nitroanthracene crystal forces apparently result in minimum energy when the twist is 85°. In solution the angles are the same in both molecules, the exact values possibly depending on solvent–solute interactions.

The present communication describes the extension of these investigations to nitromesitylene; the angle between the plane of the nitro group and the aromatic plane has been determined by an accurate X-ray analysis of the crystals, and the resultant resonance inhibition has been correlated with the characteristic vibration frequencies of the nitro group, both in the solid state and in solution.

EXPERIMENTAL

Infrared Spectra

The spectra measured (Fig. 1) were those of pure nitromesitylene in carbon tetrachloride solution and dispersed in a Nujol mull, as observed with a Perkin–Elmer model 21 infrared spectrophotometer with a rock salt prism.

X-Ray Analysis

Crystals of nitromesitylene are orthorhombic with four molecules in a unit cell of dimensions $a = 15.14$, $b = 8.41$, $c = 7.26$ Å, space group $Pna2_1$. The structure was determined from projections along the three principal crystallographic axes. All the carbon atoms and the nitrogen atom lie on one plane, but the oxygen atoms lie one above and one below this plane at distances of 0.95 Å, so that the nitro group is twisted very markedly out of the plane of the aromatic ring about the C—N bond, the angle between the planes of the benzene ring and the nitro group being 66.4°. Figure 2 shows a projection of the structure along the *b*-axis; the benzene ring is perpendicular to the plane of projection so that the individual atoms are not resolved, but the large deviation of the oxygen atoms from coplanarity is well illustrated. Full details of the crystal structure analysis are published elsewhere (2).

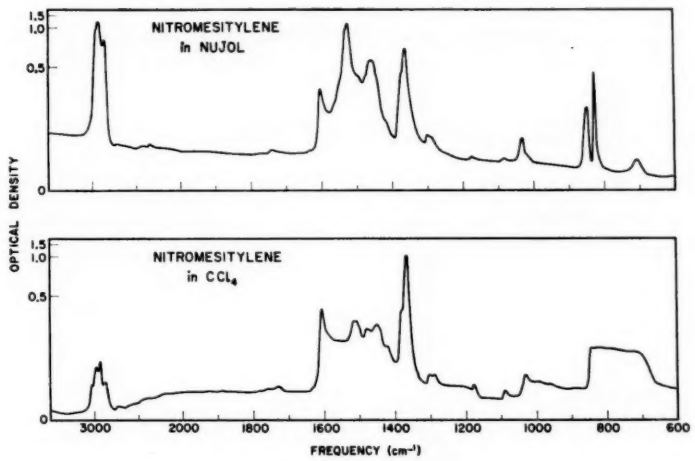

FIG. 1. Infrared spectra.

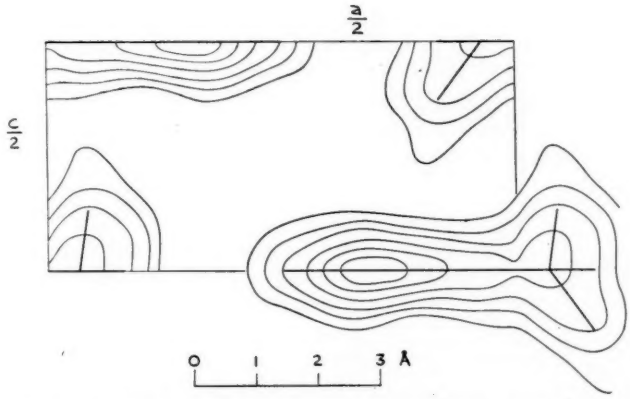

FIG. 2. Projection of the structure of nitromesitylene along the *b*-axis.

DISCUSSION

The spectra of nitromesitylene in the range 3500 cm^{-1} to 600 cm^{-1} in carbon tetrachloride solution and dispersed in a Nujol mull are shown in Fig. 1, and the peak positions and intensities of the absorption bands are listed in Table I, some peaks of course being masked by the carbon tetrachloride or Nujol bands. The strong absorption at 1364 cm^{-1} in solution and 1362 cm^{-1} in the solid state can be assigned to the NO_2 symmetrical stretching vibration. The NO_2 antisymmetrical stretching vibration cannot be assigned quite so unambiguously, as with the nitroanthracenes, but is probably at 1531 cm^{-1}. The absorption maximum at 828 cm^{-1} corresponds to the C—N stretching vibration.

The characteristic NO_2 frequencies in nitromesitylene are compared in Table II with the corresponding frequencies in conjugated (3) and non-conjugated (4) nitro compounds and with those in 9-nitroanthracene and 9,10-dinitroanthracene. The twists of the nitro

TABLE I

Frequencies and intensities of absorption bands

Solution (CCl_4)		Solid (Nujol mull)		
Frequency, cm^{-1}	Intensity	Frequency, cm^{-1}	Intensity	Vibration
3030	w			Aromatic C—H stretching
2975	m			CH_3 antisymmetrical stretching
2930	m			CH_3 stretching
2875	w			CH_3 symmetrical stretching
1606	m	1604	m	C=C (aromatic) stretching
		1531 (sh)	s	NO_2 antisymmetrical stretching
		1525	s	C=C (aromatic) stretching
1478	m			CH_3 bending
1450	m			CH_3 symmetrical bending
1420 (sh)	w	1419 (sh)		CH_3 bending
1380 (sh)	m	1373 (sh)	m	CH_3 antisymmetrical bending
1364	s	1362	s	NO_2 symmetrical stretching
1303	w	1300	w	
1288	w	1288 (sh)	w	
1178	w	1177	w	
1090	w	1085	w	Characteristic aromatic bands
1031	w	1033	w	
		849	m	Aromatic C—H out-of-plane vibration
		828	s	C—N stretching

TABLE II

Characteristic nitro-group frequencies (cm^{-1}) and deviations from coplanarity in nitromesitylene and related molecules

Molecule	NO_2 stretching		C—N stretching	NO_2 twist, θ in degrees
	Symmetrical	Antisymmetrical		
Non-conjugated	1377	1586	800→900	90.0
9-Nitroanthracene	1374	1540	836	84.7
Nitromesitylene	1362	1531	828	66.4
9,10-Dinitroanthracene	1367	1542	831	63.7
Conjugated	1349	1518	849	0

groups out of the aromatic planes are included in the last column of the table. The NO_2 symmetrical stretching vibration in nitromesitylene at 1364 cm^{-1} in solution and at 1362 cm^{-1} in the solid state indicates, as in 9,10-dinitroanthracene, that resonance interaction between the nitro group and the aromatic π-electrons is markedly reduced in comparison with a completely conjugated nitro compound, but is not negligible. This conclusion is in agreement with the effect which would be predicted from the measured twist of the nitro group out of the aromatic plane, the predicted resonance energy being about one-fifth ($\cos^2 66.4° = 0.16$) of that for a planar model.

As with the nitroanthracenes the frequencies in solution cannot be directly correlated with the values in the crystals and with the twists of the nitro groups out of the aromatic planes, since the possible effects of solvent–solute interactions cannot be estimated; it can only be deduced that the angle in solution is between 66° and 90°.

REFERENCES

1. Wheland, G. W. Resonance in organic chemistry. John Wiley & Sons, Inc., New York. 1955.
2. Trotter, J. Acta Cryst. (In press).
3. Randle, R. R. and Whiffen, D. H. J. Chem. Soc. 4153 (1952).
4. Smith, D. C., Pan, C., and Nielsen, J. R. J. Chem. Phys. **18**, 706 (1950).

SOLVOLYSIS IN HYDROGEN AND DEUTERIUM OXIDE

III. ALKYL HALIDES[1]

P. M. LAUGHTON[2] AND R. E. ROBERTSON

ABSTRACT

Rate data for the hydrolysis of a series of α- and β-methylated allyl, benzyl, and cycloalkyl halides in light and heavy water are compared. The major factor determining the rate ratio k_{D_2O}/k_{H_2O} appears to be the relative stability of the initial solvation shell. When the relative viscosity of H_2O and D_2O is used as a measure of the relative stability of structure in bulk solvent, the observed kinetic isotope effect and the temperature dependence of the isotope effect can be rationalized in terms of accepted properties of aqueous solutions.

Attention is drawn to the anomalous rate ratio $k_{RBr}/k_{RI} > 1$ which appears to be characteristic of solvolysis of these alkyl halides in pure water in contrast to other media.

In an extension of recent solvolytic studies of strongly solvated substrates, chiefly sulphonates (1), rates were obtained for the solvolysis of a variety of halogen compounds in light and heavy water. This work was done on the premise that the isotope effect derived from the rate ratio k_{D_2O}/k_{H_2O} was insensitive to temperature, a conclusion based on earlier work on the benzenesulphonates and methanesulphonates (2). However, a recent determination of $\Delta C_p^{\ddagger}$ for isopropyl bromide in light and heavy water (3) has cast doubt on the general applicability of this assumption. Since it was not practical to determine the $\Delta C_p^{\ddagger}$ for each of the alkyl halides for which we had a rate ratio at one temperature, we give here the rate ratios at the convenient experimental temperatures, both because we propose to refer to them later and because even subject to the above proviso they provide, for the detailed mechanism of hydrolysis, clues which deserve discussion.

EXPERIMENTAL

The methods of measuring kinetic rates were similar to those used previously (4). Easily volatile solutes were added under vacuum to the reaction flask, containing deaerated water and the potassium salt of the corresponding acid (0.003 *M*) either from a gas burette or from an evacuated side arm. With some solutes of low solubility, especially the benzyl bromides, a saturated solution was formed, and a fritted glass disk in the filling line was required to remove the small undissolved globules of the halide. With these latter solutes, supersaturation difficulties were occasionally encountered, as shown by non-linear rate plots.

Most of the halides were commercial samples (chiefly Eastman Kodak-White Label), distilled before use with a Fenske (low boiling) or Vigreux (high boiling) column, and passed through an alumina column to give refractive indices in agreement with published values. The following compounds were prepared by the methods indicated: cyclopentyl chloride (5), *p*-methylbenzyl bromide (6), neopentyl bromide (7), and *t*-butyl fluoride (8).

DISCUSSION OF RESULTS

The rates of hydrolysis in light and heavy water and rate ratios for a series of saturated alkyl halides are given in Table I. Similar data for a series of unsaturated or cyclic

[1]*Manuscript received May 20, 1959.*
Contribution from the Division of Pure Chemistry, National Research Council, and the Department of Chemistry, Carleton University, Ottawa, Canada. Presented in part at the Toronto Meeting of the Chemical Institute of Canada, May 27, 1958.
Issued as N.R.C. No. 5288.
[2]*Department of Chemistry, Carleton University, Ottawa, Canada.*

TABLE I

Solvolytic rate constants for the reaction of alkyl halides, RX, in hydrogen and deuterium oxide

X	R	Temp. (° C)	$k_{D_2O}\times10^5$ sec^{-1}	$k_{H_2O}\times10^5$ sec^{-1}	k_{D_2O}/k_{H_2O}
Cl	Me[a]	89.96	4.38	5.64[b]	$.78_0$
	Et	100.00	9.33 ± .06	11.48	.81
	i-Pr	98.64	75.7 ± .03	100.0 ±1.1	$.75_7$
	t-Bu[a]	4.00	95.0	136.7[c]	.70
		14.03	473	636	.74
	n-Pr	100.00	5.58	6.81	.82
Br	Me[a]	70.50	8.55	10.65[b]	$.80_3$
		80.00	22.0	27.1	$.81_0$
		89.95	54.8	67.0	$.81_8$
	Et	98.66	113.8 ± .2	139.5 ± .4[c]	$.81_6$
	i-Pr[a]	50.00	8.84	11.29[d]	$.78_0$
	n-Pr	79.99	13.15 ± .05	16.14[e]	$.81_5$
	i-Bu	80.00	1.652	1.406	.85
		100.00	35.5 ± .1	42.5	$.83_5$
	*neo*Pen	90.00	4.25 ± .004	5.08 ± .04	$.83_8$
		100.17	13.8	16.2 ± .1	.85
I	Me	79.99	6.68 ± .04	8.19 ± .06[b]	$.81_6$
	Et	98.64	71.1 ± .1	87.8 ± .7[f]	$.81_0$
	i-Pr	80.01	211 ±1	275 ± .4	$.76_7$
	n-Pr	100.00	45.1 ± .4	54.9 ± .4	$.82_2$
	i-Bu	99.90	28.6	35.5 ± .4	.81
F	*t*-Bu	90.24	42.5 ± .02	51.8 ± .16	$.82_0$

[a]Values taken from Paper I of this series (2).
[b]Previous data by Moelwyn-Hughes (9).
[c]Data by Tommila (10, 11).
[d]Value of Winstein *et al.* (12), 1.16×10^{-4} sec^{-1}.
[e]Previous data by Fierens, 25–60° C (13).
[f]Higher than the value of Moelwyn-Hughes (9) at 100° C.

TABLE II

Solvolytic rate constants for the reaction of some allylic, benzylic, and cyclic halides in hydrogen and deuterium oxide

Halide	Temp. (° C)	$k_{D_2O}\times10^5$ sec^{-1}	$k_{H_2O}\times10^5$ sec^{-1}	k_{D_2O}/k_{H_2O}
$CH_2{=}CHCH_2Cl$	74.99	23.3± .05	29.5± .2	$.79_2$
$PhCH_2Cl$	60.00	45.8± .2	58.3± .1[b]	$.78_5$
p-$MeC_6H_4CH_2Cl$	29.98	64.4± .1	86.2± .5	$.74_7$
$PhCHCl_2$	29.98	198 ± .4	297 ±2	$.66_6$
$PhCCl_3$	5.10	307 ±15	387 ±5	.79
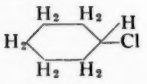	60.01	17.7± .03	23.2± .1	$.76_0$
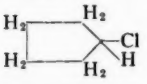	98.64	76.2± .2	93.2± .2	$.81_7$
$CH_2{=}CHCH_2Br$	60.00	69.0± .3	89.6± .4[c]	$.77_0$
$PhCH_2Br$[a]	29.98	20.2	27.5	$.73_5$
p-$MeC_6H_4CH_2Br$	20.00	104.8± .2	140.6±1.1	$.74_5$
o-$MeC_6H_4CH_2Br$	20.00	41.5± .2	56.0± .3	$.74_2$
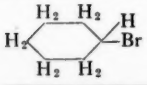	59.98	224 ±2	292 ±1	$.76_6$

[a]Data taken from Paper I of this series (2).
[b]Previous data by Olivier at 30° (15).
[c]Previous data by Fierens, 15–51° (13).

compounds are given in Table II. The rate ratios for benzal chloride and benzotrichloride were included since Bensley and Kohnstam have recently suggested (16) that these compounds react by an ionizing mechanism.

The model we have used for aqueous solutions in previous papers (4, 17) has approximated to that proposed by Frank and Evans (18). However, the term "iceberg" has a connotation of a greater degree of rigidity than is intended. The problem is to find some graphic word which will take account of the high degree of structure in water and at the same time take cognizance of the dynamic situation demonstrated by self-diffusion (19) and solvation exchange (20, 21). This semantic difficulty is both illustrated and in some degree accommodated by Frank's "fluttering cluster" hypothesis (22). For the sake of simplicity, however, we have chosen to discuss the isotope effect in terms of the static term "structure" in spite of the limitations which this abstraction implies. The opposing effects of non-electrolytes and ions on the associated water in aqueous solutions are conveniently discussed in terms of characteristic changes in structure, and when considered differentially, these changes provide a basis for interpreting the isotope effect observed when D_2O replaces H_2O as a medium for hydrolysis.

Aqueous Solutions of Non-Electrolytes and Ions

When a non-electrolyte is introduced into water, its mere presence removes some degree of librational freedom (23, 18), or in terms of Frank's "fluttering cluster" theory (22) its presence interferes with the shifting centers of organization in such a way as to cause a greater interaction between those molecules immediately contiguous to the non-electrolyte. This has been described as leading to the formation of icebergs about the solute but it is probably a better approximation to specify that a particular water molecule in the primary solvation shell spends more time in each configuration than is characteristic of bulk water (24, 25). The net effect of this loss of freedom will clearly be proportional to the number of water molecules in the surface layer thus leading to such regularities between structures and solvation parameters as are recognized in the Barklay–Butler rule (26).

Evidence that the stability of the solvation shell about non-electrolytes in aqueous solutions decreases with rising temperature is derived from the decrease in the negative enthalpy characterizing the gas–solution equilibria (i.e. $\delta_s C_p$ is positive). In the activation process for hydrolysis the energy required to break down this initial state solvation shell ($\Delta F^{\ddagger}_{str}$) will also be expected to show a similar temperature dependence. This has been invariably found (17) with the obvious difference that since $\Delta H^{\ddagger}$ is positive, $\Delta C^{\ddagger}_p$ is negative for the latter process.

The added energy required to reorganize this initial state solvation shell is given formal recognition in equation [1]

$$[1] \qquad \Delta F^{\ddagger} = \Delta F^{\ddagger}_{I} + \Delta F^{\ddagger}_{str} - \Delta F^{\ddagger}_{R^{\delta+}} - \Delta F^{\ddagger}_{X^{\delta-}}$$

where $\Delta F^{\ddagger}$,* the free energy of activation, is shown to be the difference between (*a*) the energy of bond breaking plus the energy required for the breakdown of the initial state solvation shell and (*b*) the sum of the two terms representing the interaction of the water with the transition state. The intention here is ***not*** to suggest that complete charge development has necessarily been achieved in the transition state but rather to emphasize interaction with the cationic and anionic functions of the solute.

Ions of intermediate size such as $Cl^{\ominus}$, $Br^{\ominus}$, or $I^{\ominus}$, in contrast to non-electrolytes, appear to have a net structure-breaking effect on water (17), or to use the Bernal–Fowler

*Symbols are the same in this paper as in ref. 17.

description, such ions raise the structural temperature of the water (27). The specific effect will be strongly dependent on the charge density at the surface of the ion, and for singly charged ions this leads to the well-known gradation of solvation properties with size (28, 29). The extension of such considerations to the effect of charge development on adjacent water molecules in the activation process would seem obvious. The majority of salts are known to be more soluble in H_2O than in D_2O (30) presumably because the former already has a less stable structure (see below), and it would seem equally probable that in the hydrolysis of neutral esters, the transition state would be favored by H_2O over D_2O in agreement with the observed isotope effect. It is unlikely, however, that this is the major factor determining the k_{D_2O}/k_{H_2O} ratio.

Kinetic Isotope Effect

In all of those experimental situations where a breakdown of water–water structure is involved, e.g. viscosity (31), mobility of ions (32), self-diffusion (19), dielectric relaxation (33), D_2O invariably gives evidence of a greater degree of structure than H_2O at the same temperature. Since each of the above physical reorganization processes appears to depend on the same elementary step, the similarity found for the isotope effect in each of these processes is to be expected. In terms of the formalism noted above we have adopted this isotope ratio as a measure of the relative structural stability of D_2O versus H_2O toward reorganization. Since the activation process for the hydrolysis of the alkyl halides will involve a reorganization of solvent from a condition characterizing the solvation of non-electrolytes to that characterizing the solvation of the quasi-ionic transition state, it would seem reasonable that the above norm when coupled with recognized differences in the structural stability of water contiguous to non-electrolytes and to ions would provide a convenient basis for discussing the observed isotope effects (k_{D_2O}/k_{H_2O}). To use viscosity as a measure of structural stability in a kinetic equation is by no means novel (34, 35), although this factor is normally considered to have negligible effect on the reaction rate (36).

Formal representation of the kinetic isotope effect follows directly from equation [1]

$$[2] \qquad -RT \ln k_{D_2O}/k_{H_2O} = \delta_M \Delta F^{\neq} = \delta_M \Delta F^{\neq}_{str} - \delta_M \Delta F^{\neq}_{R^{\delta+}} - \delta_M \Delta F^{\neq}_{X^{\delta-}}$$

and in the following an attempt will be made to evaluate the relative contribution of the three factors on the right-hand side of equation [2].

If we consider the isotope effect for fluidity (ϕ_{D_2O}/ϕ_{H_2O}) as a normal value for the relative stability of water structure toward reorganization, then it will be apparent that the kinetic isotope effect at any temperature as indicated by the rate ratio (k_{D_2O}/k_{H_2O}) tends toward values either below or above this norm (Fig. 1). This grouping of relative kinetic isotope effects with respect to the assumed "norm" follows, to a remarkable degree, the changes to be expected in the relative stability of the initial state solvation shell.

Just as small ions may be regarded as raising the structural temperature of the water molecules associated with them, so non-electrolytes may be considered to lower the structural temperature of the surrounding water molecules. For solutes such as the alkyl halides, which do not interact strongly with the primary solvation shell, the isotope effect arising from the breakdown of the more stable initial state solvation shell will reflect this added stability, and hence will correspond to a lower temperature, that is, a larger isotope effect than for the corresponding "normal" ϕ_{D_2O}/ϕ_{H_2O} value which reflects the relative stability of the water structures at the experimental temperature. Since on this hypothesis the kinetic isotope effect (k_{D_2O}/k_{H_2O}) will largely arise from water–water

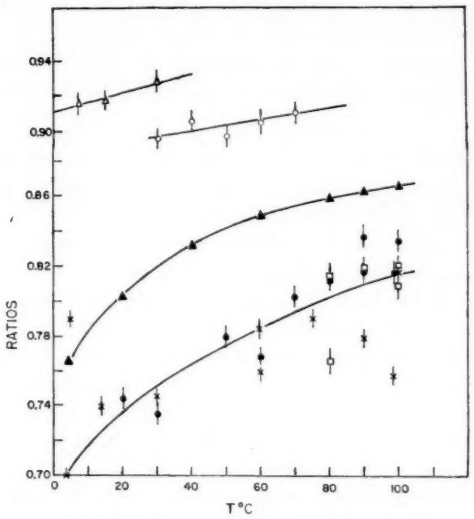

FIG. 1. The kinetic isotope effect caused by a change of medium from H_2O to D_2O over a range of temperatures compared with the corresponding isotope effect expressed by the relative fluidities of the two solvents.

△ Isopropyl benzenesulphonate (ref. 1).
○ Methyl benzenesulphonate (ref. 2).
× Chlorides (Tables I and II).
● Bromides (Tables I and II).
□ Iodides (Tables I and II).
▲ Relative fluidities (ref. 31).

interaction, this ratio will tend to be the same for all esters at a given temperature, a conclusion supported by the results in Tables I and II. That this conclusion is not exactly true is not too surprising, since small effects will be expected to arise as a consequence of characteristic differences in the solvation of the alkyl halides and differentially result in the observed scatter of points (Fig. 1). On the other hand, esters containing the sulphonic group show a much smaller isotope effect and in terms of the present formalism may be regarded as raising the structural temperature of the water solvating the initial state, thus decreasing the relative difference between rates in D_2O and H_2O. The difference between the halides and the sulphonates becomes larger at lower temperatures, the characteristic curve for the halides lying below and roughly paralleling the "normal" viscosity isotope curve while the isotope ratios for the solvolysis of the sulphonates change by but a few per cent through the temperature range 5–80° C.

Apparently *t*-butyldimethylsulphonium ion with a rather weak field also belongs to the class of molecules that interact strongly, like the sulphonates, and hence have a reduced isotope ratio ($k_{D_2O}/k_{H_2O} = 0.94$). On the other hand, methyl nitrate (0.83 at 85° C) and benzenesulphonyl chloride (0.63 at 10° C) and methanesulphonyl chloride (0.63 at 20° C) do not. Indeed the latter compounds, along with benzal chloride (0.66 at 30° C) and benzotrichloride, (0.79 at 5.1° C) show such wide deviations from the norm as to suggest major differences in mechanism.

There appears to be a minor trend toward a decreased isotope effect through the α-methylated series (Table I) and a tendency for some of those molecules which from other considerations would be expected to have a greater degree of charge development in the transition state to give isotopic ratios which lie below the "normal curve". If these molecules were more ionic in the initial state the predicted ratio would lie above

the normal curve as shown by the sulphonates. An opposite effect would suggest some minor contribution to the isotope effect from $\delta_M \Delta F^{\ddagger}_{R\,\delta+}$ and $\delta_M \Delta F^{\ddagger}_{X\,\delta-}$ as discussed above. Before any particular significance can be attached to such deviations, however, the temperature dependence of the ratios must be examined for the individual solutes.

The Halide Anomaly

While it is not the purpose of this paper to discuss the effect of changes in structure on the rate of alkyl halides hydrolyzing in water, although this would appear to be the first time that such data have been published for many of the substrates in Tables I and II, it is of interest to note that the relative rates of hydrolysis of alkyl halides are in the unusual order $k_{bromide} > k_{iodide} > k_{chloride}$. This order was first noted by Moelwyn-Hughes 20 years ago (9) for the methyl compounds and is now seen to be characteristic of other alkyl halides hydrolyzing in water. The "normal" order of reactivity $k_{iodide} > k_{bromide}$ is found for all bimolecular displacement reactions at a saturated carbon atom of which we are aware (see the recent review by Streitwieser for a summary (37)) save for displacement by OH^- in water (9), and is also the order for the solvolysis of tertiary halides in 80/20 ethanol–water where the mechanism has been assumed to approach a limiting (11), i.e. an ionization or S_N1, type.

Since this reversal of order cannot be attributed to a change in the alkyl group from one which requires a large degree of nucleophilic interaction (primary halides) to the tertiaries where this requirement is reduced if not absent, and since the order for the so-called border line compounds (the isopropyl halides hydrolyzing in 60/40 ethanol–water (37)) is also the normal order $k_{iodide} > k_{bromide}$, we are led to conclude that the the reverse order found for halides in pure water derives from some peculiarity in ion–dipole interaction which favors the bromide in the above reactions: note for example the order of the mobilities Br > I > Cl.

ACKNOWLEDGMENT

We wish to acknowledge the careful technical assistance of Mr. S. Sugamori throughout the course of this investigation.

REFERENCES

1. Robertson, R. E. and Laughton, P. M. Can. J. Chem. **35**, 1319 (1957).
2. Laughton, P. M. and Robertson, R. E. Can. J. Chem. **34**, 1714 (1956).
3. Heppolette, R. L. and Robertson, R. E. Unpublished work.
4. Robertson, R. E. Can. J. Chem. **33**, 1536 (1955).
5. Yarnall, W. A. and Wallis, E. S. J. Org. Chem. **4**, 284 (1939).
6. Atkinson, E. F. J. and Thorpe, J. F. J. Chem. Soc. **91**, 1687 (1907).
7. Sommer, L. H., Blankman, H. D., and Miller, P. C. J. Am. Chem. Soc. **76**, 803 (1954).
8. Cooper, K. A. and Hughes, E. D. J. Chem. Soc. 1183 (1937).
9. Moelwyn-Hughes, E. A. Proc. Roy. Soc. A, **164**, 295 (1938).
10. Tommila, E., Tülikainen, M., and Voipoi, A. Ann. Acad. Sci. Fennicae, A, **II**, 26 (1955).
11. Tommila, E. Suomen Kemistilehti, A, **29**, 205 (1956).
12. Winstein, S., Grunwald, E., and Jones, H. W. J. Am. Chem. Soc. **73**, 2700 (1951).
13. Fierens, P. J. C. and Kruys, P. Bull. soc. chim. Belges, **64**, 542 (1955).
14. Scott, J. M. W. and Robertson, R. E. Unpublished work.
15. Olivier, S. C. J. Rec. trav. chim. **33**, 891 (1934).
16. Bensley, B. and Kohnstam, G. J. Chem. Soc. 287 (1956).
17. Robertson, R. E., Heppolette, R. L., and Scott, J. M. W. Can. J. Chem. **37**, 803 (1959).
18. Frank, H. S. and Evans, M. J. Chem. Phys. **13**, 507 (1945).
19. Wang, J. H. J. Phys. Chem. **58**, 686 (1954).
20. Posey, F. A. and Taube, H. J. Am. Chem. Soc. **79**, 4285 (1957).
21. Connick, R. E. and Poulson, R. E. J. Chem. Phys. **30**, 759 (1959).
22. Frank, H. S. and Wen, Yen-Yang. Discussions Faraday Soc. **24**, 133 (1957).
23. Eley, D. D. Trans. Faraday Soc. **35**, 1421 (1939).
24. Haggis, G. H., Hasted, J. B., and Buchanan, T. J. J. Chem. Phys. **20**, 1452 (1952).

25. SAMILOV, O. Discussions Faraday Soc. **24**, 141 (1957).
26. BARKLAY, I. M. and BUTLER, J. A. V. Trans. Faraday Soc. **35**, 1445 (1939).
27. BERNAL, J. D. and FOWLER, R. H. J. Chem. Phys. **1**, 1 (1933).
28. LAIDLER, K. J. Can. J. Chem. **34**, 1107 (1956).
29. GURNEY, R. W. Ionic processes in solution. McGraw-Hill Book Co., Inc., New York. 1953. Chap. 10.
30. TAYLOR, H. S., CALEY, E. R., and EYRING, H. J. Am. Chem. Soc. **55**, 4334 (1933).
31. HARDAY, R. C. and COTTINGTON, R. L. J. Research Natl. Bur. Standards, **42**, 573 (1949).
32. CHITTUM, J. P. and LA MER, V. K. J. Am. Chem. Soc. **59**, 2425 (1937).
33. COLLIE, C. H., HASTED, J. B., and RITSON, D. M. Proc. Phys. Soc. **60**, 145 (1948).
34. MOELWYN-HUGHES, E. A. J. Chem. Soc. 95 (1932).
35. MOELWYN-HUGHES, E. A. Trans. Faraday Soc. **33**, 91 (1937).
36. GLASSTONE, S., LAIDLER, K. J., and EYRING, H. The theory of rate processes. McGraw-Hill Book Co., Inc., New York. 1941. p. 401.
37. STREITWIESER, A., JR. Chem. Revs. **56**, 571 (1956).

SYNTHESIS OF CYCLIC PHOSPHOROUS ACID ESTERS BY TRANSESTERIFICATION[1]

ALEXIS A. OSWALD

ABSTRACT

Five- and six-membered cyclic phosphorous acid esters were synthesized by transesterification of phosphites with 1,2- and 1,3-glycols: Diethyl hydrogen phosphite was transesterified to give cyclic hydrogen phosphites. Partial transesterification of tris-2-chloroethyl phosphite resulted in cyclic 2-chloroethyl phosphites.

Organic phosphites are potentially important chemicals as antioxidants in the petroleum and plastics industry (1, 2, 3). Their usefulness is limited, however, by their hydrolytic instability. Recently, the extreme resistance of *cis*-1,3-cyclohexylidene phosphate to hydrolysis was reported (4). This report together with earlier knowledge (5) regarding the stability of 2,3-dimethyl-2,3-butylene hydrogen phosphite initiated the present work of synthesizing new cyclic phosphites.

SYNTHESIS OF CYCLIC HYDROGEN PHOSPHITES

One of the earliest methods for synthesizing dialkyl esters of phosphorous acid is the direct esterification (6, 7) by heating phosphorous acid with the appropriate alcohol. The first syntheses of cyclic hydrogen phosphites were probably accomplished by starting from phosphorous acid and various glycols. However, there is little evidence of a single pure product being isolated (8).

Another method for the synthesis of cyclic hydrogen phosphites is the hydrolysis of cyclic chlorophosphites (5, 9, 10, 11) or alkyl phosphites (5). Saunders and his co-workers (12) reported the synthesis of a cyclic secondary diphosphite by reacting phosphorus trichloride with an excess of ethylene glycol.

In the course of this work, the transesterification of diethyl hydrogen phosphite with 1,2- and 1,3-glycols was accomplished. When 3-chloro-1,2-propylene glycol was used for transesterification, the known 3-chloro-1,2-propylene hydrogen phosphite or 2-hydroxy-4-chloromethyl-1,3,2-dioxaphospholane (13) was obtained. Analogously, the formation of other cyclic hydrogen phosphites with five-membered (dioxaphospholane) and six-membered (dioxaphosphorinane) ring structures was presumed according to the following equations:

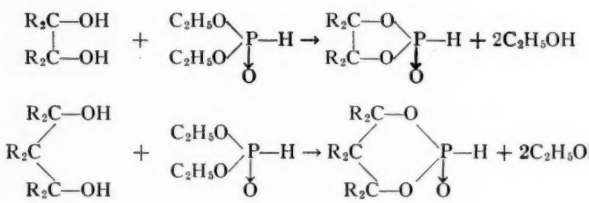

R = H or alkyl

In the transesterification experiments, 1 mole of 1,2- or 1,3-glycol was used per mole of hydrogen phosphite. The reactions were carried out between 130 and 140° C at

[1]*Manuscript received April 23, 1959.*
Contribution from the Research Department, Imperial Oil Limited, Sarnia, Ontario, Canada.

120–150 mm. When the liberation of the by-proudct ethanol ceased, the remaining crude product was fractionated at pressures between 2 and 3 mm. The purified compounds are liquids with the exception of the white crystalline 2-hydroxy-5,5-dimethyl-1,3,2-dioxaphosphorinane. Some of the physical and analytical data and the yields of the compounds obtained are shown in Table I.

TABLE I

Cyclic hydrogen phosphites

Formula	B.p. (° C/mm)	Refractive index (n_D^{20})	Phosphorus (%)		Yield (%)
			Calc.	Found	
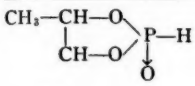	84–86/2.3	1.4580	25.4	23.9	78
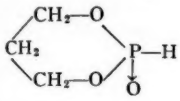	97–98/2.5	1.4522	25.4	24.9	79
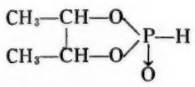	84–85/2.3	1.4616	22.8	23.1	75
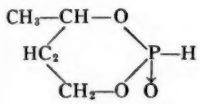	103–104/2.3	1.4547	22.8	22.8	76
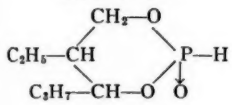	117–118/2.5	1.4600	16.1	16.3	78
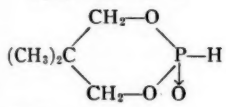	103–104/2.3	m.p. 53–55°	20.6	20.2	85
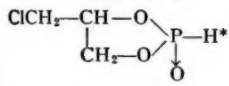	125–126/2.3	1.4910	19.8	19.7	83
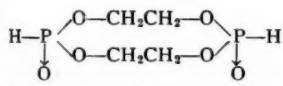	117–118/2.3	1.4751	28.7	28.2	56

*First synthesized by Arbuzov and Zoroastrova (10).

Unequivocal syntheses of the cyclic butylene hydrogen phosphites were also carried out to prove the five- and six-membered ring structures respectively. These syntheses started from the appropriate butanediols and phosphorus trichloride. In this manner, the corresponding cyclic chlorophosphites (11, 12) were prepared. These compounds yielded the cyclic hydrogen phosphites after hydrolysis with the stoichiometric amounts of water.

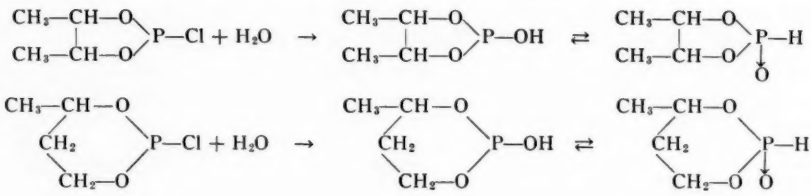

It can be assumed from the high yield of the product of hydrolysis that the water attack results in the selective removal of the chlorine without ring opening. The identity of the infrared spectra of the compounds obtained in this manner with the butanediol transesterification products verifies the assumed five- and six-membered ring structures.

All the liquid cyclic hydrogen phosphites prepared are highly viscous materials with high boiling points. These properties probably indicate intermolecular association as shown by B. A. Arbuzov and Vinogradova (13) in the case of dialkyl phosphites. In the case of the hydrogen phosphite tautomer such an association can be depicted as follows:

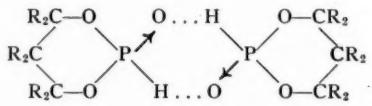

This assumption is supported by the observation that the cyclic hydrogen phosphites prepared from the chlorophosphites became viscous only after several days' standing after distillation.

Transesterification with ethylene glycol resulted in a compound having an identical boiling point with the cyclic diethylene diphosphite mentioned previously.

SYNTHESIS OF CYCLIC PHOSPHITES

Transesterification of phosphite esters was first performed by Milobendzki and Szulgin (14). They prepared propyl- and butyl-diphenyl phosphite from triphenyl phosphite by the action of the corresponding sodium alcoholates according to the following equation:

$$(Ph—O)_3P + NaOR \rightarrow (Ph—O)_2POR + Ph—ONa.$$

Some patents claim transesterification of triarylphosphites with alcohols (1, 2); for example, the synthesis of alkyl diaryl phosphites by the following reaction:

$$(ArO)_3P + HOR \rightarrow (ArO)_2POR + HOAr.$$

A recent German patent (15) claims the transesterification of tris-2-chloroethyl phosphite with several alcohols. However, in this work the transesterification reaction with polyhydric alcohols was mentioned as giving polymeric products.

The reinvestigation of the latter transesterification in these laboratories revealed some new facts suggesting the formation of monomeric cyclic phosphite esters by partial transesterification of tris-2-chloroethyl phosphite with 1,2- and 1,3-glycols.

In previous work, cyclic phosphite esters have also been synthesized from the corresponding cyclic chlorophosphites, which in turn were prepared from phosphorus trichloride and diols; in both cases with the help of an acid-binding agent (pyridine) (10, 11, 16, 17).

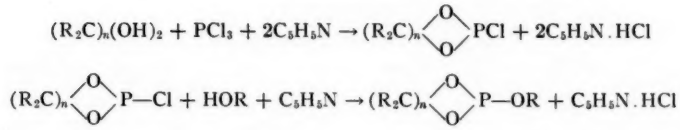

Similar compounds can be synthesized starting with an alkyl dichlorophosphite and a diol.

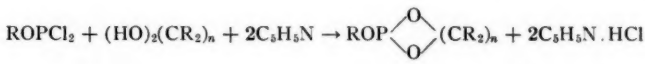

Cyclic catechol phosphites were prepared by an analogous method starting from catechol and phosphorus trichloride (18, 19). Chloroethyl catechol phosphite was synthesized by reacting ethylene oxide with catechol chlorophosphite according to the following reaction equation (20):

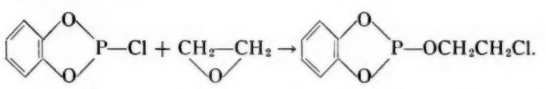

The stability of the cyclic phosphite esters is greatest for six-membered rings (10, 11, 16, 17).

Partial transesterification of 1 mole of tris-2-chloroethyl phosphite with 1 mole of 1,2- or 1,3-glycol was attempted. At elevated temperature and reduced pressure about 2 moles ethylene chlorohydrin per mole of phosphite was removed from the reaction mixture as indicated by the amount of the distillate in the receiver and the weight loss of the reaction mixture. After redistillation, the distillate was identified as ethylene chlorohydrin by boiling point, refractive index, and infrared spectrum. The formation of five- and six-membered cyclic chloroethyl phosphites is suggested according to the following general equations:

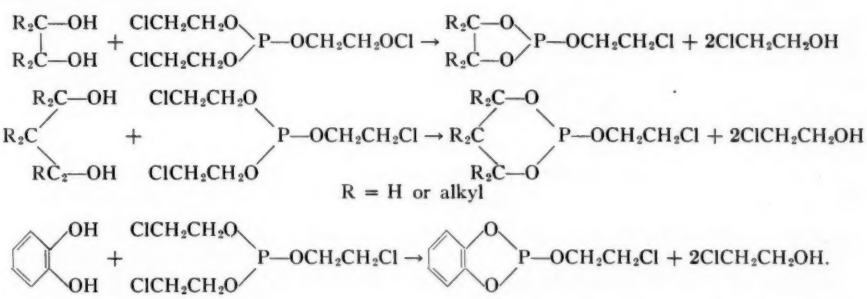

The lower glycols used in these reactions were not miscible with the tris-2-chloroethyl phosphite, but after standing at room temperature homogeneous mixtures were obtained. For preparative purposes, the reaction was performed by heating the ingredients between 60 and 100° C *in vacuo*, and the ethylene chlorohydrin distilled as it was formed. The remaining crude product was fractionated *in vacuo* yielding the purified, colorless cyclic chloroethyl phosphites usually as liquids, immiscible with water. Some of the physical and analytical data and the yields obtained are shown in Table II.

TABLE II

Cyclic 2-chloroethyl phosphites

Formula	B.p. (° C/mm)	Refractive index (n_D^{20})	Chlorine		Yield (%)
			Calc.	Found	
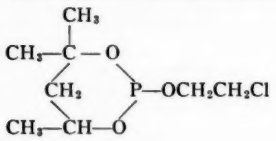	105–107/2	1.4534	15.67	16.05	80
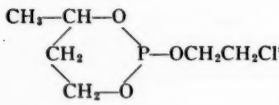	98–100/2.5	1.4680	17.88	18.30	75
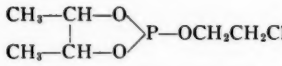	107–109/3	1.4650	17.88	17.90	70
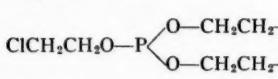	108–110/2	1.4898	20.82	19.85	20‡
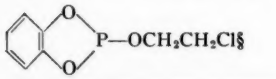	82–84/2	1.5390	16.24	16.50	85

*For data on compound prepared by independent synthesis see Experimental part.

†Highly viscous liquid; tentative formula. For ethylene-2-chloroethyl phosphite Arbuzov (10) gives the following data: b.p. 78.5–79.5° at 65 mm, n_D^{20} 1.4755.

‡The greater part of the raw product is polymeric material, which cannot be distilled.

§Previously prepared by Kabachnik (20), who found b.p. 107–108° at 2.5 mm and n_D^{20} 1.5430. Catechol-2-chloroethane-phosphonic acid has b.p. 167–170° at 4.5 mm and n_D^{20} 1.5502 as reported by Kabachnik and co-workers (21).

Unequivocal syntheses of the cyclic butylene 2-chloroethyl phosphites were also carried out to prove the five-membered 1,3,2-dioxaphospholane and the six-membered 1,3,2-dioxaphosphorinane ring structures respectively. In these syntheses the corresponding cyclic chlorophosphites (10, 11) were reacted with ethylene chlorohydrin to give the cyclic 2-chloroethyl phosphites.

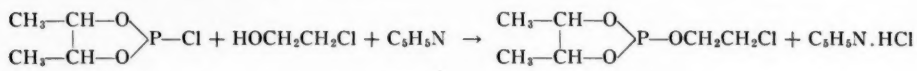

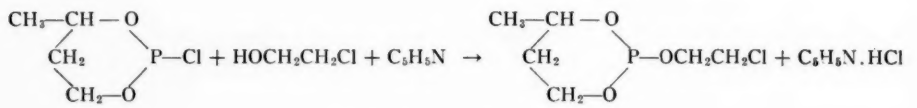

In the course of these reactions, if carried out below room temperature, Arbuzov transformation and ring opening are not likely to occur. Therefore, the identity of the infrared spectra of the compounds with the corresponding transesterification products supports the presence of the cyclic phosphite structures. A further indication of this structure is given by the comparison of the boiling point and refractive index of the catechol transesterification product with catechol 2-chloroethyl phosphite prepared by Kabachnik (20) from catechol chlorophosphite.

EXPERIMENTAL

Preparation of Cyclic Hydrogen Phosphites by Transesterification

Diethyl hydrogen phosphite (27.6 g, 0.2 m (mole)) and 1,2- or 1,3-glycol (0.2 m) were placed in a round bottom flask connected to a Claisen head fitted with a downward condenser and a receiver for vacuum distillation. The resulting solution was heated to 130° C at 120–160 mm pressure under nitrogen. The reaction proceeded as shown by the distillation of ethanol. Ethanol evolution ceased after about 3 hours' heating at the above temperature.

The remaining crude product was fractionated at 2 to 3 mm. The cyclic hydrogen phosphites were obtained as very viscous, colorless liquids. The yields and other data are given in Table I. Some high boiling materials remained in the distillation flask and were probably polymeric.

Preparation of Cyclic Chlorophosphites

To a solution of phosphorus trichloride (68.7 g, 0.5 m) in anhydrous ether (200 ml) a mixture of 2,3- or 1,3-butanediol (45 g, 0.5 m), pyridine (79 g, 1 m), and ether (200 ml) was added with vigorous stirring, while the temperature was kept below −5° C. The precipitated pyridinium chloride was removed by filtration and washed with ether. The combined clear filtrate was fractionated. After the removal of the ether, the cyclic chlorophosphites were distilled in vacuum and were obtained as colorless liquids.

Starting from 2,3-butanediol, 67 g (87%) 2-chloro-1,3,2-dioxaphospholane boiling at 54–56° C at 10 mm was obtained. The refractive index was n_D^{20} 1.4700. (Lucas and co-workers (11) obtained apparently the same product without an acid-binding agent. It had a boiling point of 66° C at 15 mm and a refractive index of n_D^{20} 1.4696.)

When 1,3-butanediol was used, the method gave 2-chloro-4-methyl-1,3,2-dioxaphosphorinane (69.5 g, 98%) boiling at 55–57° C at 10 mm. The refractive index of this product was n_D^{20} 1.4670. (Arbuzov and Zoroastrova (10) reported b.p. 65° C at 12 mm and n_D^{20} 1.4700. Lucas and co-workers (11) gave b.p. 66.6–67.5° C at 15 mm and n_D^{20} 1.4884.)

Synthesis of Cyclic Hydrogen Phosphites by the Hydrolysis of Cyclic Chlorophosphites

To a mixture of water (3.6 g, 0.2 m) and benzene (100 ml), the solution of the chlorophosphite (0.2 m) in benzene (250 ml) was added, while it was shaken. The reaction mixture was then stirred for one-half hour. The resultant clear, homogeneous solution was fractionated in vacuum, when the benzene solvent was removed at first under 160 mm pressure. The raw product was then distilled at 2 mm of mercury.

2-Chloro-4,5-dimethyl-1,3,2-phospholane gave on hydrolysis 2-hydroxy-4,5-dimethyl-1,3,2-phospholane (26 g, 95%). The product was obtained between 81° and 83° C at 2 mm and had a refractive index, n_D^{20} 1.4610. Comparison of infrared spectra showed identity with the 2,3-butanediol transesterification product.

Similarly, by the hydrolysis of 2-chloro-4-methyl-1,3,2-phosphorinane, this procedure resulted in the formation of 2-hydroxy-4-methyl-1,3,2-dioxaphosphorinane obtained as a colorless liquid (25 g, 92%) between 101 and 102° C at 2 mm. The refractive index is n_D^{20} 1.4528. Although this product was a mobile liquid after distillation, it became quite viscous after a few days and was similar to the transesterification product with 1,3-butanediol. The identity of the two products was then proved by comparison of their infrared spectra.

Preparation of Cyclic 2-Chloroethyl Phosphites by Transesterification

Tris-2-chloroethyl phosphite (26.9 g, 0.1 m) and 1,2- or 1,3-glycol (0.1 m) were placed in a round bottom flask connected with a Claisen head, downward condenser, and receiver

for vacuum distillation. The contents became homogeneous within 5 minutes when heated in a water bath. Reaction was performed at 18 mm under nitrogen. The heating was continued for about 1 hour, during which time the evolution of ethylene chlorohydrin was complete.

The colorless crude product was fractionated at 2–3 mm pressure to obtain the pure products as clear, colorless liquids, immiscible in water. See Table II for properties and yields.

Preparation of Cyclic 2-Chloroethyl Phosphites from Cyclic Chlorophosphites

To a solution of the cyclic chlorophosphite (30.9 g, 0.2 m) (2-chloro-4,5-dimethyl-1,3,2-dioxaphospholane and 2-chloro-4-methyl-1,3,2-dioxaphosphorinane respectively) in ether (200 ml), ethylene chlorohydrin (16.1 g, 0.2 m) and subsequently pyridine (15.8 g, 0.2 m) were added dropwise with stirring at 0° C or lower. After the addition, the reaction mixture was allowed to come to room temperature with continued stirring. Pyridinium chloride was removed by filtration and the filtrate was fractionated.

In this manner, beginning with 2-chloro-4,5-dimethyl-1,3,2-dioxaphospholane between 56 and 60° C at 1 mm, 31 g (79%) 2-(β-chloroethoxy)-4,5-dimethyl-1,3,2-dioxaphospholane (2,3-butylene-2-chloroethyl phosphite) was obtained, n_D^{20} 1.4659. The spectrum of this compound was identical with the product of transesterification reported in Table II.

When the same method was used, 2-chloro-4-methyl-1,3,2-phosphorinane gave 33 g (86%) 2-(β-chloroethoxy)-4-methyl-1,3,2-dioxaphosphorinane distilled between 54 and 56° C at 1 mm and having a refractive index of n_D^{20} 1.4697. This compound had an identical spectrum with the corresponding transesterification product reported in Table II.

ACKNOWLEDGMENTS

The author is greatly indebted to Mr. A. J. Stephenson for the infrared spectra, to Mr. E. G. Ulbricht and Miss A. F. Fischel for the phosphorus analyses, and to Mr. J. F. Eagen for the chlorine analyses.

REFERENCES

1. Reuter, R. U.S. Pat. No. 2,280,450 (1942).
2. Gzemski, F. C. U.S. Pat. No. 2,353,558 (1944).
3. Hecker, A. C. and Leistner, W. E. U.S. Pat. No. 2,860,115 (1958).
4. Brown, D. M. and Higson, H. M. J. Chem. Soc. 2034 (1957).
5. Arbuzov, A. E. and Azanovskaya, M. M. Izvest. Akad. Nauk S.S.S.R. Otdel. Khim. Nauk, 473 (1949).
6. Arbuzov, A. E. J. Russ. Phys. Chem. Soc. **46**, 291 (1914).
7. Baker, A. A. and Brown, J. H. U.S. Pat. No. 2,670,368 (1954).
8. Kosolapoff, G. M. Organophosphorus compounds. J. Wiley & Sons, Inc., New York. 1950. p. 189.
9. Carré, M. P. Compt. rend. **136**, 756 (1903).
10. Arbuzov, A. E. and Zoroastrova, V. M. Izvest. Akad. Nauk S.S.S.R. Otdel. Khim. Nauk, 208 (1948).
11. Lucas, H. J., Mitchell, F. W., Jr., and Scully, C. N. J. Am. Chem. Soc. **72**, 5491 (1950).
12. Cook, H. G., Ilett, J. D., Saunders, B. C., Stacey, G. J., Watson, H. G., Wilding, J. G. E., and Woodcock, S. J. J. Chem. Soc. 2921 (1949).
13. Arbuzov, B. A. and Vinogradova, V. S. Izvest. Akad. Nauk S.S.S.R. Otdel. Khim. Nauk, 507 (1952).
14. Milobendzki, T. and Szulgin, K. Chemik Polski, 66 (1917); Chem. Abstr. **13**, 2867 (1919).
15. Gumlich, W. and Wriss, F. A. German Pat. No. 1,011,866 (1957).
16. Arbuzov, A. E. and Zoroastrova, V. M. Izvest. Akad. Nauk S.S.S.R. Otdel. Khim. Nauk, 770 (1952).
17. Arbuzov, A. E. and Zoroastrova, V. M. Izvest. Akad. Nauk S.S.S.R. Otdel. Khim. Nauk, 799 (1952).
18. Arbuzov, A. E. and Valitova, F. G. Izvest. Akad. Nauk S.S.S.R. Otdel. Khim. Nauk, 529 (1940).
19. Reich, W. S. Nature, **157**, 133 (1946).
20. Kabachnik, M. J. Izvest. Akad. Nauk S.S.S.R. Otdel. Khim. Nauk, 631 (1947).
21. Kabachnik, M. J., Rossiiskaya, P. A., and Novikova, N. N. Izvest. Akad. Nauk S.S.S.R. Otdel. Khim. Nauk, 97 (1947).

L'ARYLATION DES QUINONES PAR LES SELS DE DIAZONIUM

V. SUR LA SYNTHÈSE DE 5-ARYLTOLUQUINONES[1]

P. BRASSARD ET P. L'ÉCUYER

RÉSUMÉ

Tout comme la chloroquinone la toluquinone réagit en milieu tampon avec les sels de diazonium aromatiques pour donner des monoaryltoluquinones. Cependant, par contraste avec les réactions de la première, qui donnent naissance à deux isomères monoarylés, les réactions de cette dernière n'ont permis d'isoler qu'un seul isomère monoarylé. Celui-ci est fort probablement la 2-méthyl-5-aryl-1,4-benzoquinone, car il a été vérifié dans un travail ultérieur que tel est bien le cas pour la 2-méthyl-5-phényl-1,4-benzoquinone.

Diverses 1,4-benzoquinones monosubstituées réagissent en milieu tampon avec les sels de diazonium pour donner des 1,4-benzoquinones bisubstituées. Ainsi, selon ces conditions, une monoaryl-1,4-benzoquinone (I = Ar) donne naissance à une 2,5-bisaryl-1,4-benzoquinone (II, X = Ar) (1, 2), tandis que la chloroquinone (I, X = Cl) fournit un mélange de deux monoaryl-1,4-benzoquinones isomères que nous avons d'abord cru être la 2-chloro-3-aryl-1,4-benzoquinone et la 2-chloro-6-aryl-1,4-benzoquinone (II, X = Cl) (3, 4).

X = Cl, CH_3 ou Ar Ar = groupe aryle

Tout comme la chloroquinone, la toluquinone (I, X = CH_3) en milieu tampon aqueux réagit avec les sels de diazonium aromatiques. La réaction est cependant beaucoup plus lente avec cette dernière, à moins que l'activité du sel de diazonium ne compense partiellement la faible réactivité de la toluquinone. Nous avons réalisé la synthèse de diverses monoaryltoluquinones (Tableau I) et nous n'avons toujours isolé qu'une seule substance, bien qu'il soit possible qu'un autre isomère soit présent dans le produit d'au

TABLEAU I

2-Méthyl-5-aryl-1,4-benzoquinones

1,4-Benzoquinone	P.f., °C	Solvant	Formule	Analyse	
				% calculé	% trouvé
2-Méthyl-5-phényl-	107–109	Méthanol–acétone–eau (2:1:1)	$C_{13}H_{10}O_2$	C, 78.77 H, 5.09	C, 78.9 H, 5.0
2-Méthyl-5-(*o*-bromophényl)-	133–134	Acétone	$C_{13}H_9O_2Br$	C, 56.34 H, 3.27 O, 11.55 Br, 28.84	C, 56.0 H, 3.3 O, 11.4 Br, 28.8
2-Méthyl-5-(*p*-chlorophényl)-	128–130	Méthanol–acétone–eau (2:1:1)	$C_{13}H_9O_2Cl$	C, 67.11 H, 3.90	C, 66.9 H, 3.9
2-Méthyl-5-(*o*-nitrophényl)-	130–131.5	Acétone–méthanol	$C_{13}H_9O_4N$	C, 64.20 H, 3.73 N, 5.76	C, 64.1 H, 3.8 N, 5.7
2-Méthyl-5-(*m*-nitrophényl)-	185–185.5	Acétone	$C_{13}H_9O_4N$	C, 64.20 H, 3.73 N, 5.76	C, 64.2 H, 3.8 N, 5.8
2-Méthyl-5-(*p*-nitrophényl)-	156–158	Éthanol–acétone	$C_{13}H_9O_4N$	C, 64.20 H, 3.73 N, 5.76	C, 64.7 H, 3.9 N, 6.0

[1]*Manuscrit reçu le 1 juin 1959.*
Contribution du Département de Chimie, Faculté des Sciences, Université Laval, Québec, Qué.

moins quelques réactions. L'isomère isolé est fort probablement la 2-méthyl-5-aryl-1,4-benzoquinone (II, X = CH_3). C'est du moins la conclusion qu'il s'impose de tirer d'un travail ultérieur (5) dans lequel nous avons pu vérifier que, dans le cas de la condensation de la toluquinone avec le chlorure de benzène–diazonium, c'est bien la 2-méthyl-5-phényl-1,4-benzoquinone que l'on obtient.

Les monoaryltoluquinones sont des solides cristallins jaunes. Elles s'obtiennent avec des rendements variant de 20 à 85% selon les difficultés qu'on a à surmonter lors de leur purification.

(I) (II)

PARTIE EXPÉRIMENTALE[2]

On diazote, entre 0 et 5°, l'amine (0.05 mole) dissoute dans un mélange de 12.5 ml d'acide chlorhydrique concentré et de 50 ml d'eau, en ajoutant une solution de nitrite de sodium (3.5 g) dans de l'eau (10 ml). La solution limpide du sel de diazonium est ensuite versée dans un mélange de 6.8 g (0.055 mole) de toluquinone, de 20.4 g (0.3 mole) d'acétate de sodium trihydraté et de 500 ml d'eau, qui est agité mécaniquement. Sauf pour les sels de diazonium les moins actifs, le dégagement d'azote se produit lentement même à la température ambiante. Sinon, on porte le mélange à 35–40° en plongeant le récipient dans un bain-marie. On continue d'agiter pendant quelques heures et on abandonne ensuite le mélange réactionnel à la température ambiante jusqu'à ce que le dégagement gazeux soit terminé (12 à 24 heures). On filtre ou décante la solution aqueuse, lave à l'eau le précipité ou le résidu et sèche ce dernier.

Il est quelquefois assez difficile de purifier l'aryltoluquinone, car elle est parfois contaminée par une quantité variable de résines. Celles-ci sont très solubles dans l'acétone, moins dans le méthanol et presque pas dans l'éther de pétrole. Par ailleurs, les aryltoluquinones sont aussi passablement solubles dans l'acétone, moins dans le méthanol et peu dans l'éther de pétrole. En conséquence, on ne réussit quelquefois à se débarasser complètement des résines par cristallisation dans le méthanol qu'en faisant bouillir à plusieurs reprises la solution avec du noir animal. D'autre part, en cristallisant dans l'acétone (noir animal) non dilué, on obtient vite l'aryltoluquinone à l'état pur. Dans les deux cas toutefois, le rendement s'en trouve considérablement diminué.

Les deux meilleures façons de procéder pour la purification des aryltoluquinones semblent les suivantes: (*a*) Comme la 2-méthyl-5-phényl-1,4-benzoquinone est relativement soluble dans l'éther de pétrole (p.é. 65–110°) bouillant, on l'extrait à plusieurs reprises dans ce solvant, on évapore les extraits à siccité sous pression réduite et on cristallise ensuite dans le mélange acétone–méthanol–eau (1:2:1); (*b*) quant aux autres aryltoluquinones qui sont trop peu solubles dans l'éther de pétrole bouillant, on les cristallise directement dans un mélange de méthanol–acétone ou méthanol–acétone–eau et on les décolore au noir animal.

[2]*Les points de fusion (p.f.) ne sont pas corrigés. Ils ont été déterminés dans un appareil de Vanderkamp.*

REMERCIEMENTS

Nous remercions la Shell Oil Company of Canada et le Conseil National de Recherches du Canada pour des bourses d'études qu'ils ont accordées à l'un d'entre nous (P. B.).

BIBLIOGRAPHIE

1. KVALNES, D. E. J. Am. Chem. Soc. **56**, 2478 (1934).
2. BRASSARD, P. et L'ÉCUYER, P. Can. J. Chem. **36**, 700 (1958).
3. GÜNTHER, F. Brevet allemand 508,395 (1924).
4. BRASSARD, P. et L'ÉCUYER, P. Can. J. Chem. **36**, 814 (1958).
5. HOEGERLE, K. et L'ÉCUYER, P. Can. J. Chem. (Soumis).

EBULLIOMETRY AND THE DETERMINATION OF THE MOLECULAR WEIGHTS OF POLYMERS

PART I. THE SMALL EBULLIOMETER[1]

W. R. BLACKMORE

ABSTRACT

An ebulliometer that has been in routine use for the determination of the number average molecular weight of polymers is described. The results obtained with two different series of polythenes (which were also measured elsewhere) are given. These results show this ebulliometer to be subject to experimental difficulties which limit it to number average molecular weights of perhaps 20,000 depending on the precision required.

INTRODUCTION

Ebulliometry is the measurement of the difference in boiling point between a solution and a pure solvent at the same pressure. The technique may be used to measure the number average molecular weight of a polymer.

In the earliest work in ebulliometry, Beckmann (1) submerged one of his thermometers directly in the boiling liquid, first in the solvent and then in the solution, but the temperature difference thus determined was not accurately reproducible. It was found that there was superheat in the liquid and this was subject to large random fluctuations. Molecular weights of only the simplest compounds could be determined in this way. The situation was markedly improved by Cottrell (2), who first suggested the use of a vapor-lift pump. It was found that when pumped liquid was allowed to trickle down over a surface so that a thin film of liquid was in contact with solvent vapor, then temperature equilibrium was rapidly established. Furthermore this temperature was much more constant than in the main body of the boiling liquid itself (3).

Once the Cottrell pump had been introduced and the noise level reduced so greatly, it was not long before two transducers (4, 5) more sensitive than Beckmann thermometers were used in ebulliometry. These are still used in modern times (6, 7). After World War II new temperature-sensitive resistors, called thermistors (8), were developed to the point of being made available commercially. As applied in ebulliometry a steady-state temperature difference is established between two thermistors, each forming one arm of a Wheatstone bridge circuit. The temperature difference causes a resistance difference between the thermistor arms and this, in turn, produces an unbalance voltage which is amplified and recorded. In our apparatus the measured change in this unbalance voltage corresponding to the addition of weighed polymer pellets permits the polymer number average molecular weight $\bar{M}_n$ to be computed.

APPARATUS

Description of Glassware

The ebulliometer is shown in Fig. 1. This modified form of Ray ebulliometer (7) was designed in the Research Department of the Plastics Division of Imperial Chemical Industries Limited. The drawing was provided through the courtesy of Dr. Burnett.

[1]*Manuscript received April 3, 1959.*
Contribution from the Central Research Laboratory, Canadian Industries Limited, McMasterville, Que. A preliminary account of this work was presented to the Chemical Institute of Canada Meeting, Vancouver, June 1957.

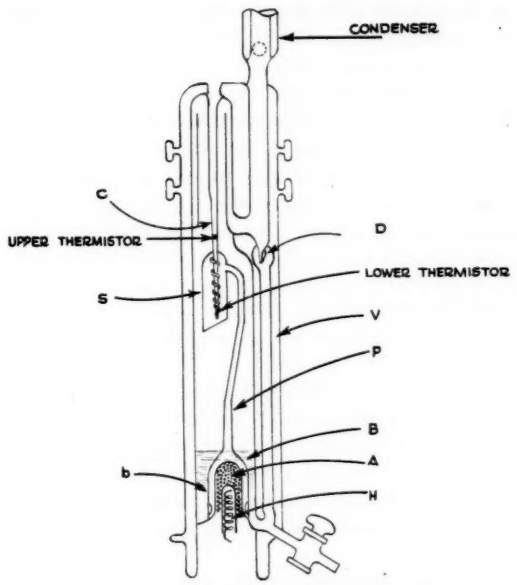

FIG. 1. The small ebulliometer.

The ebulliometer proper is protected from ambient temperature fluctuations by the silvered, vacuum jacket (V). Initially solvent is maintained at its boiling point in the boiler (B) by a bayonet heater (H) which heats by radiation and is not in contact with the boiling liquid. Polymer additions are made through the condenser. The stippled region (A) of the figure indicates crushed glass which has been fused to the inner surface of the boiler to promote boiling. The Cottrell pump (P) consists of a bell (*b*) and the stack up which boiling liquid is lifted by bubbles of vapor. When the liquid is ejected by the pump it is channelled by a spiral down the central core (C) which houses both thermistors. The shield (S) protects the lower tip of the well from any condensate which might roll down from the uppermost regions of the ebulliometer. The positioning of the thermistors is approximately as shown. The drop-counter (D), after Swietoslawski (3), was intended to provide a measure of the boil-up rate. In fact, it is frequently a source of experimental difficulty. Polymer pellets which only dissolve slowly may stick there temporarily and plug the condenser return line. This spreads a film of polymer on the upper reaches of the ebulliometer and spoils the run. The difficulty may be avoided by eliminating the drop-counter entirely. To protect the ebulliometer from atmospheric pressure fluctuations, it is connected by a wide-bore glass tube (2 in. diameter) to a 25-liter surge bottle which vents to the atmosphere through a length of capillary tubing. This does not reduce the pressure fluctuations within the ebulliometer produced by the surging liquid itself but it does remove the effects of draughts. Since improperly matched thermistors in Wheatstone bridge circuits may be very sensitive to atmospheric pressure changes it may be necessary to protect the ebulliometer from relatively long-term pressure drifts during the day. To do this a Cartesian Diver manostat (10) may be employed to control the pressure in the surge bottle.

Another experimental problem is that of thermal e.m.f.'s. Since a direct-current

thermistor bridge has been used with this ebulliometer, room temperature changes may produce drifts in the thermal e.m.f.'s which are large enough compared to the signals which are to be measured to seriously affect the results. This problem has been brought under control by mounting the ebulliometer and its associated electrical equipment in a thermostatted air bath. The design is not critical, the only requirement being that the box be large enough. The temperature is controlled at 34±0.5° C with a thermistor controller (11). The thermistor (32A11 V.E. Co.) (12) is situated close to the fan and main heater so that the response time may be fast. It should be pointed out that thermostatting does not remove the problem of thermal e.m.f.'s but merely renders the effects tractable.

Description of Electrical Components

The Wheatstone bridge is made up of two 52A11 V.E. Co. (12) thermistors which have been calibrated and matched in a manner to be described below. The remaining two arms of the Wheatstone bridge are fixed wire-wound resistors of accurately known resistance (nominally 2500 Ω) in series with a decade resistance box. Initially a Leeds–Northrup Model 9835-B, direct-current microvolt amplifier was used as the bridge output detector but this was replaced several years ago by a Liston–Becker (9), Model 14, breaker-type d-c. amplifier. The latter instrument is more sensitive. The amplifier output is fed through a resistance–capacitance network into a Brown "Electronik" potentiometer recorder (10 mv full scale).

It has been found desirable to use shielded cabling throughout. In those places where space was limited, for instance in the thermistor well, the Teflon coated leads were covered by a braided shield which was slipped as close to the extremities as possible. Thermal-free solder (with a low thermal e.m.f. to copper), supplied by the Liston–Becker Company (9), was used on all bridge connections. Originally all connections in the bridge were soldered. But during the course of time it has been found that it is more useful to have the leads from the bridge resistors enter a shielded junction box fitted with four double-pole single-throw heavy copper switches. With this arrangement it is easily possible to change thermistors, or to substitute wire-wound resistors for the thermistors if the electrical circuitry must be tested. All shields are connected directly to one ground point to avoid ground loops.

Thermistor Calibration

The thermistors which are to be calibrated are maintained at whatever temperature is desired in a large copper block. This copper block is heated by radiation and may be maintained (11) at any temperature, at least up to 300° C, with a precision of 0.001° C. The temperature of the copper block is measured with a platinum resistance thermometer and a Mueller bridge. The thermometer was calibrated at the National Physical Laboratory, Teddington, England. The resistances of the thermistors are measured with a Wheatstone bridge (Type 3352) manufactured by the Tinsley Company (13). A microvolt d-c. amplifier has been used to detect unbalance when thermistors are being calibrated, and this has been either a Liston–Becker (9) or the Leeds and Northrup. The unbalance voltage is fed from the amplifier to a Brown Electronik recorder. It is thus possible to follow slight changes in block temperature as well as measure the thermistor resistance simultaneously. The thermistor current normally used in calibrating a thermistor is about 25 μa so that the thermistor is only heated to a small fraction of a degree above its ambient temperature. Generally four or five thermistors are suspended in oil in the central well of the copper block simultaneously. It is thus possible to measure their

resistances consecutively at any one temperature before shifting the block temperature one or two degrees and taking another series of measurements.

BRIEF DESCRIPTION OF THEORY AND CALCULATION OF RESULTS

Fundamentally the apparatus behaves as follows: the two thermistor arms of the Wheatstone bridge are maintained at slightly different temperatures, because one thermistor is at the boiling point of the solvent while the other thermistor is at the boiling point of the solution. This difference in temperature, between the two thermistors, produces a resistance difference between them, and this, in turn, produces an unbalanced voltage signal from the bridge which is amplified and then displayed on the recorder. The actual value of the unbalance voltage which appears with a solution in the ebulliometer is of no particular significance. The only subject of concern is the *change* in this voltage produced when a pellet of solute of known weight is added to the boiling solution (or solvent).

It can be shown (14) that for any Wheatstone bridge in which all arms are of resistance R, except for one which has a resistance $R+\Delta R$, the unbalance voltage e_b appearing at the detector is given by an expression of the form

[1] $$e_b = k \,.\, i_b \,.\, \Delta R$$

where k is a constant,
i_b is the bridge current,
and ΔR the difference in resistance between the arms of the bridge.

The equation relating the resistance of a thermistor and its temperature (8) is

[2] $$R = R_0 e^{B/T}$$

where R is the thermistor resistance at temperature T °K,
R_0 is the thermistor resistance at some arbitrary reference temperature,
B is a constant related to the material of which the thermistor is made,
and T is the absolute temperature at which the resistance is desired.

Hence, assuming that we have two perfectly matched thermistors with the same R_0 and B, then if these are maintained at two slightly different temperatures T and $T+\Delta T$ their resistances will differ by an amount

[3] $$\Delta R = \frac{-B}{T^2} \,.\, R \,.\, \Delta T \,.$$

Thus substituting [3] into [1] we obtain an expression for the unbalance voltage obtained from a Wheatstone bridge when the two thermistor arms are maintained at temperatures differing by $\Delta T°$. This expression is

[4] $$e_b = \frac{-kB}{T^2} \,.\, i_b \,.\, R \,.\, \Delta T \,.$$

The boiling point elevation (15) for an ideal solution (or any solution at infinite dilution) is given by

[5] $$\Delta T = \frac{R_g T^2}{L_g} \,.\, N_2$$

where R_g is the gas constant,
L_g the molar heat of vaporization,
T the boiling point in degrees Kelvin,
and N_2 the mole fraction of solute.

When [5] is substituted in [4] and the constants are combined, an expression of the form

[6] $$e_5 = Ki_b \,.\, R \,.\, N_2$$

is obtained. This relates the unbalance voltage to the mole fraction of solute in the solution. But as has been mentioned earlier, the *change* in unbalance voltage with *change* in solute concentration is the only measurement actually used in this work. That is

[7] $$\Delta e_5 = Ki_b \,.\, R\Delta N_2.$$

Now $N_2 = n_2/(n_1+n_2)$ where n_1 is the number of moles of solvent; and for dilute solutions $n_1+n_2 \simeq n_1$. Therefore $N_2 \simeq n_2/n_1$ and since $n_2 = w_2/M_2$ where w_2 is the weight of solute of molecular weight M_2, equation [7] becomes

[8] $$M_2 = K \,.\, i_b \,.\, R \,.\, \frac{M_1}{w_1}\frac{\Delta w_2}{\Delta e_5}$$

and the molecular weight M_2 of the desired component is given in terms of quantities which are either measurable or known. When the second component is a polymer then M_2 is identical with $\bar{M}_n$, the number average molecular weight (16). Equation [5] for the boiling point elevation was used for simplicity and is not strictly applicable to polymer solutions. An equation of the type used by Smith (17) would be more precise.

During the course of a run the values of interest are the changes in e_5 brought about by the addition of a series of polymer pellets. The cumulative shift ($\Sigma\Delta s$) of the recorder pen, which is proportional to the boiling point elevation, is plotted versus the cumulative weight Σw (proportional to the concentration) of polymer added. It is found experimentally that for low molecular weight materials the cumulative shift so obtained is frequently a linear function of the total weight of material added, i.e.

[9] $$\Sigma\Delta s = a \,.\, \Sigma w;$$

but as the molecular weight of the material increases it is sometimes necessary to go to a quadratic equation

[10] $$\Sigma\Delta s = a_0\Sigma w + a_1\Sigma w^2.$$

This, however, is quite a common finding with polymer solutions (e.g. with osmotic pressures) and it is only in the limit of infinite dilution that one might expect a simple linear relation to hold. In the case where the linear relationship holds, the value of interest is the slope of the plot of $\Sigma\Delta s$ versus Σw. In the quadratic case ($\Sigma\Delta s/\Sigma w$) is plotted versus Σw and the value of the intercept at $\Sigma w = 0$ is used. The values of ($\Sigma\Delta s/\Sigma w$) for the polymer so obtained must then be related to the molecular weight of the polymer. The simplest method of doing this is to use a standard material, the molecular weight of which is known. Then using the relation

[11] $$\bar{M}_n\left(\frac{\Sigma\Delta s}{\Sigma w}\right)_{\text{polymer}} = M_s\left(\frac{\Sigma\Delta s}{\Sigma w}\right)_{\text{standard}}$$

it is possible to calculate the molecular weight of the unknown. This comparative procedure is recommended by Swietoslawski ((3), pp. 171–173). The technique, as we have used it frequently, consists of adding benzil pellets (the standard material) consecutively to establish the benzil sensitivity, i.e. the ($\Sigma\Delta s/\Sigma w$) for benzil for that day; then polymer pellets are added to this benzil solution and the $\Sigma\Delta s/\Sigma w$ for the polymer determined. The molecular weight of the polymer is then calculated using equation [11].

It may be objected at this point that the possibility of interaction between polymer and standard when both are added to the same solvent would vitiate this procedure entirely. This problem is discussed in greater detail later (21). Our results to date indicate that the procedure is safe, at least for benzil and polythene.

It may be mentioned as an aside, at this point, that the sensitivity attainable with thermistors and high gain amplifiers is so great that choosing a solvent because of its high ebullioscopic constant is no longer meaningful. Most ebullioscopic constants are within a factor of 10 of each other and any change in this value from solvent to solvent is easily compensated for by increasing the amplifier gain. A similar argument may be applied to the question of using a two-thermistor bridge or a four-thermistor bridge. The latter has twice the sensitivity of the former but the difficulty of matching four thermistors is more than twice that of matching two. Hence a two-thermistor bridge is used and gives more than adequate sensitivity.

EXPERIMENTAL RESULTS

The small ebulliometer has been in routine use for 4 years. During this time a large number of different samples has been determined with molecular weights ranging from the low hundreds to about 30,000. Rather than reproduce all the results, two series only will be discussed. These show, as well as any, the nature of the difficulties encountered. Furthermore each series was independently determined in another laboratory so that a check is provided. Those polymers other than polythene which have been measured gave similar problems.

The first series tested consisted of four polythene fractions (17) which had been prepared at Imperial Chemical Industries Limited, Alkali Division, where they were designated 47A/3/1, 2, 4, and 9. The results obtained at Imperial Chemical Industries Limited and Canadian Industries Limited are listed in Table I.

TABLE I

Comparison of I.C.I. and C-I-L results with some polythene fractions

	I.C.I. ebulliometer		C-I-L ebulliometer		
Sample No.	CCl_4	Toluene	CCl_4	Toluene	No. of runs
47A/3/1	4500	4000	4300	4320±130	2
47A/3/2		7090		6910, 6950, 6870	3
47A/3/4		11700		10000, 10500	2
47A/3/5	17280	13000			
47A/3/9	29400	20300	28200	16000, 17800	2

Sample No. 47A/3/5 has been included in this table even though it was not measured at Canadian Industries Limited because a tentative explanation for the different results obtained with the two solvents will be given in the discussion.

The next series of comparative determinations was performed by Dr. F. Sirianni of the Division of Applied Chemistry, National Research Council, Ottawa. The apparatus employed (18) permits a measurement of the depression of the vapor pressure over a solution compared with that over the solvent. His measurements were made with toluene solutions at 75° C. The results are listed in Table II.

One other sample has been determined both elsewhere and at Central Research Laboratory. This was a polystyrene which had been characterized both by osmometry and the method of radioactive end groups (22). The results were given as 24,000 and 20,000 respectively. Our result was 17,000.

TABLE II

Comparison of N.R.C. and C-I-L results with whole polythene samples

Alkathene melt index	N.R.C. results	C-I-L	
		CCl_4	Toluene
200000	2550	2400	2500
20000	4800	4680	4660
7000	6850	7100	7300, 6900
700	7750		7200, 6700
2	14150		10400
0.2	24350		18400

DISCUSSION OF RESULTS

It will be seen from Table I that the results obtained with the same samples in both ebulliometers agree quite well. The uncertainty with any one sample in toluene in the Canadian Industries Limited ebulliometer was least for low values of M_n and increased to about 10% at the highest M_n. The individual results are plotted in Fig. 2.

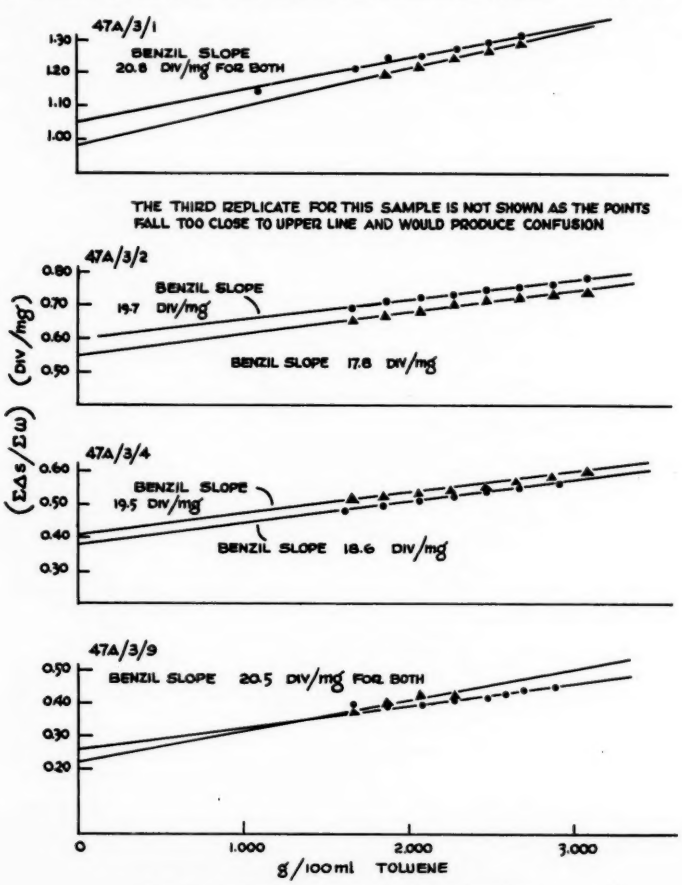

FIG. 2. Replicate runs on polythene fractions.

Two major points concerning the results in Table II and Fig. 2 should be discussed. The first is the remarkably large discrepancy between the value of M_n for sample 47A/3/9 in toluene compared with CCl_4, both at Imperial Chemical Industries and Canadian Industries Limited. A tentative explanation is that the high molecular weight species present in each added pellet do not dissolve in CCl_4 because of its low boiling point. Richards (19) and Myers (20) have both shown that the solubility of a polythene may be very sensitive to temperature. The percentage deviation between the results in CCl_4 and toluene increases as the value of M_n increases, which is in keeping with this explanation. Experimentally, since polythene floats on CCl_4, undissolved portions of the added pellets would be difficult to see because of the foam and the narrow viewing slit in the small ebulliometer. This explanation is, however, only tentative because Smith (17) also obtained high results in *n*-octane (boiling point 125° C) where the effect should not occur.

The second major point concerns the foam level during these runs. The "constant foam level" zone (see Foam, Part II (21)) was reached by using about 250 mg polythene in 15 ml solvent as the first addition. Subsequent additions were about 30 mg each. This means that the error introduced by the "foam shift" is hidden in the first value of $\Delta s/w$. Since this initial value of $\Delta s/w$ affects all subsequent values when the cumulative sums in $\Sigma\Delta s/\Sigma w$ are formed the error must be transmitted to the whole line. The magnitude of this error is unknown but the fact that it exists probably explains the increasing difference in results obtained between the next series measured at the National Research Council and Canadian Industries Limited.

The results of the second comparative series are shown in Table II. The agreement is good for the low molecular weight materials but there is an increasing disparity as the value of M_n increases. It is believed that the fault lies in the ebulliometer. This series provided a more stringent test of the ebulliometer for two reasons: (1) whole polymer produced more foam at lower polymer concentrations than did a fraction of comparable molecular weight and (2) the initial polymer concentration was low in each run of this series. This meant usually that the foam level changed during the run with consequences which are discussed later (21).

ACKNOWLEDGMENTS

The author wishes to thank Dr. D. C. West for his assistance in the early stages of this study, Mr. E. Lister for the skill and willingness with which this and other ebulliometers were constructed, Messrs. D. Hudson and R. Richard, by whom most of the measurements were made. The author is also indebted to Mr. H. Smith, Imperial Chemical Industries, Alkali Division, for having provided the series of polythene fractions; to Dr. A. F. Sirianni, National Research Council, Ottawa, for having performed the comparative measurements on the whole polythene samples; to Dr. H. T. Hookway for providing the polystyrene sample which had been characterized osmotically at the National Chemical Laboratory, Teddington, England, and which had been prepared and characterized radioactively by D. P. W. Allen of the British Rubber Producers Research Association.

REFERENCES

1. BECKMANN, E. Z. physik. Chem. **4**, 532 (1889).
2. COTTRELL, F. G. J. Am. Chem. Soc. **41**, 721 (1919).
3. SWIETOSLAWSKI, W. Ebulliometric measurements. Reinhold Publishing Corp., New York. 1945.
4. MENZIES, A. W. C. J. Am. Chem. Soc. **43**, 2309, 2314 (1921).
5. SAXTON, B. and SMITH, R. P. J. Am. Chem. Soc. **54**, 2626 (1932).

6. MORAWETZ, H. J. Polymer Sci. **6**, 117 (1951).
7. RAY, N. H. Trans. Faraday Soc. **48**, 809 (1952).
8. ADEY, A. W. Radio Physics Lab. Defence Research Telecommunications Establishment, Ottawa, Project Report No. 22-1-2 (1957).
9. LISTON-BECKER INSTRUMENT COMPANY, Stamford, Connecticut.
10. MANOSTAT CORPORATION, 20 N. Moore Street, New York 13, N.Y.
11. WOOD, H. H. Canadian Industries Ltd., McMasterville, Que., Report CRL-57-30. 1957.
12. VICTORY ENGINEERING CORPORATION, Springfield Road, Union, N.J.
13. H. TINSLEY & COMPANY, Smiths Falls, Ontario.
14. HARRIS, F. K. Electrical measurements. John Wiley & Sons, Inc., New York. 1952.
15. GLASSTONE, S. Textbook of physical chemistry. 2nd ed. D. Van Nostrand Company, Inc., New York. 1946.
16. HILDEBRAND, J. Solubility of non-electrolytes. 3rd ed. Reinhold Publishing Corp., New York. 1950.
17. SMITH, H. Trans. Faraday Soc. **52**, 402 (1956).
18. TREMBLAY, R., SIRIANNI, A. F., and PUDDINGTON, I. E. Can. J. Chem. **36**, 725 (1958).
19. RICHARDS, R. B. Trans. Faraday Soc. **42**, 10 (1946).
20. MYERS, C. S. J. Polymer Sci. **13**, 549 (1954).
21. BLACKMORE, W. R. Can. J. Chem. **37**, 1517 (1959).
22. ALLEN, P. W. and PLACE, M. A. J. Polymer Sci. **26**, 386 (1957).

EBULLIOMETRY AND THE DETERMINATION OF THE MOLECULAR WEIGHTS OF POLYMERS

PART II. BACKGROUND NOISE IN THE SMALL EBULLIOMETER[1]

W. R. BLACKMORE

ABSTRACT

It is shown that the usual form of ebulliometer is subject to at least three sources of noise. Those discussed here are (1) pressure fluctuations over the boiling liquid surface, (2) the Cottrell pump, and (3) the foam which appears on many polymer solutions when maintained at the boiling point. Background noise in this, and other ebulliometers commonly employed, may be large compared to the size of the signals expected for dilute high polymer solutions. Consequently further progress in ebulliometry is dependent on the development of a new ebulliometer with a much lower background noise.

INTRODUCTION

In any measurement the most important quantity is the signal-to-noise ratio. In ebulliometry, with high polymer solutions, the signal is frequently only a small boiling point elevation of perhaps 1000 microdegrees (μ° C). But the ebulliometer itself, because of the nature of its operation, introduces random temperature fluctuations, called noise. This noise is often an appreciable fraction of the signal to be measured. Thus even with pure solvent boiling and being pumped, the noise may be ± 150 μ° peak to peak, while as the concentration of polymer increases the noise also increases and may rise by a factor of five or six over the pure solvent noise. It is obvious that reducing the noise in an ebulliometer is greatly to be desired. The object of this work was to discover the sources of noise in the small ebulliometer (1).

EXPERIMENTAL SECTION

(1) *To Show the Principal Source of Background Noise*

The thermistor bridge normally used in the small ebulliometer only measures differential temperatures. To discover at which thermistor the noise is greater, the thermistor bridge was opened and the behavior of the thermistors was followed individually. To do this the Tinsley Wheatstone bridge (1), the Leeds and Northrup microvolt d-c. amplifier, and the Brown recorder were used. To facilitate the measurements the conditions were chosen so that the background noise would be much greater than normal. The ebulliometer was connected to a 25-liter surge bottle which was closed off from the atmosphere. The three traces obtained are shown in Fig. 1. It is obvious that most of the temperature fluctuation is produced at the lower thermistor which is exposed to the pumped liquid. The fluctuations recorded for the lower thermistor represent peak-to-peak fluctuations of ± 2.7 m° C. By comparison the upper thermistor trace shows only a slow drift produced by a slight increase in pressure in the surge bottle. The third trace is also most instructive. This was obtained when the tube connecting the ebulliometer to the surge bottle was closed off near the ebulliometer. This meant that pressure waves travelling up inside the ebulliometer from the surging boiling surface were now unable to dissipate themselves in the surge bottle and were reflected back down into the ebulliometer. The disastrous effect on

[1]*Manuscript received April 3, 1959.*
Contribution from the Central Research Laboratory, Canadian Industries Limited, McMasterville, Que.

the temperature stability at the upper thermistor is obvious. This noise represents peak-to-peak temperature fluctuations of ± 4.8 m° C. It must be emphasized that these conditions have been chosen for purely illustrative purposes; in normal operation the noise level is considerably lower.

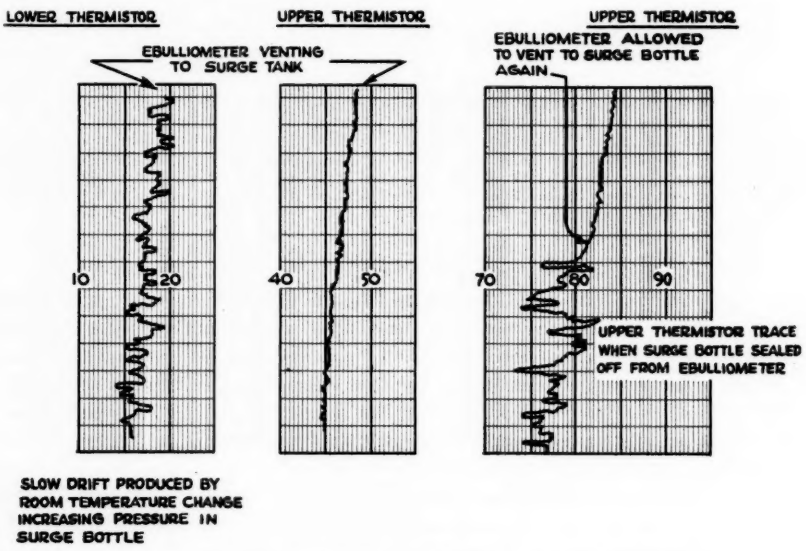

FIG. 1. Temperature fluctuations at individual thermistor wells.

The similarity of the trace obtained from the lower thermistor compared with that from the upper thermistor when the ebulliometer was closed off from the surge bottle raises one of the fundamental questions about background noise in ebulliometry. The question is this. The lower thermistor is subject in this ebulliometer to pressure fluctuations coming from (*a*) the boiling surface in the pot and (*b*) vapor puffs as the liquid is ejected by the the pump. Are these responsible for the noise at the lower thermistor? Under normal operating conditions the trace noise is of the order of $\pm(100 \rightarrow 150)$ μ° C for toluene. Differences of only $\pm(2 \rightarrow 3)$ μ Hg in the pressures of the vapors around each thermistor region would produce temperature fluctuations of the order mentioned.

(*2*) *To Show the Effects of the Boil-up Rate and Radiation from the Pump Heater on the Thermistors*

The first method used to investigate the effect of heater current variations was to follow the unbalance voltage from the differential bridge as a function of heater current, with a constant volume of solvent in the ebulliometer and the amplifier gain set high enough so that the background noise was clearly visible on the recorder. A curve typical of the results obtained is shown in Fig. 2. This curve was calculated from the differential thermistor bridge output by attributing the temperature changes to the lower thermistor and assuming the upper thermistor temperature was constant. The vertical bar at each point on the graph indicates the peak-to-peak noise level. The volume chosen was 15 ml of pure toluene for which the minimum heater current required in order for the pump just to operate is 3.0 amperes. The unbalance voltage from the thermistor bridge at this heater

current was chosen as the arbitrary zero. For any heater current above or below 3.0 amperes the trace indicated that the lower thermistor came to an equilibrium temperature which was higher than its temperature at the minimum heater current required for pumping. The noise increased with increased current too.

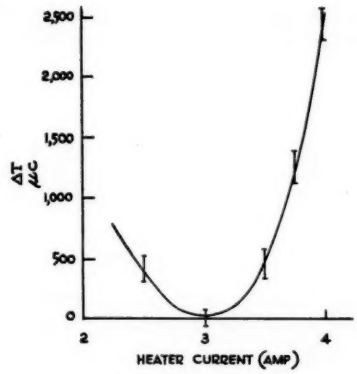

FIG. 2. Temperature difference between thermistors vs. pump heater current.

To understand this it was necessary to open the thermistor bridge and measure the resistances of the thermistors individually with the Tinsley Wheatstone bridge. The results obtained are indicated graphically in Fig. 3. The temperature change experienced by each thermistor was calculated relative to its temperature at the lowest heater current shown; pressure corrections were applied where necessary. No attempt to establish

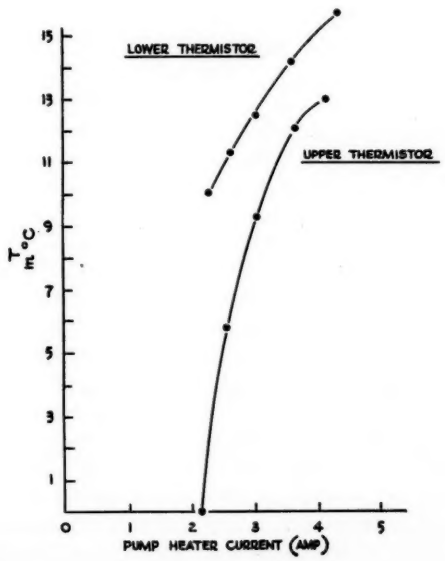

FIG. 3. Individual thermistor equilibrium temperature vs. pump heater current.

the absolute true minimum temperature difference between the thermistors was made since equipment of greater precision would have been required. For any one heater current each thermistor assumed an equilibrium temperature which was quite stable. Since the same form of curve was obtained with 10 ml in the boiler the relationship was not a function of the pumping rate. The results were attributed to (1) the changed boil-up rate, which established a new pressure head within the ebulliometer, and (2) radiation from the heater, which affected each thermistor, after multiple reflections by the silvered wall of the vacuum jacket.

(*3*) *The Cottrell Pump*

It seems reasonable to suppose that the energy required for any Cottrell pump to just operate must be proportional to the height through which the liquid is to be lifted and the mass of liquid to be pumped. Thus the energy required may be written as equal to

$$k.h.V.d.g.,$$

where k is a constant relating to pump efficiency, h is the height from boiling surface to pump exit, V and d are the volume and density of the fluid in the pump stack, and g is the acceleration due to gravity. This expression was tested by comparing CCl_4 and toluene at heater currents such that the pump just worked. From the equation we have $h_2d_2 = h_1d_1$, and since the density of CCl_4 (2) at its boiling point (76.7° C) is 1.483 g/ml while that of toluene at its boiling point (110.6° C) is 0.779 g/ml we would expect that the pump would only operate if the height for CCl_4 were half of that for toluene. An experimental check showed qualitative agreement with this analysis. The height was altered by working with different volumes of solvent. This relation also shows why a Cottrell pump works so much more easily (with less energy input from the heater) when foam, with its low density, is being pumped.

(*4*) *To Show the Effect of Hydrostatic Head on Superheat*

The unbalance voltage from the thermistor bridge was measured as a function of different volumes of solvent in the boiler. The heater current was held constant and the ebulliometer surge bottle was closed off from the atmosphere so that the pressure would not change. The experiment was started with 30 ml of toluene in the ebulliometer. After enough of a trace had been taken to allow a measure of the noise and to prove that this value of unbalance voltage was constant at that volume, 5 ml of toluene were allowed to drain out the stopcock without disturbing the heater current or the pressure. The recorder pen shifted to its new position and the whole procedure was repeated until the final volume was 10 ml. Once again the temperature difference between thermistors was least when the pump was just working. And the pump noise was also least at this point. When the volume was so low that the pump no longer worked the upper thermistor temperature was lower compared with that of the lower thermistor than it had been. To make sure that this interpretation was correct once again the thermistor bridge was opened up and the resistances of the individual thermistors followed separately. The curve obtained with the differential bridge is shown in Fig. 4 while the other two are given in Fig. 5. The curve shown in Fig. 4 was calculated from the thermistor bridge output by attributing the temperature changes to the lower thermistor and assuming the upper thermistor temperature was constant. In Fig. 5 the temperature change experienced by each thermistor was calculated relative to its temperature at a volume of 20 ml. A vapor ring was visible in the condenser at all volumes.

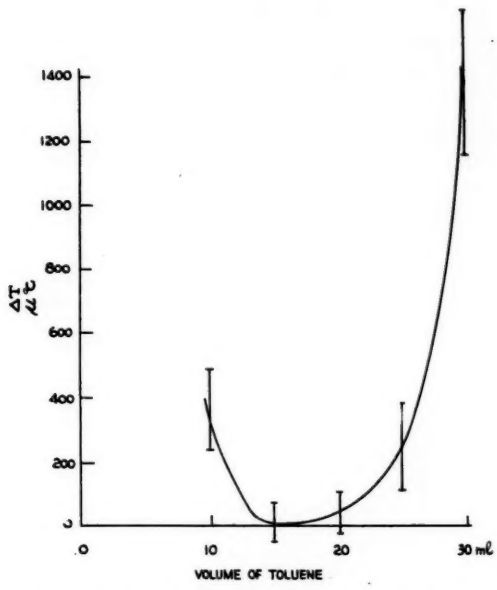

FIG. 4. Temperature difference between thermistors vs. volume of pure toluene in boiler at constant heater current (2.8 amperes).

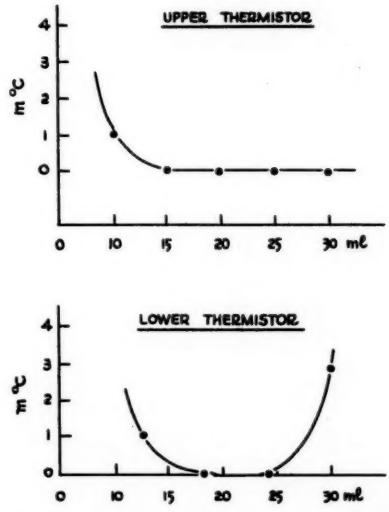

FIG. 5. Individual thermistor equilibrium temperature vs. volume of toluene in the boiler at constant heater current (2.8 amperes).

When these results are interpreted we are almost forced to conclude that the superheat in the liquid leaving the pump does not flash off immediately but rather requires more time to come to equilibrium than is available in the short run down the spiral around the

thermistor well. Since the hydrostatic head acting on the liquid in the pump bell is greatest at 30 ml, and the superheat and the pump rate are also greatest at this point the relatively vast quantity of liquid pouring over the lower thermistor may not have time to come to true equilibrium.

(*5*) *To Demonstrate the Effects of Foam in an Ebulliometer*

Many polymer solutions produce foam in the ebulliometer when maintained in a state of vigorous boiling. We have found, as did Smith (3), that both increasing molecular weight and wider molecular weight distribution in a polymer increase the amount of foam formed in the ebulliometer. Usually all the foam does not appear at once. Thus for a given polymer, in a low concentration region, there may be no foam, then in a slightly higher concentration zone there is increasing foam until finally another concentration zone of constant foam appears. Graphically this may be illustrated as in Fig. 6. When different

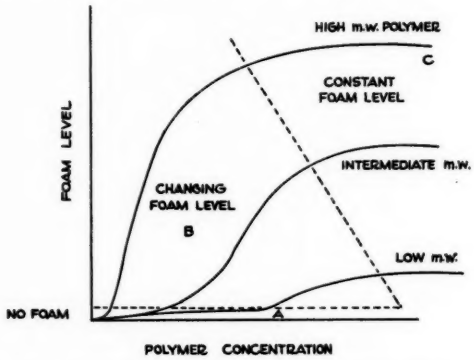

FIG. 6. Schematic representation of the foam level vs. polymer concentration for polymers of increasing molecular weight.

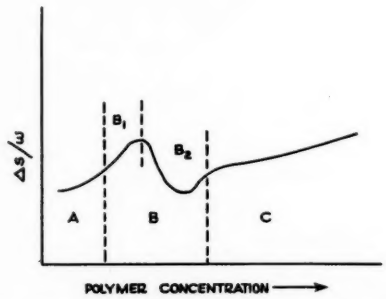

FIG. 7. Schematic representation of effect of foam level on sensitivities of successive polymer additions.

solvents are compared it is found that the behavior is similar but the "changing foam level" zone may have shifted along the concentration axis. For instance a polythene in CCl_4 produces more foam at lower concentrations than the same polythene in toluene.

Experiments to show the "foam shift" are reported below, but meanwhile a schematic representation will be given, which shows the effect most simply. Suppose successive polythene pellets, each of the same weight, are added to an ebulliometer operating with pure solvent in the boiler. Depending on the molecular weight of the material, we might obtain a curve such as that shown in Fig. 7. In region A no foam is present. In region B_1

foam begins to be established and the measurement indicates a total elevation which is the sum of the true boiling point elevation plus an elevation associated with the change in foam level. In region B_2, although the foam increases slightly, one measures lower values for $\Delta s/w$. Finally in region C the foam level is constant and $\Delta s/w$ increases with Σw as one expects for a polymer. Quite obviously the presence of changing amounts of foam accompanies serious changes in the polymer sensitivity.

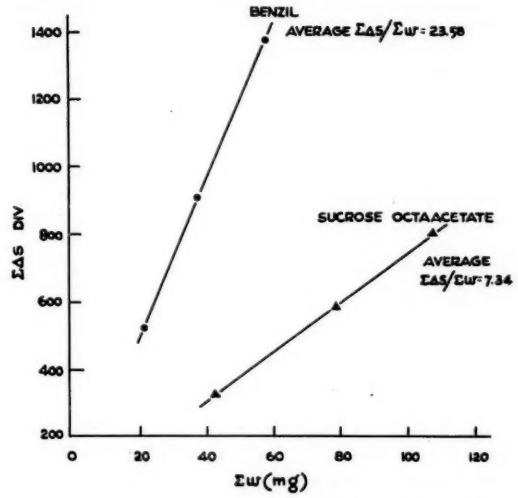

FIG. 8. Typical plots of $\Sigma\Delta s$ vs. Σw for alternate additions of low molecular weight materials.

Some experiments with foam will now be described. The first demonstrates that once the foam level is constant the sensitivity is constant. This fact was established as follows: the small ebulliometer operating with toluene was given a few benzil additions and the sensitivity measured. Then 60 mg of a polythene known to produce a great deal of foam were added, and the benzil sensitivity was measured again. The results are given in Table I.

TABLE I

Effect of foam on benzil sensitivity

Foam level	Trace noise, div peak-to-peak	Benzil		
		Δs, div	w, mg	$(\Delta s/w)$, div/mg
None	±2	54	4.3	12.6
None	±2	39	3.1	12.6
	Polythene foamer added			
Large amount of foam	±3	69	4.7	14.7
	±3	70	4.8	14.6
	±3	139	9.5	14.6
	±4	109	7.5	14.5
	More foamer added			
Extremely heavy foam	±9	161	8.9	18.1
	±9	143	8.8	16.3
This solution boiled all night and another benzil addition was made in the morning				
	±9	126	7.4	17.0

It is now necessary to establish whether (*a*) the changing foam level, (*b*) the different polymer concentration, or (*c*) the different benzil concentration produces the different benzil sensitivity. First it will be established (Table II) that the benzil sensitivity is independent of the benzil concentration.

TABLE II

Benzil sensitivity as a function of benzil concentration in toluene

Noise, div	Δs, div	w, mg	$(\Delta s/w)$, div/mg	$(\Sigma\Delta s/\Sigma w)$, div/mg
±2	45	3.86	11.7	11.7
±2	87	7.35	11.8	11.8
±2	90	7.64	11.8	11.8
±2	36	3.02	11.9	11.8
±2	94	7.75	12.1	11.9
±2	65	5.50	11.8	11.9

Next, the results in Table III show that the benzil sensitivity increases slowly with polymer concentration but not with the amount of foam present, while the individual polymer sensitivities change with the foam level established by the particular polymer addition. In the final stages of the polymer additions when the amount of foam present is not altered by an addition then the $\Sigma\Delta s/\Sigma w$ increases with Σw along a respectable straight line.

TABLE III

Effect of foam on polythene sensitivity

Substance added	Noise level	Δs, div	w, mg	$(\Delta s/w)$	Σw	$(\Sigma\Delta s/\Sigma w)$	Comments
Benzil	±2	79	6.45	12.2	6.45	12.2	No foam
	±2	51	4.00	12.8	10.45	12.4	
Polythene	±2	34	32.4	1.05	32.4	1.05	
Benzil	±2	42	3.15	13.3	13.60	12.6	
	±2	48	3.80	12.6	17.40	12.6	
Polythene	±2	39	32.0	1.22	64.4	1.13	Slight foam on surface
Benzil	±2	43	3.30	13.0	20.70	12.7	of boiling liquid but
	±2	43	3.34	12.9	24.04	12.7	none around thermistor well
Polythene	±2	87	60.1	1.45	124.5	1.29	Definite small surface
Benzil	±3	65	5.1	12.7	29.14	12.7	foam and slight froth
Polythene	±3	80	62.5	1.28	187.0	1.28	in umbrella at lower
Benzil	±3	48	3.75	12.8	32.89	12.7	thermistor. Remains
Polythene	±3	91	61.9	1.47	248.9	1.33	approximately con-
Benzil	±3	44	3.2	13.8	36.09	12.8	stant hereafter
Polythene	±3	100	63.7	1.57	312.6	1.38	
Benzil	±3	72	5.3	13.6	41.39	12.9	

(*6*) *Solvent Purity and Benzil–Polymer Interaction*

In this work the comparative method requiring the addition of a standard substance to the solution of the unknown has been employed for the reasons advanced by Swietoslawski ((4), pp. 171–173). The solvent used has been toluene ("from Sulfonic Acid") produced by Distillation Products Inc. It was assumed that neither the polythenes nor the benzil would associate with any impurity. Given this, the only difficulty which

might have arisen was a volatile impurity. To measure the effect of a volatile impurity increasing concentrations of water were added to boiling toluene in the small ebulliometer with the results given in Table IV.

TABLE IV

% water, g/100 cc	Ratio of wet toluene noise to noise for pure dry toluene
0	1
1.4	5
4.8	7
12.0	20

The toluene normally used was tested with Karl Fischer reagent and found to be dry (.0016 g/100 cc). No regularly repeating fluctuations were ever observed in a trace which would have indicated a volatile impurity. The reasons for using benzil (diphenyldiketone) as a reference substance are that it is (1) easily purified, (2) stable to heat and light, (3) non-hygroscopic, and (4) easily soluble in common organic solvents.

The next problem is whether the introduction of benzil may produce some interaction with the polythene solutions. To test this several experiments were performed. First a series of benzil additions was made to pure boiling toluene. This gave a completely linear plot of cumulative shift $\Sigma\Delta s$ versus total weight added Σw. The relationship has been proved linear up to concentrations as high as 10% (g/cc). The next experiment was to measure the benzil sensitivity ($\Delta s/w$) for alternate additions both before and after the introduction of a quantity of low molecular weight material, e.g. sucrose octaacetate. No change in sensitivity (Fig. 8) could be detected. If the formula weight for benzil is assumed known the molecular weight calculated for sucrose octaacetate from the data in Fig. 8 is 676.7, which is in error by 0.28%. This proved the feasibility of the method for solutions in which neither sensitivity was a function of the concentration. The next step was to do a run on a pure polythene solution. This was a low molecular weight material ($M_n = 3000$) and a plot of ($\Sigma\Delta s/\Sigma w$) versus Σw for this polymer was a straight line. No attempt was made to calculate a molecular weight from this series of polythene additions; the run was being used simply to determine whether the polymer sensitivity ($\Delta s/w$) increased with Σw. It did, in fact, quite slowly. Then a new run was made; this time the benzil sensitivity was measured after each polythene addition. It was found that the benzil sensitivity increased with increasing polymer concentration with the same slope as had the polymer plot of ($\Sigma\Delta s/\Sigma w$) versus Σw. Consequently it was concluded that the benzil did not affect the polymer, and conversely.

DISCUSSION OF RESULTS

The problems which may arise from (*a*) pressure fluctuations in the ebulliometer, (*b*) changes in the boil-up rate, (*c*) radiation from the heater acting on the thermistors, and (*d*) uneven delivery from the pump each may be corrected by fairly obvious changes in design. This has, in fact, been done with an ebulliometer to be described later in this series.

The real problems are to understand (1) why polymer solutions produce noise which increases as a function of the concentration and (2) how to explain the "foam shift". From the foregoing results it appears that a constant amount of foam in the ebulliometer is not troublesome. The principal difficulty arises when the amount of foam is changed by the addition of polymer for then the shift measured is not necessarily the true boiling point elevation but also has associated with it what is called a "foam shift".

The first attempt to explain the foam shift was an argument to the effect that the dissipation constant of foam at the lower thermistor was less than that of liquid. Consequently, since thermistors must always float slightly above the ambient temperature, if less heat were taken away from the lower well by foam than by liquid, then the boiling point elevation measured on the addition of a material which changed the foam level would be greater than the true value. Unfortunately, measurements of the dissipation constant proved that this was not the case. The dissipation constant was unchanged whether foam or liquid engulfed the well.

The next approach was to consider the hypothesis advanced by Smith (3) to explain the curves he obtained. It was supposed there that adsorption in the foam at low bulk concentrations gave a polymer "excess" in the foam which consequently produced a greater boiling point elevation than that expected. At higher polymer concentrations this foam adsorption represented a much smaller percentage of the material present and, as well, approached a saturated value so that the measured elevations corresponded much more closely to the true values. This satisfactorily explained the shape of the curves obtained with toluene. But the same shape curve was not obtained with CCl_4 although foam (3) appeared even earlier in this solvent. Hence surely the effect should have been found there too.

CONCLUSIONS

The results quoted have shown three sources of noise in an ebulliometer of a design similar to most now employed throughout the world. These are:

(1) instantaneous pressure differences in the vapors surrounding each detector element,

(2) remnants of superheat in the liquid ejected by the Cottrell pump, and

(3) the foam produced by most polymer solutions when maintained at the boil.

Each of these may be corrected by fairly obvious changes in design. This has been done with the new ebulliometer to be described later in this series.

ACKNOWLEDGMENTS

The author wishes to thank Drs. A. T. Williamson and S. S. Grimley for the many clarifying discussions of the problems mentioned in this paper.

REFERENCES

1. BLACKMORE, W. R. Can. J. Chem. **37**, 1508 (1959).
2. TIMMERMANS, J. (*Editor*). Physical chemical constants of pure organic compounds. Elsevier Press, Inc., N.Y. 1950. pp. 152, 224.
3. SMITH, H. Trans. Faraday Soc. **52**, 402 (1956).
4. SWIETOSLAWSKI, W. Ebulliometric measurements. Reinhold Publishing Corp., New York. 1945.

ELECTROMIGRATION OF IONS ABSORBED BY FILTER PAPER[1]

R. A. BAILEY[2] AND L. YAFFE

ABSTRACT

The variation with absorbance of the zone mobilities and obstructive factors for a number of inorganic ions has been investigated in acetic acid and in ammonium hydroxide at several concentrations. The results agree with the form of the semiempirical equation of Crawford and Edward. For a given ion the apparent obstructive factor defined as

$$\rho_{app} = \frac{\text{zone mobility}}{\text{free solution mobility}}$$

remains fairly constant as the concentration of the background electrolyte is changed, except in the very dilute region. However, the apparent obstructive factor varies with the ion and the background electrolyte indicating that specific effects, which are not considered in the equation, are important.

INTRODUCTION

The separation of ions by electromigration in paper has received much attention in recent years, but it is for the most part an empirical technique. Theories have been proposed to account for the behavior of ions under the conditions which prevail in this process and, although they are based on a somewhat naive model, they seem to be at least qualitatively valid. In order to see to just what extent these theories are applicable, there is a great need for accurate and reproducible measurements of zone mobilities under conditions where all of the many variables are fixed. This is especially so in the case of inorganic ions. In this paper we shall show that, while the zone mobilities (defined as the velocity under unit voltage gradient of the zone of ions on the paper) of inorganic ions in paper do follow the existing theories in a general manner, specific effects are present which cannot be accounted for satisfactorily.

Electromigration of ions in paper was first treated fundamentally by Kunkel and Tiselius (1). Their treatment was later modified by Edward (2). In the model used, the zone mobility U_z of an ion migrating in paper is given by the expression

$$U_z = \rho U_F \qquad [1]$$

where U_F is the mobility of the ion in free solution, and ρ is a correction factor called the obstructive factor (2) which is the reciprocal of the square of the conventional tortuosity factor (3). This correction factor stems from the fact that the path followed by the ion in paper would be more tortuous than in free solution since the ion must now detour around the inert fibers of the paper.

If L is the length of the paper and L^1 the length of the crooked channel in it, which the ion must follow, it is readily shown that

$$\rho = \left(\frac{L}{L^1}\right)^2 = \frac{K^1}{K} \qquad [2]$$

where K^1 is the conductance of the solution when it is in the paper, and K its conductance in the free state. It is possible, then, to estimate the value of the obstructive factor from conductance measurements.

[1]*Manuscript received May 25, 1959.*
Contribution from the Radiochemistry Laboratory, Department of Chemistry, McGill University, Montreal, Que. with financial assistance from the National Research Council of Canada, Ottawa, Canada.
[2]*Holder of National Research Council Studentships, 1957–58 and 1958–59.*

Crawford and Edward (4) have considered the variation of the obstructive factor ρ with the volume of liquid present per unit weight of paper (the absorbance) and, in certain cases, their results make it possible to calculate this obstructive factor. Their treatment was based on a semiempirical equation devised by Biefer and Mason (5) giving the conductance of pads of randomly oriented, non-conducting, non-swelling fibers, which in turn was obtained from the theoretical equation

[3] $$K^1 = \frac{kf(\theta)A\epsilon}{L}.$$

Here, k is the specific conductivity of the solution, A is the cross-sectional area of the pad and solution, L is its length, and ϵ is its void fraction:

$$\epsilon = \frac{V_L}{V_L + V_s}$$

where V_L is the volume of the liquid, and V_s the volume of the solid fibers. $f(\theta)$ is an orientation factor which was originally equated to the void fraction on experimental grounds. Subsequent work (5) has shown that better agreement with experiment is obtained if $f(\theta) = \alpha\epsilon$ where α is a constant which is close to unity. Measurements with cellulose acetate, Dacron, nylon, and glass fibers give a mean value of 0.955 (5). Then

[4] $$K^1 = \frac{kA\alpha\epsilon^2}{L}.$$

Since $A = (V_L + V_s)/L$, then substituting for A and ϵ gives

$$\alpha\epsilon = \frac{K^1L^2}{kV_L},$$

but

[5] $$\rho = \frac{K^1}{K} = \frac{K^1L^2}{kV_L}.$$

Thus

$$\alpha\epsilon = \rho.$$

The absorbance a is

$$a = \frac{V_L}{\text{weight of solid}}.$$

Applying this we get

[6] $$\rho = \alpha\left(\frac{a}{a + v_s}\right)$$

where v_s is the specific volume of the fibers.

Cellulose fibers are known to swell in aqueous solution. If X is the fractional increase in fiber volume that is effective in hindering ion migration, then

$$\epsilon = \frac{V_L - XV_s}{V_L + V_s}.$$

Then, from equations [4] and [5]

[7] $$\rho = \alpha\left(\frac{a - 2v_sX}{a + v}\right).$$

Crawford and Edward, using conductance measurements, found that values of X between 0.1 and 0.2 fitted most of their experimental obstructive factors for inorganic salt solutions; α was taken as unity.

From equation (6) it is possible to calculate the obstructive factor for non-swelling fibers such as glass, if the theory is correct. The only uncertain factor in the equation is α. This can be assumed to be unity with only a small error, or it can be taken as 0.96 from the work of Biefer and Mason. The expression $f(\theta) = \alpha\epsilon$, on which equations [6] and [7] depend, is admittedly empirical, but it does seem to be well founded experimentally.

The above model makes no allowance for specific interactions between the ions and the fiber. It is true that the value of ρ obtained from conductance measurements may include effects of adsorption and may therefore show a dependence on the electrolyte used, but the measurements so far made in this connection have been with solutions of much higher concentrations than is usual for the ions moving in a separation, so that the paper is 'overloaded'. It is possible that adsorption effects at low concentrations are more marked. Furthermore, the background electrolyte itself may well affect the way in which the ion interacts with the paper. This would not be shown from conductance measurements.

By the use of radioactive tracers, we have been able to check any low concentration effects and test the validity of these empirical equations.

EXPERIMENTAL

The paper was placed between two brass plates, 60×25 cm in size, and insulated by polythene film of about 0.01-in. thickness. Water from a constant temperature bath (25.0±0.5° C) was circulated through copper tubing which was soldered to the backs of these plates. In a few experiments at lower temperature, the control was not as good. Measurements with a thermocouple in contact with the paper showed that at an applied potential of 30 v/cm, a current of 1 milliampere could be carried for each centimeter width of the paper with an increase of less than 0.5° C in the actual temperature of the strip. This is approximately the rise calculated by assuming an equilibrium between the amount of heat generated in the paper and that conducted across the polythene insulation.

Wood and Strain (6) have shown that electroosmotic flow of the background electrolyte is largely eliminated if the electrodes are placed in direct contact with the paper. We used this arrangement and, when necessary, prevented interference from the electrolytic products by moistening the zones at the ends of the paper with a suitable buffer solution which trapped the ions so formed without itself giving an interfering ion. These buffer zones also served to keep the voltage drop across the electrodes nearly constant without manual control. This procedure was chosen in preference to correcting for electroosmotic flow by the motion of zones of uncharged substances. Such corrections are always subject to uncertainty about the relative effects of adsorption on the motion of the ion and the indicator substance. Also, if the flow of electrolyte is not uniform, as when the liquid flows from both ends of the strip toward the center (the 'wick effect') (7), the effect of this flow on the migrating ion is difficult indeed to determine from the motion of the indicator zones. When uncharged materials, particularly H_2O_2, were used as indicators in our technique, these materials showed no measurable motion.

Voltages were measured by means of a vacuum tube voltmeter connected to platinum probes that were at some distance from the ends of the paper strip so that voltage

drops across the platinum foil electrodes and the buffer zones were not considered. Separate measurements showed that the voltage gradient in that part of the strip where the migration took place was uniform, and remained so for the duration of an experiment.

In order to obtain known reproducible absorbances of the paper, the desired volume of electrolyte was spread as uniformly as possible over the strip from a pipette. The buffer zones were moistened to the same absorbance. The electrolyte was allowed to spread for ½ hour or more and the solution to be investigated was applied at the starting line as a spot or a streak. This method of moistening the strip was quite satisfactory except at very low absorbances.

There are certain advantages in using radioactive materials in this work. The zones of material are very easily detected by their radiations so that no chemical tests are necessary, and exceedingly small amounts of material can be used so that the ionic strength of the moving zone is not appreciably different from that of the background solution. Although the influence of concentration of the moving ion on its zone mobility has not yet been adequately studied, it is known that there is an effect. Our work indicates that, at least in non-complexing media, the zone mobility decreases slowly with increasing concentration, while at the same time the zone becomes broader. The latter was reported also by Maki (8). The solutions used here were sufficiently dilute to render the effects of concentration entirely negligible; indeed, the Na^{22} was effectively 'carrier-free', i.e. ca. 10^{-8} molar.

Na^{22}, Cs^{137}, Tl^{204} (as Tl^{+}), Cl^{36} (as chloride), Co^{60}, and Zn^{65} were the radioactive tracers used. Inactive Cu^{++}, Cd^{++}, and Fe^{+++} were used in the form of 0.001 *M* solutions of the nitrate; some of the experiments with Zn^{++} and Co^{++} were done with similar inactive solutions. The volume applied was in most cases 10 microliters. The volume of Tl^{+} was usually 5 μl, however, and in other cases some experiments were made with 20 or 50 μl of solution.

The active ions were detected by cutting the strip into sections 1 cm (occasionally 0.5 cm) broad, and measuring each with a Geiger counter. The inactive ions were detected with a solution of dithizone in CCl_4 or by exposure to H_2S.

The papers used were Whatman No. 52 chromatography paper, 5.1 cm wide, and Reeve Angel 934AH glass fiber filter paper, 2.9 cm wide. The length of the paper available for migration varied in different experiments from 20 to 50 cm, and actual distances of migration ranged from about 15 to 50 cm.

RESULTS AND DISCUSSIONS

In order to calculate the zone mobility, U_z, it is first necessary to determine U_F, the mobility of the ion in question in the solution used as background electrolyte. This must be estimated from the ionic conductance at infinite dilution by taking into account the effects of ionic strength and viscosity. We must consider the effects of foreign ions and uncharged molecules on the ion studied, and this makes an accurate calculation of U_F very difficult. For instance, the value of the dielectric constant, which enters into all conductance equations, is probably appreciably different in 6 *M* acetic acid from what it is in pure water, but we are unable to make a satisfactory allowance for such changes. Fortunately all solutions used have quite a low ionic strength, and the correction given by the limiting form of the Onsager equation, taking the constants to be those for pure water, probably serves as well as that which could be obtained from more complicated equations which are largely untested under conditions such as we are considering. In addition, the change in mobility due to ionic strength alone is small

compared with the effect of viscosity. Therefore, we have corrected for ionic strength by the Onsager equation and divided this result by the relative viscosity to get U_F. The result, although perhaps crude, is not likely to involve an error greater than that in the experimentally determined zone mobilities.

Each of the zone mobilities included in these results represents the mean of three or more experiments, usually carried out with different voltage gradients and migration times. Figure 1 shows the variation of the zone mobilities of Fe^{+++}, Co^{++}, Ni^{++}, Cu^{++}, Zn^{++}, and Cd^{++} with absorbance in 2.36 M acetic acid at 5° C. The curves are linear in most cases. The precision of these measurements is not sufficient to show the slight curvature that would be present if equation [7] were valid.

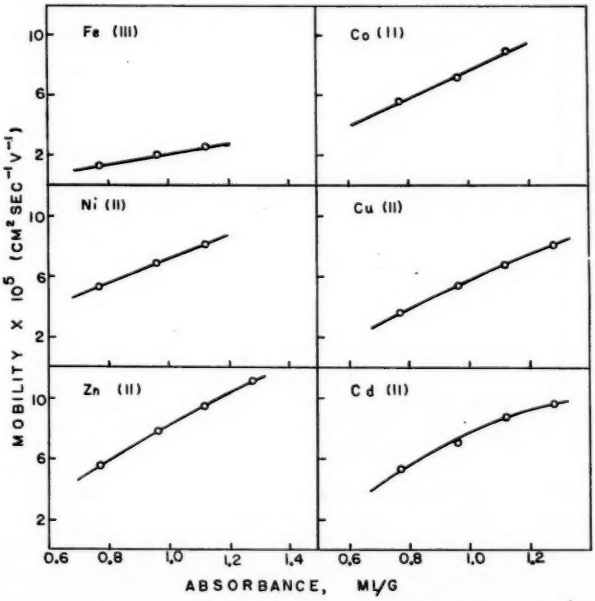

FIG. 1. Zone mobility vs. absorbance for several positive ions in 2.36 M acetic acid. Whatman No. 52 paper; 5±1° C.

Results for Cs^+ at 25° C in a variety of background electrolyte solutions are given in Fig. 2. They show the same nearly linear form as do the previous examples. In Fig. 3 the apparent obstructive factor is compared with the obstructive factor calculated from equation [7] using the values of X that give the best over-all fit for the experimental data. The calculated and experimental curves agree very well in most instances.

It is of interest to consider ρ_{app}, i.e. zone mobility/free solution mobility, as a function of concentration of background electrolyte at fixed absorbance. This is given for a number of ions in acetic acid and ammonium hydroxide in Tables I and II. The zone mobility is plotted as a function of concentration for Cs^+ in acetic acid, in Fig. 4, and is typical of all examples investigated. At acetic acid concentrations above about 0.05 M, the curve of zone mobility concentration decreases. This is the sort of behavior that would be expected from ionic strength and viscosity considerations. In this region, ρ_{app} has a nearly constant value for most ions, although there seems to be a tendency

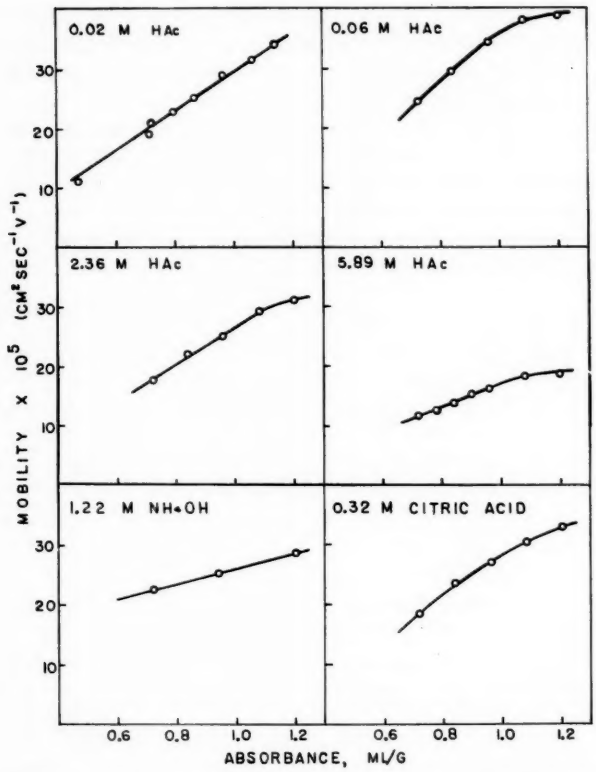

FIG. 2. Zone mobility vs. absorbance for Cs^+ in several background electrolytes. Whatman No. 52 paper; 25.0±0.5° C.

for it to fall off to some extent at higher concentrations. In the more dilute region, the zone mobility decreases quite markedly, and consequently ρ_{app} decreases also. Although this would require a corresponding increase in X if equation [7] were to be obeyed, there is no suggestion that the swelling of the cellulose fibers undergoes any particular change at this point. In fact the reduction of mobility with decreasing concentration seems to set in at a value more characteristic of the valence type of the moving ion than of the nature of the background electrolyte. The maximum zone mobility seems to occur close to 0.06 M for the univalent ions in both acetic acid and ammonium hydroxide, but at 0.5 M for the bivalent ions in acetic acid. Extensive measurements in this dilute region have been made only with Cs^+, however, and for other ions mainly the behavior at the higher concentrations is considered.

The cause of the decrease in zone mobility at low background electrolyte concentrations may be due to adsorption effects, since considerable trailing of the zones occurs, and the spots have the 'comet' shapes typical of adsorption (9). The fact that, in the more highly ionized citric acid, the decrease does not occur until a considerably lower concentration is reached indicates that the ionic strength may be important in this connection, and there are also other factors that cannot be excluded.

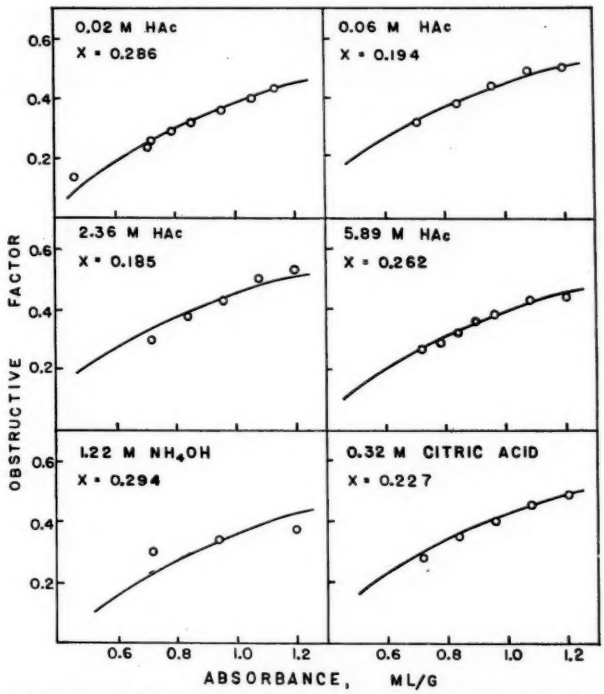

FIG. 3. Comparison of calculated and experimental (or apparent) obstructive factors as a function of absorbance for Cs^+ in several background electrolytes. The curves are calculated from equation [7] using the values of X indicated. The circles represent experimental points. Whatman No. 52 paper; 25.0±0.5° C.

Equation [7] assumes that there is no specific interaction between the migrating ion and the paper, and that consequently the obstructive factor is the same for all ions. That this is not the case is shown by the data in Tables I and II. ρ_{app} differs quite appreciably from ion to ion, and for the same ion in different background electrolytes. Evidently, since Na^+ has the largest ρ_{app}, it is the least obstructed, or hindered, of the ions studied, followed by Cs^+ and then by Tl^+. Zn^{++} and Cd^{++} are hindered somewhat more, while Cu^{++} shows the lowest ρ_{app} and is slowed to the greatest extent. It is obvious that the picture of an ion moving down a crooked channel is too simple to explain this process completely. By postulating absorption, one can explain the variation of ρ_{app} on the basis of different strengths of binding between the cellulose and the various ions. It is known that ions may travel through a portion of the swollen fiber (i.e. that the fractional increase, X, that is effective in hindering ion migration is less than the total fractional increase in volume on swelling (10, 11)). The bivalent ions seem to be more hindered than the univalent, but there are not enough examples to make any generalization between ρ_{app} and size or charge. Greater interaction with the negative acetate ions may be in part responsible for this increased hindrance.

A negative ion such as Cl^- might have different absorptive properties with respect to cellulose, but for the most part there seems to be little difference in its behavior, as shown in Table III. The mobility drops sharply in very dilute solutions, as for positive ions.

TABLE I

Zone mobilities of several positive ions in various concentrations of acetic acid

Ion	Concentration of acetic acid, moles/liter	U_s, $cm^2\ v^{-1}\ sec^{-1} \times 10^5$	ρ_{app}
Cs^+	0.01	27.8	0.35
	0.02	28.8	0.36
	0.04	31.2	0.40
	0.06	34.5	0.44
	0.59	30.9	0.43
	1.18	28.8	0.43
	2.36	25.1	0.43
	5.89	16.2	0.38
Na^+	0.06	24.8	0.49
	0.59	22.1	0.47
	1.18	20.7	0.48
	2.36	18.1	0.48
	5.89	13.4	0.49
Tl^+	0.06	27.0	0.36
	0.59	25.4	0.36
	2.36	21.1	0.37
	5.89	13.4	0.32
Cu^{++}	0.06	10.2	0.18
	0.59	10.4	0.20
	1.18	11.0	0.22
	2.36	9.0	0.21
	3.40	7.2	0.19
	5.89	5.1	0.17
Zn^{++}	0.06	15.7	0.30
	0.59	15.8	0.33
	1.18	16.1	0.35
	2.36	12.6	0.32
	3.40	10.7	0.31
	5.89	7.7	0.27
Cd^{++}	0.06	14.9	0.30
	0.59	15.3	0.33
	1.18	15.1	0.36
	2.36	11.6	0.32
	3.40	9.4	0.29
	5.89	6.9	0.26

NOTE: Absorbance, 0.96 ml/g, Whatman No. 52 paper, 25.0±0.5° C.

TABLE II

Zone mobilities of some positive ions in various concentrations of ammonium hydroxide

Ion	Concentration of NH_4OH, moles/liter	U_s, $cm^2\ v^{-1}\ sec^{-1} \times 10^5$	ρ_{app}
Cs^+	0.06	28.9	0.37
	0.61	26.1	0.34
	2.4	23.8	0.33
	6.1	21.5	0.33
Na^+	0.06	21.3	0.42
	0.61	19.9	0.41
	2.4	19.6	0.43
	6.1	17.9	0.43
Tl^+	0.06	15.6	0.21
	0.61	12.4	0.17
	1.22	11.8	0.16
	2.4	10.7	0.15
	6.1	9.5	0.15

NOTE: Absorbance 0.94 ml/g, Whatman No. 52 paper, 25.0±0.5° C.

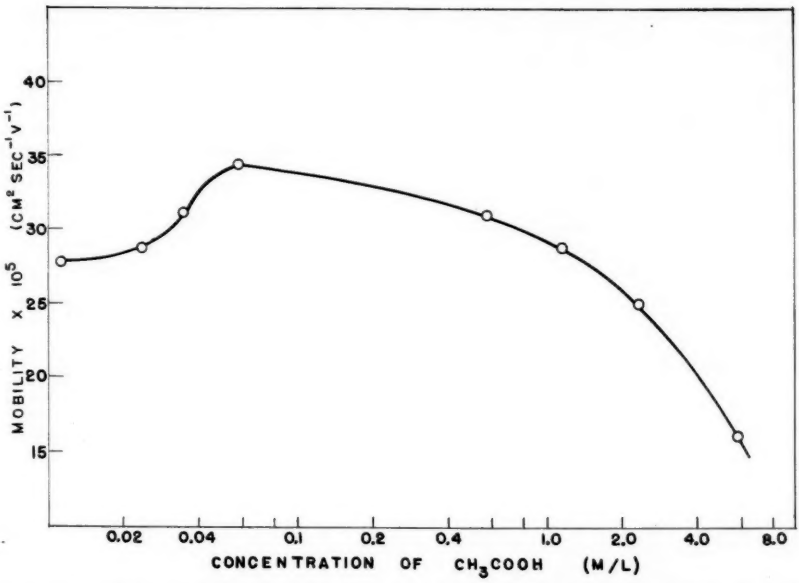

FIG. 4. Zone mobility vs. concentration for Cs^+ in acetic acid. Absorbance 0.96 ml/g; Whatman No. 52 paper; 25.0±0.5° C.

TABLE III

Zone mobility of Cl^- in varying concentrations of acetic acid and ammonium hydroxide

Background electrolyte	Concentration of background electrolyte, moles/liter	U_z, $cm^2\ v^{-1}\ sec^{-1} \times 10^5$	ρ_{app}
Acetic acid	0.02	15.2	0.20
	0.06	30.3	0.39
	0.59	26.3	0.37
	1.18	24.1	0.36
	2.36	20.1	0.35
	5.89	16.0	0.38
NH_4OH	0.6	24.8	0.33
	2.4	24.0	0.34
	6.1	22.2	0.34

NOTE: Absorbance 0.96 ml/g, Whatman No. 52 paper, 25.0±0.5° C.

Fibers such as glass do not swell in aqueous solutions, so it should be possible to apply equation [6] to electromigration in glass fiber filter paper. In Figs. 5 and 6 are shown the mobilities of Na^+ and Cl^- respectively, in such a medium with acetic acid as background electrolyte. Glass paper appears to absorb positive ions to a much greater extent than does cellulose paper. At any rate both Cs^+ and Tl^+ showed very extensive trailing, and Na^+ trailed considerably in acetic acid of less than 1 *M* concentration. The calculated value of ρ, assuming v_s to be 0.43 and α to be 0.96, is 0.84 for the absorbance used. In the high-concentration regions (above 1 *M*) U_z, calculated using this value of ρ, agrees fairly well with the experimental value, considering the errors involved in both the experimental and the calculated values.

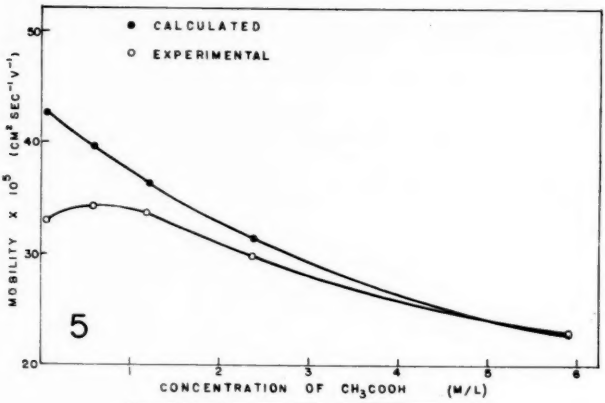

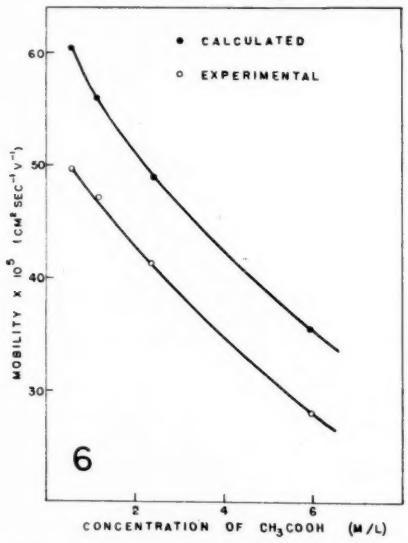

FIG. 5. Comparison of experimental zone mobilities of Na^+ in acetic acid with those calculated from equation [6]. Reeve Angel 934AH glass fiber filter paper; absorbance 3.36 ml/g; 25.0±0.5° C.

FIG. 6. Comparison of experimental zone mobilities of Cl^- in acetic acid with those calculated from equation [6]. Reeve Angel 934AH glass fiber filter paper; absorbance 3.36 ml/g; 25.0±0.5° C.

However, the data for Cl^- under the same conditions show very poor agreement between calculated and experimental results; the hindrance of Cl^- in glass is considerable compared with that for Na^+.

The results shown here indicate that specific interactions of appreciable magnitude can affect the zone mobilities of ions in both cellulose and glass papers. The equation of Crawford and Edward, relating obstructive factor to absorbance for cellulose papers, gives an approximate fit to the experimental results if the value of the swelling factor is properly chosen. In general, this factor varies for each ion and for each background electrolyte, usually falling between 0.13 and 0.45. It is apparent that these changes in X reflect factors other than swelling of the fibers. These may include adsorption of the ions and migration through the swollen volume of the fiber.

Using glass fiber paper, it is possible to calculate an idealized obstructive factor free from any uncertain swelling factor, and for Na^+ in fairly concentrated acetic acid the calculated zone mobilities agree quite well with the experimental. For Cl^-, on the other hand, they do not. Most of the ions studied so far in glass paper showed a large amount of trailing indicative of adsorption. It is clear that further work in this or in a similar non-swelling material with ions which show no adsorption is required.

REFERENCES

1. KUNKEL, H. G. and TISELIUS, A. J. Gen. Physiol. **35**, 89 (1951).
2. EDWARD, J. T. J. Chromatography, **1**, 446 (1958).
3. SCHEIDEGGER, A. E. The physics of flow in porous media. University of Toronto Press, Toronto. 1957.
4. CRAWFORD, R. and EDWARD, J. T. Anal. Chem. **29**, 1543 (1957).
5. BIEFER, G. J. and MASON, S. G. Trans. Faraday Soc. (In press).
6. WOOD, S. E. and STRAIN, H. H. Anal. Chem. **26**, 1869 (1954).
7. STRAUCH, L. and ANDREC, K. Vestnik. Sloven. kemi. društva, **3**, 127 (1956).
8. MAKI, M. Japan Analyst, **4**, 377 (1955).
9. WEBER, R. Helv. Chim. Acta, **36**, 424 (1953).
10. BIKERMAN, J. J. J. Phys. Chem. **46**, 724 (1942).
11. GORING, D. A. I. and MASON, S. G. Can. J. Research, B, **28**, 307 (1950).

THE STRUCTURE OF AN ARABOGALACTAN FROM MONTEREY PINE (PINUS RADIATA)[1]

D. J. BRASCH[2] AND J. K. N. JONES

ABSTRACT

The two major components of the water-soluble polysaccharides from Monterey pine (*Pinus radiata*) are an arabogalactan and a glucomannan. The arabogalactan contained L-arabinose and D-galactose in the ratio 1 to 8. The polysaccharide is highly branched in structure and contains end groups of L-arabofuranose and of D-galactopyranose. Removal of the L-arabinose residues leaves a highly ramified galactan.

INTRODUCTION

When wood meal which has been extracted with organic solvents is exhaustively washed with cold water a mixture of polysaccharides is readily obtained. The quantities and constituents of this mixture vary widely with the species of wood used, but usually the polysaccharides isolated are one or more of four general types: wood starches, pectic materials, arabogalactans, or glucomannans.

Starch is known to occur to the extent of 0.5% to 5% in woods and can be detected by the usual blue coloration with iodine. Care must be taken in the interpretation of this test since certain wood hemicelluloses are also stained blue with iodine (1). When starch is present it usually occurs in the sapwood, and often the starch granules can be detected microscopically. Wood starches on hydrolysis give mainly D-glucose, although a starch-like polysaccharide which apparently contained uronic acid groups has been isolated from oakwood.

The second group of polysaccharides which may occur in the cold water extracts of wood are the pectic materials. The main polysaccharide of the pectic group is a polymer of α-1 $\rightarrow$ 4-linked D-galacturonic acid units which are either fully or partly esterified and which may have attached to them residues of L-arabinose or D-galactose. Araban and galactan are frequently found associated with pectic acid.

The term arabogalactan has been given to the third group of polysaccharides occurring in the cold water extracts, especially of coniferous woods, since these polysaccharides on hydrolysis give mainly L-arabinose and D-galactose. Western larch (*Larix occidentalis*) contains up to 15% of an arabogalactan (2), European larch (*Larix decidua*) yields the so-called ϵ-galactan (3), while many other gymnosperms (4, 5, 6, 7, 8, 9, 10) contain lesser amounts of polysaccharides which are structurally similar to the arabogalactan of western larch. It is not yet clear whether or not the arabogalactans are homogeneous polysaccharides, (but see (2)).

The last of the types of polysaccharides which occurs in the aqueous extract of coniferous woods belongs to the glucomannan group. Several coniferous woods are known to yield polysaccharides of this type (11, 12, 13), but their chemistry has not yet been investigated in such detail as that of the associated arabogalactans.

When wood meal from Monterey pine (*Pinus radiata*) is extracted with water a complex mixture of polysaccharides is obtained. These can be separated, as described by Adams (10) and by Jones and Painter (11) into a polysaccharide fraction which is

[1]*Manuscript received May 4, 1959.*
Contribution from the Department of Chemistry, Queen's University, Kingston, Ontario.
[2]*Present address: Dominion Laboratory, Department of Scientific and Industrial Research, Wellington, New Zealand.*

precipitated by Fehling's solution; the glucomannan fraction; and one which is not precipitated by this reagent, the arabogalactan. This paper discusses the chemistry of the arabogalactan.

The polysaccharide was obtained as a white, water-soluble powder which on hydrolysis gave L-arabinose and D-galactose in a ratio of 1 to 8.2. All attempts to separate this polysaccharide into fractions with different properties were unsuccessful even when the polysaccharide, its acetate, or methyl ether was used.

Oxidation of the polysaccharide with sodium metaperiodate resulted in the consumption of approximately 1 mole of metaperiodate and the formation of 0.35 mole of formic acid per 162 g of polysaccharide. These figures indicate that for every sugar unit which is oxidized with the production of formic acid one other sugar residue is oxidized without the formation of formic acid, and one sugar residue is unattacked. This suggested that the polysaccharide is highly branched or that it consists of a linear polymer which contains a variety of differently linked sugars.

When the polysaccharide was hydrolyzed under mild conditions oligosaccharides were produced and two were tentatively identified as 6-*O*-β-D-galactopyranosyl- and 3-*O*-β-D-galactopyranosyl-D-galactose.

The methylated polysaccharide on hydrolysis gave a complex mixture of sugars. The following major constituents were identified: 2,3,5-tri-*O*-methyl-L-arabinose (I), 2,3,4,6-tetra-*O*-methyl-D-galactose (II), 2,4,6-tri-*O*-methyl-D-galactose (III), 2,3,4-tri-*O*-methyl-D-galactose (IV), and 2,4,-di-*O*-methyl-D-galactose (V).

The molar ratio of sugars I + II:III + IV:V was approximately 1:1:1. This proves that the polysaccharide is of the branched-chain type. When the arabogalactan was heated in dilute oxalic acid solution (14) all the L-arabinose was eliminated together with a small quantity of D-galactose and traces of other sugars. The ease of elimination of the L-arabinose indicated that it was all present in the polysaccharide in the furanoside form and probably as end group since no L-arabinose-containing oligosaccharides were isolated.

The arabinose-free polysaccharide termed "galactan" had a low positive rotation which indicated that the sugars were united by β-galactosidic linkages. The galactan was oxidized by sodium metaperiodate, approximately 1.1 moles of periodate were consumed and 0.5 mole of formic acid produced per 162 g of polysaccharide. The increase in yield of formic acid indicated that removal of the L-arabinose residues (probably from the —OH at C_3 of D-galactose) has resulted in the exposure of D-galactose residues which possess hydroxyl groups on each of three adjacent carbon atoms. These hexose residues thus become end groups or 1,6-linked D-galactose residues.

The methylated "galactan" on hydrolysis gave sugars II, III, IV, and V. The ratio of these sugars was II:III + IV:V of 1.0:1.1:1.0. The amount of 2,4,6-tri-*O*-methyl-D-galactose (III) was 10 times less than that of 2,3,4-tri-*O*-methyl-D-galactose (IV). It is evident that the formic acid produced on oxidation of the galactan by metaperiodate was derived almost equally from the end groups D-galactopyranose residues and from 1,6-linked D-galactopyranose residues.

These results do not allow the advance of a unique structure for the arabogalactan. However, it can be said that the polysaccharide is of the branched-chain type and that it resembles in structure the several other arabogalactans which have been isolated by other workers (4, 5, 6, 7, 8, 9, 10).

The structure of the glucomannan which is associated with arabogalactan will form the subject of a later communication.

EXPERIMENTAL

All melting points are uncorrected. Optical rotations were determined at 25° C and in water unless otherwise stated. All solutions were concentrated under reduced pressure and at a temperature not exceeding 40° C.

Sheet paper chromatography was carried out on Whatman No. 1 chromatographic paper by the descending method (15). The following solvent systems were used: A_1, ethyl acetate:acetic acid:formic acid:water (18:3:1:4); A_2, ethyl acetate:acetic acid:water (9:2:2); B, butan-1-ol:pyridine:water (10:3:3), and C, butan-1-ol:ethanol:water (10:3:3, all v/v). After development the sugars and derivatives were located on the chromatograms by spraying them with a 1% solution of *p*-anisidine hydrochloride in butan-1-ol (16) or with a 1% solution of silver nitrate in acetone followed by spraying with 2% ethanolic sodium hydroxide (17). The rates of movements of sugars are quoted relative to a standard sugar, e.g. R_{gal} (relative to galactose), while the movement of methyl sugars is quoted relative to tetramethyl-D-glucose (i.e. the R_g value). Infrared absorption spectra were recorded using a Perkin–Elmer Model 21 instrument in conjunction with potassium bromide pellets or 7% chloroform solution (w/v) in sodium chloride cells.

Description and Preparation of Wood Sample

The sample of Monterey pine wood used in this work was from a 25-year-old tree grown in North Island, New Zealand. The wood was received in log form, each log being about four feet long. The wood showed 2.8 to 4.2 annual growth rings per inch. It was converted into wood meal using a circular wood-working saw and air-dried to a moisture content of 9.8%. The wood (3 kg) was then extracted under reflux with ethanol (95%):benzene (2:1, v/v) for 16 hours. The residue was then extracted with ethanol (95%) under reflux for 8 hours, and dried in air.

Isolation of the Water-soluble Polysaccharide

The air-dried wood meal (500 g) was extracted with stirring, with water (10 liters) at 20° C for 16 hours. During this process toluene was added to the top of the slurry to obviate bacterial action. The wood was filtered through linen, and the process repeated using fresh water. The combined washings from 3 kg of wood were concentrated to 1 liter and centrifuged. The clear solution was then poured into ethanol (12 liters) which contained a little barium chloride and the precipitate collected. The precipitate was redissolved in water (200 ml) and reprecipitated by the addition of ethanol (800 ml). Repetition of this process (twice) gave a white product (4.3 g). Anal. ash, 2.9%; Klason lignin, 3.4%.

A sample of the product (50 mg) was hydrolyzed with 2 *N* sulphuric acid for 6 hours at 98° C. Paper chromatographic examination of the hydrolyzate (solvents A_1, A_2, and C) revealed the presence of arabinose, galactose, glucose, and mannose together with traces of xylose, rhamnose, and uronic acid.

Separation of Polysaccharides by Electrophoresis on Glass Paper

The crude polysaccharide was examined by electrophoresis on glass fiber paper (18) using both borate buffer (0.025 *N*) and sodium hydroxide (2 *N*). In one experiment at 400 v and 40 ma for 2 hours, using buffer at pH 10.7, the crude polysaccharide was separated into two distinct components. It was possible to repeat the separation, though reproducibility was not always satisfactory. In all experiments the endosmosis was considerable. Two components were also indicated by electrophoresis at 120 v, 60 ma, using sodium hydroxide (2 *N*) to dissolve the polysaccharide.

Fractionation of the Crude Polysaccharide by Copper Complex Formation

The polysaccharide (25 g) was dissolved in water (3 liters) and the solution centrifuged. Fehling's solution (100 ml) was added to the clear solution and, after 4 hours, the precipitated copper salts were collected. The top clear solution was dialyzed and, when the solution was free from copper salts, it was concentrated to 1 liter and Fehling's solution again added. The precipitated copper complex was collected and the top clear solution dialyzed until it was free from salts. The solution was concentrated and poured into alcohol and the precipitated polysaccharide (11.2 g), an *arabogalactan*, was collected. The combined precipitated copper complexes were washed with water and decomposed by maceration for 1 minute with ice-cold ethanol which contained concentrated hydrochloric acid (1% v/v). The residue was washed with ethanol and then redissolved in water. It was purified via its copper complex twice more and finally isolated as a white powder (10.7 g), a *glucomannan*.

Characterization of the Sugars from the Arabogalactan

The polysaccharide (0.30 g) was hydrolyzed for 6 hours with *N* hydrochloric acid at 100° C. The sugar mixture was isolated and separated chromatographically. L-Arabinose, $[\alpha]_D$ +96° (*c*, 2.0), was characterized as its diphenylhydrazone, m.p. 201° C, not depressed in admixture with an authentic specimen, and D-galactose, $[\alpha]_D$ +78° (*c*, 0.5), was characterized as its *N*-methyl-*N*-phenyl hydrazone, m.p. and mixed m.p. 190° C. The ratio of sugars, determined chromatographically (19), was found to be 1:8.2 (mean value). (Attempts to separate an araban from the arabogalactan by extracting the solid with 70% ethanol (v/v) were unsuccessful.)

Acetylation of Arabogalactan

The arabogalactan (0.20 g) was dissolved in formamide (10 ml), pyridine (10 ml) was then added followed by acetic anhydride (20 ml), which was added in 10 portions of 2 ml over a 2-hour period. After 16 hours the solution was poured on to ice and the precipitate collected. The dried product was reacetylated as described above and yielded arabogalactan acetate, $[\alpha]_D$ −5° (*c*, 1.2 in chloroform), which was readily soluble in dioxane, chloroform, and acetone. All attempts to fractionate this material were unsuccessful.

Periodate Oxidation of the Arabogalactan

A sample of arabogalactan was deionized by passing its solution in water through columns of Amberlite Resin IR-120 (H form) and Duolite A-4 Resin (OH form), and the polysaccharide was isolated.

Duplicate samples (approximately 50 mg each) were dissolved in water. Sodium metaperiodate solution (3 ml, 0.3 *M*) was added and the solution was made up to 100 ml. Oxidations were carried out at 23° C with the exclusion of light. At intervals aliquots (5 ml) were withdrawn and the amounts of metaperiodate consumed and formic acid liberated were determined. Found: moles of metaperiodate consumed and formic acid produced per mole of anhydro hexose: 0.52, 0.20 (3 hours); 0.91, 0.36 (8 hours); 1.04, 0.39 (20 hours); 1.10, 0.43 (44 hours); 1.19, 0.51 (68 hours).

Methylation of the Arabogalactan Acetate

Acetylated arabogalactan (6.9 g) was dissolved in acetone (500 ml) and methylated by the dropwise addition of sodium hydroxide (30% w/v; 150 ml) and dimethyl sulphate (50 ml) in the usual way. The resulting partially methylated polysaccharide (5.5 g) was remethylated as described above. After eight such treatments examination of the product in the infrared indicated that the amount of free hydroxyl groups had become small and constant. The product was therefore methylated by the procedure of Kuhn *et al.*

(20) and a practically completely methylated product was isolated. The pale yellow solid (3.9 g) had $[\alpha]_D$ −57° (*c*, 4.5 in chloroform) and $[\alpha]_D$ −37° (*c*, 3.9 in acetone). The infrared spectrum showed a very low concentration of hydroxyl (band at 3500–3600 cm^{-1}). Attempts to fractionate the methylated product by solution in chloroform – light petroleum (b.p. 60–80° C) were unsuccessful. Practically all the material dissolved when a ratio of chloroform – light petroleum of 3:1 (v/v) was reached.

Hydrolysis of the Methylated Arabogalactan

The methylated galactoaraban (2.5 g) was dissolved in formic acid (50% v/v) and heated at 97° C until no further change in optical rotation occurred (6 hours). The water was distilled off and the residual formic acid was removed by three codistillations with water. The hydrolysis was completed by dissolving the syrup in sulphuric acid (2 *N*) and heating the solution at 90° C for 4 hours. The cooled solution was neutralized ($BaCO_3$), centrifuged, and the clear solution concentrated with the addition of 1 drop of acetic acid. The syrup (2.1 g) had $[\alpha]_D$ +55° (*c*, 3.1 in methanol) and contained at least five components (paper chromatography).

Separation of the Methylated Sugars

A portion (1.7 g) of the mixture of methylated sugars was separated by partition chromatography on a column of powdered cellulose (21) using butan-1-ol and light petroleum (b.p. 100–120° C) (3:7) as eluent. The solvent mixture was later changed to a 1:1 ratio, followed by pure butan-1-ol and then by water. The following seven fractions were collected and their components identified.

Fraction 1. The first fraction (141 mg) was chromatographically identical with 2,3,5-tri-*O*-methyl-L-arabinose in solvents A and B. A portion (0.12 g) of the syrup was oxidized with bromine water and converted to 2,3,5-tri-*O*-methyl-L-arabonic acid which was characterized as its derived amide. The product had m.p. 134–135° C, not depressed on admixture with an authentic specimen, and $[\alpha]_D$ +20° (*c*, 2.0).

Fraction 2. This fraction (155 mg) was a mixture of 2,3,5-tri-*O*-methyl-L-arabinose and 2,3,4,6-tetra-*O*-methyl-D-galactose (which could be separated paper chromatographically) (solvents A_1, B, and C). The ratio of sugars was judged to be approximately 2:1 from chromatographic evidence. It was not further examined.

Fraction 3. Fraction 3 (133 mg) behaved in solvents A and B like 2,3,4,6-tetra-*O*-methyl-D-galactose. It had $[\alpha]_D$ +102° (*c*, 1.5) but did not crystallize. When a portion of the syrup (0.1 g) was heated with ethanolic aniline for 3 hours 2,3,4,6-tetra-*O*-methyl-*N*-phenyl-D-galactosylamine crystallized, it had m.p. and mixed m.p. 196° C and $[\alpha]_D$ −80° (*c*, 2.0 in acetone). No other sugar could be identified in this fraction.

Fraction 4. This fraction (30 mg) crystallized. The crystals possessed properties which were indistinguishable from those of 2,4,6-tri-*O*-methyl-D-galactose, m.p. 99–100° C, $[\alpha]_D$ +85° (*c*, 1.1). On heating its solution in ethanol with aniline, needlelike crystals of 2,4,6-tri-*O*-methyl-*N*-phenyl-D-galactosylamine separated, m.p. and mixed m.p. 178° C.

Fraction 5. This fraction (208 mg) consisted of two components which moved at the same rate as 2,3,4- and 2,4,6-tri-*O*-methyl-D-galactose. The syrup was heated with ethanolic aniline for 8 hours and the solvent then removed. The residue on recrystallization from ethanol yielded a mixture of needle- and plate-like crystals, the latter predominating. The two products were separated by hand picking. The needlelike crystals were identical with 2,4,6-tri-*O*-methyl-*N*-phenyl-D-galactosylamine, m.p. 175° C. The plates were not distinguishable from 2,3,4-tri-*O*-methyl-*N*-phenyl-D-galactosylamine, m.p. 162–164° C not depressed on admixture with an authentic specimen. No other derivative was isolated.

Fraction 6. Fraction 6 (315 mg) contained one component only. This sugar was indistinguishable from 2,3,4-tri-*O*-methyl-D-galactose on paper chromatograms (solvents A and B). With ethanolic aniline it yielded 2,3,4-tri-*O*-methyl-*N*-phenyl-D-galactosylamine, m.p. and mixed m.p. 166–168° C, $[\alpha]_D$ −60° → +40° (equil.) (*c*, 1.3 in methanol).

Fraction 7. The last fraction (521 mg) crystallized. Recrystallization from acetone–light petroleum yielded 2,4-di-*O*-methyl-D-galactose, monohydrate, m.p. 98–100°, $[\alpha]_D$ 119° → 85° (24 hours) (*c*, 2.0). When the sugar was heated with ethanolic aniline it gave the derived *N*-phenyl-galactosylamine, m.p. 218°–220° C, $[\alpha]_D$ −180° (*c*, 1.0 in pyridine).

The molar ratios of the sugars were determined by the method of Hirst and Jones (19). Found: total end group in molar ratios (0.97), tri-*O*-methyl fraction (1.0), di-*O*-methyl fraction (1.0).

Partial Hydrolysis of the Arabogalactan

The arabogalactan (0.10 g) was hydrolyzed for 1 hour at 95° C with sulphuric acid (0.1 *N*). Chromatographic analysis of the neutralized solution revealed the presence of substantial amounts of galactose and arabinose plus minor amounts of three oligosaccharides with (*a*) R_{gal} 0.34 (solvent A_1) and 0.42 (solvent A_2), (*b*) R_{gal} 0.20 (solvent A_1) and 0.26 (solvent A_2), and (*c*) R_{gal} 0.13 (solvent A_1) and 0.14 (solvent A_2). The oligosaccharide (*a*) and (*b*) moved at rates very similar to those of galactobiose (1,6-β-linked) and galactobiose (1,3-β-linked). In a second experiment arabogalactan (4.98 g) was dissolved in oxalic acid solution (0.026 *N*, 200 ml) and heated at 95° C for 5 hours. The cooled solution was neutralized ($CaCO_3$), centrifuged, the clear solution concentrated, and the concentrate poured into ethanol. The precipitated degraded polysaccharide was collected, washed with ethanol, dissolved in water, and reprecipitated in ethanol, yield 3.49 g. The supernatant solutions were concentrated and the syrupy concentrate (1.19 g) was examined chromatographically (solvents A_1, A_2, and C). The major component of the syrup was arabinose; associated with it were significant quantities of galactose and trace quantities of xylose and rhamnose. The ratio of arabinose to galactose was 2 to 1.

The degraded polysaccharide, henceforth termed *galactan*, on hydrolysis yielded D-galactose only (paper chromatography).

The galactan had $[\alpha]_D$ +13° (*c*, 3.5) and contained 0.9% ash and 0.3% Klason lignin. Attempted fractionation of the galactan by (*a*) ethanol precipitation from neutral or acidic aqueous solution, (*b*) by copper complex formation, and (*c*) by glass paper electrophoresis was unsuccessful.

Periodate Oxidation of the Galactan

The galactan (ash-free) was oxidized with sodium metaperiodate solution as described for the oxidation of the arabogalactan. Found: moles of metaperiodate consumed and moles of formic acid produced per anhydrohexose residue: 1.17, 0.60 (8 hours); 1.35, 0.80 (25 hours); 1.61, 1.12 (48 hours); 1.95, 1.45 (72 hours). Extensive over-oxidation had occurred.

Methylation of the Galactan

Prior to methylation the galactan was reduced with sodium borohydride. The galactan (2.97 g) was dissolved in water (50 ml), and a solution of sodium borohydride (25 mg) in water (10 ml) was added. After 4 hours acetic acid (1 ml) was added and the reduced polysaccharide was methylated by adding dropwise to its solution sodium hydroxide (300 ml, 30%) and dimethyl sulphate (100 ml) during 5 hours. After 16 hours the partially methylated product (2.71 g) was isolated and the methylation procedure was repeated. The product was then methylated (twice) by the Kuhn procedure (20) in dimethyl-

formamide. The resultant methylated polysaccharide (2.1 g) was a crisp pale yellow solid. Anal. Found: OMe, 45.3%. The product had $[\alpha]_D$ −49° (*c*, 5.3 in chloroform) and −29° (*c*, 4.9 in methanol). Infrared examination of the solid indicated that it contained very little free hydroxyl.

An attempt was made to fractionate the methylated polysaccharide by dissolution in a series of mixtures of boiling *n*-hexane and chloroform in the usual way. Almost all of the material (1.58 g) was soluble in the solvent when the ratio of *n*-hexane to chloroform was 4:1 (v/v).

Fission of the Methylated Galactan

The methylated galactan (1.4 g) was dissolved in formic acid (90% v/v) and the solution was heated at 95° C for 6 hours. The solution was evaporated to dryness and formic acid removed by three codistillations with water. The hydrolysis was then continued by heating the syrup in *N* sulphuric acid for 5 hours at 95° C. The mixture was cooled, neutralized ($BaCO_3$), and centrifuged. The top clear solution was acidified (acetic acid) and evaporated to a syrup, (1.2 g), $[\alpha]_D$ +65° (*c*, 2.0 in methanol).

Isolation of the Methylated Sugars

Paper chromatographic examination of a portion (1 g) of the syrup indicated the presence of at least four methylated sugars. These were separated on a column of cellulose using the procedure described above.

Fraction 1. The first component (0.34 g) eluted from the column behaved chromatographically like 2,3,4,6-tetra-*O*-methyl-D-galactose (solvents A_1 and B) and had $[\alpha]_D$ +112° (*c*, 1.4). A sample when heated with ethanolic aniline yielded 2,3,4,6-tetra-*O*-methyl-*N*-phenyl-D-galactosylamine, m.p. 195–197° C, not depressed on admixture with an authentic specimen.

Fraction 2. The second fraction (0.03 g) was identified chromatographically as 2,4,6-tri-*O*-methyl-D-galactose (solvents A_1 and B) and was characterized as the *N*-phenyl-D-galactosylamine derivative, m.p. and mixed m.p. 179° C.

Fraction 3. This fraction (0.08 g) was a mixture of two methyl sugars. The slower moving and major component moved at the same rate as 2,3,4-tri-*O*-methyl-D-galactose. It gave a characteristic brown color with the *p*-anisidine hydrochloride spray, while the faster moving component gave a pink color and was indistinguishable from the 2,4,6-tri-*O*-methyl isomer. The mixed sugars were converted into the mixed crystalline *N*-phenyl-D-galactosylamines which were separated by hand.

Fraction 4. Fraction 4 (0.15 g) was homogeneous and identical with 2,3,4-*O*-trimethyl-D-galactose. Treatment with ethanolic aniline yielded the corresponding D-galactosylamine derivative, m.p. and mixed m.p. 167–169° C, $[\alpha]_D$ −65° → 45° (5 hours) *c*, 1.1) in methanol.

Fraction 5. This fraction (0.27 g) crystallized and was identified as 2,4-di-*O*-methyl-D-galactose monohydrate, m.p. and mixed m.p. 100° C, $[\alpha]_D$ 116° (5 minutes, *c*, 1.7). When it was heated with ethanolic aniline 2,4-di-*O*-methyl-*N*-phenyl-D-galactosylamine, m.p. and mixed m.p. 216° C was obtained.

Fraction 6. The last fraction (0.005 g) was eluted from the column with water. It represented 0.5% of the original hydrolyzate and was probably a monomethyl galactose.

Estimation of Molar Ratios of the Methylated Sugars

The molar ratios of the methylated sugars in the hydrolyzate were determined by the method of Hirst, Hough, and Jones (19). Anal. Found: ratio of 2,3,4,6-tetra-, to tri-,

to 2,4-di-*O*-methyl-D-galactose: 1.0:1.1:1.0. The ratio of 2,4,6-tri-*O*-methyl- to 2,3,4-tri-*O*-methyl-D-galactose was 1 to 10 as determined from the weight of fractions isolated from the cellulose column.

ACKNOWLEDGMENTS

The authors thank the National Research Council for a grant. They gratefully acknowledge the award of a scholarship by Canadian Industries Limited to one of them (D.J.B.). They also thank Dr. L. E. Wise and The Institute of Paper Chemistry, Appleton, Wisconsin, U.S.A., for the supply of sawdust.

REFERENCES

1. CAMPBELL, W. G. Biochem. J. **29**, 1068 (1935).
2. BOUVENG, H. O. and LINDBERG, B. Acta Chem. Scand. **12**, 1977 (1958).
3. PETERSON, F. C., MAUGHAN, M., and WISE, L. E. Cellulosechemie, **15**, 109 (1934).
4. WISE, L. E., HAMER, P. L., and PETERSON, F. C. Ind. Eng. Chem. **25**, 184 (1933).
5. NIKITIN, N. I. and SOLOVIEV, I. A. J. Appl. Chem. (U.S.S.R.), **8**, 1016 (1935); Chem. Abstr. **30**, 5563 (1936).
6. ITO, T. Cellulose Ind. **13**, 4 (1937); Chem. Abstr. **31**, 6872 (1937).
7. SCHORGER, A. W. and SMITH, D. F. J. Ind. Eng. Chem. **8**, 494 (1916).
8. BRAUNS, F. E. Science, **102**, 155 (1945).
9. BISHOP, C. T. Can. J. Chem. **35**, 1010 (1957).
10. ADAMS, G. A. Can. J. Chem. **36**, 755 (1958).
11. JONES, J. K. N. and PAINTER, T. J. Chem. Soc. 573 (1959).
12. SMITH, F. Paper presented at 128th Meeting of the American Chemical Society, Minneapolis, Minn. Sept. 1955.
13. DUTTON, G. S. and HUNT, K. J. Am. Chem. Soc. **80**, 5697 (1958).
14. BYWATER, R. A. S., HAWORTH, W. N., HIRST, E. L., and PEAT, S. J. Chem. Soc. 1983 (1937).
15. PARTRIDGE, S. M. Biochem. J. **42**, 238 (1948).
16. HOUGH, L., JONES, J. K. N., and WADMAN, W. H. J. Chem. Soc. 1702 (1950).
17. TREVELYAN, W. E., PROCTOR, D. D., and HARRISON, J. S. Nature, **166**, 444 (1950).
18. SMITH, F. and LEWIS, B. A. J. Am. Chem. Soc. **79**, 3929 (1957).
19. HOUGH, L., HIRST, E. L., and JONES, J. K. N. J. Chem. Soc. 928 (1949).
20. KUHN, R., TRISCHMANN, H., and LÖW, I. Angew. Chem. **67**, 32 (1955).
21. HOUGH, L., JONES, J. K. N., and WADMAN, W. H. J. Chem. Soc. 528 (1949).

THE PHOTOOXIDATION OF AZOMETHANE. III[1]

F. WENGER[2] AND K. O. KUTSCHKE

ABSTRACT

It is confirmed that the yields of all products in the photooxidation of azomethane at relatively high oxygen pressure depend on conversion in a manner which would be explained if a reactive hydrogen donor were produced in the early stages of the reaction. Evidence is presented which indicates that formaldehyde cannot be active as an inhibitor in the system at 162° C. It is suggested that methyl radicals react with oxygen in two ways. The third order formation of methyl peroxy radicals leads to methoxy radicals and, eventually, to methanol, while the bimolecular reaction between methyl radicals and oxygen leads to a vibrationally excited state of formaldehyde. The latter is thought to undergo oxidization to performic acid, which acts as the inhibitor in the system. Yields of formaldehyde, of nitrogen in excess of that formed in the primary process, and of nitrous oxide are linearly related regardless of the conversion up to about 4%. Methanol is a major product of the oxidation and, if account is taken of its yield, a carbon balance of the order of 90% is obtained.

INTRODUCTION

In view of the convenience of azomethane as a photochemical source of methyl radicals, this compound has been used in the past for studies of the reaction of methyl radicals with oxygen (1, 2, 3). While it was possible to obtain an approximate value for the rate constant of this association reaction (1), assuming it to be bimolecular (see (3) and (4) for a discussion of this point), many of the features of the over-all photooxidation remained unsettled. This was particularly true with respect to the dependence of the rates of formation of most of the products on the extent of conversion.

Earlier work was hampered by the lack of reliable techniques for formaldehyde detection (1) and measurement (2). The present report describes the techniques for measurement of formaldehyde and methanol yields. Experimental conditions have been limited to the region of high oxygen pressure where methane and ethane are absent (1), an observation which was confirmed in the present study. The absence of methane renders highly improbable the participation of "hot" methyl radicals such as have been postulated from other methyl radical sources (5). Data have been obtained at 121° and 161° C. The lower limit was chosen to ensure that formaldehyde would not polymerize in the system, while the upper limit was dictated by the appreciable rate of a thermal reaction at temperatures slightly above it.

EXPERIMENTAL

Apparatus

The apparatus was basically the same as used in an earlier investigation (2). Improvements in the thermostatted air bath housing the cell lowered local temperature differences from point to point within the oven to 1° C. The volume of the reaction system—U-tube, reaction cell, and circulating pump—was 255 cm^3; that of the cell itself, 180 cm^3. Some changes were made in the analytical system to permit the use of the modified procedures for liquid product analysis described below. Actinic light, mainly of 3660 Å, was obtained from a Hanovia S-500 mercury arc and a Corning 5860 filter (6).

Materials

Azomethane was obtained from Merck of Canada (Montreal). After several bulb-to-bulb distillations a middle fraction was stored at room temperature in a blackened bulb

[1]*Manuscript received May 8, 1959.*
Contribution from the Division of Pure Chemistry, National Research Council, Ottawa, Canada.
Issued as N.R.C. No. 5295.

[2]*National Research Council Postdoctorate Fellow 1955–57. Present address: Mellon Institute, 4400 Fifth Avenue, Pittsburgh 13, Pa., U.S.A.*

behind a mercury cutoff. Oxygen was prepared by heating potassium permanganate and purified by passage through a trap at −196° C. Formaldehyde-O^{18} was obtained as paraformaldehyde from Dr. L. C. Leitch of these laboratories; it had been prepared by exchange of the polymer with enriched water under reflux. Heating of the polymer liberated the monomer, which was freed of residual water by distillation from −78° to −196° C. Mass spectrometric analysis indicated an O^{18} content of 2.4%, although the water used in the exchange was more highly enriched. It is thought that only the surface layers of the polymer had been exchanged by the treatment used.

The trisodium salt of chromotropic acid (4,5-dihydroxy-2,7-naphthalene disulphonic acid, trisodium salt) used in formaldehyde and methanol analyses was prepared by titration of an aqueous solution of Eastman Kodak chromotropic acid, disodium salt. On adding ethanol a white, crystalline material separated, which was filtered and dried. This crude material soon turned violet when left to stand. The substances causing the colored oxidation products—impurities and probably the quarternary salt of the acid—were less soluble in ethanol–water mixtures and were removed by fractional precipitation. Material prepared in this manner was stored for months in the dark with no change in its analytical behavior.

Photooxidation Procedure

Azomethane was outgassed in the storage bulb prior to each run; the required pressure, as measured on a manometer at room temperature, was built up in the hot cell; and the contents of the reaction system were condensed at −196° C in the U-tube. Oxygen was admitted to the reaction system to the required pressure and measured on a McLeod gauge external to the oven. The volume of the cold U-tube was small relative to that of the whole reaction system so that negligible error was introduced by measuring oxygen pressure with the U-tube at −196° C. After the valve leading to the storage and measuring manifold was closed, the U-tube was heated to the cell temperature and the gases mixed by means of the circulating stirrer.

Considerable care was taken in the experiment with added formaldehyde to ensure that the results would not be uncertain due to polymerization of that material. An accurately known amount of formaldehyde was introduced as follows. Two bulbs of known volume ratio and equipped with breakoff points were connected via stopcocks to a manifold containing formaldehyde vapor at approximately the required pressure. After time was allowed for pressure equilibration, the stopcocks were closed, the formaldehyde condensed at −196° C, the bulbs detached from the stopcocks at a sealoff point, and the contents of one bulb analyzed by the chromotropic acid procedure (see below). From the known volume ratio, the quantity in the second bulb could be calculated. This second bulb was sealed to the reaction system in the oven, and azomethane was introduced as usual and stored temporarily outside the oven in a trap on the analytical system. The breakoff was broken, the monomeric formaldehyde condensed in the U-tube at −196° C, and the formaldehyde introduction bulb sealed from the system. Azomethane was returned to the cold U-tube, oxygen introduced as usual, and the gases mixed.

Analysis of Products

(*a*) *Gaseous Products*

After photolysis the contents of the reaction system were condensed in a trap at −196° C and the non-condensable gases (N_2, CO, and O_2) were transferred to a gas burette, measured, and analyzed over copper–copper oxide at 250° C with a contact time of 2 hours as described earlier (1, 2). The contents of the trap were allowed to warm to room

temperature in a volume of connecting tubing defined by the valve leading to the reaction system and a stopcock near the trap, and were recondensed and warmed three times thus polymerizing the bulk of the formaldehyde (2). Unpolymerized material was transferred to a LeRoy still (7) held at −196° C. Nitrous oxide, carbon dioxide, unpolymerized formaldehyde, and some of the azomethane were transferred at −130° C from this still to a second at −196° C. By heating the second still to −160° C, nitrous oxide and carbon dioxide were transferred to the gas burette, measured, and submitted for mass spectrometric examination. By following this procedure in detail less than 1% formaldehyde impurity was found in the carbon dioxide – nitrous oxide fraction.

(*b*) *Formaldehyde*

A method based on the chromotropic acid procedure (8) was used. Formaldehyde and any azomethane from the second LeRoy still, along with the formaldehyde from the U-tube (depolymerized by heating), were condensed with liquid nitrogen on top of 4 ml of a frozen aqueous solution containing 150 mg of the trisodium salt of chromotropic acid contained in a small pear-shaped reaction flask. The flask was removed from the vacuum system at a ground joint, warmed to room temperature, and mixed well. Azomethane was removed by bubbling a stream of water-saturated nitrogen through the solution. Blank experiments showed that this procedure removed completely the excess azomethane and retained formaldehyde quantitatively. The solution was acidified with 12 ml concentrated H_2SO_4, heated in boiling water for 30 minutes, and cooled. After dilution the extinction at 570 mμ was measured on a Beckmann DU spectrophotometer and the amount of formaldehyde determined from a calibration curve. For samples expected to contain more than 200 γ formaldehyde proportionally larger quantities of reagents were used.

(*c*) *Methanol*

Products remaining in the first LeRoy still (mainly methanol, water, and the bulk of the unreacted azomethane) were distilled to a reaction flask containing 4 ml distilled water. Azomethane was removed on a stream of nitrogen as before; 400 mg chromotropic acid, disodium salt, and 0.5 ml concentrated H_2SO_4 were added and a 3-ml fraction, containing all the methanol (as shown by calibration experiments), was transferred by distillation to a second reaction flask. Methanol was oxidized by potassium permanganate and the resulting formaldehyde determined with chromotropic acid as described above (9). A set of similarly treated methanol standards was used to construct the calibration curve of extinction vs. amount of methanol.

Since the yield in the oxidation step of this procedure is small ($\sim$10%) small amounts of formaldehyde, present in this liquid product fraction or produced by hydrolysis of azomethane or other products of the photooxidation, if carried over in the distillation step will yield high values for the amount of methanol. In using the method of Bricker and Vail (10) to separate synthetic methanol – formaldehyde mixtures, formaldehyde was always found in the methanol fraction. This could be prevented by heating the solution to 100° C for a half an hour prior to distillation or by maintaining a low pH during the distillation as was outlined above. This latter method was adopted because the liquid products from the first LeRoy still appeared to contain small amounts of unidentified compounds, presumably products of the addition of radicals to azomethane. These compounds were not removed by the stream of nitrogen. Moreover, they did not react with the chromotropic acid salt (as would free formaldehyde if present) so that they appeared in the methanol distillate where they were hydrolyzed to formaldehyde during subsequent acid treatment causing high methanol yields. The addition of sulphuric acid prior to distillation yielded a distillate free of formaldehyde and hydrolyzable substances.

In some parallel experiments the methanol determination was verified by gas chromotography or, after removal of the bulk of the azomethane by distillation, by infrared analysis.

RESULTS

Analyses are given for the amounts of nitrogen, carbon monoxide, carbon dioxide, methanol, and formaldehyde formed and for oxygen disappearance. Water was detected mass spectrometrically and the rough estimate of its yield on this basis was in essential agreement with that calculated from a consideration of the hydrogen and oxygen material balances. Formic acid and acetaldehyde were detected mass spectrometrically in very small yields in the liquid product fraction. An otherwise unidentifiable peak at mass number 104 was tentatively assigned to the compound $CH_3OOCH_2N_2CH_3$. It is possible that this compound is an important intermediate in nitrogen production at low oxygen pressure.

In the early series of experiments (Table I and Fig. 1) methanol analyses were not attempted and formaldehyde yields are probably low due to adsorption or polymerization on room temperature connecting tubing; this was corrected in the later experiments by heating the tubing to about 140° C.

TABLE I

Products of azomethane photooxidation

p_{azo} = 57 mm, p_{O_2} = 8.5 mm at 0° C, Temp. = 119° C

Time (minutes)	μmoles of:					
	N_2	CO	CO_2	N_2O	CH_2O	$-O_2$
			$I_a = 1.3\times10^{13}$, quanta/cm³ sec			
10	2.36	0.36	0.27	0.54	0.80	—
20	5.44	1.03	—	—	1.47	—
40	11.28	2.45	0.54	2.10	—	—
60	15.4	4.24	0.80	2.54	4.28	—
90	23.1	7.36	1.52	3.26	5.31	45
150	39.7	14.3	2.27	3.61	6.91	78
210	49.7	22.1	4.19	5.66	8.34	97
90	21.4		Oxygen absent			
			$I_a = 6.3\times10^{13}$, quanta/cm³ sec			
5	6.56	1.47	0.13	0.94	2.10	
11	15.6	3.97	0.54	2.19	2.77	
20	24.1	7.81	0.94	2.10	4.50	
30	35.8	12.6	1.25	2.81	6.78	
40	46.2	17.8	1.56	3.48	8.12	
20	22.5		Oxygen absent			

Table I shows the data for a set of experiments at 120° C using two different light intensities. An examination of these data shows that light intensity changes of a factor of about five have little effect on product ratios for any given degree of conversion as indicated by the amount of nitrogen and nitrous oxide found. The data for the lower intensity are plotted in Fig. 1 showing the general trend of the amounts of the various products formed with illumination time. Both the very small intensity dependence and the trend shown in Fig. 1 confirm results reported previously (2).

The data shown in Table II were taken after the improvements in the analytical system noted above had been achieved. If it is assumed that each molecule of azomethane which is decomposed leads to either a molecule of nitrogen or of nitrous oxide, then the

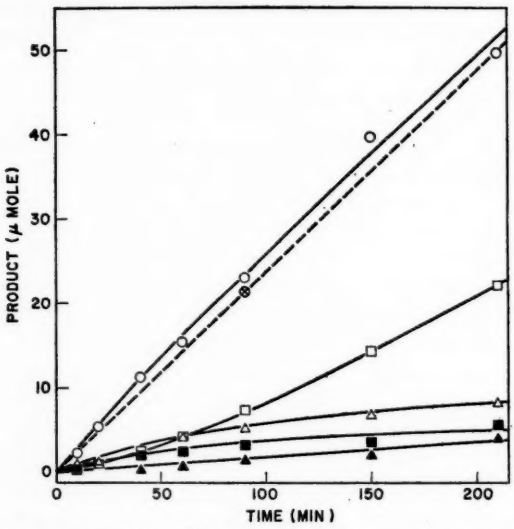

FIG. 1. Time dependence of products, 119° C. ○ N_2; ⊗ N_2, oxygen absent; □ CO; ■ N_2O; △ CH_2O; ▲ CO_2.

ratio $(n_{N_2}+n_{N_2O})/n_A$ is an approximate measure of the fractional conversion of the azomethane. Here $n_{N_2}+n_{N_2O}$ represents the total number of moles of nitrogen and nitrous oxide found and n_A represents the initial number of moles of azomethane in the reaction system (255 cm^3). This corresponds to the conversion D_1 of the earlier work (2); to obtain conversions based on the cell volume (D_2 of (2)) multiply by 1.42. By plotting the data against fractional conversion rather than time of illumination at least some compensation is achieved for the effects of small variations in light intensity from one experiment to another.

TABLE II

Products of azomethane photooxidation
p_{azo} = 57 mm, p_{O_2} = 7 mm at 0° C

Time (minutes)	μmoles of:							% of:			
	N_2	CO	CO_2	N_2O	CH_2O	CH_3OH	$-O_2$	m_C	m_H	m_O	m_I
Temp. = 121° C; $I_a = 4.5\times10^{13}$ quanta/cm^3 sec											
5	4.24	1.56	0.09	0.71	1.47	4.55	—	77	71	—	103
9	7.58	1.56	0.13	1.12	2.23	8.34	—	70	73	—	66
15	—	—	0.58	1.92	—	—	—	—	—	—	—
20	17.1	5.35	0.80	2.41	5.93	16.7	—	74	67	—	104
30	—	—	—	—	8.16	26.4	—	—	—	—	—
40	30.6	11.19	1.69	3.30	10.39	31.4	—	80	72	—	110
20	16.0	Oxygen absent									
Temp. = 121° C; $I_a = 3\times10^{11}$ quanta/cm^3 sec											
520	3.17	0.67	0.36	1.65	2.77	6.91	3.84	111	115	166	65
960	5.84	1.56	0.98	2.50	3.39	12.6	14.9	100	103	74	59
1500	9.46	2.54	1.78	3.79	4.37	16.2	24.4	94	93	62	69
Temp. = 162° C; $I_a = 4.7\times10^{13}$ quanta/cm^3 sec											
5	4.77	1.16	0	2.10	3.43	7.36	7.7	87	88	91	78
10	9.05	2.94	0.71	3.39	5.40	12.3	16.4	86	80	78	98
20	16.8	7.09	1.47	4.82	7.18	22.7	—	89	81	—	101
31	25.0	11.6	2.05	6.29	9.28	34.3	42	91	83	78	101
30	21.1	Oxygen absent									

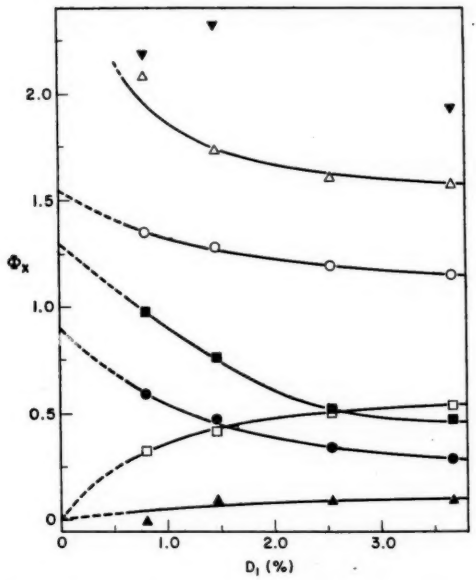

FIG. 2. Dependence of quantum yields on conversions, 162° C. ○ N_2; ● N_2O; □ CO; ■ CH_2O; △ CH_3OH; ▲ CO_2; ▼ O_2.

Figure 2 contains the data taken at 162° C (Table II) plotted as apparent quantum yields Φ_X, calculated as the ratio of the amount of product X actually found to the amount of nitrogen which would have been formed had oxygen been absent in the experiment. Extrapolations to zero conversion are arbitrary except in the case of carbon monoxide where the shape of the amount vs. time curve (similar to that of Fig. 1) strongly suggests that the quantum yield vanishes at zero conversion. The large increase in Φ_{CO} is accompanied by a decrease in Φ_{N_2O} and Φ_{CH_2O}. The actual decrease in Φ_{CH_3OH} might not be as large as indicated because the curve drawn is strongly dependent on the yield at the lowest conversion where small errors in the analytical method would be exaggerated. However, it seems quite certain that Φ_{CH_3OH} does decrease as conversion is increased.

Data for the lower temperature experiments are illustrated in Fig. 3. Instead of Φ_X the quantity ρ_X, defined as $n_X/(n_{N_2}+n_{N_2O})$, is plotted against conversion. ρ_X is a measure of the yield of the product X per molecule of azomethane decomposed. The use of ρ eliminates any assumption regarding the comparison of experiments in the presence and absence of oxygen and the possibility that such a comparison is not valid over a large range of intensity. In general the trends of ρ_X with conversion are similar to those of Φ_X except when X is N_2. ρ_{N_2} decreases at low conversion because of the increase in the relative amount of nitrous oxide, although Φ_{N_2} in fact increases in this region in a manner analogous to that shown in Fig. 2. Values of Φ_X at 120° C, read from a graph similar to that of Fig. 2 at conversions such that the yields had attained their approximately steady values, are, $\Phi_{N_2} \sim 1.0$; $\Phi_{N_2O} \sim 0.1$; $\Phi_{CO} \sim 0.4$; $\Phi_{CO_2} \sim 0.06$; $\Phi_{CH_3OH} \sim 1.0$; $\Phi_{CH_2O} \sim 0.2$. In drawing curves to obtain these values, no account was taken of the very low intensity experiments in Table II; owing to the lack of data at high conversion and low intensity it is not possible to make an estimate of limiting quantum yields for these conditions. However, it would seem definite that all Φ_X increase at low intensity. This fact, together with

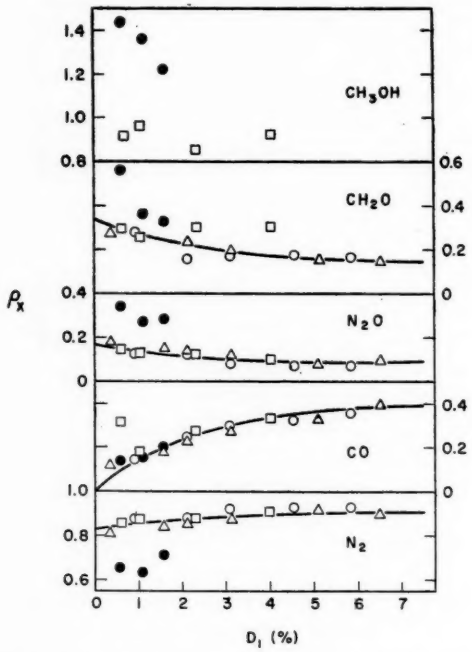

FIG. 3. Change of product ratios (ρ_x) with conversion, ~ 120° C. ○ Table I, $I_a = 6.3\times10^{13}$; □ Table II, $I_a = 4.5\times10^{13}$; △ Table I, $I_a = 1.3\times10^{13}$; ● Table II, $I_a = 2.7\times10^{11}$.

Φ_{CH_3OH} 2.5 at about 1% conversion strongly suggests that a short chain is operating which is inhibited at higher conversions and higher light intensity. Inhibition of a chain by increase in oxygen pressure is suggested by other work, but the present data are taken at an oxygen pressure such that any inhibition from this source should be fully developed.

Earlier work on this problem (1, 2) as well as other photooxidation studies has been hampered by very low product balances. Using the assumption mentioned earlier, to the effect that nitrogen and nitrous oxide found are proportional to azomethane decomposition, it is seen that carbon recovery in per cent is given by $m_C = (100/2)\Sigma\rho_X$ where the summation extends over all products containing carbon. Similarly, the hydrogen recovery is $m_H = (100/6)\,(4\rho_{CH_3OH}+2\rho_{CH_2O})$. Oxygen recovery is given by $m_O = 100(n_{CO}+2n_{CO_2}+n_{N_2O}+n_{CH_2O}+n_{CH_3OH})/2n_{O_2}$ where the n_X is the numbers of moles of products X recovered and n_{O_2} is the oxygen consumption. Values calculated on this basis are reported in Table II; the data of Table I have not been treated in this way since methanol was not determined. Rather surprisingly, methanol yields are sufficiently large to raise the carbon balance to reasonably high values. It would thus appear that no major products of the reaction have been neglected. One possibility cannot be ruled out entirely. If some high molecular weight nitrogenous compound were produced possessing a carbon to nitrogen atomic ratio less than unity, the balances cited would be too large. It is difficult to visualize the formation of such compounds in this system, however. The converse hypothesis, that high molecular weight products are formed, but that they possess a carbon–nitrogen

ratio greater than unity, is probably true and could account for $m_C < 1$. Such compounds could be formed by radical addition to the nitrogen–nitrogen double bond, a reaction of considerable importance in the absence of oxygen (1, 6).

DISCUSSION

Nitrogen, Formaldehyde, and Nitrous Oxide

Following our earlier work (1) it is considered that the primary process in the photolysis is unaffected by the presence of oxygen.

$$CH_3N_2CH_3 + h\nu \rightarrow 2CH_3 + N_2 \quad [1]$$

The strongest evidence supporting this hypothesis is data taken at low azomethane pressure, high oxygen pressure, and low temperature. It was shown (1) that for these conditions $-\Phi_{azo} = \Phi_{N_2} \sim 1$, which could hardly be true if deactivation of excited molecules were occurring. The low temperature is expected to favor deactivation if it occurred.

For other conditions values of $\Phi_{N_2} > 1$ have been observed here and in earlier work (1, 2). A similar observation has been made in the azoethane photooxidation (11). The data may be correlated empirically as is done in Fig. 4. In this plot, at 162° C, the amount of formaldehyde produced is linearly related to the amount of nitrous oxide, as is the amount of secondary nitrogen. The latter is defined as the nitrogen produced in excess of that which would have been formed had oxygen been absent in the experiment. Although curvature may be present in these plots, a linear relation represents the data adequately within experimental error. Such a correlation strongly suggests a common source for secondary nitrogen, nitrous oxide, and formaldehyde. Nitrous oxide has been considered (1) to arise via the mechanism

$$R + CH_3N_2CH_3 \rightarrow RH + CH_2N_2CH_3 \quad [2]$$

$$CH_3N_2CH_2 + O_2 \rightarrow CH_3 + N_2O + CH_2O. \quad [3]$$

Reaction [3] is written as an over-all reaction and might occur in stages involving the $CH_3N_2CH_2O_2$ radical. R is some radical in the system capable of abstracting hydrogen from azomethane. A parallel reaction yielding the secondary nitrogen might be

$$CH_3N_2CH_2 + O_2 \rightarrow CH_3O + N_2 + CH_2O. \quad [4]$$

If these are the only important reactions producing secondary nitrogen, nitrous oxide, and formaldehyde, the difference between formaldehyde and secondary nitrogen should equal the amount of nitrous oxide found. The broken line in Fig. 4, which is drawn with a slope of unity, is a reasonable representation of the data. At the lower temperature the correlation does not hold. Data at 124° C from an earlier investigation (2) show a similar trend but are rather badly scattered. Thus it is not possible to obtain the activation energy difference between [3] and [4]. From Fig. 4 a value $k_3/k_4 = 1.8$ is obtained at 162° C.

Earlier data show that [3] and [4] are slow compared to the third order (3, 12) reaction [5]

$$CH_3 + O_2 + M \rightarrow CH_3O_2 + M. \quad [5]$$

This may be seen by comparing (at 161° C) the oxygen pressure at which Φ_{N_2O} attains its approximately limiting value ($\sim$ 1 mm) with that required for Φ_{CH_4} to decrease to negligible values ($\sim$ 0.1 mm) (Figs. 3 and 4 of (1)). Thus there exists a region of oxygen pressure between these limits where CH_3O_2 and $CH_2N_2CH_3$ are present in the system. If these may react as in [6] and the resulting peroxide decomposes, in part, by [7] and [8],

Φ_{N_2} should increase at oxygen pressures below about 1 mm and decrease again at a very low oxygen pressure where [5] becomes a less predominant fate for methyl radicals.

$$CH_3O_2 + CH_3N_2CH_3 \rightarrow CH_3O_2CH_2N_2CH_3 \quad [6]$$

$$CH_3O_2CH_2N_2CH_3 \rightarrow CH_3O + OCH_2N_2CH_3 \quad [7]$$

$$OCH_2N_2CH_3 \rightarrow CH_2O + N_2 + CH_3 \quad [8]$$

A careful examination of the dependence of Φ_{N_2} on oxygen pressure (Fig. 1 of (1)) shows that such a trend exists. The tentative mass spectrometric identification of $CH_3O_2CH_2N_2CH_3$ among the products in the current work supports this hypothesis as well. An analogous effect has been observed in the photooxidation of azoethane (11), and a similar scheme might be used to explain part of the variation in Φ_{CO} with oxygen pressure in acetone photooxidation (13).

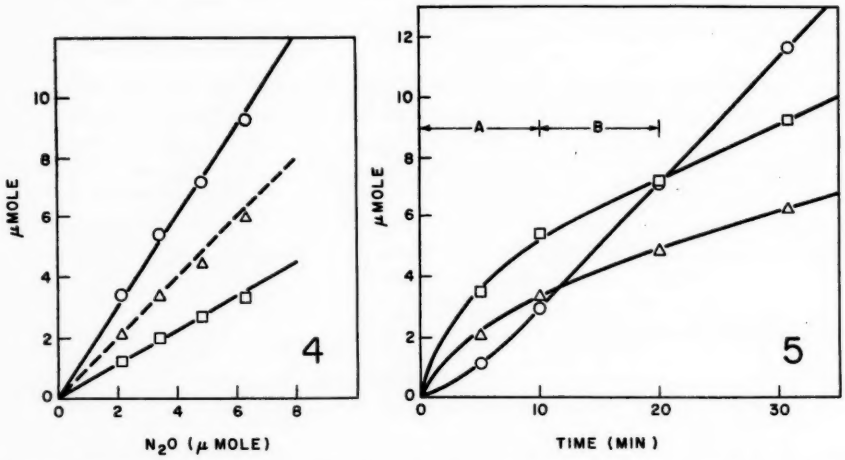

FIG. 4. Correlation of formaldehyde, secondary nitrogen, and nitrous oxide, 162° C. ○ CH_2O; □ $(N_2)_{secondary}$; △ CH_2O–$(N_2)_{secondary}$. The broken line has a slope of unity.
FIG. 5. Possible formaldehyde inhibition, 162° C. ○ CO; □ CH_2O; △ N_2O.

If the reactions analogous to [2], [3], [4], [6], [7], and [8] occur in the acetone photooxidation, the material balance method (4) of determining the third body requirement for [5] is open to some question since more than two methyl radicals are released to the system per quantum absorbed. The determination of k_5 using azomethane photooxidation (1) included the chain steps [2] and [3] but did not consider [6], [7], and [8]. Occurrence of [4] further complicates the situation in either case.

Formation of Methanol

It seems unlikely that the large yields of methanol found here can be explained without the presence of relatively high concentrations of methoxy radicals. If such is indeed the case then methanol could arise in reaction [2], with R the CH_3O radical, and possibly in [9] as well.

$$2CH_3O \rightarrow CH_3OH + CH_2O \quad [9]$$

Empirically it is found that the material balance [I] holds reasonably well over a large range of conversion and temperature.

$$CH_3OH = 2CO + CO_2 + CH_2O \quad [I]$$

This is shown in the last column of Table II as the ratio $m_I = (2CO + CO_2 + CH_2O)/CH_3OH$. At the very low intensity the relationship is no longer obeyed.

It would appear that, in addition to [2] and [9], which produce equivalent quantities of methanol and formaldehyde if [3] and [4] are the sole fates of $CH_2N_2CH_3$ radicals, there is another source of methanol. This further source involves the production of 2 molecules of methanol and 1 of carbon monoxide or 1 each of carbon dioxide and methanol. A single source need not lead to both oxides of carbon; possibly two such sources are involved. Moreover, the inclusion of carbon dioxide in [I] is somewhat dubious. Because of the relatively small yields of this product, an equally reasonable value of m_I could be obtained if carbon dioxide were not considered. Since methanol production by this means appears to be associated with carbon monoxide formation and the yield of this product depends most strongly on conversion, a discussion of the additional methanol formation is deferred to a later section.

Occurrence of [2] and [9] as sources of methanol requires the presence of methoxy radicals. Reaction [4] is not, of course, a sufficiently copious source of that radical. The product of [5] is almost certainly a methyl peroxy radical, and some scheme must be devised to transform the peroxy methyl radical to a methoxy. Using an earlier suggestion of Bell *et al.* (14) reaction [10] has been postulated for this conversion (1).

$$2CH_3O_2 \rightarrow 2CH_2O + O_2 \qquad [10]$$

Unless other fates are possible for CH_3O_2 radicals, [10] is inevitable regardless of intensity. Such another fate might be abstraction from some hydrogen donor in the system to form methyl hydroperoxide. All attempts to identify this compound have been fruitless (1). While it might be objected that mercury vapor present in the system might catalyze the decomposition of the peroxide, the results of Marcotte and Durbetaki (15) in the acetone photooxidation are inconsistent with this objection. Thus it is concluded that if [10] occurs it will be unaffected by light intensity. Recently McDowell and Sharples (16) have shown that reactions, thought to be analogous to [10], of acetyl and propionyl peroxy radicals proceed with almost unit collision yield. The products in those cases were written as diacetyl or dipropionyl peroxides and molecular oxygen, but the products were not isolated. In view of the higher temperatures used here it might be anticipated that the products would be those of O—O bond fission in the resulting peroxide. Hence [10] is considered an efficient reaction.

Other mechanisms have been suggested for this conversion. The identification of small, stationary concentrations of ozone in some photooxidation systems has led to the suggestion (3, 17) that [11] might be efficient in the transformation.

$$RO_2 + O_2 \rightarrow RO + O_3 \qquad [11]$$

Ozone is thought to be consumed by rapid reaction with alkyl radicals so that its concentration never reaches readily detectable levels.

While the precise mechanism operating in this system remains unknown, it seems necessary to postulate that the methyl radicals produced in [1], [3], and [8] are, for the most part, rapidly and efficiently converted to methoxy radicals probably via the methyl peroxy radical.

Dependence of Products on Conversion

The decrease with conversion of the apparent yields of nitrogen, nitrous oxide, formaldehyde, and methanol, as illustrated in Figs. 1 to 3, accompanied by an increase in the carbon monoxide yield, strongly suggests that an inhibitor is produced in the early stages of the reaction. Radicals, presumably mostly methoxy, react with this inhibitor

rather than with azomethane, resulting in a decreased chain length for the over-all reaction and production of carbon monoxide from the inhibitor. The time scale of the events—many minutes—precludes the possibility that the phenomenon involves a radical acting as an inhibitor.

Because of the relatively small energy requirements for abstraction of the aldehydic hydrogen, aldehydes have been thought to act in the manner required by the present observations. A scheme involving formaldehyde has been suggested in the azomethane photooxidation (2). This involved the mechanism outlined below in which the radical R is probably methoxy.

$$R + CH_2O \rightarrow RH + CHO \qquad [a]$$

$$R + CHO \rightarrow RH + CO \qquad [b]$$

$$O_2 + CHO \rightarrow CO + HO_2 \qquad [c]$$

$$R + CH_3N_2CH_3 \rightarrow RH + CH_2N_2CH_3 \qquad [d]$$

$$CH_2N_2CH_3 + O_2 \rightarrow CH_2O + N_2O + CH_3 \qquad [e]$$

If, as seems reasonable, [*c*] and [*e*] are considered to follow rapidly after [*a*] and [*d*] respectively, so that the latter reactions are rate determining, it is seen that the instantaneous rate ratio is obtained as [II]

$$[II] \qquad r_{CO}/r_{N_2O} = k_a[F]/k_d[A].$$

Figure 5 is used to test this suggestion. During the period from 10 to 30 minutes r_{N_2O} is essentially constant while the instantaneous concentration of formaldehyde, [F] of equation [II], has increased from about 2.1×10^{-5} mole/l. at 10 minutes to about 3.6×10^{-5} mole/l. at 30 minutes. Thus r_{CO} should have increased by a factor of about 1.7 if [II] is to hold. Obviously r_{CO} is essentially constant in this interval.

Further confirmation of the incorrectness of the hypothesis is obtained from the experiment with added formaldehyde-O^{18}, done at 162° C. Formaldehyde was added in an amount (5.13 μmole) calculated to be equivalent to that found at the end of a 10-minute exposure. If formaldehyde were essentially inert in the system, the amounts of various products expected are those corresponding to the time interval A of Fig. 5. Conversely, if formaldehyde acts as the inhibitor, the amounts expected are those pertaining to time interval B. Products observed and those expected under the two conditions are shown in Table III. It is seen that the observed values are in excellent agreement with those expected if formaldehyde were inert in the system.

TABLE III

Photooxidation of azomethane formaldehyde mixture
$p_{azo} = 57$ mm, $p_{O_2} = 7$ mm at 0° C
Formaldehyde added 5.13 μmole

	Products in μmole		
		Expected	
	Observed	Abstraction from H_2CO	No abstraction from H_2CO
N_2	9.19	8.03	9.05
CO	2.90	4.15	2.94
CO_2	0.85	0.76	0.71
N_2O	3.70	1.43	3.39
CH_2O	9.01	6.91	10.5

A further observation from this experiment involves the isotopic composition of carbon monoxide. This product, along with unreacted oxygen, was compressed into the copper – copper oxide furnace and the resulting carbon dioxide submitted for mass spectrometric examination. Blacet and Taylor (17) have concluded that oxygen required for the conversion of carbon monoxide to the dioxide arises solely from the excess gas phase oxygen, and that no exchange occurred. Hence it was anticipated that exchange of any CO^{18} present was unlikely. However, conditions were not identical in the two cases (especially in regard to contact time and the state of oxidation of the catalyst) so that the results might not be significant. It was observed that the carbon dioxide so formed had precisely the naturally occurring composition (obs. $CO^{16}O^{16}$ 99.59%, $CO^{16}O^{18}$ 0.41%, $CO^{18}O^{18}$ absent; natural composition $CO^{16}O^{16}$ 99.60%, $CO^{16}O^{18}$ 0.399%, $CO^{18}O^{18}$ 0.0004%). Had abstraction occurred from the added formaldehyde somewhat less than 2.4% of the carbon dioxide should have been enriched. By itself the isotopic result is of little value because of low O^{18} concentrations and lack of proved techniques. Agreement between the conclusions reached here and those outlined above, however, suggests that the results are more than fortuitous. It is hoped to continue work along these lines in the future.

On the basis of the evidence outlined, it is difficult to treat formaldehyde differently from any other product in the system. The parallelism between the yields of formaldehyde, secondary nitrogen, and nitrous oxide (Fig. 4) had already suggested this. It is, however, possible to obtain a qualitative explanation of this parallelism even if further oxidation of formaldehyde occurs (2). As shown here this explanation leads to quantitative inconsistencies and must be abandoned.

Various other intermediates have been suggested in thermal oxidation reactions but no direct evidence is available from the present work which would permit a decision in this matter. Another qualitatively correct hypothesis is worthy of examination, however. It has been suggested by Hoare and Walsh (4) and by Christie (12) that the oxidation of a methyl radical proceeds via the third order reaction [5] and a bimolecular reaction [12].

$$CH_3 + O_2 \rightarrow CH_2O + OH \qquad [12]$$

The products of [12] were not discussed in detail but Christie's evidence is strongly in favor of its occurrence; she suggests those shown as probable products. It might be pointed out further that if the products of [12] retain the energy of the exothermic reaction, it is conceivable that a goodly percentage of this energy is held by the formaldehyde. The products of [3], [4], [8], and [9], the latter being especially exothermic, are not thought to be in high vibrational levels. The activated complex for [9], for example, presumably involves a relatively simple H-abstraction type of configuration in which vibrations are not excited (18). High vibrational levels must be involved in the complex of [12], however, and it is thought that these are carried over in the formaldehyde product.

It is suggested that this excited formaldehyde is oxidizable by some mechanism which cannot be specified in detail, but which must not be available to normal formaldehyde. Such a process can be designated by the over-all reaction [13].

$$CH_2O^* + O_2 \rightarrow HCO_3H \qquad [13]$$

It is possible to devise a scheme, on the basis of performic acid as the elusive intermediate, which does in fact satisfy most of the data.

$$CH_2O + HCO_3H \rightarrow CH_3OH + CO_3H \qquad [14]$$

$$CO_3H \rightarrow CO_2 + OH \qquad [15]$$

$$CH_2O + CO_3H \rightarrow CH_3OH + O_2 + CO \qquad [16]$$

The mechanism is thought to operate in a manner generally similar to the formaldehyde mechanism discussed before. At very low conversions, $\backsim 1/2\%$ in this work, the concentration of performic acid is too low to affect the course of the reaction and a short chain reaction occurs (at 162° C $\Phi_{N_2} + \Phi_{N_2O}$ extrapolates to 2.5 at zero conversion). As conversion increases performic acid is consumed in [14], [15], and [16], leading to new products—the oxides of carbon—so that its concentration is held at a low, stationary level which was not detected analytically. This particular scheme has the advantage that the production of carbon dioxide with an induction period is also accounted for explicitly. Because of the small yields the actual presence of an induction period cannot be demonstrated conclusively (Figs. 2 and 3), but its occurrence would not be inconsistent with data. An alternative suggestion, that excited formaldehyde itself acts as the intermediate, can be eliminated on the basis of the time scale of the phenomenon.

Over-all Mechanism

Hydroxyl radicals, formed in [12] and [15], are thought to react as do methoxy. Thus [17], [18], [19], and [20] are postulated for their disappearance.

$$OH + CH_3N_2CH_3 \rightarrow H_2O + CH_2N_2CH_3 \qquad [17]$$

$$OH + HCO_3H \rightarrow H_2O + CO_3H \qquad [18]$$

$$OH + CO_3H \rightarrow H_2O + CO + O_2 \qquad [19]$$

$$OH + CH_3O \rightarrow H_2O + H_2CO \qquad [20]$$

An over-all mechanism composed of reactions [1] to [20] will explain the time dependence and is consistent with stability of formaldehyde in the system. The weakest point is, of course, the formation of performic acid for the presence of which no direct evidence has been obtained. It is seen that water is the only product not determined aside from presumably small quantities of performic acid. In the range of oxygen pressure used here, reactions [6], and thus [7] and [8], are unimportant. Conversion of methyl peroxy to methoxy is assumed to proceed via [10] only; reaction [11] is not considered here. Formaldehyde is formed in [3], [4], [9], and [20]. The difference

$$(H_2CO)_{total} - ((N_2)_s + N_2O) = (H_2CO)_{9,20} \qquad [III]$$

is shown in Fig. 4 to be negligible so that [9] and [20] cannot be significant at this temperature.

Unfortunately only the series of experiments at 162° C are sufficiently complete to be used as a test of the mechanism. In view of this, only material balances can be used to evaluate the scheme proposed. Moreover, because of the effect of conversion on the rates, comparisons can be made only after the rates have attained limiting values. These have been estimated graphically yielding limiting values at 162° C as follows; N_2 0.77, CO 0.42, CO_2 0.069, N_2O 0.14, CH_2O 0.25, CH_3OH 1.07, O_2 consumption 1.27 (all values are in μmole/minute). Since nitrogen is produced in the primary step at a rate of 0.70 μmole/minute, the limiting rate for secondary nitrogen is 0.07 μmole/minute.

If the amount of performic acid remaining at the end of an experiment can be neglected, the sum of the rate of formation of carbon monoxide and of carbon dioxide is a direct measure of the rate of [12]. Moreover, since [9] and [20] are not important, the difference between the limiting rates of formation of methanol and that of secondary nitrogen is a measure of the rate of [5]. Hence,

$$[IV] \qquad k_{12}/k_5[M] = (R_{CO}+R_{CO_2})/(R_{CH_3OH}-(R_{N_2})_s).$$

Using the limiting rates given above, $k_{12}/k_5[M] = 0.49$. A number of expressions may be derived relating $k_{12}/k_5[M]$ to the limiting rates of various products; all such expressions lead to similar values for the rate ratio. This value may be compared to that of 0.12 obtained from Christie's data (12) where M was methyl iodide. Differences in the temperature of the two experiments and possibly different efficiencies of methyl iodide and azomethane as third bodies might account for the factor of four difference. The uncertainties in both determinations are large.

It can be shown that oxygen consumption is given by either [V*a*] or [V*b*].

$$[Va] \qquad -R_{O_2} = \frac{4k_{12}+k_5[M]}{k_{12}+k_5[M]}\left((R_{N_2})_{prim}+\tfrac{1}{2}R_{N_2O}\right)+(R_{N_2})_s+R_{N_2O}-R_{CO}$$

$$[Vb] \qquad = \frac{2k_{12}+k_5[M]}{k_{12}+k_5[M]}\left((R_{N_2})_{prim}+\tfrac{1}{2}R_{N_2O}\right)+(R_{N_2})_s+R_{N_2O}+R_{CO_2}$$

[V*a*] yields 1.22 and [V*b*] 1.30 to be compared to an observed rate of 1.27 μmole/minute when limiting rate values are used. Thus the mechanism suggested yields the observed rate with reasonable success once approximately steady rates are reached.

Since water was not determined quantitatively it is not possible to test the predications of the mechanism for this product. It might be pointed out, however, that if each hydroxyl radical formed in [12] and [15] abstracts hydrogen to form water (as suggested by [17], [18], [19], with [20] thought not important) then the rate of water production when steady rates are attained is given by

$$[VI] \qquad R_{H_2O} = R_{CO}+2R_{CO_2}.$$

If [VI] is evaluated using the limiting rates, $R_{H_2O} = 0.56$ μmole/minute corresponding to a limiting value of the quantum yield of 0.8. The mechanism also predicts that

$$[VII] \qquad R_{CH_3OH}+R_{H_2O} = (R_{N_2})_s+R_{N_2O}+2R_{CO}+R_{CO_2}.$$

Comparison of [I] and [III], which are correct empirically as demonstrated earlier, with [VII] suggests that the yield of water should be negligible, which cannot be reconciled to the prediction of [VI]. Until more extensive data are available it seems fruitless to speculate further in regard to the formation of water.

A decrease of intensity yields an increase in the relative yields of products formed in propagation reactions (Fig. 3). However, the fact that the rates depend on conversion as well makes an investigation of the effect of intensity difficult to interpret until more data are available at various conversions and intensities.

It is concluded that the mechanism suggested is not complete, especially in regard to water formation, but that the trends of the product yields are reasonably well accounted for by that mechanism.

ACKNOWLEDGMENTS

The authors wish to thank Dr. E. W. R. Steacie for his continued interest in this work and to acknowledge the assistance of Mrs. Frances Kutschke and Miss Bernice Thornton with the mass spectrometric analysis.

They also wish to thank Dr. J. G. Calvert for manuscript copies of his papers (see ref. 3) prior to publication.

REFERENCES

1. HOEY, G. R. and KUTSCHKE, K. O. Can. J. Chem. **33**, 496 (1955).
2. STRONG, R. L. and KUTSCHKE, K. O. To be published.
3. HANST, P. L. and CALVERT, J. G. J. Phys. Chem. **63**, 71 (1959). SLEPPY, W. C. and CALVERT, J. G. J. Am. Chem. Soc. **81**, 769 (1959).
4. HOARE, D. E. and WALSH, A. D. Trans. Faraday Soc. **53**, 1102 (1957).
5. MARTIN, R. B. and NOYES, W. A., JR. J. Am. Chem. Soc. **75**, 4183 (1953).
6. JONES, M. H. and STEACIE, E. W. R. J. Chem. Phys. **21**, 1018 (1953).
7. LEROY, D. J. Can. J. Research, B, **28**, 492 (1950).
8. BRICKER, C. E. and JOHNSON, H. R. Ind. Eng. Chem. **17**, 400 (1945).
9. BOOS, R. N. Anal. Chem. **20**, 964 (1948).
10. BRICKER, C. E. and VAIL, W. A. Anal. Chem. **22**, 720 (1950).
11. CERFONTAIN, H. and KUTSCHKE, K. O. To be published.
12. CHRISTIE, M. I. Proc. Roy. Soc. (London), A, **244**, 411 (1958).
13. MARCOTTE, F. B. and NOYES, W. A., JR. Discussions Faraday Soc. **10**, 236 (1951); J. Am. Chem. Soc. **74**, 783 (1952).
14. BELL, E. R., ROLEY, J. H., RUST, F. F., SEUBOLD, F. H., and VAUGHAN, W. E. Discussions Faraday Soc. **10**, 242 (1951).
15. MARCOTTE, F. B. and DURBETAKI, A. *Quoted by* W. A. Noyes, Jr. Discussions Faraday Soc. **10**, 308 (1951).
16. MCDOWELL, C. A. and SHARPLES, L. K. Can. J. Chem. **36**, 251, 258, 268 (1958).
17. BLACET, F. E. and TAYLOR, R. P. Ind. Eng. Chem. **48**, 1505 (1956). SHUBERT, C. C. and PEASE, R. N. J. Chem. Phys. **24**, 919 (1956); J. Am. Chem. Soc. **78**, 2044 (1956).
18. BYWATER, S. and ROBERTS, R. Can. J. Chem. **30**, 773 (1952).

THE SYNTHESIS OF 5-DEOXY-5-*S*-ETHYL-D-THREO-PENTULOSE[1]

J. K. N. JONES AND D. L. MITCHELL

ABSTRACT

The microbiological oxidation of 1-deoxy-1-*S*-ethyl-D-arabitol by *Acetobacter suboxydans* has yielded syrupy 5-deoxy-5-*S*-ethyl-D-*threo*-pentulose from which a crystalline phenylosazone identical with the one prepared from 5-deoxy-5-*S*-ethyl-D-*xylo*-pentose was obtained. A syrupy 3,4-*O*-isopropylidene-5-deoxy-5-*S*-ethyl-D-*threo*-pentulose and its crystalline 2,5-dichlorophenylhydrazone were prepared.

INTRODUCTION

The microbiological oxidation of terminal substituted polyhydric alcohols by *Acetobacter suboxydans* has been the subject of investigation in several laboratories (1, 2, 3). Recently, we reported that 1-deoxy-1-*S*-ethyl-D-glucitol was oxidized to 6-deoxy-6-*S*-ethyl-L-sorbose (3), and in this communication we report the microbiological oxidation of a structurally similar polyol, 1-deoxy-1-*S*-ethyl-D-arabitol (I), to 5-deoxy-5-*S*-ethyl-D-*threo*-pentulose (II). The ω-deoxy analogue, 5-deoxy-D-*threo*-pentulose, $[\alpha]_D$ −5° in water, has been prepared by an aldolase-catalyzed condensation between acetaldehyde and dihydroxyacetone monophosphate (4); it was also most likely obtained when 1-deoxy-D-arabitol was oxidized by *A. suboxydans* (1).

When the culture medium contained sorbitol (0.4%), 1-deoxy-1-*S*-ethyl-D-arabitol was completely oxidized after 10 days to a strongly reducing compound. Copper reducing values previously published also support this conclusion (3). However, when sorbitol was not included in the medium, oxidation proceeded at a slower rate and was incomplete after 8 days. The oxidation product (II), $[\alpha]_D$ −41° in ethanol, which was obtained as a chromatographically pure syrup, revealed a strong absorption band in the carbonyl stretching frequency at 1710 cm^{-1}, while the corresponding 5-deoxy-5-*S*-ethyl-(D-*xylo*- and L-*arabino*-pentoses) possessed only a trace of carbonyl absorption and must therefore exist almost entirely as furanoses. Periodate oxidation of (II) at pH 3.7 followed by an estimation of the liberated formaldehyde (0.6 mole) indicated that the reducing compound had a primary alcohol group and that the site of enzymic oxidation was not at carbon 1. It appeared that periodate oxidation took place mainly between carbons 1 and 2. However, cleavage between carbons 2 and 3, or carbons 3 and 4, is possible although it could lead to an intermediate (i.e. glycollic acid) which is very stable to further attack by periodate ion (5). If enzymic oxidation occurred at a site other than the first carbon atom, the formation of a furanol ring system would be prohibited and the molecule would most likely exist in a zigzag conformation. The hydroxyl groups at carbons 3 and 4 would then be favorably situated for scission by periodate ion and also for ketal formation. Reaction of the ketose (II) with acidified acetone led to the formation of a strongly reducing *O*-isopropylidene derivative which possessed strong absorption at the carbonyl and carbon–hydrogen stretching frequencies. Considerable reduction of the absorption peak in the hydroxyl region of this compound was observed when its spectrum was compared with that of the ketose (II). Periodate oxidation of the *O*-isopropylidene derivative at pH 7 liberated formaldehyde (0.6 mole), which indicated

[1]*Manuscript received May 19, 1959.*
Contribution from the Department of Chemistry, Queen's University, Kingston, Ontario.

that carbons 1 and 2 were not involved in ketal formation. Reaction of the *O*-isopropylidene derivative (III) with 2,5-dichlorophenylhydrazine produced a small amount of the crystalline 2,5-dichlorophenylhydrazone (IV) which gave absorptions in the infrared corresponding to hydroxyl, —C=N—, and ketal groups (6). This evidence indicates that the biochemical oxidation product is the acyclic 2-pentulose, 5-deoxy-5-*S*-ethyl-D-*threo*-pentulose (II) and that the derived ketal is 3,4-*O*-isopropylidene-5-deoxy-5-*S*-ethyl-D-*threo*-pentulose (III). These conclusions are also consistent with the well-known enzyme specificity for oxidations at pH 6.

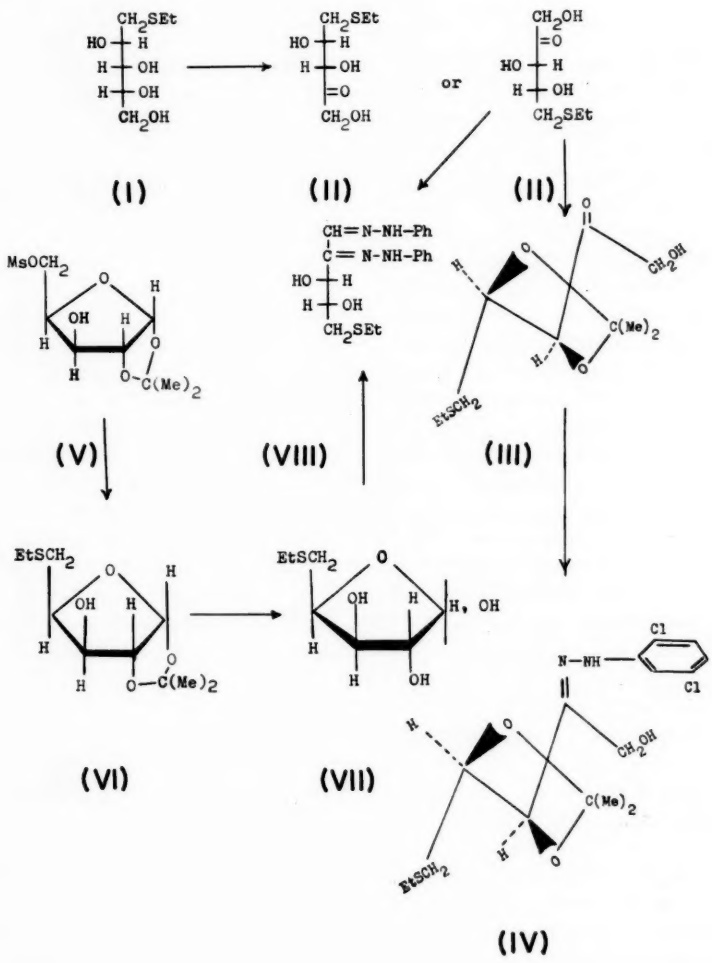

Independent proof of the structure (II) was obtained through the synthesis of 5-deoxy-5-*S*-ethyl-(D-*xylo*- (VII) and L-*arabino*-pentose) via the 1,2-*O*-isopropylidene-5-*O*-toluene-*p*- (or methane-) sulphonyl ester (e.g. (V) → (VI)). The thioethyl aldoses (VII) displayed physical properties different from the thioethyl ketose (II). However, 5-deoxy-5-*S*-ethyl-

D-*xylo*-pentose gave a phenylosazone (VIII) identical with that which was prepared from (II) but which differed from the phenylosazone of 5-deoxy-5-*S*-ethyl-L-*arabino*-pentose. Therefore, the hydroxyls at carbons 3 and 4 of (II) possess the D-*threo*-configuration.

EXPERIMENTAL

Solutions were concentrated under reduced pressure (ca. 15 mm) and at 40° C or less. Melting points were uncorrected and optical rotations were determined in water unless otherwise stated. Paper chromatography was carried out by the descending method on Whatman No. 1 filter paper using the following solvent systems (v/v): (*a*) ethyl acetate – acetic acid – formic acid – water (18:3:1:4); (*b*) ethyl acetate – acetic acid – water (9:2:2); (*c*) butan-1-ol–ethanol–water (9:3:3); and (*d*) butan-1-ol–pyridine–water (10:3:3). Non-reducing compounds were detected on paper chromatograms with an alkaline silver nitrate spray reagent (7) and reducing compounds were detected with *p*-anisidine hydrochloride reagent (8). The rate of movement of the compound on paper chromatograms is quoted relative to that of rhamnose (R_{Rh} value). Infrared absorptions were measured as solutions in chloroform or as a powder suspended in a potassium bromide pellet on a Perkin–Elmer Model 21 spectrophotometer and wave numbers are given to within ± 10 cm^{-1}.

*5-Deoxy-5-S-ethyl-*D*-threo-pentulose*

A broth consisting of 1-deoxy-1-*S*-ethyl-D-arabitol (3) (0.42 g), sorbitol (0.2 g), yeast extract* (0.1 g), and potassium dihydrogen phosphate (0.01 g) in tap water (50 ml) was autoclaved (15 p.s.i., 30 minutes), cooled, inoculated with *Acetobacter suboxydans* (A.T.C.C. No. 621), and stored at 28° C for 10 days. Paper chromatographic examination of the medium then indicated the formation of a single major reducing constituent, besides sorbose, which gave an orange-red (apricot) color with the *p*-anisidine hydrochloride reagent. Chromatographic comparison with 5-deoxy-5-*S*-ethyl-L-*arabino*-pentose and 5-deoxy-5-*S*-ethyl-D-*xylo*-pentose, which both gave bright pink colors with the same reagent, indicated that it was a different compound because its rate of movement was slower in solvent systems (*c*) and (*d*). The rates of movement were practically identical in solvent systems (*a*) and (*b*). With the orcinol – trichloroacetic acid spray reagent no color reaction was produced but with the silver nitrate reagent a very rapid formation of silver resulted.

The broth was poured with stirring into ethanol (150 ml) and the cell debris was separated by filtration. After concentration of the filtrate, the oxidation product was separated on Whatman 3 MM filter paper and was obtained as a chromatographically pure syrup (0.20 g, 67%). The syrup was soluble in water, ethanol, acetone, and chloroform. A specimen which was dried *in vacuo* for 4 days was dissolved in chloroform (3% w:v) and its absorption measured in the infrared. A strong, sharp peak in the carbonyl stretching frequency at 1710 cm^{-1} was observed; $[\alpha]_D$ $-41° \pm 2°$ (*c*, 0.9, ethanol). After 3 weeks' storage at room temperature, the syrup was re-examined by paper chromatography, and revealed streaking in the vicinity of the constituent, presumably due to the development of isomers via keto $\rightleftarrows$ enol tautomerism. Some time later a second reducing constituent appeared with a rate of movement approximately that of rhamnose (solvent *a*).

In another experiment, *Acetobacter suboxydans* was grown on the same medium described above except that sorbitol was not included. After 8 days' oxidation, the

**Nutritional Biochemicals Corporation, Cleveland, Ohio, U.S.A.*

substrate and oxidized product appeared to be present on paper chromatograms in a ratio of 1:1.

TABLE I

Paper chromatographic values

Solvent system	(*c*)	(*d*)
R_{Rh} value of:		
5-Deoxy-5-*S*-ethyl-L-*arabino*-pentose	2.11*	1.98*
5-Deoxy-5-*S*-ethyl-D-*threo*-pentulose	2.02	1.86
5-Deoxy-5-*S*-ethyl-D-*xylo*-pentose	2.14	2.00

*Mean of two measurements.

5-Deoxy-5-S-ethyl-D-threo-pentulose Phenylosazone

A portion of the syrupy 5-deoxy-5-*S*-ethyl-D-*threo*-pentulose (ca. 50 mg) was dissolved in a mixture of phenylhydrazine (0.1 ml), acetic acid (0.2 ml), and water (2 ml) and the solution was heated to 80° C for 2 hours. The derived phenylosazone was collected after the solution had been cooled and diluted with water. It was recrystallized from a small volume of ethanol and the product was washed with cold (−60° C) ethanol. Several recrystallizations gave a product of constant melting point 158–159° C (decomp.) which possessed an infrared absorption spectrum identical with that of the phenylosazone derived from 5-deoxy-5-*S*-ethyl-D-*xylo*-pentose. Mixed melting point [155–156° C, $[\alpha]_D^{20}$ −29°±4° (*c*, 1.2, pyridine). Anal. Calc. for $C_{19}H_{24}N_4O_2S$: C, 60.0; H, 6.7. Found: C, 59.5; H, 6.4.

3,4-O-Isopropylidene-5-deoxy-5-S-ethyl-D-threo-pentulose

Syrupy 5-deoxy-5-*S*-ethyl-D-*threo*-pentulose (ca. 75 mg) was dissolved in acetone (50 ml) containing concentrated sulphuric acid (1 drop) and the solution was shaken for 18 hours. After neutralization with barium carbonate, filtration, and concentration of the filtrate, the resulting syrup was examined by paper chromatography and infrared spectroscopy. A compound which moved much faster than the original material and which had R_{Rh} 2.7 (solvent (*a*)) was detected on the chromatogram as an orange-colored spot (*p*-anisidine hydrochloride); it also gave an immediate reaction with the silver nitrate – sodium hydroxide reagent. Traces of acetone were removed by repeated codistillation with chloroform, and a chloroform solution of the *O*-isopropylidene derivative was examined in the infrared. It possessed a medium weak absorption band at 3350 cm^{-1} and a medium strong absorption band at 1709 cm^{-1}. When the syrup was examined chromatographically in high concentration, a trace of 5-deoxy-5-*S*-ethyl-D-*threo*-pentulose was detected, $[\alpha]_D$ 21.5° (*c*, 0.6, ethanol).

3,4-O-Isopropylidene-5-deoxy-5-S-ethyl-D-threo-pentulose 2,5-Dichlorophenylhydrazone

A solution of the syrupy *O*-isopropylidene derivative (30 mg) and 2,5-dichlorophenylhydrazine (30 mg) in methanol (10 ml) were heated under reflux for 3 hours. After removal of the solvent, the light brown syrup was redissolved in *n*-hexane (5 ml), the solution was chilled in a solid carbon dioxide – ethanol mixture, and crystallization was induced by rubbing the walls of the flask with a spatula. The white powder (10 mg), m.p. 89–91° C, absorbed strongly in the infrared at 1595 cm^{-1} and the carbonyl absorption at 1710 cm^{-1} was present as a very weak peak barely detectable over the background fluctuation. Absorptions were also recorded at 1458 (m), 1378 (vs), 1250 (s), 1234 (vs), 1200 (s), 1160 (vs), 1087 (vs), 1033 (vs), and 794 (s) cm^{-1}. Anal. Calc. for $C_{16}H_{22}Cl_2N_2O_3S$: C, 48.8; H, 5.6. Found: C, 48.5; H, 5.4.

*1,2-O-Isopropylidene-5-deoxy-5-S-ethyl-*D*-xylo-pentose*

1,2-*O*-Isopropylidene-5-*O*-methanesulphonyl-D-xylose (1.08 g, m.p. 136–137° C (9)) and freshly prepared sodium thioethylate (0.70 g) in acetone (25 ml) were heated to 100° C in a pressure bottle for 2 hours. The solution was cooled and concentrated, and the acetone removed by several codistillations with water. The aqueous solution was extracted thrice with ether and the ethereal extracts were shaken once with ice cold, dilute sulphuric acid, twice with water, and were finally dried (Na_2SO_4). The ethereal extract was concentrated and the residual pale yellow syrup was dissolved in a small volume of *n*-hexane and the solution was cooled in a solid carbon dioxide – ethanol mixture. Crystallization was induced by rubbing the walls of the vessel with a spatula. The product (0.4 g, 42%) was collected and washed thoroughly with cold (−60° C) *n*-hexane. The product had m.p. 64–65° C, and $[\alpha]_D$ −58° (*c*, 0.9, ethanol).

The reported constants were: m.p. 66.5–67.5° C, $[\alpha]_D$ −57.5° (ethanol) (10).

A test portion of the product was hydrolyzed with acetic acid for 3 hours under reflux. Removal of the solvents and acetic acid left a syrup which was soluble in chloroform. Examination of this solution in the infrared revealed only a trace of absorption in the vicinity of 1710 cm^{-1}.

*5-Deoxy-5-S-ethyl-*D*-threo-pentose Phenylosazone*

A solution of 1,2-*O*-isopropylidene-5-deoxy-5-*S*-ethyl-D-*xylo*-pentose (100 mg) in 50% aqueous alcohol (10 ml) and glacial acetic acid (5 drops) was hydrolyzed by heating for 3 hours under reflux. Water was added and the ethanol and acetone were removed by several codistillations with water. Phenylhydrazine (0.2 ml) and acetic acid (0.2 ml) were added and the phenylosazone was prepared according to the method previously described. The bright yellow product after recrystallization from a small volume of ethanol followed by washing with cold (−60° C) ethanol melted at 155–156° C, $[\alpha]_D^{20}$ −28°±4° (*c*, 1.1, pyridine). Anal. Calc. for $C_{19}H_{24}N_4O_2S$: C, 60.0; H, 6.7; S, 8.4. Found: C, 59.9; H, 6.3; S, 8.3.

*1,2-O-Isopropylidene-5-deoxy-5-S-ethyl-*L*-arabino-pentose*

1,2-*O*-Isopropylidene-5-*O*-toluene-*p*-sulphonyl-L-arabinose (1.09 g, m.p. 129–130° C (11)) and freshly prepared sodium thioethylate (0.5 g) in acetone (25 ml) were heated at 100° C in a pressure flask for 2 hours. Water was added and the acetone was removed by several codistillations with water. The aqueous solution was then extracted twice with chloroform and the chloroform extracts were washed successively with cold, dilute sulphuric acid and then with water. The dried (Na_2SO_4) solution was concentrated to a crystalline mass which was readily recrystallized from a small volume of *n*-hexane to yield needles (0.61 g, 82%) melting at 88° C, $[\alpha]_D$ 1.3° (*c*, 0.8, ethanol). Anal. Calc. for $C_{10}H_{18}O_4S$: C, 51.3; H, 7.7; S, 13.7. Found: C, 51.2; H, 7.8; S, 13.8.

*5-Deoxy-5-S-ethyl-*L*-arabino-pentose*

1,2-*O*-Isopropylidene-5-deoxy-5-*S*-ethyl-L-*arabino*-pentose (0.46 g) was hydrolyzed for 3 hours with Amberlite IR-120 (H) resin (20 cc, wet volume) suspended in 50% aqueous ethanol (25 ml). The solution was filtered through a charcoal pad, concentrated, and the resulting syrup was redissolved in ethyl acetate. The solution was clarified by percolation under gravity through a fine porosity sintered glass funnel. Concentration yielded a colorless syrup (0.38 g) which revealed a single reducing constituent by paper chromatography and possessed no carbonyl absorption in the infrared; $[\alpha]_D$ −32°±2° (*c*, 0.9, ethanol).

Further hydrolysis with 0.05 *N* hydrochloric acid for 1.5 hours at 80° C, followed by deionization on Duolite A-4 (OH) resin, yielded a colorless syrup with $[\alpha]_D$ −29.5° (*c*, 3.3, ethanol). Since the optical rotation of the product was not significantly changed by the second acid hydrolysis, hydrolysis by the resin was considered complete.

*5-Deoxy-5-S-ethyl-*L*-erythro-pentose Phenylosazone*

The crystalline phenylosazone was prepared from syrupy 5-deoxy-5-*S*-ethyl-L-*arabino*-pentose (66 mg) in the usual way to yield a product that melted at 157° C after recrystallization from aqueous ethanol. The infrared absorption spectrum differs in minor features from 5-deoxy-5-*S*-ethyl-D-*threo*-pentose phenylosazone; the major difference was the absence of a peak at 817 cm^{-1} in the 5-deoxy-5-*S*-ethyl-L-*erythro*-derivative. The mixed melting point with both specimens of 5-deoxy-5-*S*-ethyl-D-*threo*-pentose phenylosazone was 120–135° C; $[\alpha]_D^{20}$ +19°±4° (*c*, 0.9, pyridine). Anal. Calc. for $C_{19}H_{29}N_4O_2S$: C, 60.0; H, 6.7; S, 8.4. Found: C, 59.5; H, 6.8; S, 8.7.

Determination of the Formaldehyde Liberated

Samples (0.5–1.5 mg; accurately weighed) were dissolved in buffer solution or 40% aqueous pyridine containing 0.3 *M* sodium metaperiodate solution (0.5 ml) and were made up to 10 ml. At intervals, aliquot samples (1 ml) were withdrawn and the formaldehyde was estimated by the chromotropic acid method (12). A trial experiment indicated that pyridine did not interfere in the estimation.

TABLE II

Liberation of formaldehyde during periodate oxidation

Compound	pH	Time (hours)				
		0.08	0.25	0.50	1.0	20
5-Deoxy-5-*S*-ethyl-D-*threo*-pentulose	3.7[a]	0.60[c]		0.63	0.60	
	40% pyridine		0.64			0.59
3,4-*O*-Isopropylidene-5-deoxy-5-*S*-ethyl-D-*threo*-pentulose	7.6[b]	0.33				0.61
	40% pyridine		0.38			0.43

[a], [b]0.5 *M* acetate buffer.

[c]Moles of formaldehyde liberated per mole of substrate.

ACKNOWLEDGMENTS

The authors wish to thank Dr. N. K. Richtmyer of the National Institute of Arthritis and Metabolic Diseases, National Institute of Health, Bethesda, Maryland, for cultures, and Dr. D. H. Ball for generous specimens of 1,2-*O*-isopropylidene-5-*O*-methane-sulphonyl-D-xylose and 1,2-*O*-isopropylidene-5-*O*-toluene-*p*-sulphonyl-L-arabinose. One of us (D.L.M.) thanks the Ontario Research Foundation for a scholarship.

REFERENCES

1. Bollenback, G. N. and Underkofler, L. A. J. Am. Chem. Soc. **72**, 741 (1950).
2. Richtmyer, N. K., Stewart, L. C., and Hudson, C. S. J. Am. Chem. Soc. **72**, 4934 (1950).
3. Hough, L., Jones, J. K. N., and Mitchell, D. L. Can. J. Chem. **37**, 725 (1959).
4. Gorin, P. A. J., Hough, L., and Jones, J. K. N. J. Chem. Soc. 2140 (1953).
5. Fleury, P., Courtois, J., Perles, R., and Le Dizet, L. Bull. soc. chim. France, 347 (1954).
6. Barker, S. A., Bourne, E. J., Pinkard, R. M., and Whiffen, D. H. J. Chem. Soc. 807 (1959).
7. Trevelyan, W. E., Proctor, D. P., and Harrison, J. S. Nature, **166**, 444 (1950).
8. Hough, L., Jones, J. K. N., and Wadman, W. H. J. Chem. Soc. 1702 (1950).
9. Ball, D. H. Unpublished work. Department of Chemistry, Queen's University, Kingston, Ontario.
10. Raymond, A. L. J. Biol. Chem. **107**, 88 (1934).
11. Levene, P. A. and Compton, J. J. Biol. Chem. **116**, 189 (1936).
12. O'Dea, J. F. and Gibbons, R. A. Biochem. J. **55**, 580 (1953).

SODIUM DITHIONITE, DECOMPOSITION IN AQUEOUS SOLUTION AND IN THE SOLID STATE[1]

M. W. Lister and R. C. Garvie

ABSTRACT

The decomposition of sodium dithionite has been investigated in alkaline aqueous solution. Under these conditions it decomposes by a first order reaction with a rate constant of 4.5×10^{-4} min^{-1} at 88.5° C and an activation energy of 26.5 kcal/g-molecule. The ionic strength, and the concentration of the sodium hydroxide also present, affect the rate to some extent. A possible mechanism is suggested. The decomposition of solid sodium dithionite was also examined, and was found to give the best fit to the equations deduced assuming random nucleation, followed by linear growth of nuclei, with possible ingestion and interference of reacting zones. The activation energy of nucleus growth is 32 to 33 kcal/g-molecule, and that for nucleation probably between 40 and 45 kcal/g-molecule.

The decomposition of aqueous solutions of sodium dithionite was examined by K. and E. Jellinek (1). They established that the products were sodium thiosulphate and bisulphite, so that the equation for the reaction is:

$$2Na_2S_2O_4 + H_2O \rightarrow Na_2S_2O_3 + 2NaHSO_3.$$

The quantities of the various products agreed with this equation. They measured the rate of decomposition in solutions containing varying, but usually large, amounts of sodium bisulphite. From the ionization constants of sulphurous acid (2), the pH of these solutions must have been about 4.5. They found a second order reaction, fairly rapid even at room temperature: the rate constant was 0.044 $(g\text{-molecule/l.})^{-1}$ min^{-1} at 32° C. The rate constants at various temperatures give only a moderately straight line in a plot of log (rate constant) against 1/temperature (they did not themselves put their results in this form); the activation energy appears to be close to 8 kcal/g-molecule.

This is a remarkably low activation energy, when it is remembered that the mechanism proposed is one involving the collision of two doubly charged ions, followed by the breaking of at least one chemical bond. The details of the reaction are not entirely clear, but whatever mechanism is suggested must include at least one bond rupture. The most obvious solution of this difficulty would be to suppose that at the pH used, the dithionite is partly present as $HS_2O_4^-$, or even as $H_2S_2O_4$ molecules, and that these react. Accordingly, experiments were made on the decomposition of sodium dithionite in alkaline solution; and, as will be seen below, these show that the rates in alkaline solution are quite different from those reported by K. and E. Jellinek. The reaction was examined over a range of ionic strength and temperature.

The decomposition of solid sodium dithionite has been examined by Deines and Elstner (3), who found the products to be sodium thiosulphate and sulphite and sulphur dioxide. This is sufficiently similar to the reaction in solution that it seemed worth while to obtain some quantitative information on the decomposition of the solid, particularly in order to compare the activation energies of the reaction under the different circumstances.

EXPERIMENTAL

The chief difficulty in these experiments is that sodium dithionite solutions can be

[1]*Manuscript received April 17, 1959.*
Contribution from the Department of Chemistry, University of Toronto, Toronto, Ontario, Canada.

Can. J. Chem. Vol. 37 (1959)

oxidized by atmospheric oxygen, so air must be rigorously excluded, both during the run, and during manipulation of samples. The apparatus used was similar to that of K. and E. Jellinek, modified only in details. The solutions were made up in a flask under a positive pressure of purified nitrogen. During the run this flask was immersed in a water thermostat, and the contents were stirred with a mercury sealed stirrer. At intervals samples were sucked up into a nitrogen-filled burette, and then a measured volume of solution was immediately run into excess oxidizing agent. The details of the analysis are given below.

In the experiments with solid sodium dithionite, the apparatus consisted of a long pyrex tube, with a sintered glass disk fixed across the middle of it. The tube was wound with suitable resistance wire and insulation, and a thermocouple was placed just above the glass disk. During the actual run the thermocouple was embedded in the sodium dithionite. The temperature at the thermocouple was maintained constant by connecting it to a potentiometer, and sending the off-balance current through a light-and-mirror galvanometer, the light being reflected on to a photocell. The photocell activated a relay which introduced a small extra resistance into the heating circuit when the temperature rose. The temperature was thus controlled to 0.1° C. Nitrogen was passed through the tube and disk, and, for a run, sodium dithionite was placed on the disk. As soon as it had come to temperature, a sample was removed by a small glass scoop, weighed, and analyzed; further samples were taken at suitable intervals.

In the solution runs, the solutions were always kept alkaline with sodium hydroxide. This is slowly used up, as the total reaction is:

$$2Na_2S_2O_4 + 2NaOH \rightarrow Na_2S_2O_3 + 2Na_2SO_3 + H_2O,$$

but the runs were never carried beyond the point where the sodium hydroxide was exhausted. The ionic strength was adjusted by addition of sodium fluoride. This salt was chosen because it did not interfere with the analyses, and is of a simple ionic type. As the equation shows, the ionic strength rises during the reaction. In the results given below, the initial ionic strength is recorded. Most of the runs were kept fairly short, so that the change in ionic strength was not above 0.05, as it was expected that the rate would vary considerably with ionic strength. As it turned out, there is some such variation, but it was not very large. For the most part, evidence of the order of the reaction was obtained by starting runs at different dithionite concentrations, but in the run shown in Fig. 1, the analyses were continued long enough to give fairly definite evidence of this from this run alone.

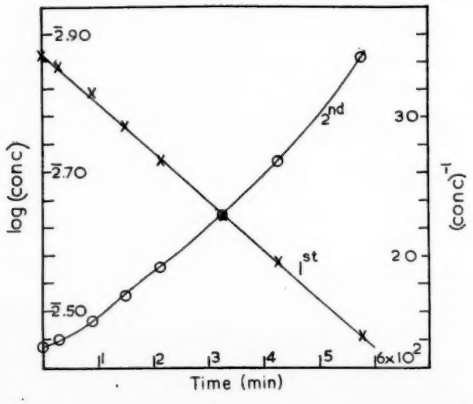

FIG. 1.

The analysis for dithionite in alkaline solution presents some difficulties that are not encountered in neutral or weakly acid solution. K. and E. Jellinek used the reduction of ammoniacal copper (II) sulphate for their analyses. In alkaline solution this reagent gives a heavy black precipitate (probably a sulphide) with dithionite, and the method is impracticable. Hahn (4, 5) used titration with ferric chloride, in the presence of a mixed indicator of potassium thiocyanate and ferricyanide, but this was found to give irregular results in alkaline solution. However, it worked well for the analyses of solid sodium dithionite, and was used in runs with the solid. The method finally used in the solution runs was that due to Smith (6). A known volume of dithionite was run into excess ammoniacal silver nitrate; silver is then precipitated. This was filtered off, washed, dissolved in nitric acid, and titrated with chloride by the Volhard method. The chief difficulty was that sometimes the precipitate was so finely divided that filtration was virtually impossible, and samples were occasionally lost because of this.

The reagents used were all of analytical reagent quality, with the exception of the sodium dithionite. The purest available solid was about 90% sodium dithionite, the main impurities being the decomposition products, sodium thiosulphate and sulphite. Recrystallization did not much improve this as some decomposition always occurred. Solutions were made from this, and were then analyzed in order to be able to calculate the ionic strength. This was then adjusted to the desired value by adding sodium fluoride.

RESULTS

The runs were generally not long enough to distinguish unambiguously the order of the reaction solely from one run. Accordingly in Table I the results are given in the form of the best values of the first order rate constants (k_1), and the second order rate constants (k_2), obtained in the usual way from a plot of time against log (concentration) or (concentration)$^{-1}$. This table also gives runs at various ionic strengths, at various temperatures, and at various initial sodium hydroxide concentrations.

TABLE I

Decomposition of sodium dithionite in aqueous solution

Run	Temp., °C	Initial ionic strength	Initial ($Na_2S_2O_4$), molar	Initial (NaOH), molar	k_1, min^{-1}	k_2, (g-molecule/l.)$^{-1}$ min^{-1}
1	88.5	0.70	0.064	0.10	4.3×10^{-4}	7.4×10^{-3}
2	88.5	0.67	0.062	0.10	4.4	8.0
3	88.5	0.70	0.034	0.10	4.6	15.1
4	88.5	0.70	0.123	0.10	4.6	4.0
5	88.5	0.70	0.069	0.20	6.3	10.6
6	88.5	0.70	0.130	0.20	6.4	6.1
7	88.5	0.71	0.142	0.20	6.1	5.6
8	88.5	0.74	0.067	0.05	4.3	7.0
9	88.5	0.70	0.067	0.15	5.5	9.6
10	88.5	0.35	0.068	0.10	2.9	4.5
11	88.5	0.99	0.063	0.10	5.0	7.5
12	88.5	1.53	0.065	0.10	5.8	10.5
13	98.0	0.71	0.065	0.10	11.3	18.9
14	84.1	0.70	0.065	0.10	3.0	5.15
15	79.4	0.69	0.059	0.10	1.65	3.0
16	98.0	0.70	0.074	0.20	16.0	35.8

The first thing that is apparent from this table is that the reaction is first order in dithionite. Runs 1 to 4, or 5 to 7, where all other variables are kept constant show this clearly. Figure 1 shows a plot of log (concentration) and (concentration)$^{-1}$ against time for run 16. This gives a better straight line for a first order reaction. This, as well as the great differences in over-all rate, proves that the reaction in alkaline solution is not the

same as that examined by K. and E. Jellinek. The obvious explanation of this is that under the conditions of their experiments the solution contained $HS_2O_4^-$ or $H_2S_2O_4$, and that these decompose faster than $S_2O_4^{--}$. Similar behavior is, of course, found with other acids and their salts, e.g. thiosulphates and hypochlorites. There seem to be no reliable values of the ionization constants of dithionous acid, so it is impossible to calculate the concentrations of $HS_2O_4^-$ or $H_2S_2O_4$ in K. and E. Jellinek's experiments. With an activation energy as low as 8 kcal, as calculated from their results, it seems quite probable that molecules of dithionous acid are reacting.

The effect of varying concentrations of sodium hydroxide can be seen from runs 8, 1, 9, and 5. The rate increases somewhat at higher sodium hydroxide concentrations, but the change is very small at lower concentrations. Presumably hydroxide ions catalyze the reaction to some extent, but the effect is not proportional to their concentration.

Ionic strength was varied in runs 10 to 12, taken together with earlier runs at an ionic strength of 0.7. The results show a moderate change in rate with ionic strength, higher ionic strengths giving increased rates. Somewhat similar behavior is, of course, found in other ionic reactions.

Variation in temperature in runs 13 to 15 gave rate constants which show a reasonably linear plot of log k against $1/T$ of the usual sort. The activation energy is 26 kcal/g-molecule (or perhaps, $26\frac{1}{2}$ kcal/g-molecule). If $k = A\,e^{-E/RT}$, then, expressing k_1 in (seconds)$^{-1}$, log $A = 10.9$, or ln $A = 25.1$. This is a somewhat low figure, but not exceptionally so. This is for concentrations of hydroxide ion low enough for them apparently not to affect the rate to any great extent.

The mechanism of the reaction cannot be deduced with any certainty from these results. The most plausible suggestion, perhaps, is that the initial, and slowest, stage is a reaction with water:

$$S_2O_4^{--} + H_2O \rightarrow HSO_2^- + HSO_3^-$$

followed by a more rapid further reaction of HSO_2^- with dithionite ions:

$$HSO_2^- + S_2O_4^{--} \rightarrow HSO_3^- + S_2O_3^{--}.$$

This suggestion is very tentative. However, if it is correct, the reaction is really bimolecular, and $d[S_2O_4^{--}]/dt = -k_2[S_2O_4^{--}].[H_2O]$. Allowing for the concentration of water, and if $k_2 = A_2\,e^{-E/RT}$, then log $A_2 = 9.2$ (time in seconds), a fairly typical figure (7).

DECOMPOSITION OF THE SOLID

It seemed of interest to compare rates in the solid with those in solution, although if the above suggestion about the mechanism is correct, the reaction must necessarily go by a different route in the solid. Finely ground solid (between 100 and 200 mesh) was used, and the fraction decomposed at different times is given in Table II.

These results give typical S-shaped curves when the fraction decomposed (represented by α in the equations below) is plotted against time. Various equations have been proposed to explain similar curves for other reactions of solids (e.g. (8)), the different equations being based on different mechanisms. In applying them, there is a difficulty because the sample took a finite time to come to the temperature of the run, and consequently there is some doubt about the true zero of time for the reaction. To avoid this difficulty the method generally adopted was to plot the observed time to reach a given value of α against the calculated time to reach the same value. This was done for the range of α from 0.1 to 0.95, and a suitable equation should give a straight line for the resulting graph. Even so the decision between various equations is not too easy, since all give, if

TABLE II

Decomposition of solid sodium dithionite

Run 1: 155° C								
Time (min)	30	60	90	120	150	180	210	240
α	0.038	0.065	0.092	0.151	0.230	0.355	0.458	0.610
Time (min)	272	30	333	362				
α	0.772	0.834	0.908	0.953				
Run 2: 160° C								
Time (min)	30	60	93	120	150	165	180	195
α	0.081	0.123	0.225	0.366	0.623	0.712	0.798	0.900
Time (min)	210	225						
α	0.941	0.962						
Run 3: 165° C								
Time (min)	15	30	45	60	75	90	107	120
α	0.062	0.095	0.145	0.257	0.405	0.563	0.737	0.854
Time (min)	135	150	165					
α	0.939	0.983	0.994					
Run 4: 170° C								
Time (min)	15	30	45	60	75	90	105	
α	0.076	0.204	0.507	0.741	0.902	0.978	0.989	

α is plotted against time, roughly linear middle sections, similar to what is found experimentally; and consequently graphs of calculated against experimental times were always linear over a considerable range in the middle. Hence a decision for or against a possible mechanism largely depended on the ends of the curves.

The equations quoted by Garner (8) may be divided into those which take account of overlap and interference between growing reaction zones, and those which do not. The latter are only applicable in the early stages of the reaction, and so cannot be applied here. On the former, the following deductions seem possible.

1. Branching Nuclei, Interfering During Growth

Garner and Hailes (9) suggested that nuclei might initially form very rapidly up to a certain maximum number, and thereafter increase by branching. At the same time nuclei might disappear as centers of reaction by becoming totally surrounded by reacted material. The chance of this happening was taken to be proportional to α. If N is the number of nuclei at time, t, these assumptions mean that

$$dN/dt = k_3N - k_4\alpha N$$

where k_3 and k_4 are constants. If each nucleus grows linearly with time, $d\alpha/dt = k_1N$, the nuclei being supposed to grow out in one dimension and not as spheres. Hence the curve of α against t will have an inflexion at $\alpha = \alpha_1 = k_3/k_4$. If $N = 0$ at $\alpha = 0$, these equations lead to

$$\ln [\alpha/(2\alpha_1 - \alpha)] = k_3t + C$$

where C is an integration constant.

In the present curves α_1 is about 0.5 (as was found in other cases by Garner and Hailes), and a plot of $\ln [\alpha/(1-\alpha)]$ against t was fairly linear. The values of k_3 were calculated to be:

T	155	160	165	170	° C
k_3	1.9	3.3	5.4	8.2×10^{-2}	min^{-1}.

These values make the activation energy for the growth process 36 kcal/g-molecule.

There is some deviation from this equation if α is small, but in any case the approximations made in deriving it are not valid at low values of α. This is because the assumption that $N = 0$ at $\alpha = 0$ is not really correct. If we assume that $N = N_1$, a small number, when $\alpha = 0$, the equation becomes:

$$\ln \{(\alpha - N_1k_1/k_3)/(2\alpha_1 - N_1k_1/k_3 - \alpha)\} = k_3(1 - N_1k_1/k_3\alpha_1)t + C.$$

As α evidently approaches unity at large values of t, presumably

$$2\alpha_1 - N_1k_1/k_3 = 1.$$

Fairly good lines are obtained if $N_1k_1/k_3 = 0.04$ for all runs; the resulting values of k_3 are:

T	155	160	165	170	°C
k_3	2.35	3.65	5.6	9.05×10^{-2}	min^{-1}.

These give an activation energy of 34.1 kcal/g-molecule.

2. Random Surface Nucleation Followed by Rapid Surface Growth

Here it is proposed that random nucleation occurs, but once it has occurred on a grain of the material either the entire surface, or certain faces of it, is rapidly covered with a reaction zone, which then moves slowly towards the center. If N_0 is the total number of grains, and N of these are nucleated, then $dN/dt = k_1(N_0 - N)$. If the reaction zone moves at a constant speed, α is given by:

$$\alpha = (1/k_1t_0)\ (e^{-k_1t} + k_1t - 1)$$

where t_0 is the time any one grain takes to decompose. This is valid up to $t = t_0$, as it does not allow for some grains having totally decomposed. If $t > t_0$, α is given by:

$$\alpha = 1 - (1/k_1t_0)\ (e^{k_1t_0} - 1)\ e^{-k_1t}.$$

When these equations were compared with the experimental curves, it was not possible to get a good fit. In particular they make α rise much too rapidly at first as compared with experiment, though this improves somewhat if k_1t_0 is very large. However, it seems unlikely that this is the correct mechanism. Other assumptions about the proportion of the surface nucleated led to modified equations, but none were found to give a good agreement with experiment.

3. Random Surface Nucleation, but no Rapid Surface Growth

On this picture nucleation starts at a point on the surface of the grain, and the reacted zone spreads inwards like a growing sphere. If each grain is itself spherical, the fraction of any grain reacting in time, t, is

$$\alpha_1 = 4(t/t_0)^3 - 3(t/t_0)^4$$

where t_0 is the time for any grain to react completely. If nucleation is random the equations for α are:

[i] $t < t_0$; $\alpha = (24A^3 + 72A^4)\ (e^{-U/A} - 1) - 3U^4 + 4U^3 + 12AU^3 - 12AU^2 - 36A^2U^2 + 24A^2U + 72A^3U$

[ii] $t > t_0$; $\alpha = 1 - e^{-U/A}[24A^3 + 72A^4 - (12A^2 - 48A^3 + 72A^4)\ e^{1/A}]$

where $U = t/t_0$ and $A = 1/k_1t_0$, and k_1 is the rate constant for the nucleation process.

These equations make the rise in α too steep at first unless k_1t_0 is fairly large (about 7 or more), under which conditions the rate of nucleation is rapid compared with the time for a particle to react. However, even if k_1t_0 is large a plot of U against experimental times for the same α does not give a good straight line. Hence this is probably not the correct mechanism.

4. Random Nucleation with Ingestion of Nuclei

Here it is proposed that nuclei are formed at random throughout the material, and the radii of the nuclei grow at a constant rate. Allowance is made for the impingement of the nuclei on each other. This leads to the equation:

$$-\ln (1-\alpha) = B(e^{-U}-1+u-u^2/2+u^3/6)$$

where $u = k_1t$, and k_1 is the rate constant for nucleation. B is a constant equal to $8\pi N_0k_2^3/V_0k_1^3$, where N_0 is the total number of nuclei, k_2 is the rate of nucleus growth, and V_0 is the total volume of material (10).

The form of the curves is little altered by changes in B, so that it is not possible to deduce the best value of B with any precision. Plots of u against the experimental time for the same values of α give good lines if B is fairly large (about 10), though the data for 170° C fit a somewhat smaller value of B (about 2 to 5). If B is 10 at all temperatures, values of k_1 are:

T	155	160	165	170	°C
k_1	2.55	4.3	7.15	10.2×10^{-3}	min^{-1}.

This gives a linear plot of log k_1 against $1/T$ corresponding to an activation energy of 35.7 kcal/g-molecule.

However, B should vary with temperature, and as the activation energy of nucleation is presumably larger than that of growth, B should fall with increasing temperature. Different values of B at 170° C, with $B = 10$ at 155° C, give the following activation energies:

B (170° C)	10	5	2	1	
E_1	35.7	39.0	45.4	50.4	kcal/g-molecule
E_2	35.7	33.2	31.9	31.1	kcal/g-molecule.

Here E_1 is the activation energy of nucleation, and E_2 that of growth. If $B = 5$ at 170° C, then $k_1 = 12.0\times10^{-3}$ min^{-1}; if $B = 2$, $k_1 = 15.5\times10^{-3}$ min^{-1}, both at 170° C.

As a general conclusion, this last equation undoubtedly gives the best agreement with the experimental points, and is somewhat superior to the equation for the branching mechanism; so probably the correct mechanism is one of random nucleation and linear growth. Although some other mechanisms have been definitely excluded above, one cannot be certain that some hitherto unsuggested mechanism might not also fit the experimental points. Because of the small change in the curves representing random nucleation and linear growth as B varies, it is not possible to separate all the rate constants, but that for the nucleation rate must be approximately as indicated above. The activation energy for growth is 32 to 33 kcal/g-molecule, while the most that can be said about the activation energy for nucleation is that it is probably 40 to 45 kcal/g-molecule. As is to be expected, these are considerably larger than the solution activation energy of 26½ kcal/g-molecule.

REFERENCES

1. JELLINEK, K. and JELLINEK, E. Z. physik. Chem. **93**, 325 (1919).
2. LANGE, N. A. Handbook of chemistry. Handbook Pubs., Inc., Sandusky, Ohio. 1956. p. 1202.
3. DEINES, O. and ELSTNER, G. Z. anorg. u. allgem. Chem. **191**, 340 (1930).
4. HAHN, F. L. Anal. Chim. Acta, **3**, 62 (1949).
5. HAHN, F. L. Anal. Chim. Acta, **3**, 65 (1949).
6. SMITH, J. H. J. Am. Chem. Soc. **43**, 1307 (1921).
7. SMITH, J. H. J. Am. Chem. Soc. **43**, 76 (1921).
8. GARNER, W. E. Chemistry of the solid state. Butterworth Scientific Publications, London. 1955. Chap. 7.
9. GARNER, W. E. and HAILES, H. R. Proc. Roy. Soc. A, **139**, 576 (1933).
10. AVRAMI, M. J. Chem. Phys. **7**, 1103 (1939); **8**, 212 (1940).

GAS ADSORPTION CHROMATOGRAPHY[1]

JAMES F. HANLAN AND MARK P. FREEMAN[2]

ABSTRACT

It is found that the "retention volume" in gas adsorption chromatography may be identified in a very simple way with the concept of "apparent volume" in the equation of state for high temperature physical adsorption first derived by Halsey *et al.* It is shown that a considerable body of experimental chromatographic data reduces down to the two parameters of the theory in a reasonable way. The single parameter describing temperature dependence is seen to be related simply to the number of carbons in the skeleton for a series of hydrocarbons, while the parameter describing column capacity shows regular, though unanticipated, behavior. This theoretical connection provides a complete link between static measurements and gas adsorption chromatography.

Gas adsorption chromatography or gas solid chromatography is the name applied to the chromatographic process using an adsorbent as the fixed phase and a gas as the mobile phase. It is useful chiefly in the chromatographic separation of mixtures of permanent gases and vapors of low-boiling liquids for which purpose it seems more suitable than the more frequently encountered gas–liquid partition chromatography.

As it is commonly used, gas adsorption chromatography apparatus is very similar to that employed in gas–liquid partition chromatography with the substitution of an adsorbent for the fixed bed. It is characterized by requiring a much more sensitive temperature control for reproducible results. Elution chromatography and frontal analyses may be performed in either case, but the adsorption chromatogram is characterized by asymmetric break-through curves which have thus far defied a simple quantitative interpretation. This latter fact has complicated a theoretical interpretation by the "theoretical plate" analysis so useful in the partition chromatogram (1).

At the same time, the aforementioned sensitivity to temperature change in adsorption chromatography makes it possible to separate virtually any mixture on the same column by judiciously selecting the temperature (barring chemisorption), whereas in partition chromatography it is often necessary to change the liquid employed in the fixed phase.

This work represents an attempt to present a comprehensive theoretical framework for the interpretation of gas adsorption chromatographic results in terms of the rigorously derived equation of state for the interaction of gases and surfaces developed by Halsey *et al.* (2, 3, 4, 5, 6) also (7, 8). Such an interpretation would necessarily link gas chromatographic results to the static measurements employed in these investigations, as well as provide the desired predictive information about temperature dependence for the chromatogram.

The experimental data (9) used in the verification of the theory derived here were obtained by Dr. H. Habgood of the Research Council of Alberta, Edmonton, Alberta, Canada, and one of us (James F. Hanlan) at that laboratory.

The experimental observation made by these investigators indicating the suitability of the gas–surface interaction state equation was that when the logarithm of the retention volume (10) (which is defined as the volume of gas leaving the column while a given

[1]*Manuscript received in original form December 18, 1958, and, as revised, April 7, 1959.*
Contribution from the Department of Chemistry, University of California, Berkeley, California.
[2]*Present address: Research Division, American Cyanamid Company, Stamford, California.*

constituent is passing through the column) of gas A minus that for H_2 is plotted vs. $1/T$, a fairly good straight line relationship holds (Fig. 1). This is reminiscent of the concept of "excess volume" in the theory of Halsey *et al.* which exhibits similar behavior.

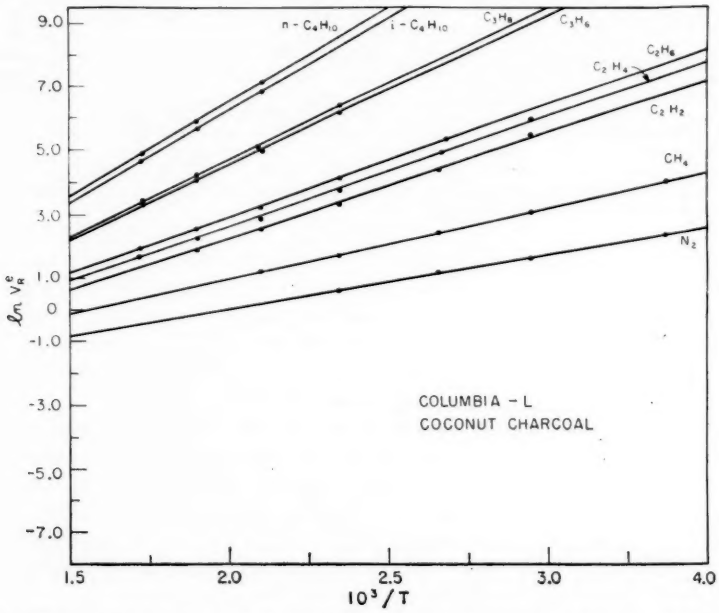

FIG. 1. The natural logarithm of the experimental excess retention volume on Columbia L charcoal plotted vs. reciprocal temperature for several gases. Five points of the original data have been discarded where marked deviations from the trend were observed. These deviations were not systematic and were probably attributable to experimental error.

THEORY

A basic underlying assumption will be implicitly made in the following derivation. Namely, it will be assumed that some sort of equilibrium exists within the gas phase passing through the column so that the gas systems (molecules or atoms) are always at their equilibrium distribution with respect to the gas surface potential well. This assumption is supported by the observation (10) that retention volume is independent of flow rate over a wide range of flow rates.

The retention volume is given as the product of retention time and flow rate through the column:

[1] $$V_R = F \cdot t_A = (\eta kT/P) \cdot t_A$$

where F is the flow rate in cm³/sec (at column temperature T and pressure P) and η is the flow rate in systems per second; t_A is the time lag between introducing the mixture and detection of constituent A at the other end. Now, the apparent volume of a vessel containing an adsorbent is just given by:

[2] $$V_a = NkT/P$$

where V_a is just the imaginary volume that would be required to hold N systems of ideal gas at temperature T and pressure P. If these two concepts are linked, a very

simple picture emerges for the adsorption chromatogram in terms of the time required for constituent A to get through the column. Namely, if all gas systems pass through the column at the same flow rate, the time to get through is going to vary directly as the apparent volume traversed. That is, one could think of equivalent empty columns of the same diameters, but of lengths proportional to the apparent volumes. This would suggest an immediate formal identification of apparent volume and retention volume so that for a pure constituent the equation of state would be immediately applicable. Unfortunately, gas chromatography always involves a mixture of gases and although the gas–surface equation of state gives an apparent volume in this case, it is not immediately obvious what this means in terms of retention volume. This becomes particularly true when considering gas imperfections and lateral interactions on the surface.

The equation of state (5) for the interaction of a binary mixture of gases and a surface is given by:

$$\frac{1}{V_a} = \frac{X_A}{V_A^0} + \frac{X_B}{V_B^0} - N\left(\frac{C_0}{V_a^{0\,3}}\right) \tag{3}$$

where the mole fraction of G is X_G(G = A, B) and

$$V_G^0 = V_{geo} + B_{GS} \tag{4}$$

and is the apparent volume for pure constituent G at zero pressure.

Further,

$$\frac{C_0}{V_0^3} = \frac{X_A^2 C_{AAS}}{(V_A^0)^3} + \frac{X_B^2 C_{BBS}}{(V_B^0)^3} + \frac{X_A X_B C_{ABS}}{V_A^0 V_B^0}\left(\frac{1}{V_A^0} + \frac{1}{V_B^0}\right) \tag{5}$$

V_{geo} is the true or geometric volume enclosed by the vessel in which the gas is interacting with the surface and excluded by a geometric surface running through the gas–solid interface beyond which gas systems are assumed not to penetrate.

$$B_{GS} = \int_{V_{geo}} [\exp\{-\phi_{ls}^G/kT\} - 1]\, d\tau_i^G \tag{6}$$

where $d\tau_i^G$ is the differential volume element for the ith gas system of species G and ϕ_{ls}^G is the potential energy function for the interaction of a specific system of this type with the surface. This integral has been tabulated for two potential energy models both of which have been quite successful in interpreting experimental results:

(1) the hard sphere–inverse cube model (2):

$$\phi_{ls}^G = -\epsilon_G^* \frac{D^3}{x^3} \tag{7}$$

where ϵ_G^* is the depth of the potential energy well at the hard sphere repulsion distance, $x = D$, and

(2) the 9-3 model (7):

$$\phi_{ls}^G = \left(\frac{3\sqrt{3}\epsilon^*}{2}\right)\left[\left(\frac{s_0}{s}\right)^9 - \left(\frac{s_0}{s}\right)^3\right] \tag{8}$$

where ϵ^* is as before and s_0 is the gas–surface separation where the attractive and repulsive energies just cancel. This second potential energy model will be used throughout the paper as it is somewhat easier to use. A reduced form of this integral (B_{GS}/As_0) (where A is the area) for this potential model is in reference (7) with three additional values tabulated in Table I.

TABLE I

Addition to the Appendix in reference 7

ϵ^*/kT	B_{AS}/As_0
13.087	8.291×10^4
14.627	3.625×10^5
16.166	1.579×10^6

$C_{GG'S}$ can be broken up into a gas imperfection factor and a term involving the simultaneous interaction of two gas systems of type G and G′ and the surface (8):

$$[9] \qquad C_{GG'S} = -2(V_G^0 + V_{G'}^0 - V_{geo})B_{GG'} + C'$$

where $B_{GG'}$ is the (mixed) second virial coefficient and

$$[10] \quad C' = \int \{\exp[-\phi_{1s}^G/kT]-1\} \int \{\exp[-\phi_{2s}^{G'}/kT]-1\}\{\exp[-\phi_{12}^{GG'}/kT]-1\}\, d\tau_1^G, d\tau_2^{G'}.$$

The most successful model for this integration to date is tabulated in the appendix of reference (8) for a single constituent. This involves the 9-3 potential model for gas–surface attraction and a hard sphere repulsion at distance $^n r_0$ between the interacting gas systems. This integral is given as a function of the reduced gas–surface potential energy and the distance ratio $\delta = s_0/^n r_0$.

Equations [3], [4], and [5] undergo considerable simplification if it is assumed that the carrier gas, B, has no net attraction to the surface or to other gas systems (apparently true for He at room temperature and above). If ideal behavior is likewise assumed for the bulk carrier phase, then

$$[11] \qquad B_{BS} = B_{BB} = B_{AB} = C_{BBS} = C_{ABS} = 0$$

and equation [5] becomes

$$[12] \qquad \frac{C_0}{V_0^3} = \frac{X_A^2 C_{AAS}}{V_A^{0\,3}}.$$

Equation [4] for the carrier reduces to:

$$[13] \qquad V_B^0 = V_{geo}.$$

Substituting [12] and [13] in [3] yields:

$$[14] \qquad \frac{1}{V_a} = \frac{X_A}{V_A^0} + \frac{X_B}{V_{geo}} - \frac{NX_A^2 C_{AAS}}{V_A^{0\,3}}.$$

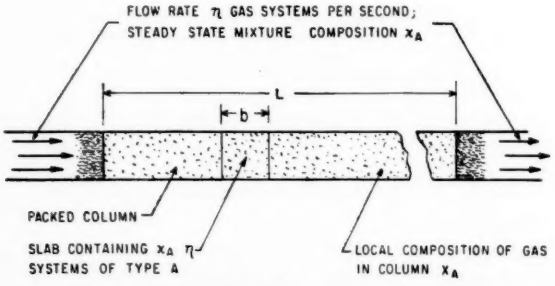

FIG. 2. Schematic representation of the adsorption chromatographic column.

To effect the necessary derivation, it is convenient to assume a steady state mixture (composition χ_A) to be flowing in and out of the column (Fig. 2) at a flow rate of η systems per second. The necessary enrichment of A in the column results in a local composition of X_A which is generally different from χ_A. Clearly $\chi_A\eta$ is the number of systems of type A leaving the column each second. The same number of systems of type A must cross every boundary in the column each second so that b, the length of a slab of column containing $\chi_A\eta$ systems of type A, divided into L, the length of the column, will give the time required for a labeled front in gas A to travel the length of the column. (This does not allow for column end effects, but this will be taken care of below.)

$$t_A = L/b \tag{15}$$

If the extensive quantities in the slab are denoted by double primes and use is made of the definition of mole fraction, then [14] may be rewritten:

$$\frac{N''}{V_{a''}} = \frac{N_{A''}}{V^0_{A''}} + \frac{N_{B''}}{V_{geo''}} - \frac{N_{A''}{}^2 C_{AAB''}}{V^{0\ 3}_{A''}}. \tag{16}$$

But by definition $N_{A''} = \chi_A\eta$. Using the assumed ideality of the carrier gas

$$N_{B''} = P_B V_{geo''}/kT = (1-\chi_A)PV_{geo''}/kT$$

and relation [2] [16] may be written:

$$\frac{P}{kT} = \frac{\eta}{V^0_{A''}} - \chi_A\eta^2 \frac{C_{AAB''}}{V^{0\ 3}_{A''}}. \tag{17}$$

If the extensive quantities per unit length are denoted by single primes, [17] becomes:

$$\frac{P}{kT} = \frac{\eta}{bV^0_{A'}}\left[1 - \chi_A\eta \frac{C_{AAB'}}{bV^{0\ 2}_{A'}}\right] \tag{18}$$

or solving for b (assuming the term on the right in the brackets, eq. [18], to be small):

$$b \approx \frac{\eta kT}{PV^0_{A'}}\left[1 + \frac{\chi_A P C_{AAB'}}{kTV^0_{A'}}\right]^{-1}. \tag{19}$$

Using relations [15] and [1] one finally obtains for V_R

$$V_{R_A} = V^0_A + \chi_A P \frac{C_{AAB}}{kT}. \tag{20}$$

The retention volume for the carrier gas by the same analysis is just

$$V_{R_{carrier}} = V_{geo}. \tag{21}$$

To be consistent with the data as they were received and to subtract out the effect of unpacked parts of the column and end effects so far as possible, one must subtract equation [21] from equation [20] to get an excess retention volume:

$$V^e_R = B_{AB}\left(1 + \frac{\chi_A P}{kT}\frac{C_{AAB}}{B_{AB}}\right). \tag{22}$$

One sees that under the conditions of the derivation if χ_A is zero then the excess retention volume is just equal to B_{AB} which is identical with

$$V_{ex}|_{p=0} = V^0_A - V_{geo} = B_{AB} \tag{22a}$$

for the static measurements. C_{AAB} has generally been observed to be negative while

B_{AS} is always positive or negligible so that the usual case will have a higher concentration of gas A going through the column faster (lower retention volume), which means that a narrow rectangular initial distribution will tend to skew forward. This is what is observed and in fact the gas adsorption chromatogram is usually characterized by sharp anterior and sloping posterior edge. At very low partial pressures where chromatograms are usually run, this will produce a negligible error if retention time is measured to the peak which is the easiest part of the chromatogram to identify. At the same time, if frontal analysis is performed at different mole fractions, one may determine C_{AAS} experimentally. This would seem like a good way to obtain this experimentally elusive parameter, which is still of considerable theoretical interest (8).

It was found necessary in the course of the derivation to assume $1 \gg \chi_A PC_{AAS}/kTV_A^0$ or its equivalent. For a specific system all these quantities may be evaluated independently by static measurements. Take as an example argon on carbon black (Black Pearls No. 71) (7) at 273° K,

$$\begin{aligned}
&\text{sample wt.} = 10.63 \text{ g},\\
&C_{AAS} = -240\times10^{-20}(\text{cm})^6,\\
&V_A^0 = 150 \text{ cm}^3,\\
&kT = 3.72\times10^{-20} \text{ cc atm},\\
&V_{geo} = 28.5 \text{ cm}^3,\\
&B_{AS} = 121.5 \text{ cm}^3,
\end{aligned}$$

or

$$\frac{\chi\Delta PC_{AAS}}{kTV_A^0} = -.43\chi_A|_{p=1 \text{ atm}}.$$

If the mole fraction of A in the gas phase is kept below, say, 0.1 then the assumption that this product is much less than unity is clearly all right for this particular assembly. It would seem that if it were not small, no peak would be distinguished, which probably sets the lower temperature limit to gas adsorption chromatography.

Enthalpy of Adsorption

Using a model for physical adsorption based on the Gibbs boundary condition, one may consider the interaction to be a phase change from the gas phase to an imaginary two dimensional phase of zero volume. It has been shown (7) that the surface excess partial molar enthalpy at zero coverage is given by the derivative:

$$[23] \qquad \frac{\partial \ln T/V_{ex}^0}{\partial\, 1/RT} = \Delta H = \frac{\partial \ln T/V_R^e}{\partial\, 1/RT}$$

where V_{ex}^0 and V_R^e are those volumes at zero pressure and mole fraction respectively. Finally, using the definition of retention volume and keeping a constant flow rate (systems/second)

$$[24] \qquad \frac{\partial \ln (t_A - t_B)}{\partial\, 1/T} = \frac{-\Delta H}{R}$$

where B is as before a noninteracting constituent. This enthalpy may be related unambiguously to the parameter ϵ^* (7) which provides a way of getting this parameter without curve fitting. The enthalpy derived thus is of questionable predictive value because of a considerable temperature coefficient, especially at high temperatures, but

it is equal to the initial calorimetric heat of adsorption (L'Hospital's rule) and as such is of interest. Equation [23] is of course easier to apply than equation [24], which has been derived by a different approach (11). These authors did not correct for the interstitial dead space, but they did correct for the time spent in the unpacked region of flow at the ends of the column.

Effect of a Column Pressure Differential

Because of the short loosely packed columns and low rate used in gas adsorption chromatography, one would not expect the relatively large difference between P_i (inlet pressure) and P_o (outlet pressure) encountered in gas–liquid partition chromatography. However, in the framework of this theory any differential that exists can be handled readily.

Recognizing that [1] holds in any differential slab of the column, we obtain

$$\frac{\partial t_A}{\partial \zeta} = \frac{P(\zeta)}{\eta k T} \frac{\partial V_R}{\partial \zeta} \tag{25}$$

where ζ is the distance from the exit of the column. Making use of d'Arcy's formula for the laminar seepage of a perfect gas through a long capillary* and our boundary conditions,

$$P_{(\zeta)}^2 = P_o^2 + \frac{P_i^2 - P_o^2}{L} \zeta. \tag{26}$$

From differentiation of [20]

$$\frac{\partial V_R}{\partial \zeta} = V_{A'}^0 + \frac{\chi_A C_{AAS'}}{kT} P_{(\zeta)} \tag{27}$$

where the primed quantities are again the values per unit length. One may now write an expression for the retention time (using [25], [26], and [27]):

[28]

$$t_A = \int_{\zeta=0}^{\zeta=L} \frac{\partial t_A}{\partial \zeta} d\zeta = \frac{V_{A'}^0}{\eta k T} \int_{\zeta=0}^{\zeta=L} \left(P_o^2 + \frac{P_i^2 - P_o^2}{L} \zeta \right)^{\frac{1}{2}} d\zeta + \frac{\chi_A C_{AAS'}}{\eta (kT)^2} \int_{\zeta=0}^{\zeta=L} \left(P_o^2 + \frac{P_i^2 - P_o^2}{L} \zeta \right) d\zeta.$$

Integrating the right-hand side of equation [28] yields:

$$t_A = \frac{2 V_{A'}^0}{3 \eta k T} \left\{ \frac{P_i^3 - P_o^3}{P_i^2 - P_o^2} \right\} + \frac{\chi_A C_{AAS}}{\eta (kT)^2} \{ (P_i + P_o)^2 - 2 P_i P_o \} \tag{29}$$

where V_A^0 and C_{AAS} are those quantities for the entire volume. If one makes the approximation that the geometric mean pressure is equal to the arithmetic mean pressure P_m, (a completely justified approximation if $P_i \leqslant 1.30\ P_o$)

$$P_m^2 = \left[\frac{(P_i + P_o)}{2} \right]^2 = P_i P_o. \tag{30}$$

Equation [29] may be written

$$t_A = \frac{V_A^0}{\eta k T} P_m + \frac{\chi_A C_{AAS}}{\eta (kT)^2} P_m^2. \tag{31}$$

*Suggested by referee I.

Leaving P in equation [1] undefined for the moment, one may substitute from [31] for t_A and solve for the measured V_R:

$$[32] \qquad V_R = V_A^0 \frac{P_m}{P} + \frac{\chi_A C_{AAS}}{kT} \frac{P_m^2}{P}.$$

In practice, the flow rate is determined in a measuring device at some other temperature and pressure and is corrected to column conditions assuming ideal gas behavior. If the P used in the correction is the mean column pressure, then clearly

$$[33] \qquad V_R = V_{geo} + B_{AS} + \chi_A \frac{C_{AAS}}{kT} P_m.$$

Comparing [20] and [22*a*] with [33] it is apparent that if the mean pressure is used a column pressure drop introduces no difficulty in the interpretation of the data in terms of the integrals B_{AS} and C_{AAS}.

It may be pointed out that the correction factor for pressure drop along the column (12) proposed by James and Martin:

$$\frac{2}{3} \frac{(P_i/P_o)^3 - 1}{(P_i/P_o)^2 - 1}$$

reduces to

$$P_m/P_o$$

(where P_i, P_o, and P_m have the same significance as above) if the approximation [30] is assumed valid.

Effect of Another Elutant

Helium is moderately hard to obtain and so the question arises whether this theory can be used with a cheaper elutant such as hydrogen or nitrogen. An analysis of the behavior of B_{AS} and the relations leading to the derivation of equation [22] leads to the following conclusions:

(*a*) If the elutant is hydrogen, He may be used as the marker with no other modification.

(*b*) If the elutant is N_2 or a heavier gas, He or H_2 may still be used as the marker. The mixture must be run at a somewhat lower mole fraction for each constituent in order to preserve peaks.

(*c*) Even if the parameter C_{AAS} is quite large the pressure behavior will be dominated (5) (and hence obscured) by $C_{N_2N_2S}$.

Clearly this theory should be no more difficult to use for N_2 than for He but the sensitivity will necessarily be decreased due to the requirement of lower mole fraction for the major components and of course the fact that nitrogen is quite likely to be less different from the gas analyzed for than is He or H_2.

It is interesting that there is nothing in this theory to contradict the notion that a helium marker can move through the column considerably faster than the eluting nitrogen. This is probably easiest to understand in terms of the motion of equivalent empty columns.

Interpretation of Data

The data received by the authors were in the form V_R^e as a function of T. However, the V_R^e had been corrected to 273° K and were converted back to column temperature for application of the theory. The adsorbents used were three coconut charcoals designated Columbia L, BC-4, and BC-90. The last two charcoals were identical except for degree of activation. A hydrogen marker was used to measure the retention time of the

helium, which introduced some error because of the higher interaction energy of hydrogen and the surface, but an attempt to estimate the effect of this error on the part of the authors showed the error to be negligible within experimental error. The time interval was measured between the peak of the hydrogen marker and the peak of the constituent. As the authors had no way of determining this peak height all data were assumed to be at zero-mole fraction of A. The usual practice does not exceed this by much. The V_R°'s received had been divided by the weight of the adsorbent, but this is by no means necessary for use of the theory.

To fit the data and evaluate the parameters As_0 and ϵ^*/k, it is convenient to use a plot (7) of

$$\ln \frac{B_{AS}}{As_0} \quad \text{vs.} \quad \epsilon^*/kT.$$

One then estimates an ϵ^*/k and plots

$$\ln V_R^\circ \quad \text{vs.} \quad \left(\frac{\epsilon^*}{k}\right)_{\text{trial}}.$$

Next a

$$\ln As_0$$

is chosen for the data such that the sum of the deviations is zero when

$$\ln \frac{V_R^\circ}{As_0} \quad \text{vs.} \quad \left(\frac{\epsilon^*}{k}\right)_{\text{trial}}$$

is plotted. The trial value of ϵ^*/k is then systematically varied until the sum of the squares of the deviations of the data from the theoretical plot is a minimum. This procedure may be programed for an electronic computer and the result obtained accurately and rapidly as was done for this work. The final values of ϵ^*/kT and $\ln (B_{AS}/As_0)$ are shown in Table II along with the standard deviation from the curve. A deviation of .03 represents, for example, an average error in V_R° of 3%. The data are shown thus fitted in Fig. 3. The fit is entirely satisfactory. The values of the parameters required are given in Table III. Since one has two parameters characterizing the chromatogram it would be desirable to make them independent of the amount of column packing used. By its nature ϵ^*/k is already this way, but, of course, the product As_0 is simply extensive in the area (and presumably in the weight) of the packing material. One way to reduce this product to a reproducible parameter would be to divide by the weight of packing material as was done here. Another way would be to subtract the logarithm of As_0 for some calibrating gas such as nitrogen from $\ln As_0$ for each gas and thereby remove the extensive element.

How reproducible any of these parameters would be when determined by different investigators with different columns is of course not known, nor has an attempt been made as yet to directly compare parameters derived from chromatographs with those from static measurements.

Analysis of Trends in the Parameters

Once ϵ^* is known, the complete temperature dependence of V_R° is known so that it is of interest to see what sorts of predictions one might make about this quantity. The data presented here correlate well with several molecular and bulk properties, but the best correlation for the hydrocarbon series is to the number of carbon atoms in the skeleton (Fig. 4). This is clearly a good linear correlation suggesting the possibility that

TABLE II

Gas	Surface BC-4			Surface BC-90		
	ϵ^*/kT	ln (B_{AS}/As_0)	Standard deviation	ϵ^*/kT	ln $B_{AS}/As_0)$	Standard deviation
N_2	6.945	5.586	.0164	5.090	3.940	.0642
	6.251	4.962		4.537	3.457	
	5.532	4.327		4.032	2.016	
	4.962	3.829		3.641	2.672	
CH_4	8.587	7.086	.0363	5.006	3.867	.0231
	7.724	6.293		4.462	3.392	
	6.837	5.488		3.966	2.958	
	6.151	4.873		3.581	2.619	
	5.500	4.299		—	—	
	4.981	3.845		—	—	
C_2H_4	10.045	8.443	.0537	8.010	6.555	.0558
	9.063	7.527		7.140	5.762	
	8.086	6.625		6.345	5.047	
	7.336	5.940		5.730	4.502	
	6.566	5.246		5.220	4.054	
C_2H_6	10.545	8.914	.0535	8.552	7.053	.0836
	9.493	7.927		7.623	6.201	
	8.489	6.995		6.775	5.432	
	6.878	5.525		5.573	4.364	
C_3H_6	10.782	9.136	.0152	8.493	6.998	.0283
	9.786	8.201		7.670	6.243	
	8.760	7.246		6.987	5.624	
	—	—		6.465	5.155	
C_3H_8	11.121	9.457	.0231	10.152	8.544	.0296
	10.109	8.503		9.022	7.488	
	9.049	7.514		8.147	6.681	
	—	—		7.422	6.019	
	—	—		6.868	5.516	
i-C_4H_{10}	—	—	—	9.953	8.356	.0212
	—	—		9.067	7.530	
	—	—		8.390	6.903	
n-C_4H_{10}	—	—		10.415	8.792	
				9.488	7.923	.0475
				8.780	7.264	

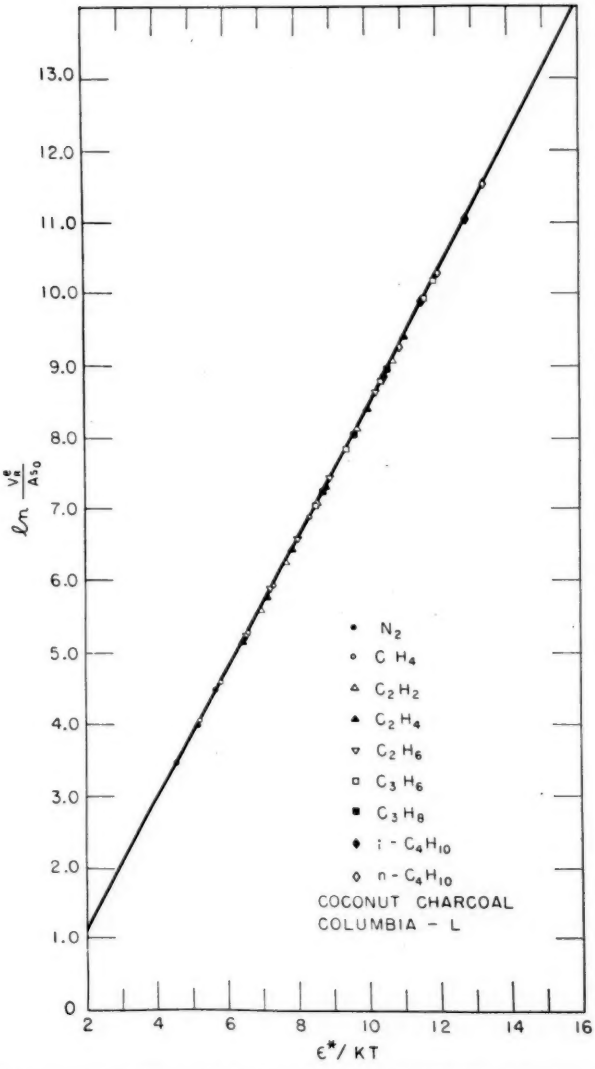

FIG. 3. Fit of the chromatographic results to the reduced curve of the theory for several gases interacting with Columbia L charcoal.

TABLE III

Surface	Gas	ϵ^*/k (° K)	ln As_0 (units of cm³/g)	ln $\frac{As_0\|A}{As_0\|N_2}$
Columbia L	N_2	1938	−2.83	—
	CH_4	2484	−2.83	0.0
	C_2H_2	3656	−3.69	0.86
	C_2H_4	3758	−3.48	0.65
	C_2H_6	3820	−3.30	0.47
	C_3H_6	4945	−3.77	0.94
	C_3H_8	5062	−3.81	0.98
	i-C_4H_{10}	6078	−4.20	1.37
	n-C_4H_{10}	6320	−4.40	1.57
BC-4	N_2	2078	−3.34	—
	CH_4	2570	−3.07	0.27
	C_2H_4	3789	−3.58	−0.24
	C_2H_6	3969	−3.64	−0.30
	C_3H_6	5055	−4.04	−0.70
	C_3H_8	5219	−4.20	−0.86
BC-90	N_2	1906	−2.94	—
	CH_4	1875	−1.87	1.07
	C_2H_4	3000	−2.46	0.48
	C_2H_6	3203	−2.53	0.41
	C_3H_6	4016	−2.75	0.19
	C_3H_8	4266	−3.03	−0.09
	i-C_4H_{10}	5211	−3.51	−0.57
	n-C_4H_{10}	5453	−3.75	−0.81

in a more heterogeneous series one could sum over different types of heavy atoms or functional groups in the molecule to obtain an accurate estimate of ϵ^*/k. This possibility should be thoroughly checked because of the obvious analytical applications of such a correlation.

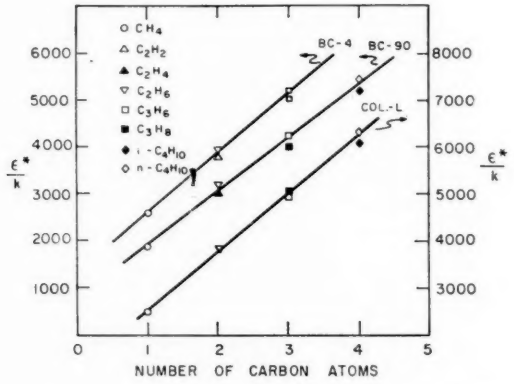

FIG. 4. Observed trends in the value of the parameter ϵ^*/k for all hydrocarbon assemblies analyzed as a function of the number of carbon atoms in the interacting gas.

The parameter As_0 when suitably normalized is as characteristic of a given gas–surface interaction as is ϵ^*/k, and so the two parameters together should serve as positive means to identify a particular molecular species for a precalibrated solid whether or not the column itself has been precalibrated. The detailed behavior of As_0 as an area-depen-

dent parameter is somewhat less satisfactory than has been observed for rare-gas atoms on carbon blacks. Even in this case there was the rather remarkable phenomenon that As_0 decreased as atomic size (and interaction energy) increased. For a constant area, this could mean a somewhat closer distance of balanced attractive and repulsive potentials. Likewise, it could mean a considerable area of small crevices or capillaries more accessible to the smaller atom than the larger. Finally, it could indicate the presence of hot-spots (7) (portions of the surface with much higher energy of interaction). This effect is much magnified in these chromatographic data (possibly because of the nonspherical systems?). For example, the parameter As_0 for Columbia L charcoal increases by 400% in going from normal butane to methane, whereas by way of comparison, changing from argon to helium on carbon black with static measurements increased As_0 by only 30%. Finally, note that when the charcoal is activated as in going from BC-4 to BC-90 (presumably by the water gas or some similar reaction) the energy of interaction for all hydrocarbons drops by about 20–30% at the same time the specific values of the parameters As_0 increase by a factor of 3.25. This is in contrast to the behavior of nitrogen which decreases in energy by 2.6% and increases in the value of the product As_0 by 52% in the same activation process.

In Table IV can be seen the increase of the area with activation. This calculation, of course, requires the approximation that s_0 be nearly the same for a given gas on the two

TABLE IV

A	$\ln \frac{As_0 \mid \text{BC-90}}{As_0 \mid \text{BC-4}}$	$\frac{A \mid \text{BC-90}}{A \mid \text{BC-4}}$
CH_4	1.17	3.22
C_2H_4	1.29	3.63
C_2H_6	1.11	3.04
C_3H_6	1.12	3.06
C_3H_8	1.20	3.32
Mean value	1.178	3.25

different surfaces. The values for the different gases are remarkably uniform with a mean value of 3.25 for the ratio of the area of charcoal BC-90 to that of BC-4. This compares well with the monolayer areas of 630 and 200 m^2/g respectively (9). If s_0 is estimated as one half the interlayer thickness of graphite, 1.7 Å, (13) plus one half the van der Waal's radius of the adsorbate, the area is calculated from the parameter As_0 to be of the order of the monolayer area. The decrease of ϵ^* with activation points to surface heterogeneity, for example, crevices which upon widening with activation would permit fewer adsorbent nearest neighbors per adsorbed molecule. This might be expected to appear under these conditions, i.e., low pressure and high temperature, where such effects would not be "washed out" by large numbers of strong lateral interactions. The similarity of the ratios of the monolayer areas and of our A's may be taken to mean that all portions of a heterogeneous surface increase equally. On the other hand, this may be interpreted as indicating that the surface is, in fact, homogeneous. More work is definitely indicated in this area.

Note that acetylene stands out as being rather exceptional. This gas was used on the BC-4 charcoal where it gave a reasonable value of ϵ^*/k but an apparently anomalous

value of the parameter As_0. At the time the experiments were performed the investigators felt that this gas was somehow interacting chemically with the column and therefore did not use it, throughout their experiments.

DISCUSSION

It has been shown that the concept of excess retention volume in gas adsorption chromatography not only provides a simple physical analog in terms of equivalent empty column lengths but also relates in a simple way to the concept of excess apparent volume. This quantity was introduced by Halsey *et al.* when treating the theory of the van der Waals interaction of gas and surface in the same temperature region where gas adsorption chromatography is carried out.

A considerable number of data were fitted to the curve and were found to fit within experimental error yielding reasonable values of the two parameters. The parameter describing the temperature dependence was seen to be highly predictable from a knowledge of the number of carbons in a hydrocarbon and the parameter describing column capacity showed some interesting though as yet uninterpreted behavior. Even without this interpretation the theoretical framework should be very useful to the practicing chromatographer.

To the theoretical investigator, it is clear that gas adsorption chromatography though possibly less accurate than static measurements makes up for it in much greater speed and ease of manipulation. The use of frontal analyses to get C_{AAS} looks especially promising.

ACKNOWLEDGMENTS

The authors wish to express their appreciation for the co-operation of Dr. Habgood and the Research Council of Alberta. In addition, they would like to thank Professor T. Vermeulen of this university for many helpful discussions.

The calculations reported here were done under the free time allocation for unsupported research on an IBM 701 computer. This computer is supported jointly by the Regents of the University of California, International Business Machines Corporation, and the National Science Foundation.

REFERENCES

1. PHILLIPS, C. Gas chromatography. Butterworth Scientific Publications, London. 1956. p. 11.
2. STEELE, W. A. and HALSEY, G. D., Jr. J. Chem. Phys. **22**, 979 (1954).
3. STEELE, W. A. and HALSEY, G. D., Jr. J. Phys. Chem. **59**, 57 (1955).
4. FREEMAN, M. P. and HALSEY, G. D., Jr. J. Phys. Chem. **59**, 181 (1955).
5. KWAN, T., FREEMAN, M. P., and HALSEY, G. D., Jr. J. Phys. Chem. **59**, 600 (1955).
6. CONSTABARIS, G. and HALSEY, G. D., Jr. J. Chem. Phys. **27**, 1433 (1957).
7. FREEMAN, M. P. J. Phys. Chem. **62**, 723 (1958).
8. FREEMAN, M. P. J. Phys. Chem. **62**, 729 (1958).
9. HABGOOD, H. W. and HANLAN, J. F. Can. J. Chem. **37**, 843 (1959).
10. JANAK, J. J. Chem. Listy, **47**, 464 (1953).
11. GREENE, S. A. and PUST, H. J. Phys. Chem. **62**, 55 (1958).
12. JAMES, A. T. and MARTIN, A. J. P. Biochem. J. **50**, 679 (1952).
13. PAULING, L. Nature of the chemical bond. Cornell Univ. Press, Ithaca, N.Y. 1948. p. 172.

ALKALOIDS OF LYCOPODIUM ANNOTINUM

PART II. ISOLATION OF FOUR NEW ALKALOIDS[1, 2]

F. A. L. Anet and N. H. Khan

ABSTRACT

Countercurrent distribution of the alkaloids of *Lycopodium annotinum* gave four new bases: annofoline, lycofoline, and α- and β-lofoline. Annofoline, $C_{16}H_{25}O_2N$, contained a keto and a hydroxyl group. Lycofoline, $C_{16}H_{25}O_2N$, possessed at least one hydroxyl group and possibly a double bond. α- and β-Lofoline each had the formula $C_{18}H_{29}O_3N$ and contained a hydroxyl and an O-acetyl group.

Anet and Eves (1) described the separation of the crude alkaloid mixture from *Lycopodium annotinum* by countercurrent distribution into a "chloroform-soluble" and a "buffer- (pH 6.0) soluble" fraction. From the former fraction they isolated a new alkaloid, lycodine. In the present paper we report work on the latter fraction, as a result of which four new alkaloids have been isolated and characterized.

The buffer-soluble fraction mentioned above (1) was subjected to 57-transfer countercurrent distribution with the system chloroform–buffer of pH 7.0, with the buffer solution as the moving phase. Weight analysis of the distribution gave the pattern shown in Fig. 1A. Although the alkaloid concentration used was such that overloading resulted, causing changes in the pH of the buffer, the separation obtained was not far from that expected on the basis of a constant distribution coefficient for each alkaloid. The alkaloids in tubes 10 to 42 are at present under investigation, but it may be noted here that acrifoline (2, 3) could be isolated from tubes 26 to 34.

The peak represented by tubes 46 to 57 (Fig. 1A) was too wide to represent a single alkaloid, a conclusion supported by the results of paper chromatography and infrared analysis. Due to the high partition coefficients, however, the various components making up the peak were badly resolved. All the same, tubes 46 to 52 readily yielded a crystalline alkaloid (α-lofoline described below), but only in small yield. In order to improve the separation, the alkaloid contents of tubes 46 to 57 were mixed and subjected to another countercurrent distribution, but this time with the system chloroform–buffer of pH 8.0. The distribution (Fig. 1B) obtained showed three peaks, two of which overlapped.

The tubes 21 to 32 (Fig. 1B) yielded a crystalline alkaloid, and paper chromatography indicated that this was the main component present. The compound obtained had m.p. 211–212°, and its properties were unchanged after chromatography on alumina or after repeated recrystallizations. Analysis gave the formula $C_{18}H_{29}O_3N$ and further showed the presence of one O-acetyl group and at least two C-methyl groups. The infrared spectrum (Fig. 2A) confirmed the presence of an O-acetyl group (bands at 1720 cm^{-1} and at 1225 cm^{-1}, 1240 cm^{-1}) and also indicated the presence of a hydroxyl group (band at 3200 cm^{-1}), thus accounting for all the oxygen atoms. The general properties and formula of this compound do not correspond with any known alkaloid and we therefore propose the name α-lofoline for it. α-Lofoline gave a methiodide, m.p. 266–267°.

Paper chromatography indicated the presence of two alkaloids in tubes 36 to 51 (Fig. 1B) which were not completely resolved in the distribution. It was found best to

[1]*Manuscript received May 19, 1959.*
Contribution from the Department of Chemistry, University of Ottawa, Ottawa, Canada.
[2]*Part I of this series is considered to be the paper entitled "Lycodine, a new alkaloid of Lycopodium annotinum" by F. A. L. Anet and C. R. Eves (see reference 1).*

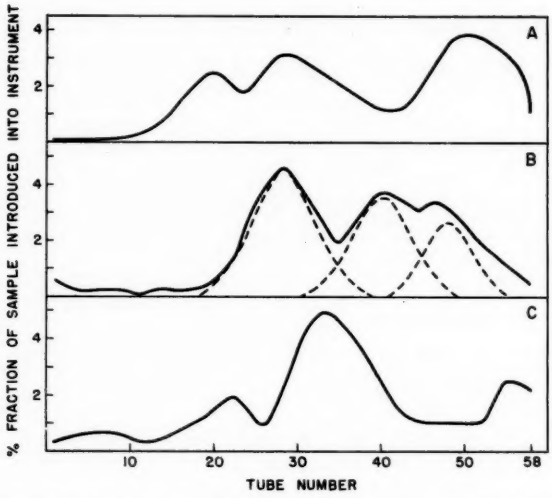

FIG. 1. Countercurrent distribution of various alkaloid fractions mentioned in the text: A, with the system chloroform–buffer of pH 7; B, chloroform–buffer of pH 8.0; C, chloroform–buffer of pH 8.2. In each case the buffer solution is the moving phase. The dotted lines represent theoretical distributions.

mix the contents of all these tubes and to separate the two components by chromatography on alumina. The first alkaloid eluted had, after recrystallization and sublimation, m.p. 156–157°. Analysis gave the formula $C_{16}H_{25}O_2N$ and showed the presence of at least one C-methyl group. The infrared spectrum (Fig. 2B) indicated a hydroxyl group (band at 3400 cm^{-1})and a carbonyl group (band at 1700 cm^{-1}, probably a ketone in a six-membered ring). The properties of this alkaloid showed it to be new, and we propose the name annofoline for it. Annofoline gave a perchlorate, m.p. 234–236°, and a methiodide, m.p. 308–309°.

The second alkaloid eluted from the alumina chromatogram had, after recrystallization, m.p. 144–145°. Analysis indicated the formula $C_{16}H_{25}O_2N$ and the presence of a C-methyl group. The infrared spectrum (Fig. 2C) showed the presence of one or more hydroxyl groups (band at 3300 cm^{-1}), but no carbonyl group. A very faint band at 1670 cm^{-1} may indicate unsaturation. This compound also appeared to be new and we have named it lycofoline. It gave a hydrobromide, m.p. 274–275°, and a methiodide, m.p. 263–264°. In the last few tubes of the distribution (Fig. 1B) there was present a small amount of a compound showing a band at 1740 cm^{-1} (in CCl_4) in the infrared, but no attempt was made to isolate the compound responsible for this absorption.

It was noticed that the distribution shown in Fig. 1A had a pronounced minimum at tube 42. It was already known (1) that alkaloids with a partition coefficient (buffer of pH 5.0 versus chloroform) near unity were not present to any appreciable extent in the crude alkaloid mixture. These facts enabled us to modify our original preliminary separation, which divided the alkaloid into two groups, into one where three groups were obtained. This was done (Fig. 3) without greatly increasing the number of transfers, and without any of the major components of the crude alkaloid mixture occurring in more than one group. The solvent system used was chloroform–buffer of pH 7.0. The buffer-soluble fractions B_1' to B_3' gave after a 60-transfer countercurrent distribution in

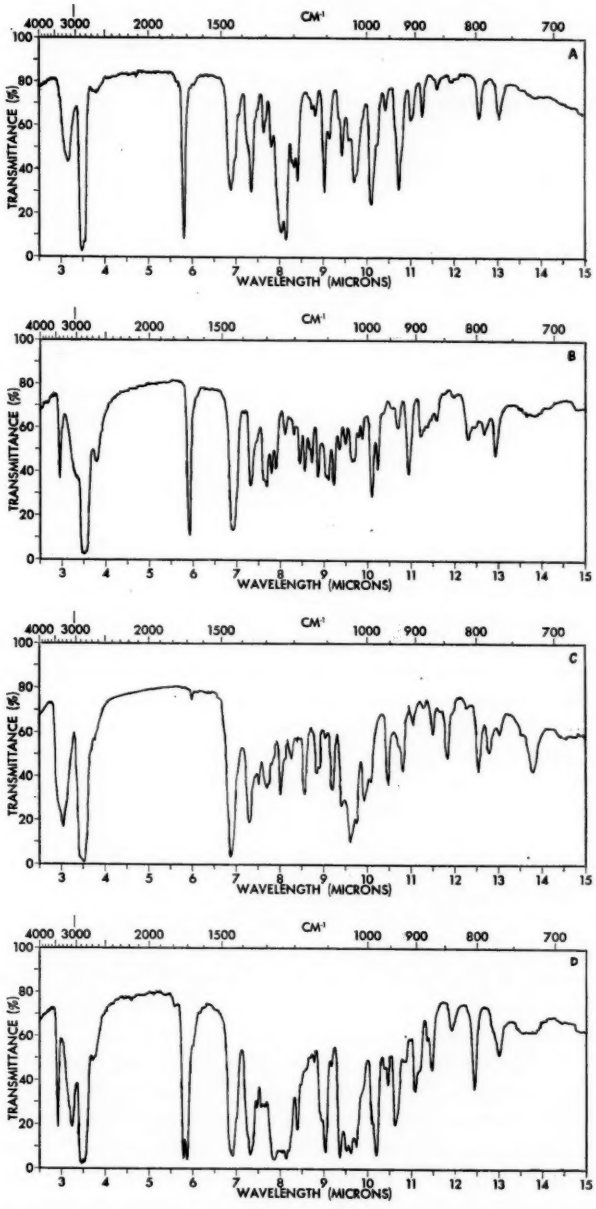

FIG. 2. Infrared absorption spectra in Nujol mull measured on a Perkin–Elmer "Infracord": A, α-lofoline; B, annofoline; C, lycofoline; D, β-lofoline.

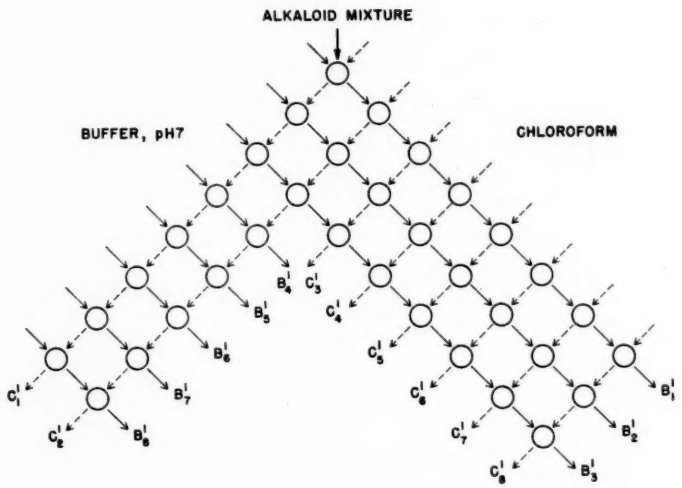

FIG. 3. Modified Bush and Densen extraction pattern. The circles represent phase separation, and the full lines show the advancement of the buffer solutions, and the dotted lines that of the chloroform solutions.

the system chloroform–buffer of pH 8.2 the pattern shown in Fig. 1C. Thus about the same separation was obtained as before but with one 60-transfer countercurrent distribution less.[3]

The distribution pattern of Fig. 1C was somewhat different from that of Fig. 1B. In the first place the peak corresponding to α-lofoline was much less intense in Fig. 1C than in Fig. 1B, and there was a new peak (tubes 52 to 58) in Fig. 1C not present in Fig. 1B. Furthermore, the peak occurring at tubes 16 to 26 contained not only α-lofoline, but also another new alkaloid resembling it closely, and which we have named β-lofoline. The two alkaloids were separated by careful chromatography on alumina. β-Lofoline had m.p. 166–167°, and analysis gave the formula $C_{18}H_{29}O_3N$ and showed the presence of one O-acetyl group and two C-methyl groups. The infrared spectrum (Fig. 2D) indicated a hydroxyl group (free hydroxyl, 3400 cm^{-1}, and bonded hydroxyl, 3100 cm^{-1}) and an O-acetyl group (bands at 1700 cm^{-1}, 1730 cm^{-1} and at 1225 cm^{-1}, 1270 cm^{-}).[1] The splitting of the carbonyl band of the acetyl group is probably related to the fact that there are two hydroxyl frequencies. In carbon tetrachloride solution both α- and β-lofoline showed only one (free) hydroxyl band and one carbonyl band (1720 cm^{-1}); therefore the effect with β-lofoline is not intramolecular. Thus in the crystals of β-lofoline the carbonyl groups of some molecules are not hydrogen-bonded whilst the carbonyl groups of other molecules are intermolecularly hydrogen-bonded. The new peak at tubes 52 to 58 (Fig. 1C) may represent hydrolysis products of α-lofoline and β-lofoline. Preliminary experiments have shown that the hydrolysis products of α- and β-lofoline have the same R_f values and partition coefficients as the alkaloids present in the new peak. This would also explain why the amount of lofolines in the second lot of alkaloid (see Fig. 1C) was less than in the first lot (Fig. 1B).

[3]*The middle fractions (B_4' to B_8' and C_3' to C_8') have been found by Mr. G. Dong in these laboratories to contain the same alkaloids as those present in tubes 10 to 42 of the countercurrent distribution given in Fig. 1A. Also, the chloroform-soluble fractions (C_1' and C_2') have been found by Mr. M. V. Rao to contain all the anno-tinine, lycodine, and lycopodine present in the original mixture.*

The pK_a's, rotations, and other properties of the alkaloids are summarized in Table I. Degradative work on these alkaloids will be reported in a future paper.

TABLE I

New alkaloids isolated from *L. annotinum*

Alkaloid	Formula	M.p.	pK_a in 50% aqueous methanol	$[\alpha]_D$ in ethanol	R_f*	Methiodide, m.p.
α-Lofoline	$C_{18}H_{29}O_3N$	211–212°	9.7	− 52°	0.58	266–267°
β-Lofoline	$C_{18}H_{29}O_3N$	166–167°	9.55	− 6°	0.51	296–297°
Annofoline	$C_{16}H_{25}O_2N$	156–157°	9.15	−131°	0.31	308–309°
Lycofoline	$C_{16}H_{25}O_2N$	144–145°	9.1	− 75°	0.53	263–264°

*Chromatography on Whatman No. 1 paper buffered to pH 7.0 and developed with *n*-butanol saturated with water (see also Experimental).

In a recent paper (4) Achmatowicz and Rodewald described the isolation of some new alkaloids, in the form of their methiodides, from *L. annotinum* of European origin. However, none of these alkaloids seems to correspond with the alkaloids which we have isolated.

EXPERIMENTAL

The infrared spectra, apart from those given in Fig. 2, were measured in carbon tetrachloride solution (1%) in a 1-mm cell on a Perkin–Elmer single-beam double-pass instrument. The paper chromatograms were obtained on Whatman No. 1 paper buffered with the pH mentioned in the text, and developed with butanol saturated with water. The absolute R_f values of the alkaloids varied appreciably, but the relative values were constant. The alkaloidal spots were revealed by spraying with a modified Dragendorff reagent (5). Equivalent weights (E.W.) and pK_a were determined by microtitrations with 0.1 *N* hydrochloric acid in 50% aqueous methanol.

Preliminary Separation of the Crude Alkaloid

The first lot of alkaloid to be investigated was the same as that described (1) previously. The crude alkaloid left after the removal of most of the annotinine by crystallization was partitioned repeatedly between chloroform and a buffer of pH 6 using the extraction scheme of Bush and Densen (6) so as to obtain six chloroform phases and six buffer phases. The alkaloid in the first four buffer phases (B1 to B4 of reference (1)) were combined for the present study and will be referred to as fraction B.

A second lot of alkaloid mother liquors from a different extraction of plant material was also investigated, but was treated differently from the above in view of the results obtained with fraction B.

Countercurrent Distribution with the System Chloroform–Buffer of pH 7.0

Fraction B (8.6 g) was dissolved in chloroform (120 ml) and the solution was placed in the first three tubes of a 60-tube Craig countercurrent distribution apparatus (7) and partitioned between chloroform and citrate–phosphate buffer of pH 7.0. Fifty-seven transfers were made, after which every third tube was analyzed. Aliquots (usually 2 ml) of each phase of a tube were removed, mixed, and made alkaline and the bases extracted with chloroform. The alkaloid left after removal of the solvent was weighed to give the distribution shown in Fig. 1A. The samples obtained from the weight analysis were submitted to paper chromatography (paper buffered at pH 6.0) and their infrared

spectra measured. Whilst α-lofoline could be crystallized from the alkaloid in tubes 46 to 52, the yield was small and it was preferable to separate the alkaloids present in tubes 46 to 57 by another countercurrent distribution.

Countercurrent Distribution with the System Chloroform–Buffer of pH 8.0

The alkaloid was recovered from tubes 46 to 57 in the usual way and submitted to 58 transfers in the above system, the alkaloid being placed in the first two tubes of the apparatus. The tubes were analyzed as described before and the distribution pattern of Fig. 1B was obtained.

Isolation of α-Lofoline

The alkaloid in tubes 21 to 32 of the above distribution was isolated and crystallized from methanol to give thick colorless prisms, m.p. 211–212°. To obtain a good yield it was found desirable to chromatograph the mother liquors on alumina, using successively benzene, benzene–chloroform, and chloroform as the eluants. α-Lofoline was very soluble in methanol and chloroform but sparingly soluble in ether or petroleum ether. The alkaloid was best recrystallized from benzene, and was sublimed (120–130° at 0.05 mm) for analysis. Calc. for $C_{18}H_{29}O_3N$: C, 70.32; H, 9.51; N, 4.56; 2C—CH_3, 9.8; O—$COCH_3$, 14.0%; M.W., 307.4. Found: C, 70.56, 70.56; H, 9.54, 9.54; N, 4.63; C—CH_3, 10.60; O—$COCH_3$, 14.21%; M.W. (Rast), 291, 312; E.W., 310, 310; pK_a, 9.7, 9.7; $[\alpha]_D$ −52° (*c*, 2.0 in ethanol).

α-Lofoline Methiodide

α-Lofoline (20 mg) was dissolved in a mixture of methanol (1 ml) and methyl iodide (0.5 ml) and the mixture was refluxed for 10 minutes. The solvent was removed by evaporation and the methiodide was crystallized from methanol–acetone. Yield, 16 mg, m.p. 266–267°. Calc. for $C_{18}H_{29}O_3N.CH_3I$: C, 50.78; H, 7.18; I, 28.24%. Found: C, 51.08; H, 7.04; I, 28.04%.

Isolation of Annofoline

The alkaloid in tubes 36 to 41 of the above distribution (with the buffer of pH 8) was isolated and crystallized from methanol–ether, but the m.p. was 115–130°. Three recrystallizations raised the m.p. to 148–150° and this changed to 156–157° after sublimation (120–130° at 0.05 mm). It was found that a much better yield of pure annofoline could be obtained by chromatography on alumina of the contents of tubes 36 to 51. Elution with benzene–chloroform gave annofoline, whilst elution with chloroform gave lycofoline (see below). Annofoline had similar solubilities to α-lofoline, and when its solution in carbon tetrachloride (but not chloroform) was allowed to evaporate in the presence of air, an intense orange-yellow residue was left. This test was not given by α- or β-lofoline but lycofoline gave a crimson-red color. For analysis a sublimed sample was used. Calc. for $C_{16}H_{25}O_2N$: C, 72.96; H, 9.57; N, 5.32; C—CH_3, 5.96%; M.W., 263.4. Found: C, 72.85, 73.05; H, 9.51, 9.59; N, 4.91; C—CH_3, 6.91%; M.W. (Rast), 270, 283; E.W., 259, 267; pK_a, 9.1, 9.2; $[\alpha]_D$ −131° (*c*, 2.0 in ethanol).

Annofoline Methiodide

The methiodide of annofoline crystallized on addition of methyl iodide (0.8 ml) to a solution of the alkaloid (60 mg) in acetone (2 ml). The mixture was refluxed for 5 minutes, cooled, and the methiodide collected. It was recrystallized from water, m.p. 308–309°. Yield, 40 mg. Calc. for $C_{16}H_{25}O_2N.CH_3I$: C, 50.37; H, 6.94; I, 31.31%. Found: C, 50.30; H, 6.70; I, 31.50%.

Annofoline Perchlorate

A methanolic solution of perchloric acid was added to a solution of the alkaloid in methanol until a slight excess was present. Ether was added to the solution and the perchlorate crystallized on scratching. After recrystallization from methanol–ether it melted at 234–236°. Calc. for $C_{16}H_{25}O_2N.HClO_4.H_2O$: C, 50.30; H, 7.65%. Found: C, 50.08; H, 7.35%.

Isolation of Lycofoline

The alkaloid in tubes 42 to 51 of the above distribution (with the buffer of pH 8.0) was isolated and converted into the hydrobromide by the addition of concentrated hydrobromic acid to the methanolic solution of the alkaloid. Addition of ether gave a crystalline salt, which after three crystallizations from methanol–ether was converted to the base. The base was sublimed (110–130° at 0.05 mm) and then crystallized from ether. Lycofoline was obtained as prisms, m.p. 144–145°. For analysis it was sublimed *in vacuo*, m.p. unchanged. Calc. for $C_{16}H_{25}O_2N$: C, 72.96; H, 9.57; N, 5.32; C—CH_3, 5.69%; M.W., 263.4. Found: C, 72.77, 72.66; H, 9.51, 9.59; N, 5.11; C—CH_3, 4.96%; M.W. (Rast), 239; E.W., 264, 267; pK_a, 9.05, 9.1; $[\alpha]_D$ −75° (*c*, 2.0 in ethanol). A better yield of lycofoline was obtained by chromatography of the mixture of annofoline and lycofoline as described in the procedure for the isolation of annofoline.

Lycofoline Hydrobromide

For analysis the hydrobromide was recrystallized from methanol–ether and dried at 117° *in vacuo*, m.p. 274–275°. Calc. for $C_{16}H_{25}O_2N.HBr$: C, 56.05; H, 7.61%. Found: C, 55.64, 55.68; H, 7.55, 7.42%.

Lycofoline Methiodide

Lycofoline (34 mg) was dissolved in methanol (1.5 ml) and the solution was refluxed for 10 minutes with methyl iodide (0.5 ml). The solvent was removed and the methiodide was crystallized from methanol. Yield, 15 mg, m.p. 263–264°. Calc. for $C_{16}H_{25}O_2N.CH_3I$: C, 50.37; H, 6.94; I, 31.31%. Found: C, 50.65; H, 6.99; I, 31.58%.

Improved Separation of Crude Alkaloid

A second batch of crude alkaloid (after removal of the annotinine) (60 g) was partitioned between chloroform and a citrate–phosphate buffer of pH 7.0 using the modified Bush and Densen extraction pattern of Fig. 3. The extractions were carried out with 1 liter of each phase. The fractions B_1' to B_3' were combined and the alkaloid extracted in the usual way. The mixture (20 g) so obtained was divided into three equal lots, and each was subjected to a 60-tube countercurrent distribution with the solvent system chloroform and boric acid – sodium hydroxide buffer of pH 8.2. The distribution pattern given in Fig. 1C was obtained.

Isolation of β-Lofoline

Annofoline and lycofoline were isolated from tubes 28 to 43 and were separated as described above by chromatography on alumina. Tubes 16 to 26, however, did not give α-lofoline in pure state easily. Indeed, paper chromatography (paper buffered at pH 7.0) showed two spots of very similar R_f values (0.58, 0.51). The mixture was therefore chromatographed on alumina. Elution with benzene, benzene–chloroform, and chloroform gave first β-lofoline, followed by α-lofoline. The β-lofoline was crystallized from methanol–ether, m.p. 160–166°, raised to 166–167° after two recrystallizations from ether. For analysis a sample was sublimed (120–130° at 0.05 mm). Calc. for $C_{18}H_{29}O_3N$: C, 70.32; H, 9.51; N, 4.56; 2C—CH_3, 9.8; O—$COCH_3$, 14.00%; M.W., 307.4. Found: C, 70.18,

70.14; H, 9.45, 9.69; N, 4.84; C—CH_3, 8.83; O—$COCH_3$, 15.6%; M.W. (Rast), 322; E.W., 311; pK_a, 9.55; $[\alpha]_D$ −6° (*c*, 2.0 in ethanol).

β-Lofoline Methiodide

To a solution of the alkaloid (20 mg) in methanol (2 ml), methyl iodide (0.5 ml) was added, and the mixture was refluxed for 10 minutes. The solvent was removed and the methiodide was crystallized from methanol. Yield, 10 mg, m.p. 296–297° (decomp.). Calc. for $C_{18}H_{29}O_3N.CH_3I$: C, 50.78; H, 7.18%. Found: C, 50.90; H, 6.80%.

ACKNOWLEDGMENTS

The authors thank Dr. Léo Marion for providing the mother liquors from the crystallization of annotinine. One of us (N. H. K.) wishes to thank the Colombo Plan authorities for the award of a scholarship and the Pakistan Council of Scientific and Industrial Research for financial support.

REFERENCES

1. Anet, F. A. L. and Eves, C. R. Can. J. Chem. **36**, 902 (1958).
2. Manske, R. H. F. and Marion, L. J. Am. Chem. Soc. **69**, 2126 (1947).
3. Perry, G. S. and MacLean, D. B. Can. J. Chem. **34**, 1189 (1956).
4. Achmatowicz, O. and Rodewald, W. Roczniki Chem. **32**, 485 (1958).
5. Munier, R. and Macheboeuf, M. Bull. soc. chim. biol. **33**, 846 (1951).
6. Bush, M. T. and Densen, P. M. Anal. Chem. **20**, 121 (1948).
7. Craig, L. C. and Post, O. Anal. Chem. **21**, 500 (1949).

SYNTHESIS OF 2,4-THIAZOLIDINEDIONE-2-AZINES AND 2,4-THIAZOLIDINEDIONE-2-DIMETHYLHYDRAZONES FROM THIOCYANOESTERS AND HYDRAZINES[1]

PAUL E. GAGNON, JEAN-L. BOIVIN,[2] AND GORDON M. BROWN[3]

ABSTRACT

Thiocyanoesters were prepared from 2-bromoesters and potassium thiocyanate, and a series of substituted thiazolidinedione-2-azines was obtained from these thiocyanoesters using hydrazine hydrate. The structure of the thiazolidinedione-2-azines was determined by hydrolysis using hydrochloric acid in ethanol. The reaction of thiocyanoesters with dimethylhydrazine, generally speaking, was analogous to their reaction with hydrazine, but there were many differences. Only 1 mole of alcohol was eliminated rather than 2, and there was no apparent reaction for the ethyl 2-thiocyanononanoate and the methyl phenylthiocyanoacetate. Furthermore, the reaction of methyl 2-thiocyanoisobutyrate with dimethylhydrazine did not give a 2,4-thiazolidinedione-2-dimethylhydrazone but rather an addition product, *N*-dimethylamino-*S*-(1-methyl-1-carbomethoxy) ethylisothiourea. To illustrate the reactivity of the thiocyano group, benzyl thiocyanate was treated with hydrazine and the product was found to be dibenzyldisulphide, and ammonia was evolved. Similarly, trimethylene dithiocyanate gave the dimer of trimethylene disulphide. Finally, benzyl thiocyanate formed an addition product with dimethylhydrazine which was *N*-dimethylamino-*S*-benzylthiourea.

INTRODUCTION

Ethyl thiocyanoacetate, which was prepared for the first time by Heintz (1) from ethyl chloroacetate and potassium thiocyanate, contains an active methylene group and, consequently, is structurally similar to ethyl cyanoacetate which is easily alkylated in the presence of a catalyst. Thus for a time it was considered that a series of thiocyanoesters might be prepared from ethyl thiocyanoacetate itself. However, Claesson (2) discovered that if ethyl thiocyanoacetate was treated with ethyl bromide, the products were ethyl thiocyanate and ethyl bromoacetate.

$$C_2H_5Br + NCSCH_2COOC_2H_5 \rightarrow C_2H_5SCN + BrCH_2COOC_2H_5$$

Therefore, the thiocyanoesters had to be synthesized from the corresponding 2-bromoesters which, in turn, were obtained by esterification of the bromoacids.

$$RCH_2COOH \rightarrow RCHBrCOOH \rightarrow RCHBrCOOR' \rightarrow RCH(SCN)COOR'$$

In 1910, Frerichs and Förster (3) reported that when an aqueous solution of hydrazine hydrate was shaken with ethyl thiocyanoacetate, an exothermic reaction ensued producing a precipitate which was insoluble in all common solvents. The analysis suggested the formula $C_6H_6N_4O_2S_2$. This compound decomposed without melting and was assigned the structure of 3,3-bis-pseudothiohydantoin.

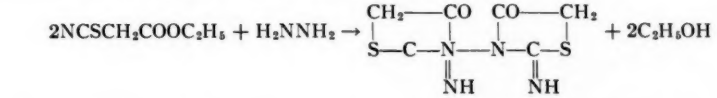

The authors also claimed that the above compound was obtained from hydrazodithiodicarbonamide and chloroacetic acid in aqueous solution.

[1]*Manuscript received May 1, 1959.*
Contribution from the Department of Chemistry, Laval University, Quebec, Que. This paper constitutes part of a thesis submitted to the Graduate School, Laval University, in partial fulfillment of the requirements for the degree of Doctor of Science.
[2]*Canadian Armament Research and Development Establishment, Valcartier, Quebec.*
[3]*Graduate student, holder of National Research Council of Canada Studentships in 1957–59.*

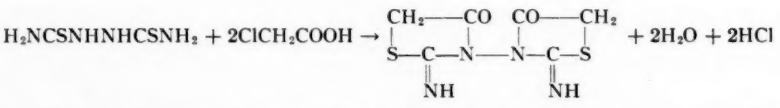

Some years later, Stephen and Wilson (4) investigated the reaction between hydrazodithiodicarbonamide and ethyl chloroacetate. They established the structure of the product by treating it with boiling concentrated hydrochloric acid in which it gradually dissolved. After evaporation, the solid obtained was extracted with hot chloroform, giving 2,4-thiazolidinedione identified by a mixed melting point with an authentic sample. The residue, after the extraction, was proved to be hydrazine hydrochloride. From the two hydrolysis products, then, it is obvious that the original compound obtained from hydrazodithiodicarbonamide and ethyl chloroacetate was 2,4-thiazolidinedione-2-azine.

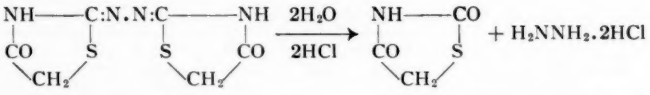

Stephen and Wilson claimed that the compound prepared by Frerichs and Förster gave the same products when boiled with concentrated hydrochloric acid. The compound of which they spoke was prepared from hydrazodithiodicarbonamide and chloroacetic acid; no mention was made of the reaction between ethyl thiocyanoacetate and hydrazine hydrate.

In 1913, Frerichs and Höller (5) studied the reactions of hydrazodithiodicarbonamide with haloacids, specifically 2-bromopropionic and 2-bromobutyric acids. The compounds obtained were regarded as substituted 3,3-bis-pseudothiohydantoins. The melting points reported by Frerichs and Höller were not sharp, which leads one to believe that difficulties in purification were encountered.

Stephen and Wilson (6) also undertook the preparation of the same compounds by the method of Frerichs and obtained from hydrazodithiodicarbonamide and 2-bromopropionic acid a solid melting at 289° C which, on hydrolysis with concentrated hydrochloric acid, gave rise to the known 5-methyl-2,4-thiazolidinedione. Similarly, the compound obtained from hydrazodithiodicarbonamide and 2-bromobutyric acid melting at 233° C gave on acid hydrolysis the known 5-ethyl-2,4-thiazolidinedione. The structure of these two compounds must be, therefore, 5-methyl- and 5-ethyl-2,4-thiazolidinedione-2-azine, respectively.

RESULTS AND DISCUSSION

Thiocyanoesters

The thiocyanoesters were prepared from the corresponding bromoesters using a 50% excess of potassium thiocyanate as recommended by Allen (7). Generally speaking, 80% alcohol was used for the lower members, and as the chain length increased to seven and eight carbons 90% alcohol was employed since the latter were not completely miscible with 80% alcohol.

The methyl phenylthiocyanoacetate was not synthesized using the sequence of reactions followed for alkyl thiocyanoacetates. Direct bromination of phenyl acetic acid puts the bromine in the ring, not in the side chain, even when no catalyst is used (8). To prepare the desired ester, then, mandelic acid was employed as the starting material. Esterification by the method of Clinton and Laskowski (9) gave the corresponding methyl

ester in good yield. The methyl phenylchloroacetate was then prepared by treatment of the mandelate with thionyl chloride in accordance with the procedure given by McKenzie and Barrow (10), and the phenylthiocyanoacetate was obtained directly from the above compound by the usual method.

It was noted that the inductive effect played a very important part in the time required to form the thiocyanoesters. In the case of ethyl chloroacetate, both the chlorine atom and the carbethoxy group are electron attracting, leaving the alpha carbon atom with a residual positive charge which attracted the attacking thiocyanate ion. The substitution, therefore, took place quite rapidly. The alpha carbon atom, in the case of alkyl-substituted thiocyanoesters, is more negatively charged than in the non-substituted ester, due to the fact that alkyl groups are electron repelling, and so the attacking thiocyanate ion approaches less rapidly as is seen by the reflux time necessary for the completion of the reaction.

The methyl 2-thiocyanoisobutyrate and the methyl 2-thiocyanoisovalerate required a much longer period of heating, due to the electron repulsion of the two methyl groups toward the same carbon atom. The approach of the negatively charged thiocyanate ion is greatly hindered by the strongly negative charges on the second carbon atom. True to the electronic theory that the inductive effect dies out after one methylene group, the preparation of methyl 2-thiocyanoisohexanoate was performed easily. In spite of the repulsion of the methyl groups, the site of the perturbation was too far removed from the second carbon atom to hinder the replacement of the bromine atom, and no extra time was required in the preparation of the above-mentioned ester. The phenylthiocyanoacetate required but a small reflux period due to the fact that the phenyl group is electron attracting, leaving the alpha carbon atom with a net positive charge and facilitating greatly the approach of the attacking thiocyanate ion.

2,4-Thiazolidinedione-2-azines

A method of improving the yields was devised for the azines by finding a suitable solvent. Methanol was finally selected as the medium in spite of the fact that it itself is a by-product of the reaction and thus tends to set up an equilibrium. If the addition of the reagent was not performed with care, the reaction mixture boiled; however, by introducing a dropwise solution of hydrazine hydrate in methanol, the temperature did not become too great and solid products were obtained.

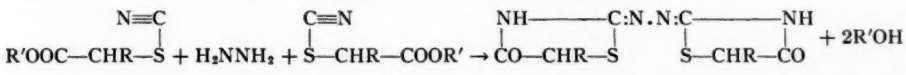

The structure was established by boiling these compounds with concentrated hydrochloric acid in ethanol (11). Substituted 2,4-thiazolidines were obtained and their melting points compared favorably with those reported in the literature. The second product of hydrolysis was identified as hydrazine hydrochloride, thus establishing without a doubt the structure of the compounds being hydrolyzed as 2,4-thiazolidinedione-2-azines.

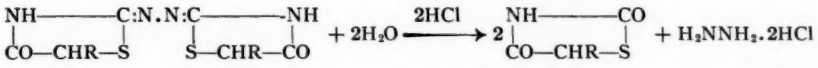

The above results prove conclusively that thiocyanoacetates and hydrazine hydrate give the same azines as hydrazodithiodicarbonamide and 2-haloacetic acids.

2,4-Thiazolidinedione-2-dimethylhydrazones

If dimethylhydrazine and thiocyanoesters, which were mutually soluble, were mixed without a solvent, the reaction, which was endothermic at the time of the addition, after a few minutes became uncontrollably exothermic with charring of the reaction mixture. It was found that for the preparation of lower molecular weight members of this series, formamide was an excellent solvent as the product was insoluble and precipitated out when the mixture was left to stand overnight.

$$RCH(SCN)COOR' + (CH_3)_2NNH_2 \rightarrow \begin{matrix} NH\text{———}C{:}N.N(CH_3)_2 \\ | \qquad\quad | \\ CO\text{—}CHR\text{—}S \end{matrix} + R'OH$$

The reaction mixture generally darkened to amber, but the reactions themselves were not exothermic, except in the case of ethyl thiocyanoacetate, which was moderately so.

Unfortunately, the complete series of thiocyanoesters was not soluble in formamide and another solvent had to be found for those of higher molecular weight. If the reaction between dimethylhydrazine and methyl 2-thiocyanohexanoate was performed using nitrobenzene as the solvent, a solid product was obtained which separated out when the mixture was left to stand overnight. No exothermic reaction was observed and the mixture darkened only slightly to yellow. The yield obtained by this method was almost the same as that obtained by using formamide. Another solvent employed was *o*-nitroanisole which gave results similar to those obtained by nitrobenzene. To determine the structure of these compounds, they were hydrolyzed with hydrochloric acid in ethanol and two products were obtained, the known 2,4-thiazolidinediones and dimethylhydrazine hydrochloride.

$$\begin{matrix} NH\text{———}C{:}N.N(CH_3)_2 \\ | \qquad\quad | \\ CO\text{—}CHR\text{—}S \end{matrix} + H_2O + HCl \rightarrow \begin{matrix} NH\text{———}CO \\ | \qquad\quad | \\ CO\text{—}CHR\text{—}S \end{matrix} + (CH_3)_2NNH_2.HCl$$

There was no apparent reaction when ethyl 2-thiocyanononanoate and methyl phenylthiocyanoacetate were treated with 1,1-dimethylhydrazine. The lack of reaction on the part of the thiocyanononanoate is not easily explained. The fact that it is an ethyl ester rather than a methyl ester might have some effect on the cyclization but could scarcely inhibit the addition of the hydrazine to the thiocyano group. Since no product was obtained, even when the solution was cooled strongly, it must be concluded that the addition did not occur which could possibly be explained by steric hindrance. Perhaps the coiled heptyl chain blocks the thiocyanate group from the attacking hydrazine. The absence of reaction of the phenylthiocyanoacetate can be theoretically explained. The triple bond in methyl phenylthiocyanoacetate is less polar than in the alkyl-substituted thiocyanoacetates, as the phenyl group is electron attracting.

In the reaction between methyl 2-thiocyanoisobutyrate and 1,1-dimethylhydrazine using the same conditions as before, it was found that the product had a much lower melting point than expected. This posed a problem until it was found that the substance was water soluble and all the 2,4-thiazolidinedione-2-dimethylhydrazones were insoluble in water. It was suspected then that the reaction between dimethylhydrazine and methyl 2-thiocyanoisobutyrate consisted of a simple addition which was confirmed by analysis. No coloration was obtained upon treatment with ferric chloride. The fact that no cyclization occurred must be due to the effect of the two methyl groups on the second carbon atom.

Disulphides

When benzyl thiocyanate was treated with hydrazine hydrate in ethanol at reflux temperature, the product was found to be dibenzyldisulphide.

$$2C_6H_5CH_2SCN + 4H_2NNH_2.H_2O \rightarrow C_6H_5CH_2SSCH_2C_6H_5 + 8NH_3 + \underset{\downarrow}{(HN{=}CH{-}N{=}N{-}CH{=}NH)} + N_2 + 2CO_2$$

The same product was formed when the reaction was carried out at room temperature although, due to occlusion of the solvent which had deepened in color to dark red, the product was not as pure. However, the yields obtained at room temperature are greater than at the reflux temperature of ethanol.

The reaction at room temperature was very interesting since certain effects were discovered which had escaped notice at the higher temperature. A strong smell of ammonia was produced, and a small amount of precipitate was obtained which contained no sulphur. This compound was suspected to contain a guanidine function and accordingly benzaldehyde and cinnamaldehyde derivatives were prepared. However, the melting points of the condensation products did not correspond with the melting points of the mono-, di-, or tri-amino/guanidine derivatives reported in the literature (12, 13). It was not possible, then, to establish the identity of this by-product.

Also trimethylene dithiocyanate was treated with hydrazine hydrate in ethanol at room temperature. A solid separated out almost immediately, which on being subjected to qualitative test showed the absence of nitrogen. Its melting point was similar to that of a compound described by Hagelberg (14), who prepared it by the treatment of trimethylene dithiocyanate with potassium hydroxide.

$$NCS(CH_2)_3SCH + 2KOH \rightarrow (CH_2)_3S_2 + KCN + KOCN + H_2O$$

However, he was not certain whether it was the simple trimethylene disulphide that was formed or its dimer. Therefore, a molecular weight determination was made using the method of Rast (15), and calculations proved that indeed the dimer hexamethylene tetrasulphide had been formed.

Isothioureas

Benzyl thiocyanate was also treated with 1,1-dimethylhydrazine. The reaction was performed at room temperature in ether, and the product started to separate almost immediately as a viscous liquid which crystallized upon standing. The suspected *N*-dimethylamino-*S*-benzylisothiourea was soluble in water as expected and the analysis was correct for $C_{10}H_{15}N_3S$.

$$C_6H_5CH_2SCN + (CH_3)_2NNH_2 \rightarrow C_6H_5CH_2SC(=NH)NHN(CH_3)_2$$

However, upon treatment of an aqueous solution of the compound with ferric chloride, a blood-red coloration was obtained, characteristic of thiocyanate ion. In addition, aqueous mercurous nitrate gave a grey precipitate of mercury, also indicative of a thiocyanate.

When the substance was dissolved in ethylene chloride and treated with concentrated sulphuric acid, a solid separated out which, according to analysis results, was the sulphate salt of 1,1-dimethyl-2-benzylhydrazine, $C_6H_5CH_2NHN(CH_3)_2.H_2SO_4$. At the same time, these results definitely eliminated the possibility of the product being a sulphate salt of the isothiourea mentioned above.

It is obvious that a rearrangement has occurred, perhaps due to the acidic medium induced by the sulphuric acid, or else by the basicity of the original mixture of benzyl

thiocyanate and dimethylhydrazine, in which case the product $C_{10}H_{15}N_3S$ must be the thiocyanic acid salt of 1,1-dimethyl-2-benzylhydrazine. If, however, the rearrangement is brought about by hydrogen ions, then treatment of the isothiourea with ferric chloride and mercurous nitrate, both of which are acidic in aqueous solution, could still conceivably give a positive test for thiocyanate ion.

The addition product obtained from dimethylhydrazine and methyl 2-thiocyanoisobutyrate gave no red coloration when treated with ferric chloride; therefore it must be an isothiourea derivative, and one would suspect the formation of a similar type of compound from the analogous reaction under discussion.

EXPERIMENTAL

2-Bromoacids

The 2-bromoacids were obtained by treatment of aliphatic fatty acids with dry bromine in the presence of phosphorus trichloride, according to the procedures of Clarke and Taylor (16) and of Marvel (17), although the conditions varied slightly from those suggested by the above authors in that, in general, the reactions were performed at lower temperatures for longer periods of time.

Methyl 2-Bromoesters

The esters were synthesized from the bromoacids by the method of Clinton and Laskowski (9). The following preparation is representative.

Methyl 2-bromoheptanoate.—2-Bromoheptanoic acid (150 g, 0.72 mole), methanol (70 g, 2.2 moles), ethylene chloride (250 ml), and concentrated sulphuric acid (3 ml) were heated under reflux for 11 hours and diluted with water. The organic layer was washed with carbonate solution and water and dried over sodium sulphate. After removal of the solvent, the ester was distilled, b.p. 87–88° C/6 mm, n_D^{25} 1.4531. Yield, 117 g (73%). Calc. for $C_8H_{15}BrO_2$: C, 43.06; H, 6.79; Br, 35.82%. Found: C, 43.18; H, 6.70; Br, 35.72%.

Methyl 2-bromoöctanoate.—This ester was obtained in the same manner, b.p. 105° C/7 mm, n_D^{25} 1.4544. Calc. for $C_9H_{17}BrO_2$: C, 45.57; H, 7.24; Br, 33.70%. Found: C, 45.86; H, 7.07; Br, 33.78%.

2-Thiocyanoesters

The bromoesters (or in the case of ethyl thiocyanoacetate and methyl phenylthiocyanoacetate, the chloroesters) were transformed into the corresponding thiocyanocompounds by the action of potassium thiocyanate in aqueous alcohol. The particulars are given in Table I.

2,4-Thiazolidinedione-2-azines

When thiocyanoesters were treated dropwise at room temperature with a solution of hydrazine hydrate in alcohol, a precipitate was produced after the whole had been left to stand overnight. The properties of the azines are recorded in Table II.

Hydrolysis of the azines.—5-Ethyl-2,4-thiazolidinedione-2-azine (1 g) was heated under reflux for 18 hours with concentrated hydrochloric acid (40 ml) and ethanol (80 ml). After the solution was evaporated to dryness, the solid was extracted several times with boiling benzene. When the benzene solution was concentrated to small volume and cooled, crystals were obtained, which upon recrystallization from benzene ligroine (2:1) melted at 64–66° C (6). The residue was dissolved in a small quantity of water and buffered with a slight excess of sodium acetate. Upon the addition of a solution of benzaldehyde in ethanol, a yellow precipitate of benzalazine was obtained, m.p. 91–93° C (18).

TABLE I

Thiocyanoesters, $R_1R_2C(SCN)COOR_3$

R_1	R_2	R_3	Time of reflux, hours	Medium	B.p. °C	B.p. mm	Yield, %	Refract. index, 25° C	Formula	Analysis: Calculated C	Calculated H	Calculated N	Found C	Found H	Found N
H	H	C_2H_5	2	80% ethanol	113–115	11.5	67	1.4677	$C_6H_7NO_2S$	*					
CH_3	H	CH_3	5	90% methanol	108–109	19	55	1.4707	$C_5H_7NO_2S$	†					
C_2H_5	H	CH_3	8	80% methanol	114–117	16	76	1.4676	$C_6H_9NO_2S$	†					
CH_3	CH_3	CH_3	10	80% methanol	88–89	9	75	1.4624	$C_6H_9NO_2S$	†					
C_3H_7	H	CH_3	6	80% methanol	114	7	70	1.4666	$C_7H_{11}NO_2S$	48.52	6.41	8.09	48.71	6.42	8.31
i-C_3H_7	H	CH_3	12	80% methanol	109	11	68	1.4674	$C_7H_{11}NO_2S$	†					
C_4H_9	H	CH_3	6	80% methanol	119–120	7	74	1.4663	$C_8H_{13}NO_2S$	51.30	7.01	7.48	51.63	6.72	7.66
i-C_4H_9	H	CH_3	7	80% methanol	115	8	68	1.4660	$C_8H_{13}NO_2S$	51.30	7.01	7.48	51.61	6.81	7.52
C_5H_{11}	H	CH_3	6	90% methanol	133–134	7	61	1.4667	$C_9H_{15}NO_2S$	53.69	7.53	6.96	53.93	7.55	6.90
C_6H_{13}	H	CH_3	6	90% methanol	143	6	67	1.4665	$C_{10}H_{17}NO_2S$	55.77	7.97	6.51	56.08	8.09	6.67
C_7H_{15}	H	C_2H_5	6	80% ethanol	164	6	75	1.4617	$C_{12}H_{21}NO_2S$	59.21	8.71	5.76	58.71	8.65	6.18
C_6H_5	H	CH_3	3	80% methanol	176	8.5	73	1.5514	$C_{10}H_9NO_2S$	57.94	4.39	6.76	57.54	4.39	7.10

*Ruhemann, S. J. Chem. Soc. **95**, 119 (1909).

†Wheeler, H. L. and Barnes, B. J. Am. Chem. Soc. **24**, 60 (1900).

TABLE II

2,4-Thiazolidinedione-2-azines, NH———C:N.N:C———NH
CO—CRR′—S S—CRR′—CO

R	R′	Reaction time, days	Solvent	M.p., °C	Yield, %	Formula	Analysis					
							Calculated			Found		
							C	H	N	C	H	N
H	H	4	Dioxane	Dec.	40	$C_6H_6N_4O_2S_2$	*					
CH_3	H	7	Dioxane	285–286	39	$C_8H_{10}N_4O_2S_2$	37.19	3.91	21.69	37.14	4.11	21.90
C_2H_5	H	14	80% dioxane	235–236	38	$C_{10}H_{14}N_4O_2S_2$	41.93	4.94	19.57	42.30	5.26	19.14
CH_3	CH_3	14	80% dioxane	342	41	$C_{10}H_{14}N_4O_2S_2$	41.93	4.94	19.57	42.41	4.96	19.39
C_3H_7	H	7	Methanol	246.5–247.5	45	$C_{12}H_{18}N_4O_2S_2$	45.83	5.78	17.82	45.78	5.82	17.73
i-C_3H_7	H	4	80% dioxane	291	54	$C_{12}H_{18}N_4O_2S_2$	45.83	5.78	17.82	46.08	5.94	17.52
C_4H_9	H	12	Methanol	233–234	38	$C_{14}H_{22}N_4O_2S_2$	49.09	6.49	16.36	49.35	6.31	16.85
i-C_4H_9	H	5	80% dioxane	274–275	39	$C_{14}H_{22}N_4O_2S_2$	49.09	6.49	16.36	49.08	6.47	16.57
C_5H_{11}	H	14	Methanol	217.5–218.5	42	$C_{16}H_{26}N_4O_2S_2$	51.86	7.09	15.12	52.31	7.19	14.81
C_6H_{13}	H	16	Methanol	218–220	28	$C_{18}H_{30}N_4O_2S_2$	54.23	7.60	14.06	54.24	7.46	13.93
C_7H_{15}	H	5	Methanol	223–224	34	$C_{20}H_{34}N_4O_2S_2$	56.29	8.05	13.13	56.00	8.05	13.01
C_6H_5	H	6	80% dioxane	307–307.5	26	$C_{18}H_{14}N_4O_2S_2$	56.52	3.70	14.65	56.07	3.98	14.06

*Frerichs, G. and Förster, P. Ann. **371**, 227 (1910).

TABLE III

2,4-Thiazolidinedione-2-dimethylhydrazones, $\begin{matrix} NH\text{———}C{:}N.N(CH_3)_2 \\ | \qquad\qquad | \\ CO\text{—}CHR\text{—}S \end{matrix}$

R	Reaction time, days	Medium	Solvent	M.p., ° C	Yield, %	Formula	Analysis					
							Calculated			Found		
							C	H	N	C	H	N
H	5	$HCONH_2$	Ethanol	199–201	21	$C_6H_9N_3OS$	37.71	5.71	26.40	37.74	5.83	26.21
CH_3	3	$HCONH_2$	Ethanol	178–180	34	$C_8H_{11}N_3OS$	41.59	6.41	24.26	41.64	6.39	24.28
C_2H_5	3	$HCONH_2$	60% methanol	158–159	35	$C_7H_{13}N_3OS$	44.89	7.01	22.44	44.93	7.01	22.24
C_3H_7	3	$HCONH_2$	60% methanol	147–148	32	$C_8H_{15}N_3OS$	47.73	7.53	20.88	47.76	7.55	20.68
i-C_3H_7	4	$C_6H_5NO_2$	70% methanol	174–177	45	$C_8H_{15}N_3OS$	47.73	7.53	20.88	47.68	7.53	21.03
C_4H_9	4	$C_6H_5NO_2$	60% methanol	138.5–139.5	39	$C_9H_{17}N_3OS$	50.19	7.97	19.52	50.15	7.93	19.79
i-C_4H_9	7	$C_6H_5NO_2$	60% methanol	166.5–168	39	$C_9H_{17}N_3OS$	50.19	7.97	19.52	50.35	7.84	19.74
C_5H_{11}	7	$C_6H_5NO_2$	70% methanol	116–117	34	$C_{10}H_{19}N_3OS$	52.35	8.36	18.32	52.46	8.33	18.07
C_6H_{13}	7	$C_6H_5NO_2$	70% methanol	118–119	34	$C_{11}H_{21}N_3OS$	54.27	8.71	17.27	54.26	8.60	17.02

2,4-Thiazolidinedione-2-dimethylhydrazones

When thiocyanoesters were treated with 1,1-dimethylhydrazine in a suitable solvent at room temperature, solids separated out after the whole had been left to stand overnight. No special precautions were required in the additions. The dimethylhydrazones prepared in this manner are listed in Table III.

Hydrolysis of the dimethylhydrazones.—5-Ethyl-2,4-thiazolidinedione-2-dimethylhydrazone (2 g) was treated with ethanol (80 ml) and concentrated hydrochloric acid (40 ml) at reflux temperature for 12 hours and the resulting solution was evaporated to dryness. After the benzene solution was extracted thoroughly with boiling benzene and concentrated to small bulk, the residue was left to stand in the refrigerator where crystals of 5-ethyl-2,4-thiazolidinedione were obtained, m.p. 63–64° C. The fraction insoluble in benzene was dissolved in water, a little sodium acetate was added, and this solution was treated with *m*-nitrobenzaldehyde in ethanol. After the solution was heated for a few minutes on a hot plate, a cloudiness developed, and solidification occurred when it was left to stand in the cold. The *m*-nitrobenzaldehyde dimethylhydrazone so formed caused no depression in the melting point of an authentic sample of this material, prepared as follows: *m*-Nitrobenzaldehyde dissolved in a small quantity of warm ethanol was treated with an excess of 1,1-dimethylhydrazine and two drops of glacial acetic acid. The solution was heated on a hot plate until little solvent remained, whereupon it was allowed to cool and the residue crystallized, m.p. 57–58° C. The compound was recrystallized from methanol, leaving the melting point unchanged. Calc. for $C_9H_{11}N_3O_2$: N, 21.75%. Found: N, 21.58%.

N-Dimethylamino-S-(1-methyl-1-carbomethoxy) Ethylisothiourea

Methyl 2-thiocyanoisobutyrate (15.0 g, 0.094 mole), dimethylhydrazine (6.0 g, 0.100 mole), and nitrobenzene (15 ml) were mixed at room temperature and allowed to stand for 4 days. After it was filtered out and washed with ligroine, the solid product was recrystallized from *t*-amyl alcohol, m.p. 136–138° C. Yield, 5.8 g (28%). Further recrystallization using the same solvent gave a sample melting at 140° C. Calc. for $C_8H_{17}N_3O_2S$: C, 43.80; H, 7.83; N, 19.16%. Found: C, 44.19; H, 7.88; N, 19.02%.

Dibenzyl Disulphide

Benzyl thiocyanate was prepared from benzyl chloride in the usual manner, m.p. 42–44° C (19). The thiocyanate (10 g, 0.067 mole) in ethanol (50 ml) was treated with hydrazine (3.4 g, 0.068 mole) at room temperature, and the resulting solution was allowed to stand for 3 days. The color of the reaction mixture deepened to dark red and a small amount of precipitate of the same color was obtained. After the solution was diluted with ether (100 ml), the product was filtered and when the filtrate was concentrated, a solid separated out, m.p. 70.5–72° C, which contained no nitrogen. Recrystallization from ethanol gave 4.2 g (51%) of the dibenzyl disulphide, m.p. 72–73° C (20).

Trimethylene Disulphide

Hydrazine hydrate (6.3 g, 0.126 mole) was added to a solution of trimethylene dithiocyanate (10 g, 0.063 mole) in ethanol (50 ml) at room temperature. The reaction was slightly exothermic, accompanied by darkening of the mixture to deep yellow. After the mixture was left to stand for 20 hours, the precipitate was filtered and washed with alcohol and ether, m.p. 73–75° C. Yield, 6.4 g (95%). Recrystallization from chloroform gave a product containing no nitrogen, m.p. 75–76° C (14). Molecular weight determinations showed that this material was in reality the dimer of trimethylene disulphide. Calc. for $C_6H_{12}S_4$: 212. Found (Rast method): 198.

N-dimethylamino-S-benzylisothiourea

Dimethylhydrazine (4.3 g, 0.072 mole) was introduced, with shaking, into a solution of benzyl thiocyanate (10 g, 0.067 mole) in ether (25 ml) at room temperature. After 5 minutes had elapsed, an oil started to separate out, and at the end of 65 hours solidification occurred. The white solid was filtered and washed with ether, m.p. 72–74° C. Yield, 12.1 g (86%). Six recrystallizations from *t*-amyl alcohol afforded a pure product, m.p. 76–77° C. Calc. for $C_{10}H_{15}N_3S$: C, 57.37; H, 7.24; N, 20.08%. Found: C, 57.56; H, 7.23; N, 20.17%.

A small quantity of the above compound was dissolved in ethylene chloride and treated with a few drops of concentrated sulphuric acid. The solution was allowed to stand overnight in a refrigerator and a solid product was obtained, m.p. 114–115° C. Recrystallization from butanol gave rise to the pure sulphate salt of 1,1-dimethyl-2-benzylhydrazine, m.p. 116° C. Calc. for $C_9H_{14}N_2 \cdot H_2SO_4$: C, 43.53; H, 6.51; N, 11.29%. Found: C, 43.80; H, 6.63; N, 11.31%.

REFERENCES

1. HEINTZ, A. Ann. **136**, 223 (1865).
2. CLAESSON, P. Ber. **10**, 1346 (1877).
3. FRERICHS, G. and FÖRSTER, P. Ann. **371**, 227 (1910).
4. STEPHEN, H. W. and WILSON, F. J. J. Chem. Soc. 1415 (1928).
5. FRERICHS, G. and HÖLLER, H. Ann. **398**, 256 (1913).
6. STEPHEN, H. W. and WILSON, F. J. J. Chem. Soc. 2826 (1928).
7. ALLEN, P., JR. J. Am. Chem. Soc. **57**, 198 (1935).
8. RADZISZEWSKI, B. Ber. **2**, 208 (1869).
9. CLINTON, R. O. and LASKOWSKI, S. C. J. Am. Chem. Soc. **70**, 3135 (1948).
10. MCKENZIE, A. and BARROW, F. J. Chem. Soc. **99**, 1917 (1911).
11. WINTHROP, S. O. and GAVIN, G. Can. J. Chem. **36**, 879 (1958).
12. STALLÉ, R. and KRAUCH, K. J. Prakt. Chem. **83**, 306 (1913).
13. LIEBER, E. and STROJNY, E. J. J. Org. Chem. **17**, 518 (1952).
14. HAGELBERG, L. Ber. **23**, 1083 (1890).
15. RAST, K. Ber. **55**, 1051, 3727 (1922).
16. CLARKE, H. T. and TAYLOR, E. R. Org. Syntheses, **4**, 9 (1925).
17. MARVEL, C. S. Org. Syntheses, **21**, 74 (1941).
18. HATT, H. H. Org. Syntheses, **16**, 51 (1936).
19. WHEELER, H. L. and MERRIAM, H. F. J. Am. Chem. Soc. **23**, 283 (1901).
20. BERGMANN, E. and HERVEY, J. Ber. **62**, 893 (1929).

THE CHEMICAL COMPOSITION OF THE HEARTWOOD EXTRACTIVES OF TAMARACK (LARIX LARICINA (DU ROI) K. KOCH)[1]

G. V. NAIR[2] AND E. VON RUDLOFF

ABSTRACT

The acetone-soluble constituents of the heartwood of tamarack have been investigated. The flavanonols taxifolin and aromadendrin were isolated in 0.30 and 0.05% yield and a trace amount of quercetin was obtained. Tropolones could not be detected, nor was there any evidence for resin acids. The major portion of the extract consisted of esters of ferulic, phthalic, and long-chain fatty acids. Eicosanyl ferulate was isolated as such, whereas the other constituents were identified after saponification. Gas liquid chromatography of the fatty acid mixture indicated the presence of palmitic, palmitoleic, oleic, linoleic, and linolenic acids as well as small amounts of C_{14}, stearic, and C_{20} acids. From the non-saponifiable portion β-sitosterol, eicosanol, and nonan-2-ol were isolated. The acetone extract also contained free D-galactose and L-arabinose.

INTRODUCTION

Whereas the heartwood constituents of pine trees (1, 2) and those of the commercially important west coast conifers (1, 2, 3) have been studied extensively, larch heartwood constituents have not been investigated to any great extent. Gripenberg (4) has isolated from *Larix decidua* (*L. europea*) taxifolin ((+)-2,3-dihydroquercetin) and aromadendrin ((+)-2,3-dihydrokaempferol) and has shown that the distylin isolated from *L. leptolepis* (5, 6) is a mixture of these two flavanonols (nomenclature (2)). Brewerton (7) made a thorough investigation of the heartwood constituents of *L. decidua* and *L. leptolepis* grown in New Zealand and found, besides taxifolin and aromadendrin, trace amounts of a flavanone (m.p. 252° C), a phytosterol, and unidentified lignin- and tannin-like material, but no resin acids.

Tamarack is a small- to medium-sized larch tree found across Canada from the Atlantic coast to northern British Columbia and in Alaska. The wood of this species is often quite oily and is resistant to decay. Although it is used for railway ties, telegraph poles, and posts, it has found little commercial use. The present study of the acetone-soluble heartwood constituent was made on mature trees obtained from the Prince Albert and the Winnipeg areas. The freshly milled heartwood contained about 2.5% (on a dry weight basis) of acetone-soluble, non-volatile extractives.

Preliminary investigation on the total extract and a saponified portion thereof, by spot tests and paper chromatography, indicated the presence of a steroid, flavanoid constituents, and free sugars. Tropolones of the thujaplicin type were not detected on a paper chromatogram (8), nor were resin acids encountered. The concentrated acetone extract deposited a mixture of sugars, consisting of D-galactose (0.15% over-all yield, based on the dry weight of heartwood extracted) and L-arabinose (0.04%). The extraction of these acetone-insoluble sugars is explained by the presence of 15% moisture in the wood. The proportion of galactose to arabinose is the same as that found by Campbell *et al.* (9) in the ε-galactan of larch wood (*Larix decidua*), and it is conceivable that the free sugars were derived from polysaccharides by hydrolysis in the plant.

[1]*Manuscript received May 25, 1959.*
Contribution from the National Research Council of Canada, Prairie Regional Laboratory, Saskatoon, Saskatchewan.
Issued as N.R.C. No. 5293.
[2]*National Research Council of Canada Postdoctorate Fellow, 1958–60.*

Conventional fractionation of the extract into petrol- or ether-soluble neutral compounds and acidic and phenolic constituents by treatment with aqueous alkali was unsatisfactory because of emulsion formation and incomplete separations. Therefore, the extract was divided into acetone-, benzene-, and petrol-soluble portions and then further fractionated as indicated (see Fig. 1). The acetone-soluble, benzene-insoluble portion (0.34%) consisted of flavonoid material. Paper chromatography of this material gave two spots corresponding to aromadendrin (R_f 0.8) and taxifolin (R_f 0.6) with the solvent system of Gripenberg (4), containing 1% acetic acid to prevent tailing. The

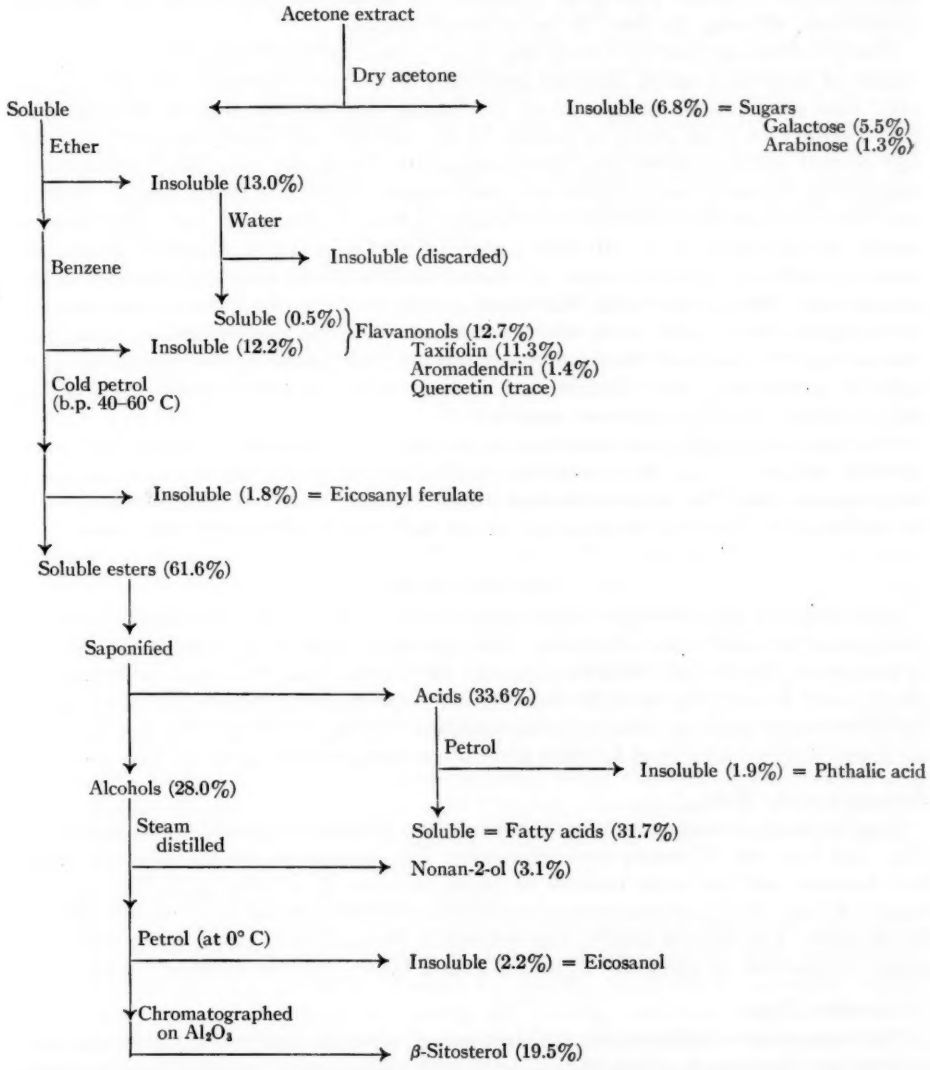

FIG. 1. Fractionation scheme and yields of compounds (based on the weight of acetone extract).

mixture was resolved almost completely on a cellulose powder column, giving an over-all yield of 0.04% of aromadendrin and 0.30% of taxifolin. When the column was washed with 50% aqueous ethanol a trace amount of quercetin was obtained.

The benzene-soluble, cold petrol-insoluble portion contained an ester, m.p. 61–62° C (0.05%), which was soluble in very dilute alkali, but which precipitated in more concentrated solutions. The infrared spectrum suggested an aromatic ester with a free hydroxyl group and a double bond in conjugation with the aromatic ring. It resembled closely the spectrum of methyl ferulate, except that the C–H absorption was much more intense. Alkaline hydrolysis produced eicosanol and ferulic acid in equimolar proportions, showing the ester to be eicosanyl ferulate.

The petrol-soluble portion formed the major part of the extract and it was comprised mainly of long-chain esters (infrared spectrum). Fractional distillation *in vacuo* did not yield pure components, and gas liquid chromatography was not feasible because of the low volatility of these esters. A portion of the material was saponified and the acidic and neutral fractions were investigated separately. From the non-saponifiable mixture nonan-2-ol, eicosanol, and β-sitosterol were isolated. From the acidic portion phthalic acid was obtained by crystallization. Phthalic acid or its esters are not often found in nature. Haagen-Smit *et al.* (10) report phthalic acid to occur in Zinfandel grapes and recently Kohlbrenner and Schuerch (11) have found *l*-2-octyl-β-sitosteryl phthalate in the extractives of Sitka spruce wood. The major portion of the acidic fraction was composed of long-chain fatty acids, with the unsaturated members predominating. Gas liquid chromatography resolved the methylated mixture and major peaks corresponding to palmitic, palmitoleic, oleic, linoleic, and linolenic acids and minor peaks corresponding to C_{14}, stearic, and C_{20} acids were recorded.

The resistance of heartwood to decay is ascribed to the presence of compounds having phenolic properties, e.g. the pinosylvins in pine heartwood (1, 12) and thujaplicins in thuja species (13). The present findings would indicate, therefore, that tamarack owes its resistance to decay to the presence of the flavanonols and ferulic acid esters.

EXPERIMENTAL

Melting points were measured with a Leitz hot stage microscope. Gas liquid chromatograms were obtained with a Beckman GC-2 chromatograph using washed silicone (14) or polyester (15) on C-22 firebrick columns (18 to 24 in. long, ¼ in. diameter). Infrared spectra were recorded by the KBr disk method or the film technique on a Perkin–Elmer Model 21 double beam recording spectrophotometer. All known compounds were identified by mixed melting point and infrared spectra comparison with authentic samples.

Extraction of the Wood

Logs of mature tamarack trees were obtained from the Prince Albert district, Saskatchewan, and from the Winnipeg area, Manitoba. The heartwood was cut out and milled in a hammer mill and then reduced to coarse sawdust in a Wiley mill. The air-dried wood (12.7 kg, 15% moisture content) was extracted with acetone in a Soxhlet extractor for 36 hours. The acetone extract was reduced to dryness by evaporation *in vacuo* in a rotary evaporator, at about 50° C, giving a dark brown, viscous material (302 g).

Preliminary Tests

The magnesium – hydrochloric acid test on an alcoholic solution of the extract was positive for flavanonols. Precipitation tests with digitonin or cyclohexylamine on the extract did not indicate the presence of free sterols or resin acids. When the test was

repeated on a saponified portion, positive results were obtained with digitonin. Paper chromatography, using *n*-butanol – acetic acid – water (4:1:1.8 v/v) (16) and *p*-anisidine spray (17) showed that the mixture contained sugars with R_f values corresponding to galactose and arabinose. With impregnated paper, petrol (b.p. 50–60° C), and diazotized benzidine spray (8) the chromatograms showed no spots corresponding to tropolones. When Gripenberg's method (4) was applied, spots corresponding to aromadendrin and taxifolin (see below) were obtained.

Isolation and Identification of Sugars

The concentrated acetone extract when left to stand yielded crystalline material (14.1 g). The total extract was then taken up in dry acetone (0.5 l.) when more solid material was deposited (6.4 g). The solid material was removed by filtration and crystallized from methanol to yield a crude product, m.p. 142–155° C, $[\alpha]_D^{24.6}$ +79.12 (*c*, 0.77, H_2O). Paper chromatography showed the presence of galactose and arabinose only, and the mixture was resolved by treatment with α-methyl-α-phenyl hydrazine (9). D-Galactose-*N*-methyl-*N*-phenyl hydrazone (1.636 g, corresponding to 80.55% galactose), m.p. 185–186° C, $[\alpha]_D^{22.8}$ −18.98 (*c*, 0.66, pyridine), and arabinose, m.p. 158–160° C, $[\alpha]_D^{23.8}$ +121.59 (*c*, 0.52, H_2O), were isolated.

Isolation and Identification of Flavanonols

The acetone-soluble material, after filtration and reduction to a small volume, was taken up in excess ether (1.25 l.). The ether-insoluble material was separated, dried (39 g), and extracted repeatedly with boiling water, the insoluble residue being discarded. The ether-soluble portion was evaporated to dryness and re-extracted with benzene. The benzene-insoluble portion (36.5 g) was combined with the water-soluble portion (1.5 g) and analyzed by paper chromatography (4). When 1% acetic acid was added to the solvent mixture (chloroform–ethanol–water, 8:2:1 v/v, lower phase) tailing of the flavanonols was prevented. With the bis-diazotized benzidine spray reagent (18) brown spots corresponding to aromadendrin (R_f 0.8) and taxifolin (R_f 0.6) were obtained. An aliquot of the mixture of flavanonols (3.75 g) was resolved on a cellulose powder column (50×4.5 cm), using the same solvent system (4.5 l.) as eluent. Fractions of 20 ml were collected and tested individually by paper chromatography. Tubes 1 to 70 contained aromadendrin (0.314 g), m.p. 236–237° C (from $CHCl_3$), $[\alpha]_D^{24.6}$ +44.72 (*c*, 0.5, water–acetone, 1:1). When the compound was recrystallized from water the m.p. was 128–130° C. This dimorphism has apparently not been noted before. Tubes 71 to 89 contained a mixture (0.077 g) of aromadendrin and taxifolin in about equal amounts. Taxifolin (3.307 g) was obtained from tubes 90 to 195, m.p. 238–240° C (from $CHCl_3$ and ethanol), $[\alpha]_D^{24}$ +47.71 (*c*, 0.75, water–acetone). When the column was washed with 50% aqueous ethanol (1:1) a yellow solid (0.006 g) was obtained on evaporation of the solvent. Crystallization from aqueous ethanol gave quercetin, m.p. 310–312° C, $[\alpha]_D^{24}$ +142.2 (*c*, 0.53, water–acetone).

Isolation and Identification of Eicosanyl Ferulate

The benzene-soluble material (191 g) was repeatedly triturated with cold petrol (b.p. 40–60° C). The petrol-insoluble material (5.5 g) on recrystallization from cyclohexane gave a compound, m.p. 61–62° C. Found: C, 75.76%; H, 10.70%; molecular weight (Rast), 533. Calc. for $C_{30}H_{50}O_4$: C, 75.95%; H, 10.54%; molecular weight, 474.52.

The ester (0.5 g) in chloroform (5 ml) was treated with excess bromine in chloroform. Evaporation of the solvent left a solid tribromide, m.p. 98° C (from petrol, b.p. 40–60° C). Found: C, 51.96%; H, 7.21%. Calc. for $C_{30}H_{49}O_3Br_3$: C, 51.65%; H, 7.03%. The ester

(2.1 g) was hydrolyzed by refluxing in a 20% aqueous potassium hydroxide solution (150 ml) containing ethanol (50 ml) for 15 hours. The ethanol was removed by distillation, and the cold aqueous residue was extracted with ether. The ether extract was washed, dried, and evaporated to dryness (1.3 g). The residue was recrystallized (from acetone) to yield *n*-eicosanol, m.p. 71–72° C. Found: C, 80.70%; H, 14.10%. Calculated for $C_{20}H_{42}O$: C, 80.53%; H, 14.06%. The aqueous soap solution was acidified to pH 2–3 with 10% aqueous sulphuric acid and extracted three times with ether. The ether extract was washed with a saturated aqueous solution of sodium chloride, dried, and the solvent was distilled off. The residual solid (0.85 g) was recrystallized from ethyl acetate – cyclohexane to give pure ferulic acid, m.p. 175–176° C. Found: C, 62.05%; H, 5.19%. Calc. for $C_{10}H_{10}O_4$: C, 61.86%; H, 5.19%.

Petrol Extract

The petrol-soluble portion formed the major part of the heartwood extract (185 g). Fractional vacuum distillation did not resolve the mixture into single components. Because of the low volatility of the mixture, gas liquid chromatography was not successful. However, an infrared spectrum of the mixture indicated the presence of a large amount of long-chain esters. An aliquot (40 g) of the material was saponified under reflux with 20% aqueous potassium hydroxide solution (200 ml) and ethanol (100 ml) for 15–20 hours. The reaction mixture was separated into non-saponifiables (18.7 g) and acids (22.25 g) in the usual manner.

The non-saponifiable material was exhaustively steam distilled, the distillate (2 l.) saturated with sodium chloride and thrice extracted with ether (200 ml each). The ethereal solution was washed with saturated sodium chloride solution, dried over anhydrous sodium sulphate, and then distilled, yielding a sweet-smelling liquid (2.3 g), b.p. 75–77° C at 12 mm. Found for a redistilled sample: C, 74.78%; H, 14.00%; n_D^{27} 1.4310. Calc. for $C_9H_{20}O$: C, 74.46%; H, 14.48%. The derived α-naphthyl urethane was crystallized from carbon tetrachloride, m.p. 55–56° C. This corresponds to the melting point of the α-naphthyl urethane of nonan-2-ol (m.p. 55.5° C) (19).

The non-volatile residue was dissolved in petrol (b.p. 40–60° C) and kept at 0–2° C for several days, when eicosanol (1.3 g), m.p. 71–72° C, crystallized. A portion of the residual material (2.4 g) was chromatographed on neutral alumina (Brockmann). Elution with petrol (b.p. 40–60° C) and ether (1:1 v/v) gave 0.3 g of unsaponified esters. With ether-ethanol (1:1 v/v) a solid (1.8 g) was eluted which had m.p. 141° C after crystallization from ethanol. It gave a positive Lievermann–Burchard reaction, and formed an acetate, m.p. 123–124° C, and a benzoate, m.p. 143–144° C, which correspond with those of β-sitosterol (20). Found: C, 83.78%; H, 12.30%. Calc. for $C_{29}H_{50}O$: C, 83.99%; H, 12.15%.

The acid mixture contained petrol-insoluble material (1.25 g) which crystallized from acetone to give phthalic acid, m.p. 201–203° C; anilide, m.p. 165–166° C. The petrol-soluble acids were converted to their methyl esters with diazomethane and analyzed by gas liquid chromatography. When the polyester column was used, peaks corresponding to two C_{14} acids (0.5% and 0.6% respectively), palmitic (7.0%), palmitoleic (7.1%), stearic (1.9%), oleic (20.0%), linoleic (31.8%), linolenic (25.2%), and two C_{20} acids (1.5% and 3.0% respectively) were obtained.

ACKNOWLEDGMENTS

We wish to express our thanks to the Forestry Branch of the Department of Natural Resources for obtaining the wood, to Mr. M. Granat for technical assistance, to Miss

I. M. Gaffney for the infrared spectra, to Mr. M. Mazurek for the microanalyses, and to Dr. C. G. Youngs for help in gas liquid chromatographic separations. We are also grateful to Professor H. Erdtman, Royal Institute of Technology, Stockholm, who kindly supplied authentic samples of taxifolin and aromadendrin, and for his advice and suggestions.

REFERENCES

1. ERDTMAN, H. *In* Progress in organic chemistry. Vol. 1. *Edited by* J. W. Cook. Butterworth Scientific Publications, London. 1952. pp. 22–63.
2. ERDTMAN, H. *In* Perspectives in organic chemistry. *Edited by* A. Todd. Interscience Publishers, Inc., New York. 1956. p. 453.
3. GARDNER, J. A. F. and BARTON, G. M. Forest Prods. J. **8**, 3 (1958).
4. GRIPENBERG, J. Acta Chem. Scand. **6**, 1153 (1952).
5. HASEGAWA, M. and SHIRATO, T. J. Chem. Soc. Japan, **72**, 223 (1951).
6. MIGITA, N., NAKANO, J., and TOROI, T. J. Japan Tech. Assoc. Pulp Paper Ind. **5**, 399 (1951); Chem. Abstr. **46**, 1254^g (1952).
7. BREWERTON, H. V. New Zealand J. Sci. Technol. B, **37**, 626 (1956).
8. WACHTMEISTER, C. A. and WICKBERG, B. Acta Chem. Scand. **12**, 1335 (1958).
9. CAMPBELL, W. G., HIRST, E. L., and JONES, J. K. N. J. Chem. Soc. 774 (1948).
10. HAAGEN-SMIT, A. J., HIROSAWA, F. N., and WANG, T. H. Food Research, **14**, 472 (1949).
11. KOHLBRENNER, P. J. and SCHUERCH, C. J. Org. Chem. **24**, 166 (1959).
12. ERDTMAN, H. Naturwissenschaften, **27**, 130 (1939).
13. ERDTMAN, H. and GRIPENBERG, J. Nature, **161**, 719 (1948).
14. CRAIG, B. M. and MURTY, N. L. Can. J. Chem. **36**, 1297 (1958).
15. CRAIG, B. M. J. Am. Oil Chemists' Soc. (In press).
16. NEISH, A. C. Can. J. Biochem. and Physiol. **35**, 159 (1957).
17. HOUGH, L., JONES, J. K. N., and WADMAN, W. H. J. Chem. Soc. 1702 (1950).
18. LINDSTEDT, G. Acta Chem. Scand. **4**, 448 (1950).
19. PICKARD, R. H. and KENYON, J. J. Chem. Soc. **99**, 56, 70 (1911).
20. COOK, J. W. and PAIGE, M. F. C. J. Chem. Soc. 336 (1944).

4-NITROPYRENE*

P. M. G. BAVIN†

Nitration of pyrene has afforded only the 1-isomer (1, 8). Since the introduction of the nitro group into polycyclic hydrocarbons through the diazonium compounds does not proceed in high yield (3), other indirect routes to the unknown nitropyrenes seemed to offer advantages.

One such alternative, the dehydrogenation of the nitrohexahydropyrene (I*a*) with chloranil, has been used to prepare 4-nitropyrene (II*a*) for the first time.

The nitrohexahydropyrene (I*a*) and the corresponding amine (I*b*) and its N-acetyl derivative (I*c*) have been described previously (7). These have been prepared again and the fluoro compound (I*d*) has been described for the first time. Other substitution products of *sym*-hexahydropyrene have been described (5, 6, 8).

It is curious that Neresheimer's work (7) was not included in Vollmann's paper (8) although carried out in the same laboratory and at the same period.

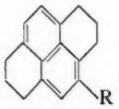

I

I*a*, R = NO_2 I*c*, R = $NH.CO.CH_3$
I*b*, R = NH_2 I*d*, R = F

II

II*a* R = NO_2
II*b* R = NH_2

EXPERIMENTAL

Melting points are uncorrected.

4-Nitro-1,2,3,6,7,8-hexahydropyrene (I*a*)

In a typical experiment, *sym*-hexahydropyrene (3 g) was nitrated with nitric acid (0.8 ml, d. 1.42) in acetic anhydride (250 ml). The solution rapidly turned red. After 48 hours at room temperature, acetic anhydride was destroyed with water and the products isolated with chloroform. Purification of the crude nitro compound by chromatography from pentane–benzene (5:1) on acid-washed alumina followed by crystallization from methanol–acetone afforded pure (I*a*) (1.9–2.4 g) as bright yellow needles, m.p. 92–93° (lit. m.p. 92–95° (7)). Calculated for $C_{16}H_{15}NO_2$: C, 75.87; H, 5.97%. Found: C, 75.97; H, 5.74%.

The impure nitro compound rapidly turned brown when exposed to light.

4-Amino-1,2,3,6,7,8-hexahydropyrene (I*b*)

4-Amino-1,2,3,6,7,8-hexahydropyrene was prepared by reducing the nitro compound (I*a*) with hydrazine and palladized charcoal (2). It crystallized from heptane as almost

*Ring index numbering.
†I.C.I. Fellow.

colorless slender needles, m.p. 132–133° (lit. m.p. 134–135° (7)). Calculated for $C_{16}N_{17}N$: C, 86.05; H, 7.67; N, 6.27%. Found: C, 86.15; H, 7.76; N, 6.28%.

N-Acetyl-4-amino-1,2,3,6,7,8-hexahydropyrene (Ic)

N-Acetyl-4-amino-1,2,3,6,7,8-hexahydropyrene crystallized from toluene as colorless slender needles, m.p. 290–292° (lit. m.p. 280–282° (7)). Calculated for $C_{18}H_{19}NO$: C, 81.47; H, 7.22; N, 5.28%. Found: C, 81.28; H, 7.28; N, 5.26%.

4-Fluoro-1,2,3,6,7,8-hexahydropyrene (Id)

4-Fluoro-1,2,3,6,7,8-hexahydropyrene, prepared in the usual way (4), crystallized from methanol as slender white needles, m.p. 111–112°. Calculated for $C_{16}H_{15}F$: C, 84.93; H, 6.68%. Found: C, 84.73; H, 6.91%.

4-Nitropyrene (IIa)

The pure hexahydro compound (Ia), (1 g), was boiled under reflux for 24 hours with a solution of chloranil (5 g) in xylene (30 ml). After it was cooled the mixture was diluted with hexane (30 ml), decanted from the dark hydroquinone, and passed through a column of alumina. Elution was continued with hexane–benzene (5:1). The eluted material was further purified by rechromatographing from hexane, only the orange-brown band eluting as a yellow solution being retained. (These colors correspond exactly to those shown by 1-nitropyrene (1).)

Crystallization from methanol containing a little acetone afforded slender orange needles, m.p. 196–197.5°. Calculated for $C_{16}H_9NO_2$: C, 77.72; H, 3.67%. Found: C, 77.40; H, 3.51%.

4-Aminopyrene (IIb)

4-Aminopyrene was prepared from (IIa) by reduction with hydrazine and palladized charcoal (2). It crystallized from heptane as bright yellow platelets, m.p. 191–193° with decomposition (lit. m.p. 182° (7)).

ACKNOWLEDGMENTS

Most of this work was completed at the University of Ottawa during the tenure of a National Research Council of Canada Postdoctorate Fellowship (1954–56). The author is indebted to Dr. W. L. Mosby (American Cyanamid Co., Bound Brook) for drawing his attention to and supplying a copy of the P.B. Report (7).

1. Bavin, P. M. G. Thesis, London. 1952.
2. Bavin, P. M. G. Can. J. Chem. **36**, 238 (1958).
3. Bavin, P. M. G. and Dewar, M. J. S. J. Chem. Soc. 4477 (1955).
4. Bavin, P. M. G. and Dewar, M. J. S. J. Chem. Soc. 4486 (1955).
5. Clar, E. J. Chem. Soc. 2168 (1949).
6. Cook, J. W. and Hewett, C. L. J. Chem. Soc. 401 (1933).
7. Neresheimer, H. P. B. Report 70840, frames 12871/6.
8. Vollmann, H., Becher, H., Corell, M., and Streeck, H. Ann. **531**, 1 (1937).

Received March 19, 1959.
The Department of Chemistry,
The University,
Kingston-upon-Hull,
East Yorkshire, England.

KINETICS OF THE THERMAL REACTION OF HYDROGEN PEROXIDE WITH HYDROGEN*

W. FORST

The thermal reaction of hydrogen peroxide with hydrogen has been studied by McLane (1), who worked around 500° C in a flow system without reaching any definite conclusions. In the present brief study it was found that under suitable conditions the reaction of hydrogen peroxide with hydrogen proceeded with a pressure increase in a closed system. This means that in addition to the over-all process

$$H_2 + H_2O_2 \rightarrow 2H_2O,$$

the reaction

$$H_2O_2 \rightarrow H_2O + \tfrac{1}{2}O_2$$

must also be occurring because it is the only conceivable process capable of increasing the number of molecules. Presence of oxygen in the system was confirmed by following the reaction to completion. The pressure in the system rose to a maximum, and then slowly declined (Fig. 1), indicating a slow hydrogen–oxygen reaction. Sometimes there occurred an explosion shortly before the pressure maximum was reached (i.e. shortly before all the

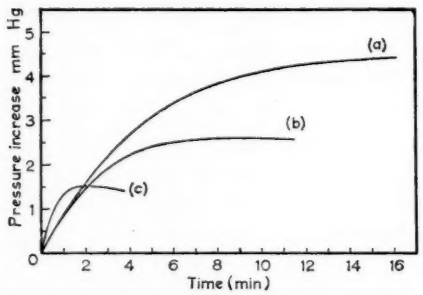

FIG. 1. Rate curves in the presence and absence of hydrogen. (*a*) Peroxide only. (*b*) Peroxide + 19.2 mm H_2 initially. (*c*) Peroxide + 96.2 mm H_2 initially. Initial pressure of peroxide 9.6 mm Hg in all three cases.

hydrogen peroxide had disappeared). This behavior finds a ready explanation in the inhibiting action of hydrogen peroxide in hydrogen–oxygen explosions at the second limit (2). Comparison of rate curves in the presence and absence of hydrogen (Fig. 1) shows that qualitatively the effect of hydrogen is twofold: (1) the rate is faster; (2) the pressure increase is smaller.

Apparatus and technique were described previously (3). All experiments were done at 431.5° C, where the slow hydrogen–oxygen reaction is not important. However, to avoid all complications arising from this reaction, only initial rates were measured and considered significant; these results are summarized in Figs. 2 and 3. Each point is the average of two successive runs on the same H_2–H_2O_2 mixture.

The interpretation of the results is complicated by two factors: (1) the time-dependence of the pressure rise in the H_2O_2–H_2 reaction system represents the rate of formation of oxygen, which, unlike in the case of the pressure rise in the H_2O_2 system, bears no simple

*This work was supported in part by the Office of Scientific Research of the U.S. Air Force under Contract No. AF 18(600)-492.

relationship to the rate of disappearance of peroxide; (2) under the experimental conditions (H_2O_2 pressure below 20 mm Hg, hydrogen pressure below 100 mm Hg) the decomposition of hydrogen peroxide is unimolecular and second order (3, 4). If the proposed (3) scheme for this decomposition is accepted, then the initial rate of oxygen formation R_0, in the presence of one inert foreign gas X, is given by (cf. eq. VII′, ref. 3)

$$[1] \qquad R_0 = (d[O_2]/dt)_{t\to 0} = a_1[H_2O_2]_0^2 + a_4[H_2O_2]_0[X]_0,$$

where the subscript zero refers to initial conditions, and

a_1 = second order rate constant for activation with peroxide,
a_4 = second order rate constant for activation with inert gas X.

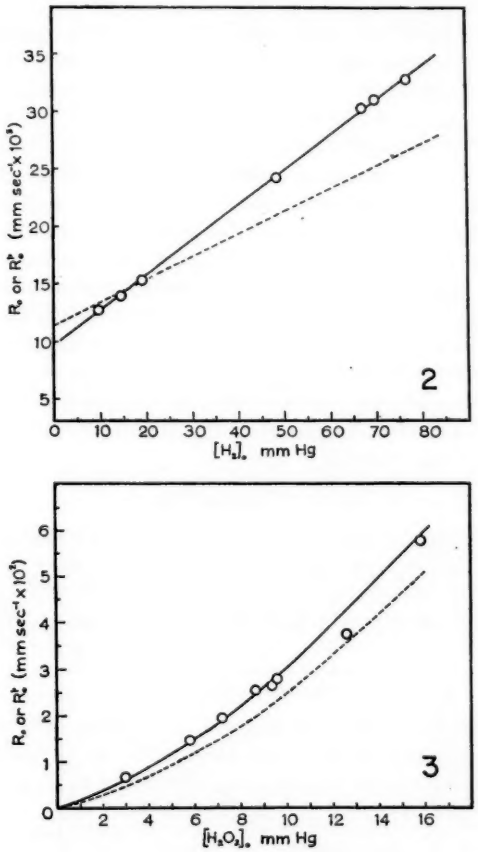

FIG. 2. Solid line: Experimental initial rate R_0 plotted vs. initial hydrogen pressure. Broken line: R_0^p (theoretical physical component of initial rate) plotted vs. initial hydrogen pressure. Initial hydrogen peroxide concentration constant at 9.6 mm Hg in both cases.

FIG. 3. Solid line: Experimental initial rate R_0 plotted vs. initial peroxide pressure. Broken line: R_0^p (theoretical physical component of initial rate) plotted vs. initial peroxide pressure. Initial hydrogen pressure constant at 57.9 mm Hg in both cases.

Equation [1] makes it at once apparent that the initial rate of oxygen formation R_0 will depend on initial hydrogen concentration even if hydrogen did not chemically react, that is, the mere presence of hydrogen as a collision medium will increase R_0. This may be referred to as the physical effect of hydrogen, the magnitude of which depends on $a_4^{H_2}$, the second order rate constant for activation with hydrogen. The experimentally determined initial rate R_0 must contain the contribution of both the physical and chemical effects of hydrogen, because it is difficult to account for the results in Fig. 1 by physical activation alone. By working out the necessary algebra it is easy to show that R_0 will be equal to the sum of the two contributions:

$$\begin{aligned} R_0 &= R_0^p + R_0^c \\ &= a_1[H_2O_2]_0^2 + a_4^{H_2}[H_2O_2]_0[H_2]_0 + R_0^c, \end{aligned}$$

where R_0^p is a term representing the physical effect and R_0^c a term representing the chemical effect of hydrogen on initial rate. This equation shows that for constant $[H_2O_2]_0$, R_0^p is linear in initial hydrogen concentration. From Fig. 2 it is apparent that for $[H_2O_2]_0$ = constant the experimentally determined R_0 is also linear in $[H_2]_0$, and therefore R_0^c must be likewise linear in initial hydrogen concentration at constant $[H_2O_2]_0$; hence the reaction is seen to be first order with respect to hydrogen.

The broken line in Fig. 2 represents a plot of R_0^p vs. $[H_2]_0$ for $[H_2O_2]_0$ = constant = 9.6 mm Hg taking $a_4^{H_2} = 2.1 \times 10^{-5}$ mm sec^{-1}, a value obtained by assuming that the collision/collision efficiency of hydrogen relative to H_2O_2 reactant is the same as that of He relative to the same reactant. This is a first approximation based on results of Volpe and Johnston (5), who found experimentally that these efficiencies were equal in the case of nitryl chloride reactant. The value of a_1 was taken from ref. 3. The discrepancy in the intercepts of the two lines is partly due to error in peroxide concentration (which enters the intercept squared), and partly to a slight shift in surface condition.

Figure 3 represents experimental results obtained at fixed initial hydrogen concentration. The broken line is a theoretical plot of R_0^p vs. $[H_2O_2]_0$ assuming $a_4^{H_2} = 2.1 \times 10^{-5}$ mm sec^{-1}, as before. If R_0^c is now written

$$R_0^c = k[H_2O_2]_0^x[H_2]_0,$$

where k = rate constant for the reaction of peroxide with hydrogen, and x = the unknown power of the peroxide concentration in the rate expression, then the plot of $R_0 - R_0^p$ vs. $[H_2O_2]_0$ will be a curve if $x > 1$, and a straight line if $x = 1$. This is plotted in Fig. 4, again for $a_4^{H_2} = 2.1 \times 10^{-5}$ mm sec^{-1}, and is seen to result in a straight line. The linearity of

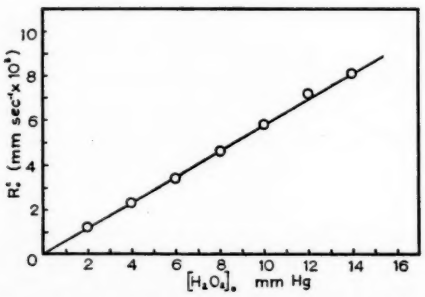

FIG. 4. The difference $R_0 - R_0^p$ (from Fig. 3) plotted vs. initial peroxide concentration, with initial hydrogen pressure constant at 57.9 mm Hg.

this plot does not depend on the assumed value for $a_4^{H_2}$, although the slope does. The reaction is thus seen to be first order in peroxide as well, and so the reaction may be described by the equation

$$R_0 = a_1[H_2O_2]_0^2 + (a_4^{H_2} + k)\,[H_2O_2]_0[H_2]_0. \qquad [2]$$

On the basis of this result some speculation may be made concerning the probable mechanism. If reactions involving oxygen are neglected on the ground that they would not affect the initial rate, hydrogen is likely to enter only into reactions

$$OH + H_2 \rightarrow H_2O + H \qquad [a]$$

$$H + H_2O_2 \rightarrow H_2O + OH, \qquad [b]$$

for which there seems to be good evidence from other sources ([*a*], ref. 6; [*b*], refs. 2, 7, 8). It turns out, however, that these two reactions, when combined with reactions postulated (3) in the decompostion of hydrogen peroxide, will not result in an increase of oxygen formation as required by eq. [2]. A closer look at the mechanism shows that there are two types of reactions that will increase the rate of formation of oxygen (but will not necessarily lead to the desired order in peroxide or hydrogen).

(1) Reactions in which one radical disappears and another radical appears, with the simultaneous formation of oxygen, for example,

$$HO_2 + H_2O_2 \rightarrow OH + O_2 + H_2O$$

or

$$HO_2 \rightarrow H + O_2.$$

These reactions do not involve the intervention of hydrogen and therefore presumably should occur also in the decomposition of pure peroxide. However, they lead there to unsatisfactory results (9, 10).

(2) Chain-branching reactions not involving oxygen. This restricts the choice of likely reactions considerably; in fact, the only reaction seems to be

$$H_2 + HO_2 \rightarrow 2OH + H \qquad [c]$$

suggested by Kassel and Storch (11) and used by them to derive a mechanism for the second explosion limit in the hydrogen–oxygen reaction. If reactions [*a*], [*b*], and [*c*] are added to the reactions postulated in the decomposition of pure peroxide (3), a rate expression for the rate of formation of oxygen may be derived which has the form [2]. However, reaction [*c*] has a very high endothermicity, some 67 kcal if $D(H–O_2)$ is taken as 47 kcal (12), so that a more direct evidence for reaction [*c*] would be required before this mechanism can be accepted.

ACKNOWLEDGMENTS

Thanks are due to Professor P. A. Giguère of Laval University for his continued interest, and to Professor O. K. Rice of the University of North Carolina for permission to write this paper during the tenure of a postdoctoral fellowship.

1. McLane, C. K. J. Chem. Phys. **18**, 972 (1950).
2. Forst, W. and Giguère, P. A. J. Phys. Chem. **62**, 340 (1958).
3. Forst, W. Can. J. Chem. **36**, 1308 (1958).
4. Hoare, D. E., Protheroe, J. B., and Walsh, A. D. Nature, **182**, 654 (1958).
5. Volpe, M. and Johnston, H. S. J. Am. Chem. Soc. **78**, 3903 (1956).
6. Lewis, B. and von Elbe, G. Combustion, flames and explosions. Academic Press, Inc., New York. 1951.
7. Geib, K. H. Z. physik. Chem. A, **169**, 161 (1934).
8. Baldwin, R. R. and Mayor, L. Paper presented at the 7th Symposium on Combustion, Oxford. 1958.

9. GIGUÈRE, P. A. and LIU, I. D. Can. J. Chem. **35**, 283 (1957).
10. CONWAY, D. C. J. Phys. Chem. **61**, 1579 (1957).
11. KASSEL, L. S. and STORCH, H. H. J. Am. Chem. Soc. **57**, 672 (1935).
12. FONER, S. N. and HUDSON, R. L. J. Chem. Phys. **23**, 1364 (1955).

RECEIVED MAY 4, 1959.
DEPARTMENT OF CHEMISTRY,
LAVAL UNIVERSITY,
QUEBEC, QUE.

TRANSIENTS IN THE FORMATION OF ANODIC OXIDE FILMS

L. YOUNG

With certain metals, in particular, tantalum (1) and niobium (2) when the ionic (film-building) current density through the anodic oxide film is suddenly increased, the field strength in the oxide "overshoots" before settling to the new steady state value corresponding to the new current density. Dewald (1) has shown that the behavior is inconsistent with the model (which he advanced to explain the Tafel slope anomalies) in which the space charge due to the mobile metal ions is uncompensated by other sources of space charge. A more realistic model would have a concentration (say, ϕ cm^{-3}) of mobile metal in the electrically neutral oxide. The net space charge may then be either negative or positive. The steady state equations for this model, with ϕ independent of field strength, have been published (3).

The purpose of the present communication is to show that Dewald's result for his case (which corresponds to $\phi = 0$) may be generalized to $\phi \neq 0$.

We have

$$\partial E/\partial t = (pI_0 - i)/KK_0 \quad \text{(differentiated Gauss' equation)}$$
$$\partial E/\partial x = q(n-\phi)/KK_0 \quad \text{(Poisson's equation)}$$
$$i = q\mu_0 \exp \beta E \quad \text{(conventional equation for the ionic current at high fields)}$$

where E = field strength in the oxide at distance x from the metal, t = time after current is changed, I_0 = current density for $t < 0$, pI_0 = current for $t > 0$, i = current in oxide at distance x from the metal, n = concentration of mobile metal ions,

$$\mu_0 = \nu \exp(-W/kT)$$

where ν = vibration frequency and

$$W = \text{activation energy at zero } E, \text{ and } \beta = qa/kT$$

where a = half ionic jump distance within the oxide. By eliminating n and i, and putting (following Dewald)

$$R = \mu_0 KK_0 \exp(\beta E)/\beta pI_0 t$$
$$T = \beta pI_0 t/KK_0$$
$$z = x/D$$

where D = total oxide thickness; with, in addition,

$$\alpha = \phi\beta Dq/KK_0$$

and

$$\epsilon = (n_0 - \phi)/\phi$$

where n_0 is the concentration of metal ions just inside the oxide for $t < 0$, we obtain

$$\partial R/\partial z+(1/R)\partial R/\partial T+\alpha R = 1.$$

The general solution is

$$f\{z+(1/\alpha)\log(1-\alpha R),\ T-\log(R/(1-\alpha R))\} = 0.$$

The boundary conditions are

$$R(z,0) = R(0,0)\{1+\epsilon(1-\exp(-\alpha z))\}$$
$$R(0,T) = R(0,0)p^r/(1+(p-1)e^{-T/r})^r$$

where r = ratio of ionic jump distance at the interface to that within the oxide.

Solutions satisfying these conditions are

$$R = \{(1-\alpha R(0,0)p)e^{-\alpha z}-1\}/\{\alpha(1-p)e^{-T}-\alpha\}$$
$$(p-1)(e^{\alpha z}e^{-T}R)^{1/r} = p(R(0,0))^{1/r}-((1-e^{\alpha z})/\alpha+Re^{\alpha z})^{1/r}.$$

These solutions join at

$$z = z_s$$

where

$$(e^{\alpha z_s}-1)/\alpha = R(0,0)(e^T-1).$$

For a given z, $\partial R/\partial T$ is always positive for $p > 1$ and always negative for $p < 1$, so that there is no overshoot.

This communication is published by permission of the Defence Research Board.

1. Dewald, J. F. J. Phys. Chem. Solids, **2**, 55 (1957).
2. Young, L. Trans. Faraday Soc. **52**, 502 (1956).
3. Young, L. Can. J. Chem. **37**, 276 (1959).

Received May 19, 1959.
British Columbia Research Council,
University of British Columbia,
Vancouver 8, British Columbia.

NOTES TO CONTRIBUTORS

Canadian Journal of Chemistry

MANUSCRIPTS

General.—Manuscripts, in English or French, should be typewritten, double spaced, on paper 8½×11 in. **The original and one copy are to be submitted.** Tables and captions for the figures should be placed at the end of the manuscript. Every sheet of the manuscript should be numbered. Style, arrangement, spelling, and abbreviations should conform to the usage of recent numbers of this journal. Greek letters or unusual signs should be written plainly or explained by marginal notes. Characters to be set in bold face type should be indicated by a wavy line below the characters. Superscripts and subscripts must be legible and carefully placed. Manuscripts and illustrations should be carefully checked before they are submitted. Authors will be charged for unnecessary deviations from the usual format and for changes made in the proof that are considered excessive or unnecessary.

Abstract.—An abstract of not more than about 200 words, indicating the scope of the work and the principal findings, is required, except in Notes.

References.—These should be designated in the text by a key number and listed at the end of the paper, with the number, in the order in which they are cited. The form of the citations should be that used in this journal; in references to papers in periodicals, titles should not be given and only initial page numbers are required. The names of periodicals should be abbreviated in the form given in the most recent *List of Periodicals Abstracted by Chemical Abstracts*. All citations should be checked with the original articles and each one referred to in the text by the key number.

Tables.—Tables should be numbered in roman numerals and each table referred to in the text. Titles should always be given but should be brief; column headings should be brief and descriptive matter in the tables confined to a minimum. Vertical rules should not be used. Numerous small tables should be avoided.

ILLUSTRATIONS

General.—All figures (including each figure of the plates) should be numbered consecutively from 1 up, in arabic figures, and each figure referred to in the text. The author's name, title of the paper, and figure number should be written in the lower left corner of the sheets on which the illustrations appear. Captions should not be written on the illustrations.

Line drawings.—Drawings should be carefully made with India ink on white drawing paper, blue tracing paper, or co-ordinate paper ruled in blue only; any co-ordinate lines that are to appear in the reproduction should be ruled in black ink. Paper ruled in green, yellow, or red should not be used. All lines must be of sufficient thickness to reproduce well. Decimal points, periods, and stippled dots must be solid black circles large enough to be reduced if necessary. Letters and numerals should be neatly made, preferably with a stencil (**do NOT use typewriting**), and be of such size that the smallest lettering will not be less than 1 mm high when the figure is reduced to a suitable size. Many drawings are made too large; originals should not be more than 2 or 3 times the size of the desired reproduction. Wherever possible two or more drawings should be grouped to reduce the number of cuts required. In such groups of drawings, or in large drawings, full use of the space available should be made; the ratio of height to width should conform to that of a journal page (5¼×7⅜ in.) but allowance must be made for the captions. **The original drawings and one set of clear copies (e.g. small photographs) are to be submitted.**

Photographs.—Prints should be made on glossy paper, with strong contrasts. They should be trimmed so that essential features only are shown and mounted carefully, with rubber cement, on white cardboard, with no space between those arranged in groups. In mounting, full use of the space available should be made. **Photographs are to be submitted in duplicate;** if they are to be reproduced in groups one set should be mounted, the duplicate set unmounted.

REPRINTS

A total of 50 reprints of each paper, without covers, are supplied free. Additional reprints, with or without covers, may be purchased at the time of publication.

Charges for reprints are based on the number of printed pages, which may be calculated approximately by multiplying by 0.5 the number of manuscript pages (double-space typewritten sheets, 8½×11 in.) and including the space occupied by illustrations. Prices and instructions for ordering reprints are sent out with the galley proof.

Contents

Printed in Canada *by* University of Toronto Press